COMPLEX COPPER COMPOUNDS WITH PENTAAMINOTETRAZOLE ARE THE NEW CHALLENGE IN TREATMENT AND PREVENTION OF FREE-RADICAL CONDITIONS

Irina Shugalei, Mikhail Ilyushin, Veronika Sokolova, Nadejda Dubjago, Irina Bachurina, Alexander Garabadzhiu*

St. Petersburg State University of Technology (Technical University)
26Moskovskyave., St. Petersburg, 190013 Russia,
Tel.+79643628922, e-mail: shugalei@mail.ruand gar-54@mail.ru

Abstract: The present article provides route of synthesis of complex copper compounds with 1.5-pentamethyltetrazole as a ligand. These compounds are considered promising antioxidants that can find application in treatment and prevention of "free radical" conditions caused by a variety of reasons, e.g. harmful environmental factors. The obtained compounds were rated by their antioxidant potential; the ability to inhibit lipid peroxidation and SOD-like activity thereof were assessed by independent experimental techniques.

Keywords: complex compounds with 1.5-pentamethyltetrazole as a ligand, antioxidants, lipid peroxidation, SOD-like activity

Introduction

Human body needs oxygen to enable active performance of its organs and systems. All major metabolic processes are based on oxidation-reduction reactions. In the mitochondria molecules of oxygen are not converted to water completely, up to 5% form highly reactive free radicals [1]. The products of free radical reactions are highly toxic oxygen containing radicals and peroxidates known as reactive oxygen species, hereinafter referred to as ROS [2]. These highly reactive ROS interact with a wide range of biomolecules [3-6]. To maintain desired level of free radical pool at the adverse environment is the critical issue of the day [7-10].

Non-specific immunity comes from the mechanism of free radical formation [11, 12]. Phagocytosis causes multiple increase of free radical amount in the phagocytizing cells and 20-fold oxygen uptake boost [13].

However, overactivation of free radical oxidation reactions presents typical pathological process that occurs during various medical conditions [14] and damaging influences. It is proved that various disease processes have free radical mechanism, e.g. shocks, atherosclerosis, brain circulation failure, peripheral circulation failure, coronary circulation failure [15], diabetes mellitis and diabetic angiopathy [16], rheumatoid, inflammatory and degenerative diseases of locomotor system, eye lesions, pneumopathy, oncopathology, thermal injuries, various toxicoses, oncological diseases [17, 18], reperfusion injuries [19-22]. Overproduction of free radicals induced by harmful factors is the general reason of premature aging [23, 24].

Human body has natural protective mechanisms from free radical loads. Multi-component antioxidant defense system includes enzymes, vitamins, low molecular weight species [25-27].

Huge loads of xenobiotics drop upon human bodies in our anthropogenic age. The body can not clear the whole amount of extra free radicals, which results in mismatch between the substances inducing free radical formation(prooxidants) and substances lowering the level of radical metabolites – antioxidants (AOs). This mistmatch leads to oxidative stress [28-30]. Hence, natural antioxidant defense system requires continuous supply of specific compounds to maintain its effectiveness [31].

These substances vary over a wide range; they have different structures and derive from different origin. Their classific concepts have been established. Currently we recognize the following groups of antioxidants:

1. Antiradical agents:
    1.1. Endogenous substances: vitamin E, vitamin C, vitamin A, carotene (provitamin A), ubiquinone, lycopene;
    1.2. Synthetic chemicals: ionol (dibunole), emoxipine, probucol (fenbutol), dimethyl sulfoxide (dimexide), olifen (hypoxene);
    1.3. Antioxidant enzymes and activators: superoxide dismutase (Erisod. Ergotein), sodium selenite;
    1.4. Free radical formation blockers: Allopurinol (Milurit), antihypoxants.

Complex compounds as antioxidants

Despite the wide range of existing drugs regulating free radical reactions within the body there is a constant search for new preparations. A recent trial explores complex compounds as antioxidants [34-37]. Currently complex compounds with nitrous ligands are considered promising antioxidants [38-40]. It is established that metal complexes

with antioxidants have a significant effect on longevity of animals in acute hypoxic states. There is evidence of distinct anti-hypoxic properties of compounds with cupric complexing agent [41-43].

In this work we have obtained new copper complexes with polynitrous ligand 1.5-pentamethyl tetrazole (corazole): copper {II} bis-(1,5-pentamethyl tetrazole) perchlorate $[Cu(PMT)_2]*(ClO_4)_2$; copper {II} tetra-(1,5-pentamethyl tetrazole) chloride $[Cu(PMT)Cl_2$, copper {II} 1,5-pentamethylene tetrazoleascorbate $[Cu(PMT)_{1/2}]*(HAsc)$ and studied their antioxidant properties.

The antioxidant properties of compounds are assessed by their ability to react with active oxygen species (AOS): H_2O_2; OH^-; O_2^-. Traditional antioxidants react with all of these ROS, but the speed of interaction depends mainly on AO structure [44]. Various AO agents react mostly with one of oxygen radicals. Various AO agents react mostly with one specific oxygen radical. The specified complex compounds will probably interact with O_2^- by accepting one electron, which leads to the termination of biomolecule radical oxidation.

We also assessed antioxidant potential of corazole (1,5-pentamethylene tetrazole) considering its significant biological properties: it is known that corazole acts as a free radical scavenger.

To make the picture complete we used several evaluation methods considering that in the standard conditions a number of AOS are generated simultaneously with their further mutual transformation.

Estimation of antioxidant potential using lipid peroxidation model

An antioxidant potential of any agent is routinely assessed by its ability to inhibit lipid peroxidation [45].
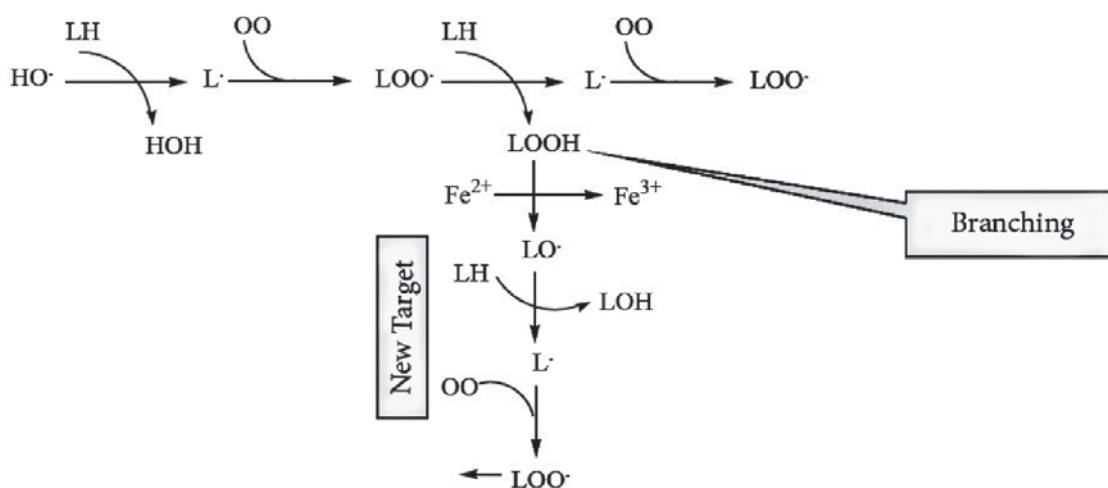

Fig. 1. Schematic diagram of lipid peroxidation

Lipids serve as one of the main substrates for free radical reactions. Among them molecules of polyunsaturated fatty acids (FA) and lipid components of very little density lipoproteins and low density lipoproteins (VLDL and LDL, respectively) stand out. The result of such interaction is complex free radical process referred to as lipid peroxidation (LP) [45-47].

Actually the process of lipid peroxidation is thoroughly studied by means of chemical kinetics and is classified as chain radical reaction [45]. General diagram of this process is given in the picture above.

This process is accompanied by slight chemiluminescence [48]. If the agent reduces chemiluminescence intensity then it is considered to have antioxidant properties.

The more chemiluminescence fades upon administration of an agent, the higher its antioxidant properties are. Studies were carried out in standard systems. A suspension of yolk liposomes in buffer solution or normal saline is a one of these systems. We have chosen a suspension of liposomes in the phosphate buffer (pH=7.4). Cystamine ($NH_2CH_2CH_2SH$) known for its scavenging and chemiluminescence reducing properties was used as a standard [50]. Compounds with thiol fragments in their chemical structure are known as effective antioxidants [51, 52].

In case of chemiluminescence fading upon the administration of ligand (1,5-pentamethyl tetrazole) we can speak of its antioxidant properties. If chemiluminescence suppression upon administration of tested compound achieves the same level of cystamine, such compound can be considered as promising antioxidants. Data for chemiluminescence suppression is summarized in Table 1.

Two criteria were used to assess chemiluminescence suppression:
- Light sum decrease;
- Reduction of peak intensity.

Table 1

Comparison of compounds in respect of their ability to quench chemiluminescence at concentration 5x10^-6 M in the liposome suspension at 20^0C, pH=7.4, c(FeSO_4)=2.4x10^-3 M

No. of compound	Compound	Light Sum, AU	Light Sum Decrease, %	Peak Intensity, AU	Decrease of Peak Intensity, %
	Control	116 ± 3	0	109 ± 3	0
I	$[Cu(PMT)_2](ClO_4)_2$	67 ± 3	42	106 ± 3	3
II	$[Cu(PMT)_4](ClO_4)_2$	108 ± 3	7	144 ± 3	Increase of 32
III	$[Cu(PMT)](Cl)_2$	51 ± 3	56	107 ± 2	2
IV	$[Cu(PMT)_{1/2}](HAsc)_2$	84 ± 2	27	123 ± 2	Increase of 13
V	PMT	84 ± 2	27	130 ± 2	Increase of 19
VI	KHAsc	96 ± 2	17	138 ± 2	Increase of 27
VII	$CuSO_4*5H_2O$	85 ± 2	27	48 ± 2	56

It should be noted that there is no symbasis in the alteration of light sum and peak intensity values. However, light sum is the most often used value for antioxidant activity evaluation. Such choice of parameter for antioxidant activity evaluation is reasonable because the process of free radical formation during chain reaction in the biological system can have an erratic character. A short-term acceleration of free radical reactionsis possible, but overall amount of radicals produced during specified time can be less. Taking light sum as a characteristic of lipid peroxidation intensity and with reference to the results shown in Table 1 all studied compounds **I-VII** are antioxidants. Administration of corazole (PMT) in the internal sphere leads to an increase of antioxidant activity. The number of coordinated corazole molecules has an impact onchemiluminescence suppression for compounds **I** and **II**. Upon administration of two corazole molecules in the internal complex sphere chemiluminescence is reduced by 42%, showing significant antioxidant activity. Administration of two more corazole moleculesresults in almost complete quenching of antioxidant properties, as evidenced by recovery of chemiluminescence up to control level.
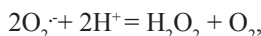
Study of SOD-like activity of complexes

There is a negligible effect of anion on antioxidant activity of the complex (compounds III, I). However, introducing of a reducing agent into external sphere, e.g. ascorbic acid (HAsc) significantly reduces antioxidant properties. We can't clearly determine correlation between antioxidant activity and nature of anion, since the number of corazole molecules coordinated in the internal complex sphere changes depending on the anion. In this regard it is interesting to study SOD-like activity of specified compounds.

This approach was chosen due to strong realization of the following processes in vivo [53, 54]:

$$Me^{n+} + O_2 \rightarrow Me^{(n+1)+} + O_2^{\cdot-} \tag{1}$$
$$Me^{n+} + O_2^{\cdot-} \rightarrow Me^{(n-1)+} + O_2. \tag{2}$$

Catalyzing ability of compounds of such form:

$$2O_2^{\cdot-} + 2H^+ = H_2O_2 + O_2,$$

or any other way to clear superoxide anion radical is called SOD-like activity [55], since this process *in vivo* is catalyzed by specific enzyme called superoxide dismutase (SOD) [56, 57].

Complex compounds can change superoxide anion radical level in biological systems [58]. SOD-like activity was assessed by the ability of compounds to inhibit rate of tetrazolium reduction to formazan in the standard conditions. Equations of test system reactions with paranitrobluetetrazolium, reduced nicotineamide-adenine dinucleotide (MADH_2), phenazinemethasulfate (PMS) are shown below (eq.(3)-(6).Products of inhibition of paranitrobluetetrazolium reduction to formazan induced by synthesized corazole complexes are shown in Table 2.

Standard method of superoxide dismutase activity determination requires presence of EDTA in the reaction medium [59].

Since EDTA is a strong complexing agent able to substitute polynitrogen ligands in the internal complex sphere [60], we decided to study its potential effect on the obtained results [61]. Similar experiments were carried out in the EDTA-free system (Table 3).
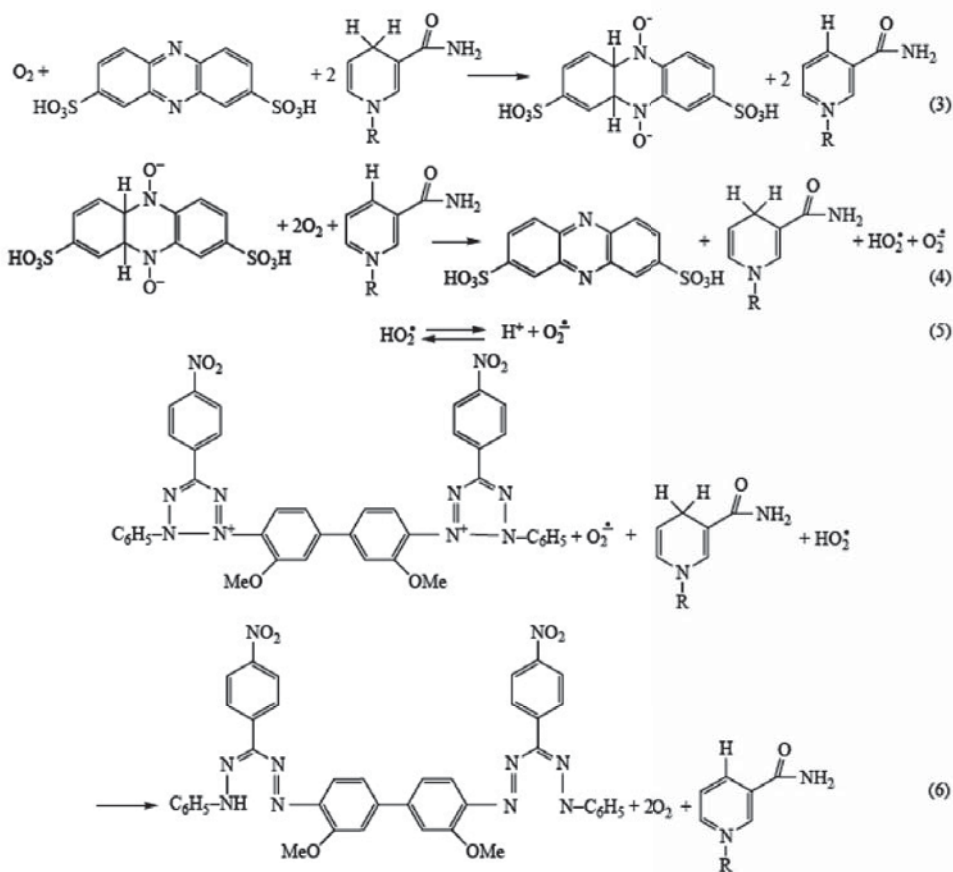
Out of the analysis of Tables 2 and 3 it can be concluded that:

(1) During the study of SOD-like activity it was found that copper sulfate **VII** has a pronounced ability for inhibition of paranitrobluetetrazolium reduction to formazan. The explored coordination compounds **I-IV** show similar activity, while free ligand and salts in the absence of copper cation don't have any antioxidant activity. Removal of O_2^- apparently depends on the presence of copper.

(2) Copper reduction reaction is as follows:

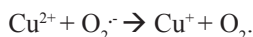$$Cu^{2+} + O_2^- \rightarrow Cu^+ + O_2.$$

Table 2

Results of SOD-like activity assessment of synthesized complexes in the presence of EDTA[a]

No of compound	Compound	Optical density, D	Quenching, %
	Control	0.268±0.02	0
I	[Cu(PMT)$_2$](ClO$_4$)$_2$	0.229±0.02	16±3
II	[Cu(PMT)$_4$](ClO$_4$)$_2$	0.223±0.02	17±3
III	[Cu(PMT)](Cl)$_2$	0.183±0.02	32±3
IV	[Cu(PMT)$_{1/2}$](HAsc)$_2$	0.199±0.02	26±4
V	PMT	0.242±0.01	10±5
VI	KHAsc	0.241±0.01	10±1
VII	CuSO$_4$*5H$_2$O	0.167±0.02	38±4

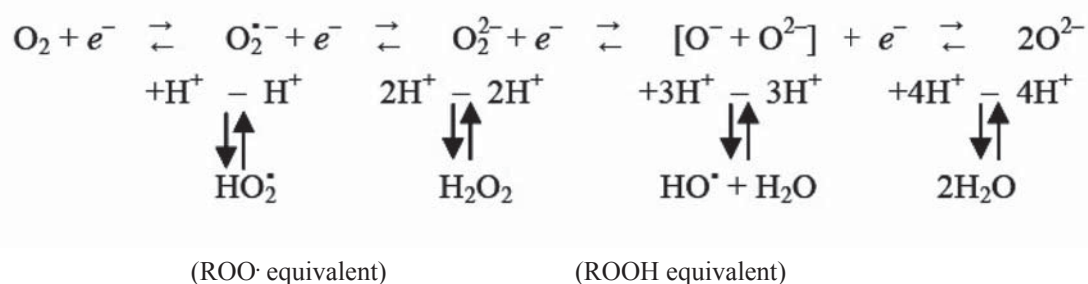[a] EDTA – ethylenediaminetetraacetate

Table 3

Results of SOD-like activity assessment of synthesized complexes in the absence of EDTA[a]

No of compound	Compound	Optical density, D	Quenching, %
	Control	0.180±0.02	0
I	[Cu(PMT)$_2$](ClO$_4$)$_2$	0.109±0.02	39±3
II	[Cu(PMT)$_4$](ClO$_4$)$_2$	0.106±0.02	41±3

III	$[Cu(PMT)](Cl)_2$	0.090±0.02	50±3
IV	$[Cu(PMT)_{1/2}](HAsc)_2$	0.094±0.02	48±5
V	PMT	0.167±0.01	7±1
VI	KHAsc	0.179±0.01	1±4
VII	$CuSO_4*5H_2O$	0.110±0.02	39±2

(3) Introduction of EDTA does not have a significant effect on the ability of copper compounds to interact with superoxide anion radical (O_2^{-}). However, when introduced in the system, it coordinates with copper ion and substitutescorazole from compounds **I** and **II** either in part or in whole, or enters into the internal sphere of complexes **III** and **IV**, increasing coordination number to four. Probably it causes inhibition of SOD-like activity of compounds **I**, **II**, **III** and **IV** in the EDTA medium relative to SOD-like activity of these compounds in the EDTA-free medium.

(4) In the EDTA system an external sphere anion affects the ability of compounds to exhibit SOD-like activity. The most decrease of reactivity was noted when perchlorate ion was used as an anion (compounds I and II).

In two independent tests the same compound $[Cu(PMT)]Cl_2$ demonstrated significant antioxidant activity. It follows that chemiluminescence quenching is probably associated withthe interruption of successive oxygen reduction chain:

$$O_2 + e^- \rightleftarrows O_2^{\cdot -} + e^- \rightleftarrows O_2^{2-} + e^- \rightleftarrows [O^- + O^{2-}] + e^- \rightleftarrows 2O^{2-}$$

$$\begin{array}{cccc} +H^+ - H^+ & 2H^+ - 2H^+ & +3H^+ - 3H^+ & +4H^+ - 4H^+ \\ \downarrow\uparrow & \downarrow\uparrow & \downarrow\uparrow & \downarrow\uparrow \\ HO_2^{\cdot} & H_2O_2 & HO^{\cdot} + H_2O & 2H_2O \end{array}$$

(ROO· equivalent)   (ROOH equivalent)

by means of O_2^- clearance. In this case hydroxyl radical – an active initiating agent of lipid peroxidation – is not produced, resulting in chemiluminescence decrease.
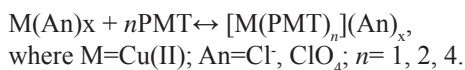
Conclusion

Compound $[Cu(PMT)]Cl_2$ can be characterized as a potential and promising antioxidant by virtue of chemiluminescencequenching and SOD-like activity.

Experimental part
General procedure of synthesis of the complex compounds

The synthesis of complexes is done according to the following reaction:

$M(An)x + nPMT \leftrightarrow [M(PMT)_n](An)_x$,
where M=Cu(II); An=Cl⁻, ClO_4^-; n= 1, 2, 4.

Aqueous solution of salt is stirred at room temperature and spiked with estimated amount of PMT. Reaction mass is then heated to 60^0C and incubated at this temperature during 3 hours. After cooling to 17^0C precipitated residue is filtered, washed with 20 ml of ethyl acetate and recrystallized from ethyl alcohol.

Synthesis of copper (II) bis-(1,5-pentamethylene tetrazole) perchlorate $[Cu(PMT)_2](ClO_4)_2$

Yield 60%.IR spectra, ν, cm⁻¹: 2860 [$ν_s(CH_2)$]; 1925 [$ν_{as} (CH_2)$]; 1470 (scissor CH_2); 1454 (N=N); 1352, 1337 (C=N); 1282, 1268 (N-N); 1100-800 (Tz). NMR spectra ¹H (DMSO0-d_6), δ, ppm: 4.41 [CH_2N^1)]; 2.92 [$CH_2(C^5)$]; 1.81, 1.70, 1.57 (CH_2-CH_2-CH_2). Found, %: C 34.99; H 5.1; N 27.49. $C_{12}H_{32}Cl_3*CoN_{12}O_{12}$. Calculated, %: C 35.4; H 5.95; N 27.5.

Synthesis of copper (II) tetrakis-(1,5-pentamethylene tetrazole) perchlorate $[Cu(PMT)_4](ClO_4)_2$

Yield was 0.61 g of light blue product (60% of theoretical). IR spectra ν, cm⁻¹: 2860 [$ν_s(CH_2)$]; 1925 [$ν_{as} (CH_2)$]; 1470 (scissor CH_2); 1454 (N=N); 1352, 1337 (C=N); 1282, 1268 (N-N); 1100-800 (Tz). NMR spectra

^{1}H (DMSO0-d_6), δ, ppm: 4.41 [CH$_2$N^1)]; 2.92 [CH$_2$(C^5)]; 1.81, 1.70, 1.57 (CH$_2$-CH$_2$-CH$_2$). Found, %: C 34.99; H 5.1; N 27.49. C$_{12}$H$_{32}$Cl$_3$*CoN$_{12}$O$_{12}$. Calculated, %: C 35.4; H 5.95; N 27.5.

If isopropyl alcohol was used as a solvent, the yield of final product was bigger. Yield was 0.81 g of light blue product (80% of theoretical). IR spectra ν, cm^{-1}: 2860 [ν$_s$(CH$_2$)]; 1925 [ν$_{as}$ (CH$_2$)]; 1470 (scissor CH$_2$); 1454 (N=N); 1352, 1337 (C=N); 1282, 1268 (N-N); 1100-800 (Tz). NMR spectra ^{1}H (DMSO0-d_6), δ, ppm: 4.41 [CH$_2$N^1)]; 2.92 [CH$_2$(C^5)]; 1.81, 1.70, 1.57 (CH$_2$-CH$_2$-CH$_2$). Found, %: C 35.2; H 5.2; N 27.5.

Synthesis of copper (II) 1,5-pentamethylene tetrazole[Cu(PMT)]Cl$_2$

Yield was 0.83 g (83% of theoretical). Calculated, %: C 21.21, H 5.31, N 16.49. CuC$_6$H$_{18}$N$_4$O$_4$Cl$_2$. Found, %: C 21.17; H 5.37; N 16.13. IR spectra, cm^{-1}: 3163 [ν$_{as}$(H$_2$O)]; 1629 (δ(H$_2$O)); 2908 [ν$_s$(CH$_2$)]; 1477 [ν$_s$(CH$_2$)]; 2943, 1535, 1421, 968 (Tetr).

PMT is an off-the-shelf product manufactured by ACROS ORGANICS, purity 98%, melting point 58.5^{0}C.

SOD-like activity measurement

We used spectrophotometry to study SOD-like activity. The following chemicals were applied during our study:
(1) Paranitrobluetetrazolium solution: 100 mg of anhydrous substance were dissolved in 50 ml of distilled water on hot water bath, filtered and stored in the dark (it is light sensitive).
(2) Phenasinemethosulfate(FMS): 1 mg was dissolved in 100 ml of distilled water and stored in the dark (it is light sensitive).
(3) Nicotineamide dinucleotide phosphate (NADH$_2$) solution: 6 mg of anhydrous substance were dissolved in 3 ml of tris-EDTA buffer (pH=8.0) and 1.8 ml of distilled water, stored in the dark (it is light sensitive).
(4) Phosphate buffer, pH=7.8.
Reaction mixture has the following composition:
(a) 0.2 ml of EDTA solution (ethylenediaminetetraacetate);
(b) 0.1 ml of gelatin solution;
(c) 0.5 ml of paranitrobluetetrazolium;
(d) 0.1 ml of FMS (phenasinemethosulfate);
(e) 2.0 ml of phosphate solution.

We did a following procedure to study the relationship between complexes and reduction of paranitrobluetetrazolium in formazan. We made two control and test sample concurrently. In the control sample were successively introduced 2.0 ml of buffer; 0.5 ml of tetrazolium solution; 0.1 ml of FMS solution; 0.2 ml of distilled water; 0.2 ml of NADH$_2$. After the introduction of NADH$_2$ we switched on a stop watch and put the samples in thermostat under darkroom conditions. Optical density of the solution was measured in 10 minutes at λ=540 nm in comparison with buffer solution. Test sample was prepared similarly, only that 0.05-0.2 ml of studied complex solution was added instead of distilled water, and diluted to volume with distilled water. Paranitrobluetetrazolium was being reduced to formazan both in control and test solutions. The effect of preparations on the reduction of paranitrobluetetrazolium to formazan was estimated by comparison of optical densities of control and test solutions. Each measurement was repeated 3-5 times.

The study of antioxidant activity by chemiluminescence quenching was carried out in standard conditions in the suspension of yolk liposomes in phosphate buffer solution with pH=7.4. Cystamine was used as a standard.

References
[1]. Ivanov, K.P. Biological Oxidation and Oxygen Supply. SPb.,"Nauka", 1993, 200 pp.
[2]. Gniseppi, J.D.; Fridovich, I. Crit. Rev. Toxicol., 1987, 12, 315–342.
[3]. Shugalei, I.V.; Lvov, S.N.; Baev, V.I.; Tselinskii, I.V.; Lukogorskaya, S.A. Accustamization to Difficult Environment, under the editorship of I.V. Shugalei. SPb.,"Aspor", 1999, p. 6-11.
[4]. Pirker, K.F.; Kay, C.W.M.; Stolze, K.; Tunega, D.; Reichenauer, T.G.; Goodman, B.A. Free Rad. Res.,2009, 43(1), 47–57.
[5]. Rice-Evans, C.A.; Miller, N.J.; Paganoja, G. Free Rad. Biol. Med., 1996, 20, 933–956.
[6]. Bielski, B.H.J.; Cabelli, D.E.; Arudi, R.L.; Ross, A.B.J. Phys. Chem. Ref. Data, 1985, 14, 1041–1100.
[7]. Vinogradov, V.M.; Krivoruchko, B.I. Psychophysiol. and Biol. Pharmacol. 2001, 1, 27-37.
[8]. Vinogradov, V.M.; Uryupov, O.Ju. Pharmacology and Toxicology, 1985, 48(1), 9-20.
[9]. Stozharov, A.N. Medical Ecology. Minsk, "Vyshajashkola", 2007, 368 pp.
[10]. Valko, M.; Phodes, C.J.; Moncol, J.; Izakovich, M.; Mazur, M. Int. J. Bioch. Cell Biol., 2007, 39, 44–84.
[11]. Buttke, T.M.; Sundstroom, P.A. Immunol. Today, 1994, 15(1), 7–10.
[12]. Knight, J.A. Ann. Clin. Lab. Sci., 2000, 30, 145–158.
[13]. Miura, Y.; Utsumi, H.; Hamada, A. Arch. BiochemBiophys., 1993, 300, 148–156.
[14]. Andersen, J.K. Nat. Med., 2004, 10, 18–25.

[15]. Zakirova, A.N. Therapeutical archive, 1996, 9, 37-40.

[16]. Davi, G.; Falco, A.;Patrono, C. Antiox. Redox Signal, 2005, 7, 256–268.

[17]. Cerutti, P.; Ghosh, R.;Oya, Y.; Amstad, P. Environ. Health Perspect, 1994, 102, (10), 123–129.

[18]. Ozben, T. J. Pharm. Sci., 2007, 96, 2181–2196.

[19]. Dizhe, G.P.; Maslova, M.N.; Dizhe, A.A.; Jakaite, V.J. Russian Physiological Journal n.a. Sechenov, 2004, 90(8), 331.

[20]. Inoue, T.; Ide, T.; Yamamoto, M.; Yoshida, M.; Tsutsumi, T.; Andou, M.; Utsumi, H.; Sinagawa, K.Free Rad. Res., 2009, 43(1), 37–46.

[21]. Yalliwell, B. Cardiovascular. Res., 2000, 47, 410–418.

[22]. Das, U. Med. Sci. Monitor, 2002, 8, 79–92.

[23]. Dasuri, K.; Nguyen, A.; Zhang, L.; Fernandez-Kim, O.S.; Bruce-Keller, H.J.; Blalock, B.A.; De Cabo, R.; Keller, J.M. Free Rad. Res., 2009, 43 (1), 28–36.

[24]. Widmer, R.; Ziaja, I. Free Rad. Res., 2005, 40, 1259–1268.

[25]. Sen, S.K. BiochemPharmacol., 1998, 55, (11), 1747–1758.

[26]. Ilyushina, T.M.; Khmelnitskaya, E.M.; Shugalei, I.V.; Sudarikov, A.M.; Lvov. S.N. XI Vyshnyakov Readings. Institutional Science for Education and Industry, under the editorship of V.N. Skvortsov. Boksitogorsk, 2008, p. 288-296.

[27]. Menschikova, E.B.; Lankin, V.Z.; Zenkov, N.K.; Bondar, I.A.; Krugovyh, N.F.; Trufakin, V.A. Oxidative stress. Prooxidants and Antioxidants. Novosibirsk, "Slovo", 2006, 553 pp.

[28]. Zenkov, N.K.; Lankin, V.Z.; Menschikova, E.B. Oxidative Stress. Biochemical and Pathophysiological Aspects. M.,"Maik, Science-Interperiodics", 2001, 343 pp.

[29]. Osipov, A,N.; Azizova, O.A.; Vladimirov, Ju. A. Progress of Biol. Chemistry, 1990, 31, 180-208.

[30]. Havinson, V.H.; Barinov, V.A.; Arutunyan, A.V. Free Radical Oxidation and Ageing.SPb.,"Nauka", 2003, 527 pp.

[31]. Lerso, M.L.; Clarkson, P.M. Toxicol., 2003, 189 (1),41–54.

[32]. Kostyul,V.A.; Potapovich, A.I. Bioradicals and Bioantioxidants. Minsk, BGU, 2004, 179 pp.

[33]. Dyumaev, K.M.; Voronina, T.A.; Smirnov, L.D. Antioxidants in the Prevention and Treatment of CNS Pathologies. M., 1995, 271 pp.

[34]. Yasnetsov, S.A.; Evseev, A.V.; Sosin, D.V. Materials of VI International Research and Practical Conference "Health and Education in XXI Century", M., 2005, RUDN, p. 500.

[35]. Evseev, A.V.; Sosin, D.V.; Evseeva, M.A.; Yasnetsov, S.A.; Orlova, O.V. Smolensky Medical Academy Bulletin, 2005, 3, 114.

[36]. Arbaeva, M.V. M.D. Author's Abstract.SPb, 2008, 39 pp.

[37]. Protasova, N.V.; Zeeva, F.N. Materials of Research and Practical Conference "Physical Culture, Sports and Health", Joshkar-Ola, 2004, p. 78-79.

[38]. Kuhareva, O.V. *M.D.* Author's Abstract. Smolensk, 2004, 25 pp.

[39]. Lebedeva, S.A. Cand. Sc (Biology) Author's Abstract. Smolensk, 2003, 23 pp.

[40]. Katunin, M.P.; Katunina, N.P.; Novikov, V.E.; Parfenov, E.A. VI International Conference "Ecology and Life Safety", Penza, 2006, p. 164-165.

[41]. Yasnetsov, S.A.; Evseev, A.V.; Parfenov, E.A. Physchopharmacol. Biol., Narcol., 2006, 6 (4), 1335-1340.

[42]. Yasnetsov, S.A. Cand. Sc (Biology) Author's Abstract. Smolensk, 2008, 23 pp.

[43]. Zaitsev, V.G.; Ostrovskiy, O.V.; Zarkevskiy V.I. Experimental and Clinical Pharmacology, 2003, 66(4), 66-70.

[44]. Vladimirov, Ju. A.; Archakov, A.I. Lipid Peroxidation in Biological Membranes, M., 1972, "Nauka", 252 pp.

[45]. Girotti, A.W. Free Rad. Biol. Med., 1985, 1, 87–95.

[46]. Baraboi, V.A. Contemporary Biology in Progress. 1991, 111(6), 923-932.

[47]. Izmailov, D.Ju. Cand. Sc (Biology) Author's Abstract. M., 2003, 25 pp.

[48]. Vasilyeva, O.V.; Lyubitskiy, O.V.; Klebanov, G.I.; Vladimirov, Ju. A. Biological Membranes, 1998,15 (2), 177-183.

[49]. Shugalei, I.V.; Sudarikov, A.M.; Voznyakovskiy, A.P.; Tselinsky I.V.; Garabadjiu, A.V.; Ilyushin, M.A. Chemistry of Detonation Nanodiamonds is a Base for Biomedical Products Development.SPb.: LGU n.a. A.S. Pushkin, 2012, 150 pp.

[50]. Powell, S.R.; McCay, P.B. Toxicol. Appl. Pharmacol., 1988, 96, 175–184.

[51]. Baev, V.I.; Lvov, S.N.; Horunjiy, V.V.; Aleksandrovich, Ju. S.; Arutsova, I. Ju.; Verevitin, M.A.; Vinogradov, M.V.; Makarova, T.P.; Oryol, O.V.; Shugalei, I.V. Population Health and Environment,under the editorship of I.V. Shugalei. SPb.,"Aspor", 2001, p. 26-29.

[52]. Shugalei, I.V.; Ivanova, A.A.; Ilyushin, M.A.; Sokolova, V.V.; Sudarikov, A.M. XI Vyshnyakov Readings. Institutional Science for Education and Industry, under the editorship of V.N. Skvortsov. Boksitogorsk, 2008, p. 334-340.

[53]. Shugalei, I.V.; Ivanova, A.A.; Ilyushin, M. A.; Tselinskiy, I.V.; Sokolova, V.V. Journal of General Chemistry, 2009, 79 (1), 132-137.

[54]. Czapski, G.; Goldstein, S. Free Rad. Res Cmmun., 1985, 1 (3), 157–161.

[55]. McCord, M.; Fridovich, I. J. Biol. Chem., 1969, 244, 6049–6055.

[56]. Chistyakov, V.A. Dr.of Biol. Sc. Author's Abstract. Rostov-na-Donu, 2011. 42 pp.

[57]. Czapsk, G.I.; Goldstein, S. Free Rad. Res. Commun., 1985, 1 (3), 157–161.

[58]. Dubinina, E. Ukrainian Biochemical Journal, 1988, 60 (3), 20-25.

[59]. Grootveld, M.; Halliwell, B. Free Rad. Res. Commun., 1985, 1 (4), 243–250.

[60]. Shugalei, I.V.; Ivanova, A.A.; Ilyushin, M.A.; Tselinskiy, I.V.; Sokolova, V.V. Journal of General Chemistry, 2010, 80 (4), 668-674.

Professor Alexander Vasilievich Garabadzhiu is a Moldovan-born Russian chemist. His research interests are biopharmaceuticals, ecological biotechnology, biomedicine, bio-organic chemistry. Currently he is the Head of the Department of Technology of Microbiological synthesis and vice rector for scientific work of the St. Petersburg State Institute of Technology (Technical University).

Author of over 200 scientific works, 3 monographs, 4 books, more than 20 patents. He guidedand mentored numerous PhD students and2 Doctors of Science (habilitations). Acts as a member of the editorial boards of journals "General chemistry" and "Scientific instrumentation" of the Russian Academy of Sciences, the chief editor of the journal "Ecological chemistry".

Professor Alexander VasilievichGarabadzhiu is a laureate of the Prize of the Government of the Russian Federation in 2006 in the field of science and technology. His duties are also related to the membership of the Interdepartmental Council of the Ministry of Education and Science of the Russian Federation on awarding the Prizes of Russian Government in science and technology (section of life sciences).

STUDYING THE RESEARCH RESULTS REGARDING FERTILIZERS USED IN THE REPUBLIC OF MOLDOVA

Tamara Leah[a], Igor Povar[b*], Tudor Lupascu[b], Serafim Andrieş[a], and Vladimir Filipciuc[a]

*[a]Institute of Pedology, Agrochemistry and Soil Protection "Nicolae Dimo", 100 Ialoveni str.,
Chisinau MD-2070, Republic of Moldova*
[b]Institute of Chemistry, Academy of Sciences of Moldova, 3 Academiei str., Chisinau MD-2028, Republic of Moldova
*E-mail: ipovar@yahoo.ca, phone: +(373 22) 73 97 36

Abstract: This paper represents an analysis of the research concerning the use of fertilizers and nutrients balance in the soils of the Republic of Moldova. The nature and effectiveness of fertilizers, their influence on the agrochemical properties of soils, the protection of the environment from the pollution by nutrients in addition to the regulatory normatives of our country developed in order to determine the necessary in fertilizers for obtaining the expected crops have been as well discussed.

Keywords: active substance, fertilizer, humus balance, pollution, soil protection

1. Introduction

According to the Statistical Yearbook of Moldova [1], on January 1, 2012 the total area of lands was 3.38 million ha, including the agricultural lands – 2.50 million ha (73.8%), forest lands – 463.1 thousand ha (13.7%). Of the total area of agricultural lands (farmlands) of 2.50 million ha, the arable lands constitute 1.81 million ha (72.6%), orchards occupy 133,3 thousands ha (5.3%), vineyards – 149.6 thousands ha (6.0%) and pastures – 350.4 thousands ha (14.0%).

The presented data shows that the share of farmlands is inadmissible large (73.8%) and for forest is of 2 - 3 times less than optimal ones. The imbalance between natural and anthropogenic ecosystems causes the amplification of the various forms of land degradation.

2. The nature and effectiveness of fertilizers

The territory of the Republic of Moldova is characterized by a rugged relief. Thus, the predominance of the slopes on 80% of the territory creates favorable conditions for the expansion of erosion processes. The average absolute altitude of the surface of the Republic of Moldova is 147 m, the maximum altitude is 429 m, and the minimum one is 5 m. The soil eroded area, which missed from 20 up to 70% of their initial fertility, is about 36% [2].

The climate of the Republic of Moldova is temperate continental [3], with a mild and short winter (the average temperature of January is $-3 \div -5^0C$) and a warm and long summer (the average temperature of July $20 \div 22^0C$). In relation to the climatic indices, the territory of Moldova was divided into three areas, which are at the same time and agro-pedoclimatic areas: North, Center and South.

The quantity of atmospheric precipitation varies within the limits of 500-630 mm in the North area and 450-500 mm in the South area [4]. The sum of temperatures higher than 10^0C constitutes $2750-2850^0C$ in the North zone and $3100-3350^0C$ in the South zone. The hydrothermal coefficient (K after Ivanov – Vîsoţchi) is 0.7-0.8 in the North zone and 0.5 -6 in the South zone of the country. The frequency of droughts in ten years is: once in the North zone, 2-3 times in the Centre zone and 3-4 times in the South zone.

The soil structure is quite complex. The main soil types and subtypes are: chernozems ("black earth"), occupying 70%; brown and grey soils – 10.2%; alluvial soils – 10.2% and the delluviale soils – 4,0% [5-7]. Soils with a high fertility coupled with the thermal favorable regime allow cultivating a wide range of valuable crops: vines, ethero-oleaginous plants, fruits, nuts, vegetables, sunflower, etc. to yield the production with a high quality taste. The current state of the quality of soil is shown in Table 1. The soils with the note of creditworthiness between 80 and 100 points occupy approximately 27% of the total area of the agricultural lands [7].

Table 1

The state of quality of the soil in the Republic of Moldova

The class of the note of creditworthiness	Note of creditworthiness, points	% from the area of agricultural lands	Area, thousands ha	Harvest of winter wheat, t/ha
I	81-100	27	689	3.2-4.0
II	71-80	21	539	2.8-3.2
III	61-70	15	382	2.4-2.8
IV	51-60	15	382	2.0-2.4

V	41-50	9	303	1.6-2.0
VI	21-40	6	153	0.8-1.6
VII	☐20	7	178	-
Average for the Republic of Moldova	**65**	**100**	**2556**	**2.6**

On these soils with a high productivity, presented as a general rule by the typical chernozems and landfill leachate (standard soils) containing organic matter of 3.6-4.5%, can be achieved at the expense of actual fertility 3.2-4.0 t/ha for the autumn wheat. The class II and III of the lands contained within the note of creditworthiness of 60-80 points is 36% or 918 thousand ha. The productivity of these soils is also quite high and constitutes 2.4-3.2 t/ha for the autumn wheat. These two classes of soils of the note of creditworthiness are often affected by the processes of humification, their diminuation in nutrient contents, destructuration and compactisation, biologycal degradation and the partial surface erosion. The soils of classes IV, V and VI of the note of creditworthiness occupy 30% from the total surface and have a note of creditworthiness of 20-60 points and a low productivity of 0.8-2.4 t/ha of the autumn wheat respectively. These soils are weak, moderately and severely degraded, especially by the erosion processes.

At present, according to the Land Cadastre of the Republic of Moldova on 01.01.2011 [2] the note of creditworthiness is 63 points. The efficient fertility of the soil assures the formation of 2.5 t/ha of winter wheat.

In the conditions of the Republic of Moldova, the soil moisture (rainfall) is one of the factors determining the formation of high and stable yields. The calculations carried out by the Institute of Pedology, Agrochemistry and Soil Protection "Nicolae Dimo" [14] shown that in a multiannual cycle the average potential harvest of the winter wheat formed from precipitations constitutes 4.3 t/ha. The difference in yield, obtained in function of the amount of rainfall and the note of creditworthiness is great and constitutes (4.3-2.5 t) 1.8 t/ha. In the conditions of insufficiency of nutritive elements, the unsatisfactory state of physical and biological characteristics of the soil, plants consume unproductively the moisture reserves accumulated in the soil fot the organic compound synthesis and as a result, harvests are small and of low quality. Those were confirmed by the research carried out in field experiences of long periods of time. It was established that for the variants fertilized optimally, the crop plants consumed 20-25% less water compared to the non-fertilized version [8]. Krupenikov I. [9] by analyzing the main forms of soil degradation (total for the 11 forms) arranged under number 1 the humic degradation and under number 2 – the agrochemical degradation agrochimică (the reduction of nutritive elements in soil). These two forms of degradation occur continuously and for all the farmlands.

The results of the multiannual field experiences have shown that in the conditions of the Republic of Moldova the use of fertilizers in the optimal doses provide a harvest enhance of 66% for sugar beet, 48% for the winter wheat and 35% for the cultivation of maize for grain and sunflower (Table 2). The productivity of the plants for the fertilized variants was 4.3 t/ha of the   winter wheat, 5.4 t/ha maize for grains, 2.0 t/ha of sunflower seeds and 34.8 t/ha of sugar beets [8].

Table 2

The effectiveness of fertilizers in the Republic of Moldova [8]

Crop plants	Harvest, t/ha		The increase in harvest	
	non-fertilized soil	fertilized soil	t/ha	%
Winter wheat	2.9	4.3	1.4	48
Maize for grains	4.0	5.4	1.4	35
Sunflower	1.5	2.0	0.5	35
Sugar beets	21.0	34.8	13.8	66

In the Republic of Moldova the regulatory normatives were developed in order to determine the necessary in fertilizers for obtaining the expected crops [10]. It was established that the use of the optimal doses of fertilizers gave a raise in the harvest of 1.2 t/ha for the winter wheat, 1.4 t/ha of maize for grains, 13.8 t/ha of sugar beets and 0.5 t/ha for sunflower seeds. From the presented data that soil fertilization and mineral nutrition of plant optimization of culture is an important factor for obtaining high crops.

3. The use of fertilizers and nutrients balance in the soil

Moldovan soils are characterized with a high fertility [6, 7, 11-13, 15, 16]. The research carried out in the 1950-1960 yrs. demonstrated that the chernozems of Moldova contained in that period 340 t/ha of humus in the layer of 100 cm. In the composition of organic matter was contained 20 t/ha of nitrogen and 5 t/ha of phosphorus. The total quantity of P_2O_5 the plowed layer was approximatively 160-180 mg and to the depth of 90-100 cm – up to 100 mg in 100 g of soil. The reserve of the total phosphorus in the layer of 1 m was 17 t/ha. Moldovan soils are rich in minerals containing potassium [17]. The total content of these soils is 10-15%. The reserve of the total potassium in the layer of 1 m of chernozems constitutes 170-290 t/ha.

In the period 1950-1960 the plant crop harvests were modest and constituted: 1.6 t/ha of winter wheat, 2.8 t/ha maize for grains, 1.5 t/ha of sunflower seeds and 11.9 t/ha of sugar beets (Table 3).

Table 3

The dynamics of the harvest of the main crops in the Republic of Moldova, t/ha

Years	Winter wheat	Maize for grains	Sunflower	Sugar beet
1963-1965	1.6	2.8	1.5	19.2
1966-1970	2.0	3.4	1.6	25.6
1971-1975	3.4	3.6	1.8	27.9
1976-1980	3.5	3.6	1.7	27.8
1981-1985	3.4	2.7	1.8	28.7
1986-1990	3.8	3.9	2.0	24.8
1991-1995	3.5	2.7	1.4	24.8
1996-2000	2.6	3.0	1.1	19.0
2001-2005	2.2	2.8	1.2	22.7
2006-2010	2.2	2.7	1.3	27.1

Obtaining the high crops was limited by two natural factors: 1) the insufficiency of moisture and 2) the low level of nutrients in the soil. The possible harvests calculated according to the degree of humidity were by 60-70% higher than those obtained of that time (Table 4).

Table 4

Field crop harvests forecast in function of the degree of water supply, t/ha [8]

Crop plants	Water consumption for obtaining 1 tonne of production, t	Soil humidity reserves (by zones), t / ha		
		North	Center	South
		4010	3620	2920
		Harvest, t/ha		
Winter wheat	820	4.9	4.4	3.6
Maize for grains	640	6.3	5.6	4.7
Sunflower	1330	3.0	2.7	2.2

These data allowed presuming that of limitative factors the first place belonged to the insufficiency of nutrients in the soil.

Generally, the effectiveness of fertilizers [E] is expressed by the equation:

$$E = R\ w.s. - R\ n., \quad \text{where}$$

$R\ w.s.$ – the harvest quantity is limited by the extent of water supply;
$R\ n.$ – the harvest quantity is determined by the contents of nutrients in the soil.

By the 1965 year, the input of fertilisers in the agriculture of Moldova was insignificant. According to the statistic data, in the period of 1961-1965 yrs. on the 1 ha of arable land and perennial plantations 6.2 kg/ha of N, 8.7 kg/ha of P_2O_5 and 3 kg/ha of K_2O that were introduced with mineral fertilizers. The average dose of organic fertilizers was 1.3 t/ha (Table 5).

Table 5

Dynamics of the use of mineral and organic fertilizers in the agriculture of Moldova

Years	Mineral fertilizers						Organic fertilizers, t/ha	Mineral and organic fertilizers (in active substances) t/ha arable land and perenian plantations		
	thousand tons (in active substances)			kg/ha (in active substances) arable land and perennial plantations						
	N	P_2O_5	K_2O	N	P_2O_5	K_2O		N	P_2O_5	K_2O
1961-1965	13.0	19.0	8.0	6.2	8.7	3.6	1.3	12.7	12.0	11.4
1966-1970	33.8	34.2	15.4	15.7	15.8	7.2	1.4	22.7	19.3	15.6
1971-1975	75.6	56.0	34.2	35.4	26.2	15.9	2.9	49.9	33.4	33.4
1976-1980	99.6	84.2	59.8	46.6	39.4	27.9	4.1	66.1	50.4	52.5
1981-1985	148.2	102.4	111.4	70.4	48.6	53.0	6.6	101.4	65.1	92.6

1986-1990	76.0	61.0	50.0	36.5	29.3	24.0	3.0	52.0	37.0	42.0
1991-1995	38.0	28.20	13.3	18.8	13.1	6.1	1.8	28.0	17.5	17.2
1996-2000	8.0	0.3	0.1	3.6	0.14	0.04	0.06	4.2	0.4	0.9
2001-2005	13.6	0.6	0.2	4.6	0.3	0.1	0.02	6.5	0.32	0.3
2006-2010	16.1	1.9	1.0	17.5	2.1	0.9	0.02	18.5	2.7	2.0

The export of nutrients from the soil by crops was significant. As a result, in the agriculture of Moldova was formed a deeply deficient of nutrients. During the considered period the deficit of nutrients per hectare was annualy: 59 kg of N, 14 kg of P_2O_5 and 80 kg of K_2O (Table 6).

Table 6

Balance of nitrogen, phosphorus and potassium in the Moldovan soils, kg/ha [8, 20]

Years	N	P_2O_5	K_2O	Sum of NPK
1913	-22	-13	-52	-92
1940	-26	-15	-62	-99
1945	-15	-15	-52	-82
1950	-27	-13	-68	-108
1951-1955	-27	-12	-62	-102
1956-1960	-40	-14	-82	-136
1961-1965	-59	-14	-80	-132
1966-1970	-36	-9	-84	-130
1971-1975	-22	-1	-79	-103
1976-1980	-15	+11	-66	-69
1981-1985	+9	+22	-33	-4
1986-1990	-15	+25	-49	-8
1991-1995	-18	-11	-80	-113
1996-2000	-30	-21	-83	-134
2001-2005	-24	-23	-81	-128
2005-2010	-26	-22	-84	-132

The research carried out in the 1955-1970 years showed that fertilizers were effective for all the cultures and for all the soils [13,18]. That conditioned the accelerate rhythms of the agriculture chimization. The volume of mineral fertilizers applied to the arable lands and the perennial plantations grew rapidly. In 1970 the agrarian sector of the Republic of Moldova received fertilizers by 2.5 times more in comparison with the 1963 year. The dose of used fertilizers accounted for 62.7 kg/ha NPK. As a result, the balance of nutrients was rapidly improved.

In the period of 1981-1988 yrs for the first time in the history of Moldova's agriculture the nutrient balance became positive.

During this period per a hectare of the arable lands and plantations of fruits, with mineral and organic fertilizers, 100 kg N, 66 kg P_2O_5 and 87 kg K_2O were applied. The average dose of manure applied in the agriculture was 6.0-6.6 t/ha. As a result the productivity of crop plants increased significantly. The average harvest of the winter wheat amounted to 3.8 t/ha, of the maize for grains was 2.4 t/ha and for sunflower was 2.0 t/ha. During the period of chimization, which lasted for 25 years (1965-1990) there were applied 1200 kg of nitrogen, 960 kg of phosphorus and 860 kg of potassium. The accumulation of nutrients in the soil was relatively small in comparison with their export throughout the entire history of agriculture. Just for 100 years on each arable land with the harvest there were exported 2300 kg of nitrogen, 1000 kg of phosphorus and 5000 kg of potassium [20].

After the 1998 year, the volume of fertilizers increased substantially, reaching the minimum level in the period of 1996-2005 yrs. During that period, there were applied about 4-6 kg of nitrogen, 0.3-0.4 kg of phosphorus and 0.3-0.9 kg of potassium per hectare. The nutritional balance again became deeply negative (Table 4), of minus 30 kg of nitrogen, 21 kg of phosphorus and 83 kg of potassium. As a result, the productivity of crop plants dropped to the level of the 60 years of the last century (Table 3).

In the recent years (2006-2012) the volume of mineral fertilizers has increased in comparison with the 1996-2006, but it has not been touched even the 1961-1965 years. Currently the fertilizers with nitrogen are preponderently applied. Practically, the fertilizers with phosphorus are not applied - the first necessary element in soils. In the last 10-12 years the dose of the applied manure in Moldova's agriculture constitutes 0.02 t/ha, the optimal rule being about 10 t/ha [13-15,18].

In the recent years (2005-2013) the average norm of fertilizers applied in Moldova's agriculture amounted to 25 kg/ha. Of fhe total dose of fertilizers about 90-95% is nitrogen one.

The largest quantities of fertilizers are applied to the production of potatoes, sugar beets and vegetable crops – 193, 70 and 52 kg/ha, respectively. The insufficient quantities of NPK fertilizers is applied to the cultivation of winter wheat (27 kg), maize and sunflower (7-12 kg/ha) (Table 7).

Table 7

Doses of mineral fertilizers applied to the crop plant fertilization, kg/ha

Crop plants	Dose of NPK, kg/ha	Harvest, t/ha
Potatoes	193	9.5
Sugar beets	70	27.0
Vegetables	52	9.0
Winter wheat	27	2.2
Maize for grains	12	2.7
Sunflower	7	1.2

The soil nutrient balance is negative (Table 6), the chemical degradation of the soil takes place and as a result the harvests are small and of low quality.

4. The influence of fertilizers on the agrochemical properties of soils

Humus is one of the main indices of the soil fertility. This fundamental component of soils determines to a great extent its chemical, physical and biological properties. The preservation of crops and biota with the mineral nutrition depends directly on the organic matter in the soil. It has been experimentally determined that increasing the content of humus with 1% gives 0.5 t/ha of the winter wheat [8].

Since the 1953 year the research institutions and universities have been carried out the agrochemical monitoring. At the same time the balance of humus in the soils has been calculated. It was established that before the period of the intensive chimization (1965-1990) the humus balance was negative (Table 8).

Table 8

The evolution of the humus balance in arable soils, kg/ha [19]

Years	Organic fertilizers applied, t/ha	Balance of humus	
		without erosion losses	with erosion losses
1971-1975	2.9	500	-900
1976-1980	3.9	400	-800
1981-1985	6.0	100	-500
1986-1990	5.6	100	-500
1991-1995	2.6	400	-800
1996-2000	0.1	700	-1100
2001-2005	0.1	700	-1100
2006-2010	0.01	700	-1100

Annually 500 kg/ha of organic matter is mineralised [18,19]. The systematic use of fertilizers, including 5-7 t/ha of manure, the cultivation of perennial grasses on about 10% of the arable land (180-210 thousand ha) contributed to the formation during the 1975-1990 years to a slightly deficient balance of humus in soils of about minus 100 kg/ha.

Over the past 10-15 years the insufficient quantities of manure (0.01-0.6 t/ha) has been incorporated into the soil. The balance of organic matter is negative, minus 700 kg/ha, while with the losses by erosion is of -1100 kg/ha.

The nitrification capacity According to the Agrochemical Research Service [24] approximately 39% of farmlands are characterized with a low content of organic matter (less than 2%), 40% with moderate (2-4% of humus) and only 20% with the humus content higher than 3.0% (Table 9).

Agrochemical characteristics of the lands of Moldova [24]

Years of the agrochemical mapping	Contents		
	low	moderate	high
Humus			
1986-1990	41	39	20
Nitrification capacity			
1986-1990	77	17	6
Mobile phosphorus			
1971-1975	68	21	11
1980-1985	50	27	23
1986-1990	31	34	35
Exchangeable potassium			
1971-1975	0	13	87
1986-1990	0	5	95

As a result, about 80% of soils are characterised by a very low and low nitrification capacity. On agricultural lands with the humus content of less than 2% by the nitrification processes in the soil only 50-60 kg/ha of nitrogen is accumulated and the soils with 3.0 - 4.5% of organic matter – up to 75 - 110 kg/ha of the mineral nitrogen. These quantities of the mineral nitrogen are sufficient for the formation of 1.7 - 2.0 t/ha and 2.5 - 3.7 t/ha respectively of the winter wheat [8, 23].

At present the content of organic matter in the soils of Moldova is about 3.0%. As a result of the mineralization of organic matter, the soils produce annually about 70 kg/ha of nitrogen. This quantity of nitrogen is sufficient for the formation of 2.4 t/ha of the winter wheat.

Phosphorus has a special role in the metabolism of plants and in the formation of the elevated harvest. Chernozems as well as the grey soils are characterized by the low content of phosphorus in soil [8, 13]. The intensity of phosphate regime has been confirmed by the research results carried out by the State Agrochemical Service [20]. In the 1971-1975 years the surface of soils with low phosphorus content was quite large and constituted approximately 68% [8].

In the period of 1965-1990 yrs about 960 kg/ha of phosphorus was incorporated into the soils [22]. This agrochemical measure influences beneficially on the phosphorus regime of soils. To the 1990 year the surface of soils with low phosphorus content decreased by 2.0 times, while that with a high phosphorus content increased by 3.0 times. On average per republic the mobile phosphorus content in the soil increased by 2.0 times, as a result the productivity of crop plants has been increased.

In the recent years (2000-2012) in Moldova's agriculture insufficient quantities of P_2O_5 (up to 1 kg/ha) were applied. The export of phosphorus with the harvest is high and constitutes annually about 25-30 kg/ha. The balance of this nutrient element is negative. Currently the postaction with phosphorus fertilizers is practically exhausted. With the natural low background of the mobile phosphorus in soil it is possible to get about 2.5 t/ha of the winter wheat. This level of harvest, usually, has been obtained within the country in recent years.

Potassium The crops for the high harvest formation extract from the soil significant quantities of potassium - 100-200 kg/ha. The soils of Moldova are rich in the total potassium. But the main reserve of available potassium for the plants constitutes the exchangeable form. It was found experimentally that the potassium content for 15-20 mg/100 g of soil is sufficient for the optimal growth and development of plants [13, 25]. According to data [24], only 13% of the farmlands are characterised with a moderate content (10-20 mg) of exchangeable potassium; 87-95% of the total area – with a high content.

The systematic use of fertilizers in the 1965-2000 years provided an equilibrated balance of potassium in soil. Therefore, the quantity of exchangeable potassium increased average by 2 mg/100 g of soil [24]. Currently, the potassic and organic fertilizers are applied in very small doses. The balance of the K_2O in soil is negative.

The soils of Moldova are rich in accessible potassium to plants, but these reserves in a quite long period (150-200 years) may be exhausted. Hence, it is necessary to maintain an optimal regime of potassium already present in the soil by applying fertilizers.

5. The requirement of mineral fertilizers in the Republic of Moldova

In the conditions of Moldova the natural factors which limit the production of high harvests are the insufficiency of nutrients in the soils as well the moisture deficit. In order to achieve the growth rate in harvest of 40-50% it is necessary to compensate the deficit of nutrients by the use of fertilizers and rational utilization of the soil moisture [8,18,19,22,25].

In determining the amount in fertilizers for agriculture of Moldova, were used the decisions of the Government of

the Republic of Moldova, of the Ministry of Agriculture and Food Industry on the development of the various branches of agriculture by the year 2020, the statistical data for the recent years, the recommendations and norms concerning the application of fertilizers, typical crop rotations models of pedoclimatic zones of the Republic of Moldova have been used. The optimal level of fertilization provides the increase of the fertility of soils, obtaining high crops and a maximum profit from a unit of agricultural land, the protection of the environment from the pollution by nutrients [18-22].

The optimal application of fertilisers is required for a level of the modern agriculture soil no-till with respecting zonal crop rotations, the soil no-till, the integrated protection of plants, extension of irrigation, the development of the livestock sector, the implementation of intensive technologies of plant cultivation. This system is based on the combined application of organic and mineral fertilizers in couple with fuller use of the biologic nitrogen.

Table 10

The optimum doses of mineral fertilizers for the fertilization of the main crop plants, kg/ha of the active substance

Crop plants	Recommended dose			Remark
	N	P_2O_5	K_2O	
Winter wheat	80	60	40	annual
Winter barley	34	60	0	*
Spring barley	34	60	0	*
Porumb pentru boabe	60	50	0	*
Maize for grains	30	20	0	*
Sugar beet	105	80	40	*
Sunflower	45	40	40	*
Tobacco	35	40	40	*
Potatoes	60	60	60	*
Vegetables	90	60	60	*
Maize for silage	40	40	0	*
Fruitful vineyards	60	60	60	once in 3 years
Fruitful orchards	60	60	60	once in 3 years
New vineyards (founding)	-	400	400	to the founding
New orchards (founding)	-	400	400	to the founding

The norms of fertilizer vary depending on the crop from 50 kg/ha NPK for peas up to 225 kg/ha NPK for sugar beets. According to the Programme [18] the average annual dose of fertilizers on the crop rotation of the agro-pedoclimatic zones constitutes:

➢ North – 5 t/ha manure and $N_{61}P_{50}K_{20}$;
➢ Center – 4 t/ha manure and $N_{54}P_{45}K_{18}$;
➢ South – 4 t/ha manure and $N_{47}P_{43}K_{18}$.

The implementation of the crop rotation with the optimum share of leguminous will allow the accumulation in soil of 30-35 kg/ha per year by the biological nitrogen fixation. The systematic application of fertilizers and organic minerals in doses of P_{55-60} will allow forming into a multiannual cycle a positive balance and an optimal level of phosphorus in the soil for obtaining high crops. The average dosage of K_{19} fertilizers will be insufficient for the stabilization of potassium in soil. The compensation of the potassium loss will be covered by the local fertilizers and the application of the secondary production as organic fertilizer. The nitrogen deficit will be compensated by the biologic nitrogen (30-35 kg/ha), manure (25-30 kg/ha) and mineral fertilizers (50-60 kg/ha). The share of nitrogen from mineral fertilizers will constitute about 50% of the total content.

The optimal demand for nitrogenous fertilizers for the crop rotation will be 82.3 thousand t of the active substance or N_{55} on average per 1 ha (Table 11).

Table 11

The annual mineral fertilizer requirements for the optimal crop fertilization, thousand tons of the active substance

Branch, crop plants	Nitrogen, N	Phosphorus, P_2O_5	Potassium, K_2O
Crop rotation	82.3	69.9	28.4
Vegetables and potatoes	6.8	9.0	6.8
Fruitful vineyards	1.5	1.5	1.5
Fruitful orchards	2.0	2.0	2.0

New vineyards	0	2.1	2.1
New orchards	0	1.0	1.0
In addition to irrigated lands	6.3	4.6	3.1
Other crop plants	1.0	1.0	1.0
Total for the Republic of Moldova	**99.9**	**91.1**	**45.9**

For potatoes and vegetable crops will be needed 6.8 thousand tons of nitrogen with the average dose for 1 ha - N_{60}. For the fruitful orchard fertilization will be needed 2.0 thousand tonnes of nitrogen, for the fruitful vineyards 1.5 thousand t. The phosphatic fertilizer requirements will constitute 69.9 thousands t for the field crops, 9.0 thousand tonnes for vegetables and potatoes, 1.5 thousand t – for the forfruitful vineyards, 1.2 thousand t for the fruitful orchards. The annual requirement of potassic fertilizers will be 28.3 thousand t for field crops, 6.8 thousand t for vegetables and potatoes and 3.1 thousand tonssuplimentary for the irrigated lands.

The total annual demand of fertilizers for the agriculture of the Republic of Moldova after 2020 will constitute 236.7 thousand tons of the active substance, including 99.9 t of nitrogen, 91.0 thousand t of phosphorus and 45.8 thousand t of potassium. This level of fertilization was reached in the 1976-1985 years by applying annually 243.6-362.0 thousand t (Tabel 5).

The use of the optimal fertilization system coupled with other technological links of cultivation of the crop plants will allow to get 4.0-4.2 t of the winter wheat, 3.6 t of grain maize and will form an equilibrated nutrient balance in Moldova's agriculture.

6. Priority measures for conservation and enhancement of soil's effective fertility

For the conservation and enhancement of soil fertility, the reasearchers of the Institute of Pedology, Agrochemistry and Soil Protection "Nicolae Dimo" developed a complex of fitotechnical, agrotechnical and agrochemical measures, which include [7,8,18,22,25,26]:

➢ optimization of crop rotation and their implementation in each pedoclimatic zone;
➢ increasing the quota of perennial grasses (alfalfa, sainfoin) in field cropping up to 10-12%;
➢ increasing the quota of annual legume crops (peas, beans, soya) in field cropping up to 10-12%. These changes in the structure of the crop rotation will allow to accumulate annually about 40-50 thousand tonnes of nitrogen or 30-35 kg/ha;
➢ annual incorporation into soil of 5-6 t/ha of manure; a total of 9-10 million tons;
➢ application of 100 thousand t of nitrogen and 90 thousand t of phosphorus; a total of 190 thousand tons;
➢ minimizing in the admissible limits of about 5 t/ha of the soil erosion.

Over the past few years the State Programs have been developed in order to remedy the chemical, physical and biological characteristics of the soil as well as for the protection of soil and water by the pollution with nutrients and substances of plant protection, including:

➢ The complex Program of valorification of the degraded lands and improvement of the soil fertility. Part I. Soil improvement approved by the Decision No. 636 of the Government of the Republic of Moldova from 26 May 2003;
➢ The complex Program of valorification of the degraded lands and improvement of the soil fertility. Part II. The improvement of the soil fertility approved by the Decision No. 841 of the Government of the Republic of Moldova from 26 July 2003;
➢ The Program for the conservation and enhancement of the soil fertility for the 2011-2020 years, approved by the Decision No. 626 of the Government of the Republic of Moldova from 20 August 2011.

These documents determine goals, actions (measures), performance indices, the terms of implementation and those responsible for implementation.

8. References

[1]. Statistical Yearbook of the Republic of Moldova; Tipografia Centrala: Chişinău, 2012; pp. 210-216 (Rom.).
[2]. Land Cadastre of the Republic of Moldova; Tipografia Centrala: Chişinău, 2009; 985 p. (Rom.).
[3]. Lase, G. A. Climate of the Moldavian Soviet Socialist Republic; Leningrad, 1978; 378 p. (Rus.).
[4]. Agroclimatic resources Moldavian CCP; Gidrometeoizdat: Leningrad, 1982; 198 p. (Rus.).
[5]. Krupenikov, I. A.; Podymov, B. P. Classification and the systematic list of the soil of Moldova; Ştiinţa: Chisinau, 1987; 157 p. (Rus.).

[6].   The soil of Moldova; Ştiinţa: Chisinau, 1984; 352 p. (Rus.).
[7].   Complex Program of valorification of degraded lands and improvement of the soil fertility. Part I. Improvement of soils; Pontos: Chişinău, 2004; 212 p. (Rom.).
[8].   Andrieş, S. Optimization of soil nutritive regimes and the productivity of crop plants; Pontos: Chişinău, 2007; 374 p. (Rom.).
[9].   Krupenikov, I. A. Chernozems. Occurrence, perfection, tragedy of degradation, ways of protection and revival; Pontos: Chişinău, 2008; 285 p. (Rus.).
[10].   Normatives on the use of mineral and organic fertilizers in the agriculture of the Moldavian Soviet Socialist Republic; Chişinău, 1987; 37 p. (Rus.).
[11].   Krupenikov, I. A. Chernozems of Moldova; Cartea Moldovenească: Chişinău, 1967; 427 p. (Rus.).
[12].   Krupenikov, I. A. Soil cover of Moldova. The past, present, management, forecast. Ştiinţa: Chisinau, 1992; 263 p. (Rus.).
[13].   The soils of Moldova; V.3. Ştiinţa: Chisinau, 1986; 336 p. (Rus.).
[14].   Rusu, V.; Postolachi, L.; Povar, I.; Alder. A. C.; Lupascu, T. Environ. Sci. Pollut. Res., 2012, 19, 3126-3131.
[15].   Lupascu, T. Buletinul ASM Seria ŞBCA 2004, 1, 170-175 (Rom.).
[16].   Lupascu, T.; Teodorescu, M. NATO Science Series. Volume "Methods and Techniques for eaning –up contaminated Sites", ESP 982358, 2008, 71-79.
[17].   Nastas, R.; Rusu, V.; Giurginca, M.; Meghea, A.; Lupascu, T. Revista de Chimie (Bucharest) 2008, 59 (2), 159-164 (Rom).
[18].   The complex Program of valorification of the degraded lands and improvement of the soil fertility. Part II. The improvement of the soil fertility; Pontos: Chişinău, 2004; 212 p. (Rom.).
[19].   Monitoring soil quality. (Bank data, forecasts, conclusions, recommendations); Pontos: Chişinău, 2010; 475 p. (Rom.).
[20].   Ursu, A. Soils of Moldova; Ştiinţa: Chişinău, 2011; 321 p. (Rom.).
[21].   Alexeev, V.E. Mineralogy of the soil formation in forest-steppe and steppe zones of Moldova; Chişinău, 1999; 87 p. (Rus.).
[22].   Bulletin of ecopedologic monitoring (Agrochemistry); The VII Edition, Pontos: Chişinău, 2000; 67 p. (Rom.).
[23].   Burlacu, I. Agrochemical preservation of the agriculture in the Republic of Moldova; Pontos: Chişinău, 2000; 228 p. (Rom.).
[24].   Zagorcea, C. The evolution of the circuit and balance the biofile elements in agrofitochenozes from the Republic of Moldova over the last century. Land and water resources. Superior valorification and their protection; V.2. Pontos: Chişinău, 1989; pp. 121-125. (Rom.).
[25].   Andrieş, S.; Lungu, V.; Donos, A. et al. Recommendations for the application of fertilizers on different types and subtypes of soil for the field crops; Pontos: Chişinău, 2012; 68 p. (Rom.).
[26].   Programme for the conservation and improvement of soil fertility for the years 2011-2020, approved by decision of the Government of the Republic of Moldova No. 626 from 20 August 2011. Published on 26.08.2011 in the Official Gazette, pp. 139-145, Article No: 696. (Rom.).

CHEMICAL COMPOSITION FROM THE DNIESTER RIVER TRIBUTARIES

Viorica Gladchi[a], Gheorghe Duca[b], Nelli Goreaceva[a], Elena Bunduchi[a], Angela Lis[a]

[a] Faculty of Chemistry and Chemical Technology,State University of Moldova, 60 A. Mateevici str., Chisinau, the Republic of Moldova
[b] Academy of Sciences of Moldova, Stefan cel Mare 1, Chisinau, the Republic of Moldova
*E-mail: vgladchi@yahoo.com; phone number: (+37322)577537

Abstract: This article presents the results obtained in the framework of the project 09.832.08.06A The role of the tributaries on formation of the Dniester river water and the study of the waters quality of sources/fountains in the catchment area of the Dniester river as sources of water supply and for irrigation in the State Program, Scientific Researches and of the management of waters quality.

Keywords: tributary, chemical composition, flow rate, mineralization, redox state

1. Introduction

This paper presents preliminary results of study on the chemical composition and impact of the right tributaries on the Dniester river waters during 2009-2010 years.

It was determined that waters of the tributaries is characterized by high mineralization (Σ_i = 892-1039 mg/dm^3), with increasing trend in the share of ions Cl$^-$, SO$_4$$^{2-}$, (Na$^+$+K$^+$) content with increasing of the mineralization.Greater water hardness (D$_{tot}$ = 8,3-11,9mmol/dm^3) is mainly conditioned by magnesium salts, with exception of the Bic river waters, where calcium and magnesium intake was approximately equal. Stability of the tributaries waters to acidulation is effectively ensured by the carbonate buffer system.The oxygen saturation of rivers waters has varied significantly: with minimum 45,4 – 69,6% and maximum 128-168%.In the Bik river waters, constant has attested oxygen deficit and even his absence with degree of oxidation (D.O.) = 0,0-0,5%.The report of chemical oxygen demandwithmanganese III reagent (COD-Mn) / chemical oxygen demand with dichromatereagent (COD-Cr) denotes that humic substances are approximately 18-24% of the total organic substances from the tributaries waters.Comparing the indicator values COD-Cr, it was established that the largest quantities of organic substances it contains in the waters of the Ichel river(43.5 mgO/dm^3) and Bic river (40.2 mgO/dm^3).In the waters of others two tributaries, the quantities are smaller: river Botna - 29.0 mgO/dm^3, river Raut - 24.2 mgO/dm^3.The biogenic elements were permanently present in high concentrations in all tributaries waters, sometimes exceeding the MAC.Average total iron content in the waters was 135.27 - 313.7 µg/dm^3 and the total copper– of 7.16 - 11.2 µg/dm^3.The highest level of peroxidase substrates was attested in river Ichel waters (1.53 µg/dm^3), followed by those of the Bic river (1.30 µg/dm^3), the Botna river (0.64 µg/dm^3), the Raut river (0.11 µg/dm^3).The values of the indicator Sk$_i$·[S$_i$] ≥ 3·10^{-5}s^{-1} denotes that tributaries waters contained the importante quantities of substances that interrupt the chain of the radical self-purification.

It was demosntrate that tributaries waters have a different impact on the main water artery of the country.

For the Republic of Moldova the study of the chemical formation composition processes of the Dniester river waters and their chemical self-purification capacity becomes an actual problem, which is substantiated by the fact that the Dniester River is a main source of surface water, which ensures the needs of urban and rural areas, the agriculture and the industrial sectors.

Currently the chemical composition and the hydrological regime of the Dniester waters suffer undesirable changes, caused by the increased anthropogenic impact. The numerous hydrotechnical constructions, changing of the river riverbed had negative consequences on the natural processes to formation of hydrological, thermic and chemical regime of the Medial and Lower Dniester [1-7].

Among other risk factors of the chemical composition and the self-purification capacity changing of the Dniester river waters in the territory of the Republic of Moldova an important role rests its tributaries.A increased risk in this sense represents the waters of the most important tributaries of the right-bank of the Dniester: Raut, Ichel, Bic and Botna rivers.

The Raut basin comprises the more watercourses with the length comprised between 40-95 km, the main ones being Copaceanca (50 km), Cubolta (92 км), Cainar (95 км), Small Ciuluc (61 км) and Cula (65 км). The river tributaries contribute to the increase of the mineralization, total hardness, pollution with biogenic substances and with organic substances of the Raut waters [11-12]. Beside these, at 212 km from the source, the Raut river accumulates the wastewaters of the municipality Balti.The tributary pours out the waters into Dniester river to 342 miles from its source, near Ustia village, the Dubasari district.

The Ichel river it pours out into the Dniester at 322 km from the mouth of the river near the village Cosernita, the Criuleni district. The tributary has a length of 101 km and an accumulation area of 814 km^2. The content of the main

ions in the river water increases from the source to the mouth, so that near of the river mouth waters reach a higher mineralization (900-1100 mg/dm³) and the total excessive hardness (8,6-10,5 mmol/dm³) [11-12].

The Bic river length is 155 km and the basin of accumulation is 2150 km². Hydrological and hydrochemical regime of the Bic river is strongly perturbed as a result of the flow rate adjustment after construction of Ghidighici dam and the discharges into river of the untreated wastewater or poorly treated of the Causeni, Straseni and Chisinau.The volume of the Chisinau municipality wastewater exceeding 3-4 times the natural flow rate of the Bic river, what leads, including, to the reduction of the total hardness and waters mineralization on the increase background of the chlorine ions content on the water course, downstream of wastewater treatment plant of the municipality [11-12].

River Botna has a length of 152 km and an area of accumulation 1540 km². The flow rate and the chemical composition determined by the natural factors are basically disturbed through total adjusting of the river course. On river is built a cascade of 3 dams with accumulation lakes, near the village Ulmu, Costesti and Rezeni.At a kilometre from the mouth in the Dniester, the river bed is jammed by a dam with gates, which currently does not work and which has a small drainage capacity of the water from the river in the Dniester, however, in periods of the high waters in the Dniester, his waters enters in the riverbed of the Botna river before and after the respectively dam [11-12].

The total area of the river basins of these tributaries is 63.44% from the accumulation basin of the Dniester waters on the country territory, including, 40% it is of the Raut river accumulation basin, the Ichel river - 4.24%, the Bic river -11.2% and the Botna river- 8%.

In watershed territory of these rivers live about 1.5 million people, activates various industrial and agricultural enterprises. Thus, these rivers are the collectors of the poorly treated or untreated household wastewater and residual waters.The high level of these rivers pollution is confirmed by results of the multiannual researche [8-11].From the ones exhibited the above it follows the need of research the chemical composition of waters of these tributaries with assessment of their impact on the Dniester river water.

To determine the chemical composition of the tributaries waters and its impact on the Dniester river waters, during 2009-2010, water samples were taken from the tributaries as well from the Dniester river, in the capture points located downstream (200-300 m) and upstream (500 m) from the confluence.

The study of the waters chemical composition in the rivers Raut, Ichel, Bic, Botna and Dniester river included the following determinations: pH, temperature, Oxidation-Reduction Potential (ORP), rH, contents of the main ions and mineralization (Σi), the degree of saturation with oxygen (DO), the concentration of dissolved organic substance (COD-Mn, COD-Cr, COB_5) and biogenic elements (N, P), the total content of metals (Cu and Fe), kinetic indicators ([Red], $[H_2O_2]$,$Sk_i \cdot [S_i]$, [OH]).

For establishing the quantities of chemicals discharged by each tributary in the Dniester river, was calculated the tributaries flow rate at the time of sampling. For this were made measurements related to the morphology of the riverbed at the river mouth and the water flux speed.

Analysis of water samples was carried out using various chemical and physico-chemical analysis methods [13-17].

2. Chemical composition and processes of self-purification of waters rivers Raut, Ikel, Bic and Botna
2.1. The contents of the main ions

The Dniester tributaries waters of the right-bank at the river mouth, during 2009-2010, can be characterized as being with the increased mineralization and advanced total hardness. The average values of the main ions content have varied insignificantly from 892 mg/dm³ up to 1039 mg/dm³. The variations of the main ions content over the years were insignificant for all rivers, except the Botna river, whose waters had considerable fluctuations of the mineralization (Tab. 1). Raut and Ichel waters are characterized with the hydrochemical index corresponding C^{Mg}_{II} and C^{Mg}_{III}. In the Bic river waters of anions, also, hydrogencarbonate ions dominate, and cations (Na⁺ + K⁺), Ca²⁺, Mg²⁺ were present in very similar quantities [18]. The Botna river waters were hydrogencarbonate and chlorides class, magnesium group and III type of quality.

For the rivers Raut, Ikel and Botna was identified well-defined linear dependence between the hydrogen ions and the total content of main ions. In waters of these tributaries was observed a clear trend of increasing the concentration of ions Cl⁻, SO_4^{2-}, of the alkali metal ions (Na⁺+K⁺) when increase the mineralization. For Bic waters not detected any correlation.

The total hardness average of the Raut, Ikel and Botna river waters constituted 11.0 - 11.9 mmol/dm³ and of the Bic - 8.3 mmol/dm³. The hardness values for this three tributaries are mainly conditioned by the presence of magnesium salts, and in the case of the Bic river, intake of calcium and magnesium salts in total hardness was roughly equal.

The contents of the main ions (Σi) and the total hardness (H$_{tot}$) of the Dniester tributaries waters from the right-bank

(to the numerator - average values, to the denominator - the limits of variation)

Tributary	H$_{tot}$, mmol dm³	Ions, mg/dm³						Σi, mg/dm³
		Ca²⁺	Mg²⁺	Na⁺ +K⁺	HCO₃⁻	SO₄²⁻	Cl⁻	
Raut	10.9±0.4 8.1-12	67.8±4.2 52-90	91.5±4.1 60.8-102	76.9±5.4 55-96	486±15.9 403-546	171±4.6 149-187	88.6±4.6 63.8-106	982±25.9 849-1082
Ichel	11.6±0.6 8-13.5	78±4.8 58-100	92.7±6.5 49.9-116	33.9±8.4 10.8-75	446±19.8 342-531	161±9.8 86-182	80.4±3.4 64-92.6	892±36 650-994
Bic	8.3±0.61 6.8-10.5	87±4.16 76-102	48.3±5.4 31-65.7	118±11.9 69.8-147	426±9.6 387-451	147±10.8 120-180	107±4.23 95.7-124	933.7±16 868.8-989
Botna	11.9±1.8 3.7-17.9	74.6±9.5 42-122	100±17.9 15.8-158	101±26.2 17.5-238	368±4.1 150-519	144±17 57.6-189	251±48.4 42.5-489	1039±132 356.7-1470

The mineralization dynamics of the Raut, Ikel and Bic rivers waters during the years was similar and deflected insignificant from the average annual values (Fig. 1). In the waters of the Botna river contents summary of the main ions varied in a wider tuning fork.
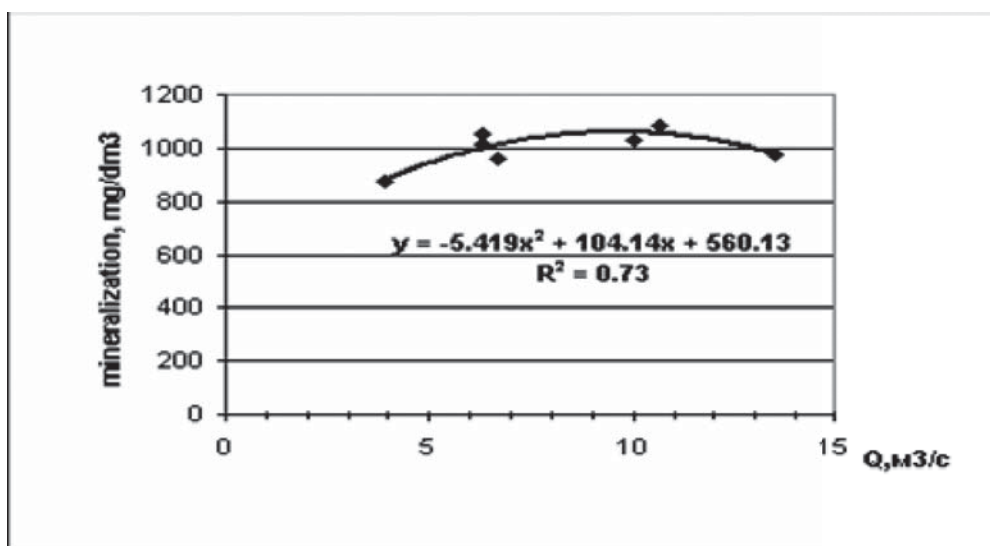
Fig. 1. Dynamics of major ions in the tributaries waters during the years 2009-2010.

For the waters of the Botna river was sudden decrease of the mineralization and total hardness values in cases of the high waters from the Dniester and thereof penetration into the mouth of shedding of the river.

For the Raut river waters was found a good correlation between the mineralization and the water flow (Fig. 2), for the Ichel and Botna rivers this dependence has a low degree of correlation.
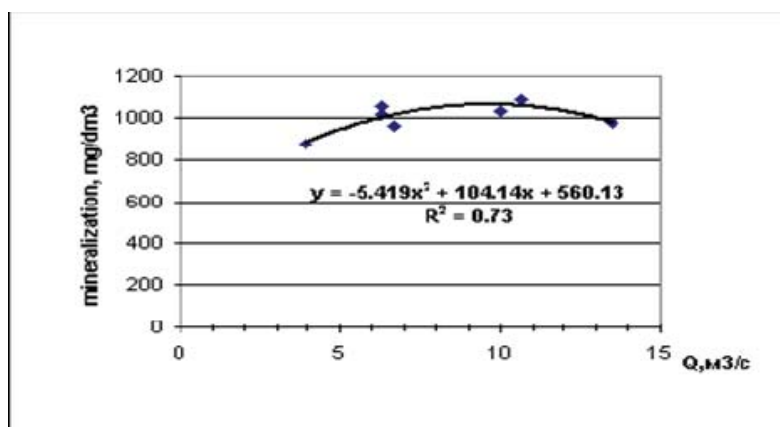
Fig. 2. The correlation between the mineralization and water flow values in the Raut river during the years 2009-2010.

2.2. The buffering capacity

Researches related to acid-base balance of the waters and their buffering capacity (after Van Slaic) have not shown the danger of acidification. For all investigated rivers is characteristic relationship stability Alk> Acid, the buffering capacity indicator has not exceeded the alkalinity.However, in water samples from Bic river has found a high content of carbon dioxide, which indicates to the intensive pollution with organic substances and spend with high speed their oxidation processes. The content of CO_2 to its mouth in the Dniester river vary between 4.9 and 32.6 mg/dm^3, averaging being of 12.13 mg/dm^3. In this river values of the waters pH was always smaller in comparison with other tributaries of the Dniester (Tab.2).

Table 2

**Parameters of acid-base balance and the buffering capacity (β)
of the Dniester tributaries waters from the right-bank**

(to the numerator - the average values, to the denominator - limits variation)

River	pH	HCO$_3^-$	Acid.	Alk.	β	pK	K* 10^7	CO$_2$ mg/dm^3
		mmol-echiv/dm^3						
Raut	8,42 / 8,2-8,9	8,33 / 6,9-10,0	0,21 / 0,0-0,94	8,33 / 6,9-10,0	0,44 / 0,3- 0,86	6,88 / 6,4-7,6	1,54 / 0,03-3,6	3,48 / 1,3-6,4
Ikel	8,25 / 7,8-8,4	7,52 / 5,2-9,1	0,23 / 0,0-0,33	7,52 / 5,2-9,1	0,51 / 0,33-0,8	6,76 / 6,5-7,2	1,92 / 0,6-3,4	5,12 / 1,7-9,9
Bic	7,83 / 7,3-8,1	7,18 / 6,4-8,3	0,61 / 0,3-1,14	7,18 / 6,4-8,3	0,91 / 0,6-1,31	6,56 / 6-6,8	3,24 / 1,8-9,1	12,13 / 4,9-32,6
Botna	8,44 / 8,0-8,8	6,15 / 2,4-8,5	0,16 / 0,0-0,62	6,15 / 2,4-8,5	0,36 / 0,2-0,48	7,18 / 6,6-7,8	0,83 / 0,17-2,4	2,18 / 0,6-4,2

K - acid-base constant

2.3. The regime ofoxygen

The content of oxygen in the studied tributaries waters and the degree of saturation of water with oxygen (D.S.) during the investigation period underwent essential variations.The most favourable situation was recorded at the mouth of shedding of the Raut river, where the degree of saturation of the waters with oxygen was maintained favourable, with except situation from 05.07.2010, when this parameter has lowered to 61.7%. In the mouths of shedding of the Botna and Ikel rivers, oxygen regime was unstable, ranging from the oxygen-deficient situations (D.S. 45.4 - 69.6%) to the supersaturation (D.S. 128-168%).At the Bic river mouth of shedding the oxygen regime was unfavourable during the whole period of monitoring, the degree of saturation in 2009 did not exceed more than 69% and in 2010 vary in the tuning fork 0.0 - 5.7%.

2.4. Organic and biogenic substances

The studied waters in the sections of shedding in Dniester are considerably the polluted with organic and biogenic substances. The average values of organic substances (O.S.), which were determined using indicator COD-Cr, is 24.2

mgO/dm³ in Raut, 29.0 mgO/dm³ in Botna, 43.5 mgO/dm³ in Ikel and 40.2 mgO/dm³ in the Bic waters. Maximum values were recorded in Ikel river waters - 126.0 mgO/dm³(Tab.3).

<div align="right">*Table 3*</div>

The contents of organic and biogenic substances in the right tributaries of the Dniester riverwaters.
(to the numerator - the average values, to the denominator - limits variation)

River	COD-Cr mgO/dm^3	COD-Mn mg_O/dm^3	BOD_5, mg_{O2}/dm^3	$\frac{BOD_5}{CCO\text{-}Cr}$	$N\text{-}NH_4^+$	$N\text{-}NO_2^-$	$N\text{-}NO_3^-$	PO_4^{3-}
					mg/dm^3			
Raut	24.2±5.87 8.0-45.0	5.05±0.66 2.6-7.55	4.4±0.59 2.0-7.0	0.25±0.1 0.07-0.75	0.54±0.24 0.01-1.91	0.042±0.02 0.003-0.150	2.72±0.73 0.50-7.02	2.64±1.33 0.43-11.4
Ikel	43.5±17.8 6.0-126.0	7.9±1.7 3.8-16.5	7.75±1.41 4.0-17.0	0.18±0.04 0.05-0.38	0.91±0.38 0.03-3.75	0.082±0.03 0.033-0.26	2.88±0.71 0.10-7.74	2.39±1.03 0.08-7.51
Bic	40.2±7.9 14.0-56.0	8.4±1.15 6.0-12.3	16.0±4.9 5.0-34.0	0.41±0.15 0.10-0.97	12.54±3.29 2.55-18.2	0.064±0.040 0.004-0.200	2.26±1.10 0.10-6.50	9.15±2.12 1.13-11.8
Botna	29±12.9 4.0-45.0	7.02±0.84 2.56-13.1	7.1±1.39 3.0-18,0	0.28±0.06 0.13-0.48	0.26±0.09 0.0-0.74	0.071±0.003 0.0-0.170	2.29±0.81 0.10-8.82	2.12±1.3 0.0-11.67

Relationship between the parameters COD-Mnand COD-Cr denotes that the tributaries water contains between 18-24% humice substances. For all tributaries are characteristics increased values of the parameter BOD_5, which characterize biodegradable organic substances [19].The highest values of the BOD_5 parameter in 2009-2010 was registered in the Bic river waters, where its values vary between 5.0 and 34.0 mgO₂/dm³. On average, in the waters of the Bic river the share of fresh organic substance formed in the totality of organic substances is 41%. In the Ikel river waters this share is the smallest (18%) and in Raut and Botna rivers waters, contents of biochemically degradable organic substances are respectively 25% and 28%.

Analysis of the determinations results for Raut river waters revealed a strong correlation between COD-Cr and COD-Mn parameters and a smaller correlation between parameters COD-Cr and the water flow in the sampling section (Fig. 3).

a)   b)
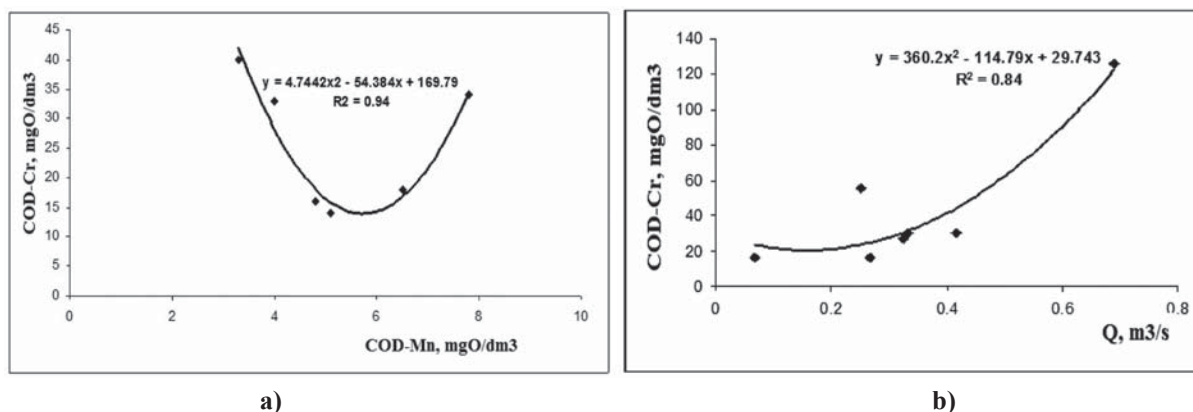
Fig. 3. Correlation between waters quality parameters of Raut river: a) COD-Cr and COD-Mn;
b) COD-Cr and debit (Q).

For the Ichel river water have been pointed correlations between parameters COD-Mn, COD-Cr and the water flow (Fig. 4).

The biogenic elements permanently were existent in the waters of all tributaries. In very scarce cases in the water of the Botna river was missing the ammoniacal nitrogen and nitrite ions. The most advanced degree of water pollution with ammoniacal nitrogen was registered in the mouths of the Ikel and Bic rivers shedding , with average values corresponding 0,91 mg/dm³ and 12,54 mg/dm³ $N\text{-}NH^{4+}$. Minimum content of this nitrogen in the Bic river water exceeded of 1.6 times maximum allowable concentration (MAC)and maximum values exceeded of 11.6 times.
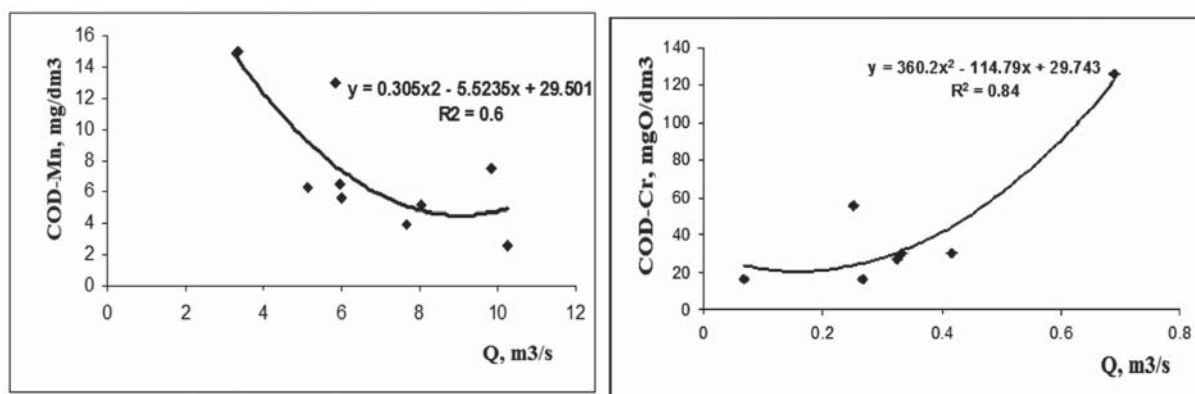
Fig. 4. The correlation between parameters COD-Mn, COD-Cr and waters flow from the Ikel river.

The waters of Dniester tributaries contained a large amount of phosphates. The average values of this parameter was 2.12 mg/dm^3 for the Botna river waters, for Ikel river - 2.39 mg/dm^3, Raut river - 2.64 mg/dm^3 and Bic river - 9.15 mg/dm^3. For the Ikel and Raut rivers waters was highlighted a strong correlation between the content of PO_4^{3-} ions and the waters flow (Q).

In the case of the Ichel river, corresponding relationship is: PO_4^{3-}, mg/dm^3 = 12.25•Q –1.159; r=0,81, for the Raut river: PO_4^{3-}, mg/dm^3 = 0,383•Q + 2,628; r = 0,64.

2.5. Metalscontent

The trend of total content of the various forms of copper and iron in the tributaries waters was decreasing from northeast to southwest. In the Raut and Ichel rivers waters the total content of copper and iron is higher in comparison with Bic and Botna rivers waters.

On an average total copper content in the Raut river waters was 11.2 μg/dm^3, and in the Ichel river - 11.55 μg/dm^3. For iron in these rivers mean values constituted respectively 313.7 μg/dm^3 and 282.3 μg/dm^3 (Fig. 5).
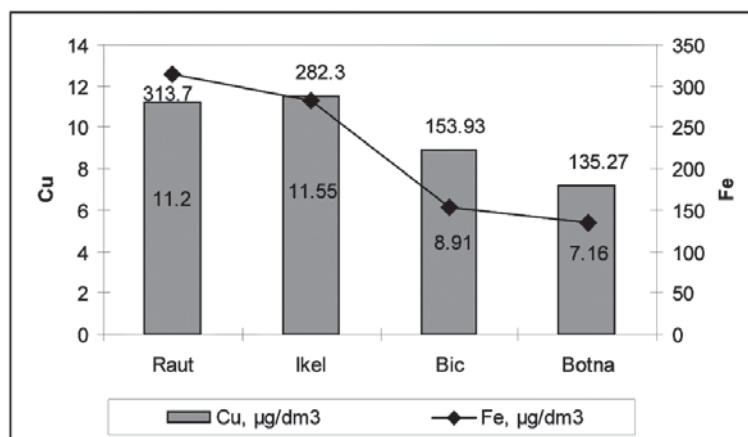
Fig. 5. The average content of copper and iron in the tributaries waters during the 2009-2010 years.

The copper was present in waters in the form of suspensions and colloidal-soluble, their share being roughly the same. Preponderant iron was registered in the form of suspensions (96,6-98,86%) (tab. 4).

Table 4

The average content of the different forms of copper and iron in the Dniester tributaries waters during the years 2009-2010

(to the numerator - the average values, to the denominator - limits variation)

River	Copper				Iron			
	SF*		CSF**		SF*		CSF**	
	μg/dm³	%	μg/dm³	%	μg/dm³	%	μg/dm³	%
Raut	6.2 1.5-12.75	50.4 27.3-76.1	5.0 2.0-8.0	49.6 23.9-80	310.5 183-482	98.86 98.4-99.6	3.2 2.0-4.0	1.14 0.41-1.61

Ikel	7.15 1.25-14.2	53.6 20-78.1	4.4 3.0-6.0	46.4 21.9-80	279.7 109.5-469	98.76 97.3-99.6	2.6 2.0-3.0	1.24 0.42-0.67
Bic	4.23 1.25-6.5	44.22 23.8-61.9	4.75 4.0-6.0	52.78 38.1-76.2	150.18 55.5-167.5	96.65 94.6-98.9	3.75 3.0-6.0	3.35 1.09-5.42
Botna	3.56 1.48-6.75	46 22.8-77.1	3.6 2.0-5.0	54 22.9-77.1	131.9 76.2-208.7	96.6 93.1-98.1	4.00 2.0-6.6	3.37 1.88-6.88

* - suspensions form (SF); ** - colloidal - soluble form (CSF).

2.6. The kinetic parameters

After kinetic parameters investigated tributaries waters can be characterized as aquatic objects with unfavourable ecological situation, well the biological value of habitation of the waters for hydrobionts was reduced (tab. 5).

The redox state of the river Raut, Ikel and Bic waters more often was reducing, in water samples was missing the hydrogen peroxide and was found substances with the reducing properties (Red). The mean values indicate that the highest content of peroxidase substrates has been attested in the Ikel river waters (1,53 μg/dm³), followed by those of the Bic river (1.30 - 1,53 μg/dm³), in the Botna river water the quantity was lower (0.64 - 1,53 μg/dm³) and the lowest quantity has been established in the Raut river water (0.11 - 1,53 μg/dm³).

Table 5

The average kinetic parameters of the Dniester tributaries waters during the years 2009-2010
(to the numerator - the average values, to the denominator - limits variation)

River	$[H_2O_2]$ μg/dm³	$[Red]$, μg/dm³	$OH_{hv} \cdot 10^{14}$ mol/dm³	$OH_{bio} \cdot 10^{17}$ mol/dm³	$\Sigma k_i \cdot [S_i] \cdot 10^{-5}$, s⁻¹
Raut	0,0 0,0-0,0	0,11 0,0-0,39	1,94 0,1-3,8	14,98 1,1-110,0	5,01 2,96-8,97
Ikel	0,0 0,0-0,0	1,53 0,0-2,42	2,15 0,31-8,8	4,54 1,2-13,8	4,38 3,4-6,82
Bic	0,0 0,0-0,0	1,30 0,82-1,90	1,4 0,0-3,2	6,26 2,04-19,0	3,38 1,9-4,9
Botna	1,06 0,0-8,5	0,64 0,0-2,4	1,96 0,0-5,1	7,94 2,4-23,0	4,22 1,6-9,2

Must to be mentioned that, during the period of monitoring, for the Botna river waters, the date of 27.09.2010, was attested superoxide status, what indicatesabout the presence in the water of this tributary of some quantities of the products and semi-products of the technology cycles, well about an aggressively anthropogenic impact. Establishing both the oxidant status, as well and reducing of the indicates on the considerable depreciation of ecological status an aquatic ecosystem.

The inhibition capacity($\Sigma k_i \cdot [S_i]$ - 5,01·10⁵ s⁻¹), which characterizes the effective constant of interaction of the OH radicals with the substances of reducing nature, demonstrates that the self-purification process with radicals had a low intake in the overall process of the Raut river water self-purification. The average values of inhibition capacity of the waters rivers Ikel (4,3810⁵ s⁻¹) and Botna (4,22·10⁵s⁻¹) shows that, in the monitored period, the contents of substances which interrupt the chain process of the radical self-purification in the waters of both rivers was roughly the same. Though the concentration of these substances in the Bic river waters was lower, however their quantity was sufficient to reduce the speed of the self-purification process with radicals (3,38·10⁵ s⁻¹).

For all monitored rivers was found the tendency of redox agents domination, formed as a result of photochemical reactions, in comparison with their training on the biotic path ($OH_\lambda > OH_{bio}$). This situation denotes that redox conditions of the waters have not been optimal for intense development of microorganisms that remove in the outer environment the products of vital activity with strong reducing and toxicproperties.

3. The influence of the right tributaries on the chemical composition of the Dniester river

The results obtained denote a negative influence of the tributaries waters on the chemical composition and chemical self-purification capacity of the Dniester river waters. The most obvious negative impact have manifested the waters of Raut and Bic rivers. In the Dniester waters downstream of the mouths of the shedding of these tributaries,

are detected the increase of main ions contents, that determines the waters mineralization (Mg^{2+}, $Na^+ + K^+$, SO_4^{2-}, Cl^-) and the values of the total hardness of waters, on average with 41% in the case of the Raut river and 26% in the case of the Bic river (fig. 6).
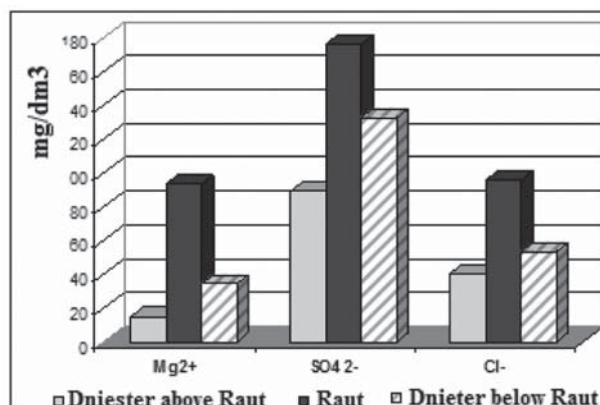

Fig. 6. Influence of the Raut river waters on the main ions content of the Dniester river.

The waters of the Raut and Bic rivers contribute to the increase in pollution of the Dniester river waters with phosphates, compounds of nitrogen, biodegradable organic substances (after the BOD_5, fig. 7). In downstream of the shedding of the rivers Raut, Ikel and Botna in the Dniester river waters increase values of the COD-Cr (fig.8-9).
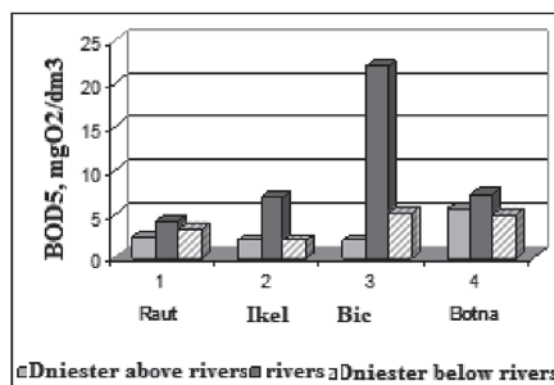
Fig. 7. The impact of tributaries on the content of biodegradable organic substances in the Dniester waters.
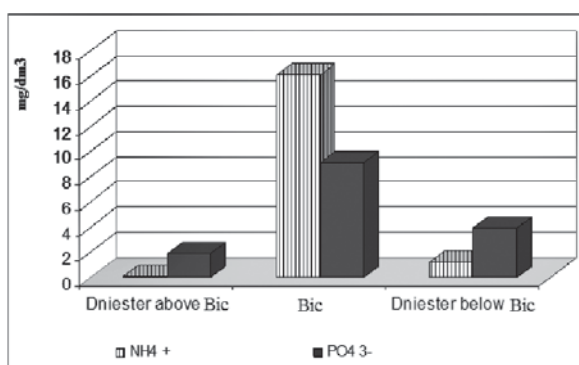
Fig. 8. The influence of Bic river on the contents of biogenic substances in the Dniester river waters.
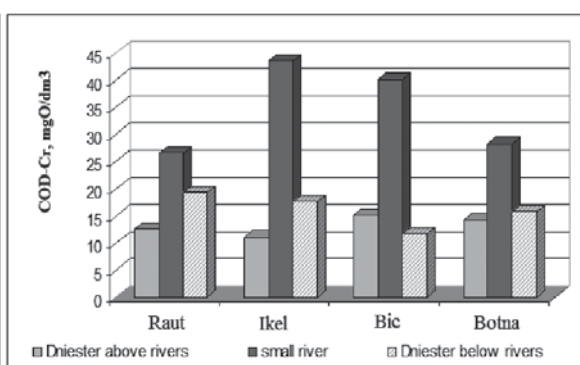
Fig. 9. The impact of tributaries on the content of organic substances in the Dniester waters.

The essential influence of small rivers on chemical composition of the Dniester waters is demonstrated by diurnal flows of some chemical substances which penetrate with the Raut river waters (tab. 6).

The penetration of the polluted waters from tributaries into the Dniester contribute to the reduction of the processes intensity of the river waters chemical self-purification, the dominance of the peroxidase type reductants, the reduction of the OH radicals content and increasing the inhibition capacity of the waters as against the conduct of the processes with participation of these active particles.

Table 6

The average diurnal values of the flow of substances which penetrate into the Dniester with the Raut river waters during the years 2009-2010, in tonnes/day

Year	Q,m³/s	Σi	SO_4^{2-}	Cl^-	C_{org}	$N-NO_3^-$	$N-NH_4^+$	PO_4^{3-}
2009	8.41	752.4	129.1	69.59	8.66	1.65	0.464	1.065
2010	10.14	848.6	144.8	68.3	5.88	1.44	0.76	4.56

Thus, conducted researches in the period 2009-2010 have demonstrated that the Dniester tributaries may be considered risk factors for the Dniester river waters and the researches in this domain must be continue for analyzing all factors that will contribute to improving the created situation.

4. Conclusions

It was been obtained the data about waters chemical composition of the Dniester tributaries (Raut, Ikel , Bic , Botna) in shedding sections in the Dniester river along the years, as well as was appreciated the chemical composition of the Dniester river in downstream and upstream ofthe tributaries shedding of the mouth and the tributaries contribution in the chemical composition formation of the Dniester river waters.

The data obtained denotes a considerable influence of the Raut river waters on the content of the main ions in the Dniester waters. In shedding downstream of the Raut river, mineral salts content in the Dniester waters increases by 41%.

The Raut and Bic rivers contribute essential to changing the chemical composition of the Dniester river:
- Is observed increaseof the total mineralization and total hardness values of Dniester river waters in downstream of tributaries;
- During the summer period, waters of the Raut and Bic rivers do not correspond the *Requirements* provided for of *Hygienic Regulation. Protection of water basins against pollution* (Chisinau, 1997);
- The advanced pollution of the Bic river with biogenic substances (NH_3, $NO_2^-$and PO_4^{3-}) contribute essential to the disruption of aquatic biocoenoses, decreased of the dissolved oxygen content and the disruption of the chemical self-purification processes of the Bic and Dniester rivers waters;
- in summer-autumn colouring is recorded the waters colouring of the Bic river in brown and presence of pronounced smell of the water, what contributes to him "death".

The influence of the Ikel and Botna rivers on the Dniester waters quality is insignificant:
- Ikel has an inessential debit that doesn't cause important changes in the chemical composition of Dniester river;
- The course of the Botna river is heavily regulated and to the shedding of the tributary in the Dniester is built a dam which basically stops the waters penetration from the Botna into the Dniester.
- Both rivers are characterized by advanced mineralization and increased content of various forms of biogenic elements, which shows a pronounced degree of anthropogenic pollution.

Bank tributary waters are polluted with mineral compounds of biogenic elements - ammonium, nitrite, nitrate, phosphate ions. Maximum concentrations were found at the shedding mouth of the Bic river. Was established trend of increasing concentration of various forms of the biogenic elements in the Dniester waters in downstream of the Bic river shedding.

Researched tributaries have an important influence on the Dniester waters after parameters BOD_5 and COD-Cr.

It was estimated redox state of the Dniester tributaries, and intensity of chemical self-purification processes of the tributaries waters to the confluence with Dniester. After kinetic indicator redox state (H_2O_2/DH_2), the rivers waters were characterized by unstable redox state (Raut river) or reducing (Ichel, Bic and Botna rivers). In the tributaries waters almost always were attested substances with reducing properties of peroxidase type, which was oxidized by H_2O_2 and thus favoured the establishment of the quasi-reducing state of these waters. Values of redox potential and of rH denotes that the state of the Dniester waters and those of the Raut, Ikel, and Botna rivers was oxidized, and those from the mouth of the Bic river shedding - reducing. The tributaries waters and those of the Dniester river contained high amounts of peroxidase substances, which has led to the establishment of redox condition unstable of these waters. Oxidation processes mediated of OH radicals arising effectively in the Dniester waters, but are slowed in those of the tributaries. The dynamics of kinetic parameters demonstrates that the self-purification capacity of the tributaries waters is less than that of the Dniester waters.

6. References

[1].   I.H. Bruma, M.A.Usatii, T.D. Sharapanovskaia, in *Environmental and economic problems of the Dniester* (Innovative-information center of Odessa "INVATS" Odessa, 1997), p. 28.

[2].   T.D. Sharapanovskaia, *in Management of Transboundary Dniester River and the Water Framework Directive of the European Union* (ECO-TIRAS, Chisinau, 2008), p. 280.

[3].   E. Zubcova, Ecology 2-3(7), p. 53 (2007).

[4].   E. Zubcova, in *Nature Conservancy of Moldova* („*Science*" Chisinau, 1988), p. 97.

[5].   I.Rusevand others, in *Integrated Management of Natural Resources in the Transboundary Dniester River Basin* (ECO-TIRAS, Chisinau,2004), p.266.

[6].   V. Gladchi, N. Goreaceva, Gh. Duca, E. Bunduchi, L. Romanciuc, I. Mardari, R. Borodaev, Chem. J. of Moldova, vol.3 (1), p. 70 (2008).

[7].   N. Goreaceva, V. Gladchi, Gh. Duca, E. Bunduchi, R. Borodaev, I. Mardari, L. Romanciuc, in *Management of Transboundary Dniester River and the Water Framework Directive of the European Union* (ECO-TIRAS, Chisinau, 2008), p.111.

[8].   N. Goreaceva, Gh. Duca, *Hydrochemistry of the small rivers of Moldova (Tom. Ed. Centre State. University, of Moldova Chisinau*, 2004), 288 p.

[9].   *Water Resources of the Republic of Moldova. The surface waters (Science, Chisinau*, 2007), 248 p.

[10].   N. Goreaceva, N.A. Guranda, *Environmental problems of Transnistria in Moldova (University, Chisinau, 1992), Causes of the degradation of the small rivers of Moldova*, p.112-119.

[11].   N. Goreaceva, in: Self-Purification Processes In Natural Waters (Bulat Art Glob Publishing Company., Chisinau, 1995), p.53-68.

[12].   E. Zubcov, N. Boicenco, D. Schlenk, L. Ungureanu, N. Zubcov, L. Biletski, Z. Bogonin, Bul. The Academy of Sciences of Moldova, 1 (290), p. 135 (2003).

[13].   *Guide for chemical analysis land waters (Hydrometeoizdat., Leningrad*, 1977), 541p.

[14].   *Advanced Water Quality Laboratory Procedures Manual* (Hach Company, USA, 1997), Rev. 1, 1140 p.

[15].   A.M. Nicanorov, I.A. Lapin,Reports Academy of Sciences of Moldova, T. 314 (6), p. 1507 (1990).

[16].   P.A. Lozovic, The water resources, T.33, p.15, (2006).

[17].   *Technique of definition of the kinetic parameters of surface water quality. Guidance Document. RD 52.18.24.83-89 (Hydrometeoizdat, Moscow*, 1990)*,* 30 p.

[18].   Gh. Duca, V. Gladchi, N. Goreaceva, E. Bunduchi, R., Borodaev, A. Lis, L.Anghel; O. Şurîghina; L. Romanciuc, Studia Universitatis, ser. natural sciences, 1(31), p. 146 (2010).

[19].   N. Goreaceva, V. Gladchi, Gh. Duca, E. Bunduchi, R. Borodaev, O. Shurigina, Studia Universitatis, ser. natural sciences, 1(31), p. 158 (2010).

ECOLOGICAL PECULIARITIES OF COPPER CHEMICAL FORMS CONTENT IN THE ERODED SOILS

Tamara Leah

"Nicolae Dimo" Institute of Pedology, Agrochemistry and Soil Protection
e-mail: tamaraleah09@gmail.com, phone: 373-22 284861, fax:373-22 284859

Abstract: The content of total and chemical forms of copper, the features of the distribution and transformation of compounds of copper in none eroded; weakly, moderately, strongly eroded; accumulative soil – deluvial of Gray soils and Calcareous chernozems from Republic of Moldova are presented. Erosion process led to increase the chemical forms associated with clay minerals, carbonates, oxides, and reducing the mobile and humus organic forms. The losses of copper in different chemical forms consist 33-35% from humus horizon of agricultural eroded soils. The data are using as ecological and diagnostically indicators of trace elements losses from soils surface.

Keywords: agriculture, chemical forms, copper, soil, transformation

1. Introduction

Chemical pollution of agricultural soils is one of the most actual problems. Avoid it completely is impossible, because pollution is consequence of the functioning of industrial society, but to be able to assess, predict and combat the negative consequences is possible. Special group of pollutant in agriculture are trace elements, inclusive copper, which have the highest rates of toxicity for environment components. The characteristics of composition and structure of the soils have a significant role as a regulator of chemical compounds of trace elements that is realized by combining the processes of migration, transformation and accumulation in the agricultural degraded soils [1].

Study the composition of the compounds of the chemical elements in soils and their transformation mechanisms have more than half a century, but their importance is growing due to the need for adequate assessment of the current state of the contaminated soil, weather changing them, finding ways to improve them. For this purpose built combined fractionation scheme of compounds of elements in series and parallel processing of soil traditionally used agents and assuming calculated by finding the content of a number of compounds of elements, which are not specifically allocated in any of the schemes [2].

To assess the migration capacity of the copper (Cu) and other trace elements in the food chain should take into account not only the total forms, but also their chemical forms associated with soil compounds, transformation in the degraded and polluted soils, as well as the ability of plants to withstand pollution. Despite intensive research, many questions of the absorption and transformation of metals in soils remain unresolved, and determine the relevance of researches. The aim of these investigations: to determinate the total forms of trace elements and verify the content of chemical forms, especially accessible for plants; to develop the ecological indicators to assessment the soil pollution in results of environment degradation.

2. Material and method

The research has been conducted on the Gray soils and Calcareous chernozems on the slope catena with different types of erosion: none eroded soil on the slope top – inter stream), strongly eroded on the slope bottom and deluvial soils in depression. The soils of catena are presented by the sequence of soils with approximate age, formed on the same parental material in similar climatic conditions, but having different characteristics in dependence of erosion degree. The purpose of researches is carrying out the features of the distribution and transformation of compounds of copper in the eroded Gray soils on the vineyards (contaminated by Cu) and arable eroded Calcareous chernozems (background concentration of Cu). The soil samples were collected from genetically humus horizon (0-20 cm) and calcareous horizon (140-200 cm). The total form of copper was determinate through classic methods of desegregations with hydrofluoric acid in combination with sulfuric acid. To research the copper fractions in eroded soils was used the parallel extraction scheme by different reagents. The total content and chemical forms of copper in soil samples were determinate by atomic absorption spectrophotometer method - AAS1.

3. Result and discussion

Systemic analysis of the chemical elements of soil reveals the relationship between their interrelations. The composition of any soil characterizes is an elementary system of chemical elements. The system of chemical elements includes in the phases of soils, influenced by interrelate processes of transformation and redistribution of matter and energy that occur in the real phase, soil profile land landscape – geochemical levels This system includes solidly associated mineral, organic and organic-mineral compounds, mobile forms of the liquid phases, the substance of the soil solution, soil air, and biota.

The total Cu includes variety chemical forms in soil, inclusive: available and inaccessible to plants. The average content of Cu in gray soils is 27 mg kg^{-1}, in calcareous chernozems – 35 mg kg^{-1}. Accumulation of Cu in humus horizons of gray soils is the result of anthropogenic contemporary actions: 135 mg kg^{-1} in none eroded soil and 82 mg kg^{-1} in strongly eroded soil. The content of Cu in calcareous chernozems are below average: 23 mg kg^{-1} in none eroded, 15 mg kg^{-1} in strongly eroded. The total content of Cu in carbonated horizons of soils are at the same level, without significant accumulation.

The accumulative deluvial soils are formed by accumulation of soil deposits rapidly increasing as a result of erosion on the slopes. Study on content and chemical forms of Cu in soils can be regarded as ecological and decisive factors of eroded and polluted soils. The total content of Cu in accumulative layers of soils under goes stratification depending on the texture and humus content. Gray soil cumulative layers I-II contains 37 mg kg^{-1} of Cu, calcareous chernozem – 14 mg kg^{-1}. In the calcareous chernozems the content of Cu is lower; the gray soil use for vineyard has a high content of total and chemical forms of Cu. The content of total Cu in soils of catena is presented in Fig. 1 and 2.
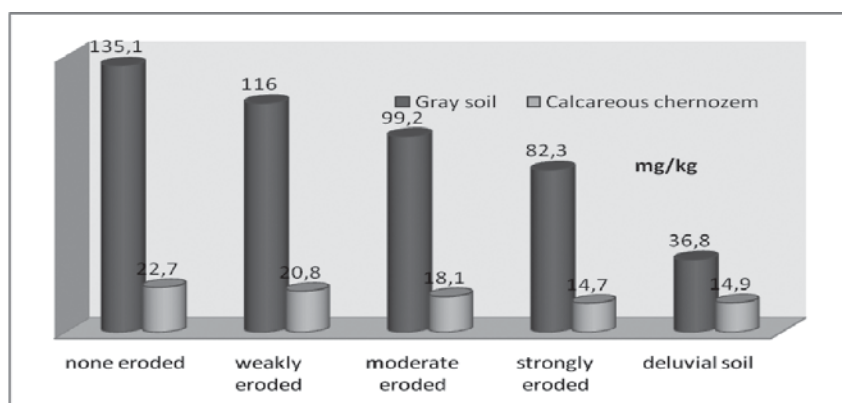
Fig. 1. The total content of Cu in humus horizon of soils
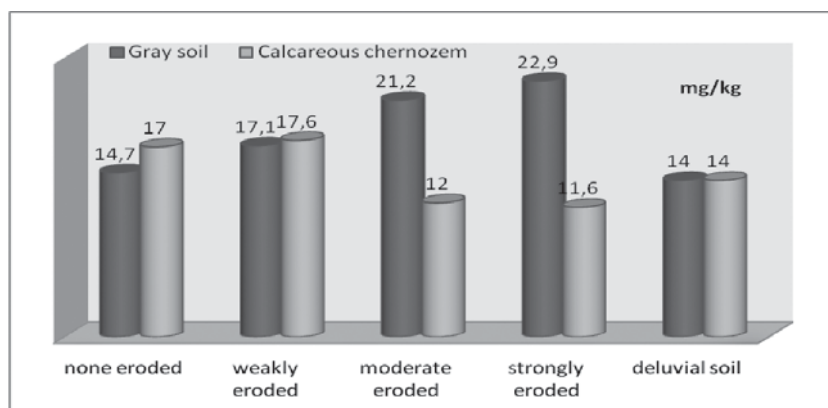
Fig. 2. The total content of Cu in calcareous horizon of soils

The chemical forms of Cu in agricultural soils and vineyard are studied more intensively. Studies in this context are reduced to the following: soil components involved in the absorption of trace elements (including Cu) are Fe-Mn oxides, organic matter, carbonates and clay minerals. These components are considered the most important groups, participating and competing among themselves in the processes of absorption, transformation and accumulation of trace elements. To trying to know the transformation of these processes it brings a contribution to pedogeochemical researches of eroded and polluted soils, included in agricultural cycle [4].

The ***mobile and accessible chemical forms of Cu*** available for plants in the gray soils consist 16-20%, in calcareous chernozems - 8-9% from total Cu. These forms are proportional and well-define correlation with global content. The ions of Cu can be easily sediment by sulfides, carbonates and hydroxides. As a result the Cu becomes an element with low mobility in carbonated soils and horizons [4]. The content of mobile Cu in superficial humus layer is 1.0-1.7 mg kg^{-1}. The mobility of Cu in eroded soils decreased in dependence by the duration of establishment of dynamic equilibrium in the soil after anthropogenic impact (fig. 3 and 4).
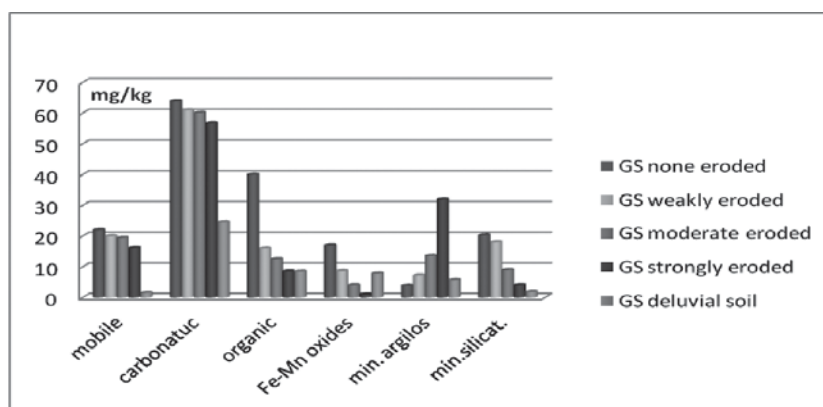
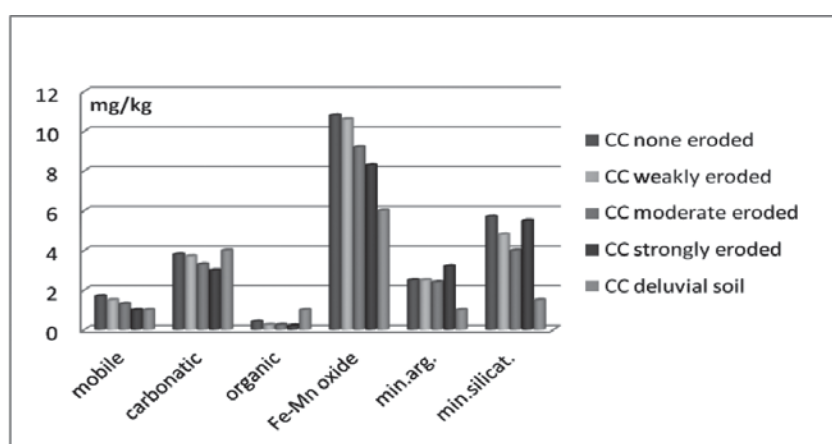**Fig. 3. Chemical forms of Cu content in the humus horizon of Gray Soils (GS)**

Fig. 4. Chemical forms of Cu content in the calcareous horizon of Calcareous Chernozem (CC)

Chemical forms inaccessible to plants find in poorly soluble or practically insoluble salts, organic and organic-mineral compounds, primary and secondary minerals. They consist up to 70-80% in the investigated soils. Copper may come inaccessible for plants through physical-chemical and biochemical mobility processes, from inaccessible to easy accessibility and ionic forms (in associate with carbonates, organic matter, Fe-Mn oxides). These forms constitute the potential mobility reserves of Cu for plants. But, practically insoluble salts and crystal lattices of minerals are locked the nutrients in inaccessible positions; these are the immobilization reserves (primary minerals).

Carbonates are a common component of soils where evaporation prevails on atmospheric precipitation. Thus, Ca^{++} is presented in soil solution. The most widespread and mobile form of calcium carbonate in soils is calcite, which has a large dispersed and actions very much on soil pH, therefore, on the behavior of soil microelements. Therefore, the Cu can be settled with the carbonates [2].

Carbonates in the soil contribute to the fixation of Cu in result of reducing the content of exchange forms, chemisorptions on the surface of the carbonates and increasing ability of the sorption Fe-Mn oxides. The chemical forms associated with carbonates consist in carbonate chernozems up 17-29% of the Cu total content, in the gray soils 47-69%. There is a proportional increase of Cu in calcareous forms with the degree of erosion and carbonates content. In accumulative layer of deluvial typical soils this forms consist 30% and 67%, respectively, with a considerable decrease in the under layer horizons.

The *organic matter* contains the necessary plant nutrients in various connections and forms. Most organic compounds are capacity to associate the Cu in the complexes, which are soluble and insoluble in soil solution, in dependence of the nature and quantity of organic matter. Formation of organic complexes has a significant practical importance to control the biological accessibility and migration of Cu in the soils. Copper content associated with organic compounds consist from 0.4 to 0.2 mg/kg in the 0-20 cm horizon of carbonated chernozems, or 2% of the total Cu. The humus horizon of gray none eroded soil contain about 40% of organically forms. In the deluvial soils were determined 7% of these forms. In humus horizons can accumulate and other organic-mineral compounds with increasing concentrations of carbonates.

Fe-Mn oxides are specific soil components and have important meaning in retaining the trace elements. Absorbed turn around Fe hydroxide the Cu ions may eventually pass in to the occluded status. A considerable quantity of copper is adsorbed by Fe-Mn oxides in higher eroded and degraded soils. Distribution of these forms in the soil profiles is similar to distribution of total Fe. The calcareous eroded chernozems of the slope contain 48-54% of compounds with Fe-Mn oxides, the gray soils – 13-20% in dependence of erosion degree.

Minerals, especially clay (argillic) are a powerful accumulator of trace elements in soils. Some part of elements are fixed of the exchange form, other is recorded in the irreversibly form. Clay minerals can retain trace elements by ion exchange, chemisorptions, adsorption and occlusion [2].

A part of copper in soil is associated by clay and silicates minerals. The minerals have capacity to adsorption the copper ions from solution, especially in soils with high clay mineral content. Soil clay minerals have a high disperse degree and specific physic-chemical characteristics. The clay minerals are the active fraction of mineral soil matter as an ecological character and factor. Together with humus, these minerals formed a clay-humid soil complex. Therefore, a considerable quantity of Cu is associated with clay and silicates minerals. With increasing of soil erosion degree the content of Cu clay minerals forms increases and accumulated in the deluvial soils.

Large part of the primary minerals may associate the copper in immobile forms, which are the most resistant chemical forms of soils. The content of forms from primary minerals are higher than secondary minerals; from 25% in 0-20 cm layer of none eroded carbonate chernozem to 37% in heavily eroded chernozem; in the gray soil, respectively – 15% and 25% from total Cu.

The eroded calcareous chernozems have a content of copper under optimal limits for plants. In carbonated chernozems dominate the chemical forms of Cu associated with primary minerals, carbonates, oxides, which are inaccessible to plants. The eroded soils of slopes need in organic fertilization which will conducting at increase the humus and capture available nutrients for plants. In the case when the soil is polluted (gray soil of vineyards), the distribution character of element on the soil compounds varies, and can serve as a diagnostic criteria in determination the type of contamination (anthropogenic or natural) and elaboration of prognoses of Cu behavior in the environment components.

4. Conclusions

Regularities of the distribution of copper chemical forms content in soils are influenced by erosion processes, agriculture use and soil composition.

1. Degree of Cu fixation by soil components showed that in the eroded soils the main role in their absorption is organic matter, Fe-Mn oxides, clay minerals. Among of these categories of chemical forms in which Cu are find in the soils, no precise separations, but gradual transition. Therefore, the great importance to separate chemical forms will determinate by the methods for establishing a balance between these forms for each type of soil.

2. The soil erosion increases the content of soluble forms and associated with clay minerals; decrease the forms of organic matter, oxides, and primary minerals. In none eroded, accumulative soils (deluvial) reduction occurs content of mobile forms, chemical forms of clay minerals compounds is lower. The content of chemical forms associated with carbonates and oxides is higher, increase in according to erosion degree on the slopes.

3. The research ecological characteristics of transformation of compounds of Cu in the soils can be used to assess the environmental impact of anthropogenic emissions. Established the mechanisms of interaction of Cu (other elements) in soils components serve to develop effective methods to remediate the contaminated soils. The revealed regularities in translocation of trace elements in plants can be used for the purposes of rationing of toxicants in soils.

4. Appropriate supervision of microelements in the eroded soils is not possible without knowing the factors which determining their mobility in soils. Knowing the chemical forms of microelements in the soils and natural anthropogenic processes that contribute to the formation and conversion of pollutant in soils, can allowing and finding ways to decontaminate the soils trough transformation one form to another form, immobilization of hazardous forms for plants and environment ambient.

5. References
[1]. Leah, Tamara (2011). *Modification of content and chemical forms of copper in agricultural grey forest soils.* Î.E.P. Ştiinţa, Comb. Polig. Chisinau, 237-240 p. (rom.).
[2]. Motuzova, G.V. (1991). *Composition of trace elements in soil: organization system, ecological importance, monitoring.* M., p. 168-170, (rus).
[3]. Minchina, T.M., Motuzova, G.V., Nazarenco, O.G. (2009). *The composition of heavy metals in soils.* Everest. Rostov na Donu. 208 p. (rus).
[4]. Leah, Tamara (2010). *Pollution of eroded soils by excess and deficiency of copper.* Scientific paper „Horticulture", LIII (53) 2010, „Ion Ionescu de la Brad", Iaşi, p. 569-572.

STUDY OF HYDROGEN SULFIDE REMOVAL FROM GRUNDWATER

Tudor Lupaşcu, Mihail Ciobanu, Victor Boţan, Taras Gromovoy [a]

Silvea Cibotaru, Oleg Petuhov, Tatiana Mitina

Institute of Chemistry of Science of Moldova, Academiei str. 3, MD 2028 Chisinau, Republic of Moldova

[a] O. Chiuco Institute of Surface Chemistry, National Academy of Science of Ukraine, 17,

General Naumov Street, Kyiv 03164 Ukraine

E-mail: lupascut@gmail.com; Phone: +373 22 725490

Abstract: The process of the hydrogen sulfide removal from the underground water of the Hancesti town has been investigated. By oxygen bubbling through the water containing hydrogen sulfide, from the Hancesti well tube, sulfur is deposited in the porous structure of studied catalysts, which decreases their catalytic activity. Concomitantly, the process of adsorption / oxidation of hydrogen sulfide to sulfate take place. The kinetic research of the hydrogen sulfide removal from the Hancesti underground water, after its treatment by hydrogen peroxide, proves greater efficiency than in the case of modified carbonic adsorbents. As a result of used treatment, hydrogen sulfide is completely oxidized to sulfates.

Keywords: catalysts, hydrogen sulfide, adsorption/oxidation, hydrogen peroxide, sulfur, sulfate

Introduction

One of the current problems of mankind is supplying quality drinking water to the population. This issue is very important for Moldova, since our country surface water sources are limited and unevenly distributed over the country, and the groundwater ($\sim$ 50%) do not meet drinking water quality indices.

Removal of hydrogen sulfide from groundwater containing sulfide concentrations ten times higher than the admissible concentration is a current problem of great importance [1-7].

Groundwater in Moldova contain quantities well above the maximum permissible concentrations of pollutants such as: sulfur ions, fluoride, ammonia, nitrates, nitrites, iron, manganese, strontium, lead, sulfides.

Presence of hydrogen sulfide in groundwater used for public supply causes various diseases of human health. In compliance with the health requirements of international standards for drinking water, concentration should not exceed 0.1 mg/L. In some geographical areas of Moldova concentration exceeds 10 mg/l. Analysis of scientific literature confirms the existence of several groundwater purification technologies to remove hydrogen sulfide. Most commonly used is the method of oxidation of sulfide ions by aeration in the presence of solid supports including activated carbon.

In this paper, as the catalytic support for removing sulfides in groundwater the industrial activated carbon BAU-A was used, intact and modified.
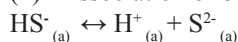
Experimental

Dissolved in water, hydrogen sulfide is included in a series of chemical reactions [1] as follows:

(1) Dissociation of molecular hydrogen sulfide to form the bisulfide ion

$$H_2S \leftrightarrow HS^-_{(a)} + H^-_{(a)}$$

(2) Dissociation of bisulfide into sulfide ion,

$$HS^-_{(a)} \leftrightarrow H^+_{(a)} + S^{2-}_{(a)}$$

(3) Ionization of water itself.

$$H_2O \leftrightarrow H^+_{(a)} + OH^-_{(a)}$$

Thus, the total concentration of hydrogen sulfide includes all sulfide species.

$$t_{H2S} = m_{H2S} + m_{HS}- + m_S2-$$

In [1] it is shown that bisulfide ion concentration increases proportionally with increasing pH in the range 1-8. In accordance with the regulations in force in the Republic of Moldova drinking water pH is between 6.5 and 9.5. The pH value of the water from the fountain subject study was 8.7.

The BAU-A activated carbon intact and oxidized was impregnated with following metal ions: Cu^{2+}, Fe^{3+}, Mn^{2+}, from individual solutions as well as with Fe^{3+} and Cu^{2+} together. The process of impregnating the activated carbon BAU-A consisted in periodical stirring of the adsorbent in the chloride 10% solution of the respective cation. The ratio between solid and liquid phase is of 1:4. The period of impregnation of the adsorbent is 4 days. Finally the solid phase is separated from the liquid, washed with distilled water until the salts excess is eliminated and dried at a temperature of 110°C to constant mass. Geometric surface and structure parameters of activated charcoal thus obtained were determined from adsorption-desorption isotherms of nitrogen measured at 1MP Autosorb instrument. Parameters of porous structure

were calculated using and the NLDFT (Density Functional Theory Non-Local) method, DR and BET equation [8].In the table 1 is prezented the parameters of the structures and geometric surface of activated carbon BAU-A intact, oxidated, modified with Mn^{2+} ions and BAU-A+ Cu^{2+} intact and BAU-A + Cu^{2+} + PDW – in the lost simples the process of adsorption/oxidation was efectuated in the dimeneralization water (PDW)..

Table 1

Geometric surface (Ssp m²/g), micropor volume (V_{mi}, cm³/g), adsorption energy (E kJ/mol), maximal adsorption volume (Vs, cm³/g) for samples of activated carbon BAU-A intact, oxidated, modified with Mn^{2+} ions and BAU-A+ Cu^{2+} intact and BAU-A+ Cu^{2+} - (PDW).

AC sample	S_{BET}, m²/g	Vs, cm³/g	Vmi, cm³/g, t-method	Ea, kJ/mol Equation DR
BAU-A intact	727,75	0,395	0,264	21,24
BAU-A+ Mn	696,31	0,396	0,241	21,22
BAU-A ox.	948,72	0,541	0,323	21,23
BAU-Aox.+ Cu	753,34	0,459	0,252	20,86
BAU-A+ Cu ²⁺ intact	**1090,7**	**0,560**	**0,405**	**20,72**
BAU-A+ Cu ²⁺ PDW	**780**	**0,354**	**0,294**	**21,29**

The data presented in Table 1 show that, after impregnation of intact activated carbon BAU-A with Cu^{2+}, Fe^{3+}, Mn^{2+} ions and of the oxidized BAU-A with Fe^{3+} + Cu^{2+} structure parameters and geometric surface of obtained samples significantly changed in the impregnation process. The process of adsorption/oxidation was conducted at the semi-pilot installation presented in Figure 1. The reactor volume was of 20l, bubbling time - 1 hour, bubbled air pressure - 2 at., the amount of water to be tested - 10 liters, the amount of carbon catalyst - 10g. The initial concentration of hydrogen sulfide in the groundwater of Hancesti was equal to 5.1 mg/l and that of sulfates - 71.2 mg/l.
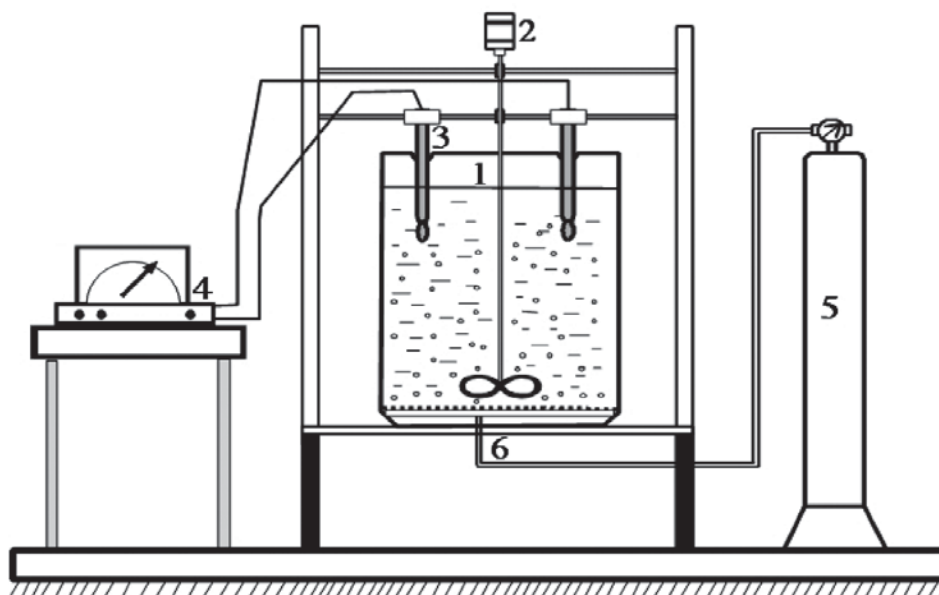
Fig. 1. Scheme of the semi-pilot installation for the study of hydrogen sulfide adsorption-desorption processes, where: 1 – reactor, 2 – stirrer, 3 - electrodes, 4 - pH/mV-meter, 5 – oxygen supply, 6 – membrane allowing the formation of a uniform gas flow in the whole volume.

Adsorption-oxidation processes of sulfide ions were determined by quantitative determinations of their concentrations and the concentration of sulfate ions. Efficiency of the carbon catalysts was established in several cycles of use. Intact and oxidized activated carbons surface chemistry was determined from the analysis of mass spectra measured with temperature-programmed desorption—mass spectrometry (TPD–MS) were performed using a custom-made system, the design and detailed explanation of which was presented in [9].(The system was based on an MX-7304A mass spectrometer(Sumy, Ukraine), with a mass range of 2–200 Da, electron impact energy of 70 eV, and sensitivity of $10-^{8}$g.

Results and discussions

Analysis of sulfide Ion concentration after completion of each cycle of investigations, using both BAU-A + Mn catalyst and BAU-A + Cu allowed to conclude that the entire amount of sulfide in groundwater disappears. To elucidate the mechanism of this process was determined the amount of sulfur ions in the initial water and that in the water which underwent oxidation. The results are presented in Table 2.

Table 2

Concentrations of sulfate and ammonia ions per cycles

Ions	Determined values				
	Cycle 1	Cycle 2	Cycle 3	Cycle 4	Cycle 5
Sulfate (SO_4^{2-}), mg/dm^3	84,9	85,2	87,4	85,0	91,5
Ammonia (NH_4^+), mg/dm^3	2,14	2,35	2,34	2,64	2,76

The data presented in Table 2 shows an increase in sulfate ions concentration from 71.2 mg/l to an average of 86.9 mg/l. This increase is due to the oxidation of sulfur that is found in groundwater according to the reaction: $S^{2-} + 2O_2 = SO_4^{2-}$. Ammonium ions are persistent and not subjected to oxidation process in those conditions.

In order to establish the chemistry and surface phenomena were analyzed mass spectra of initial carbonic catalysts and of those which underwent sulfide oxidation processes.

TPD-mass spectra of samples: BAU-A intact, BAU-Aox + Cu^{2+}; BAU-Aox.+ Cu^{2+} after 5 cycles, BAU-A + Mn^{2+}; BAU-A + Mn^{2+} after 10 cycles are shown in Figures 2 - 6. TPD-mass spectra represent qualitative information about desorption of compounds with masses of 16 a.m.u.(O), 28 a.m.u.(CO), 32 a.m.u. (S), 44 a.m.u.(CO$_2$), 48 a.m.u., 64 a.m.u. effused (formed) as function of temperature. (In the figures below, the lines representing different molecular weights are as follows:
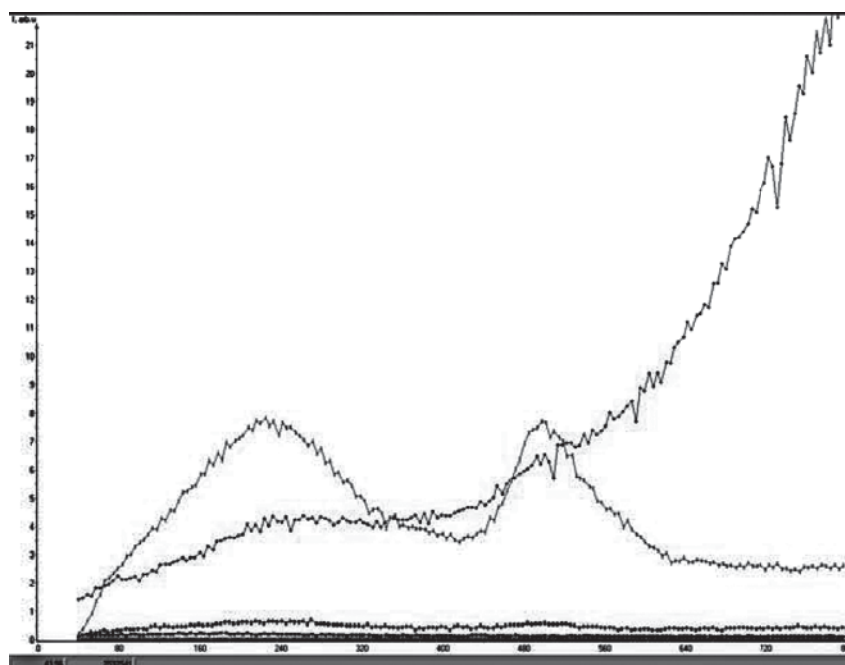
Fig. 2. TPD mass spectrum of volatile products of the intact BAU-A activated carbon sample.
$\rightarrow$ 16, $\rightarrow$ 28, $\rightarrow$ 32, $\rightarrow$ 44, $\rightarrow$ 48, $\rightarrow$ 64
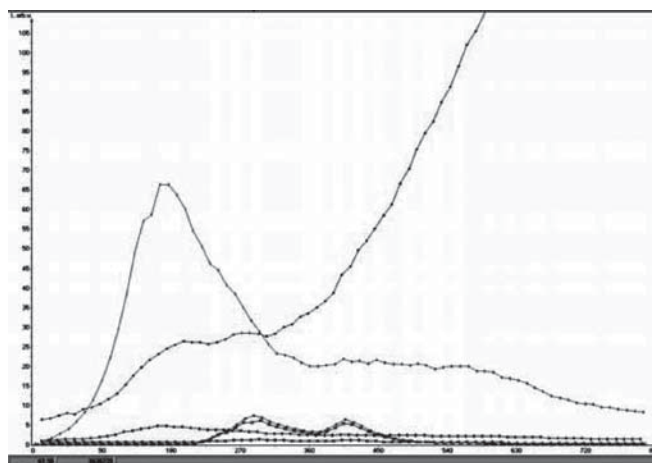
Fig. 3. TPD mass spectrum of volatile products of the BAU-A ox.+ Cu²⁺ activated carbon sample
16,   28,   32,   44,   48,   64
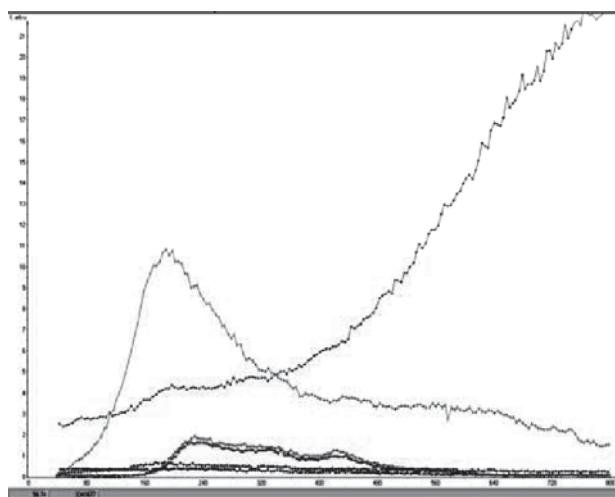
Fig. 4. TPD mass spectrum of volatile products of the BAU-A ox.+ Cu²⁺ activated carbon sample after 5 utilization cycles.
16,   28,   32,   44,   48,   64
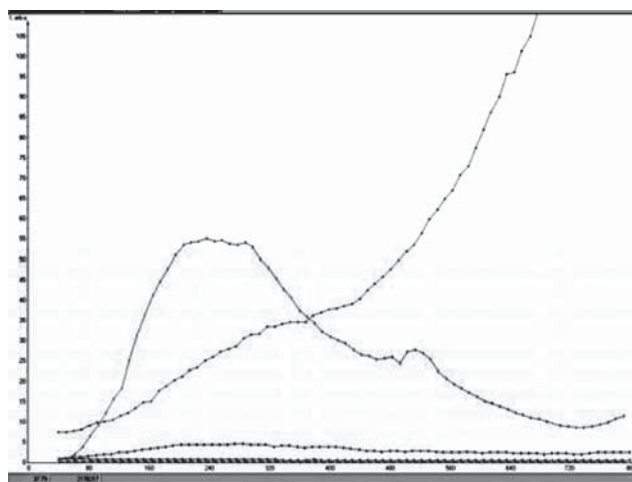

Fig. 5. TPD mass spectrum of volatile products of the BAU-A + Mn²⁺ activated carbon sample
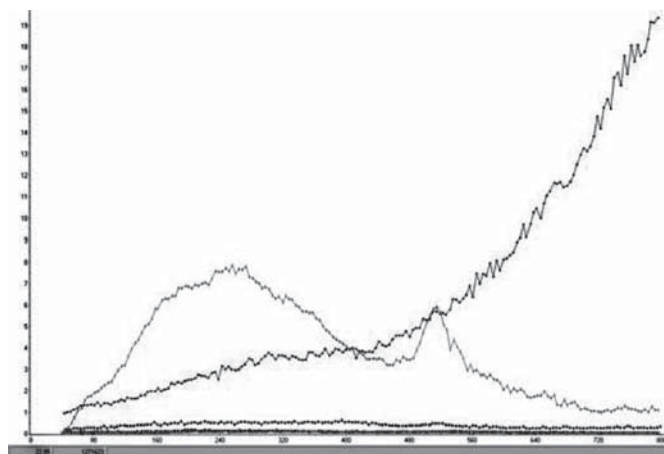16,   28,   32,   44,   48,   64

Fig. 6. TPD mass spectrum of volatile products of the BAU-A +Mn^{2+} activated carbon sample after 10 utilization cycles.

16, 28, 32, 44, 48, 64

Analysis of mass spectra allows us to make the following conclusions. TPD-mass spectra of intact and modified adsorbents by their nature can be separated into two groups: mass spectra of intact activated carbon BAU-A (Fig. 2), of the modified carbon adsorbent BAU-A + Mn^{2+} (Fig. 5) and of the carbon catalyst BAU-A + Mn^{2+} after 10 cycles of use (Fig. 6). TPD-mass spectra analysis of above mentioned results reveals that heating leads to the removal of carbon dioxide and of carbon monoxide on the surface of these spectra. Be noted that carbon dioxide is eliminated in all three cases at temperatures of about 240° C and 520° C. Carbon monoxide is smoothly eliminated in all cases to the temperature of around 500° C, followed by an intense elimination of this gas. In the second group of mass spectra are placed the spectra of oxidized active carbon BAU-A + Cu^{2+} (Fig. 3) and BAU-A ox. + Cu^{2+} after 5 cycles of use (Fig. 4). Analysis of these two TPD-mass spectra reveals that carbon dioxide is removed from the catalyst surface only at temperatures around 180°C. Carbon monoxide begins to eliminate from the surface of adsorbents intensely more quickly at a temperature of only 340 °C. In these two spectra is detected the elimination of two compounds with molecular masses of 48 a.m.u. and 64 a.m.u. at temperatures of about 290°C and 400°C for the catalyst BAU-oxidized + Cu^{2+}. For catalyst BAU-A ox. + Cu^{2+} after 5 cycles of use, these emissions is recorded at temperatures of about 240 °C and about 430°C. Different behaviors of carbon adsorbents during heating may be explained by the fact that during oxidation of the activated carbon on its surface are formed different functional groups which are removed at heat interventions. It should be noted that the mass spectrum line, corresponding to compounds with molecular mass 32 a.m.u. and 16 a.m.u. is parallel to the Ox axis at a value of approximately zero for all 5 substances investigated. From these data we conclude that in the oxidation of hydrogen sulfide colloidal sulfur is not formed, which is very important for the practical realization of technologies of hydrogen sulfide elimination from groundwater by means of catalytic oxidation.

Fig .7 shows the dependence of specific surface of oxidized activated carbon BAU-A + Cu^{2+} per cycles, which shows the decrease of Ssp (BET surface area is recommended by IUPAC) value with increasing number of cycles. Experimental points deviate somewhat from the strictly linear dependence, this can be explained by the need for continuity interference in the process to take coal samples in order to determine their specific surface. For the same reason we find deficiencies in Ssp values of oxidized intact activated carbon BAU-A + Cu^{2+} (Table 1) and Ssp of oxidized activated carbon BAU-A + Cu^{2+} after 1 cycle.
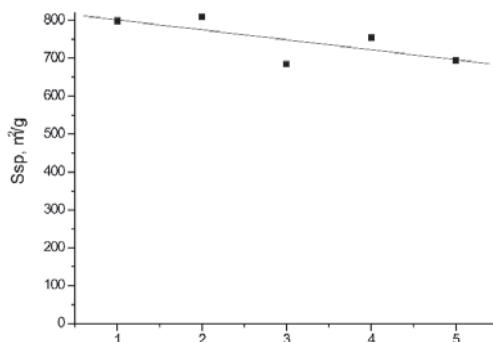

Fig. 7. Variation of the specific surface of sample BAU-A ox. Cu^{2+} per cycles.

In order to determine the influence of catalytic oxidation process with sulfides aeration the blind test was performed, i.e. the same oxidation procedure was repeated with aerated water containing no sulfides. Activated carbon used in this experience was dried to constant mass and subjected to adsorption investigations with the Autosorb 1MP.

Each cycle lasted 1 hour, after which hydrogen sulfide concentration decreased from 10 mg/l to 0 mg/l. The OH• radical which is formed at the interface oxidizes some substance, possibly heavy hydrocarbons in activated carbon BAU structure and amorphous carbon remained after its obtaining process. Bubbling oxygen through the system comprising activated carbon BAU-A + Cu^{2+} in demineralized water for 1 hour (blank sample) with subsequent determination of the structure parameters of the catalyst, can be explained if the radical OH• can oxidize (remove) from the porous structure heavy hydrocarbons, left over from industrial process for obtaining activated carbon BAU.

Conclusions

1. As a result of oxygen bubbling through the water from the fountain in Hancesti containing hydrogen sulfide, sulfur is deposited in the porous structure of studied activated carbons, which decreases its catalytic activity, but the adsorption / oxidation of hydrogen sulfide to sulfate is also produced.

2. Kinetics of hydrogen sulfide removal from water of Hancesti after treatment with hydrogen peroxide demonstrates greater efficiency compared with the use of modified carbonic adsorbents, and as a result hydrogen sulfide is oxidized to sulfate.

References

[1]. Carroll, John L.. Discussion of the Effect of pH on the Solubility of Hydrogen Sulfide. Aqualibrium. 1998-Publication Rights Reserved. P. 1-7.

[2]. Primavera, Alexandra; Trovarelli, Alexandro; Andreussi, Paolo; Dolcetti, Giuliano. The effect of water in the low temperature catalytic oxidation of hydrogen sulfide to sulfur over activated carbon. Applied Catalysis A General 173, 1998, 185-192.

[3]. Moosavi, G.R.; Naddafi, K.; Mesdaghinia, A.; Vaesi, F. and Mahmoudi, M. H$_2$S Removal in an Oxidative Packed Bed Scrubber Using Different Chemical Oxidants. Journal of Applied Sciences, 2005, 5 (4), 651– 654.

[4]. Feng, Wenguo; Kwon, Seokjoon; Borguet, Eric and Vidic, Radisav. Adsorption of Hydrogen Sulfide onto Activated Carbon Fibers: Effect of Pore Structure and Surface Chemistry. Environ. Sci. Technol. 2005, 39, 9744 - 9749.

[5]. Leuch, L.M. Le; Subrenat, A. and Le Cloirec, P. Hydrogen Sulfide Adsorption and Oxidation onto Activated Carbon Cloths: Applications to Odorous Gaseous Emission Treatments. Langmuir 2003, 19. 10869 – 10877.

[6]. Sayyadnejad, M.A.; Ghaffarian, H.R.; Saiedi, M. Removal of hydrogen sulfide by zinc oxide nanoparticles in drilling fluid. Int. J. Environ. Sci. Tehn. 2008, 5 (4), 565 – 569.

[7]. Bandosz, Tereza J. (Teaneck, NJ, US); Bahryeyev, Andriy (New York, NY,US); Locke, David C. (Brooklyn, NY,US). United States Patent Application 20110071022.

[8]. AUTOSORB AS-1. AS1Win. GAS SORPTION SYSTEM. OPERATION MANUAL. Firmware: ver 2.55. AS1Win Software: ver 2.0 and newer. Quantachrome Instruments, 2008.

[9] E.V.Basiuk, V.A.Basiuk, J.G.Bañuelos, J.M.Saniger-Blesa,V.A.Pokrovskiy, T.Y.Gromovoy, A.V.Mischanchuk, and B.G. Mischanchuk. Interaction of Oxidized Single-Walled Carbon Nanotubes with Vaporous Aliphatic Amines Chem. B v106, pp1588-1597 (2002).)

SYNTHESIS OF ACRYLIC ESTERS IN PTC: KINETICS AND ECOLOGICAL ASPECTS

G. Torosyan[1], Ghazi Aidan[2], N. Torosyan[3]

[1] *State Engineering University of Armenia, department of chemical technology & environmental engineering, Yerevan, Armenia, email: gagiktorosyan@seua.am*
[2] *National Academy of Science of Republic of Armenia Institute of Geological Researches, Yerevan, Armenia*
[3] *CSTO Institute, Yerevan, Armenia*

Abstact: Phase-Transfer Catalysis (PTC) technology is used in commercial manufacture. PTC is used also in pollution treatment processes. In the paper the synthesis of esters of acrylic, metacrylic acids, which have wide industrial application for production of unique polymeric materials, by phase transfer catalysis method is demonstrated / PTC/. It is necessary to notice, that the synthesis of acrylic acids through PTC is more important because these compounds are more sensitive to acidic and basic conditions. PTC is characterized by a high degree of useful use of substances involved in reaction, smaller consumption of materials and power resources. The work is devoted to technological problems of the synthesis of ethers in the aspect of environment's protection. The offered method for acrylic ester synthesis, in comparison with the traditional methods, has more advantages including high speed of process, soft condition of reaction allowing reduction of energy expenses, the complete exception of application of hazardous and dangerous organic solvents, by virtue of its sharp reduction of air pollution and reduction of wastewater effluent.

Keywords: Phase transfer catalysis (PTC), acrylic acid, alkyl halogenide, acrylic ester, kinetic characteristic

Introduction

In chemical technology processes, as a rule, there are many manufacturing stages, which can be supplemented by various recycling operations.

Phase Transfer Catalysis / PTC/is widely applied in the industry of organic synthesis due its advantages [1-2]. From the standpoint of the process chemistry PTC has the advantages of being a proven technology involving simple and easily evaluated procedures with high yield (often > 90%) and increased reaction rates, sometimes leading to enhanced selectivity [2]. Since a major task faced by chemical industry is the development and realization of necessary measures for exception of harmful influence of the enterprises on the environment, adoption of technologies producing fewer wastes, PTC corresponds perfectly to these criteria due to the ability to use NaOH as a base instead of more expensive and hazardous organic bases, viability in the water and avoidance of run-away conditions. PTC technology is also used in pollution prevention, pollution treatment and the removal or destruction of impurities in waste and product streams [2].

In our group it has been shown an opportunity of synthesis of ethers and esters in PTC conditions [3-5]. These investigations have allowed to develop the synthesis of unsaturated ethers such as allyl furfuryl, propargyl furfuryl ethers) and esters; esters of acrylic and methacrylic acids, which have wide application in the industry for synthesis of unique polymeric materials [6]. Furfuryl ethers and esters were used also for intramolecular Diels-Alder reaction [4].

$$CH_2=CX-COOH + RHal \longrightarrow CH_2=CX-COOR + HHal$$
$$X= H, CH_3$$
$$R= alkyl, alkenyl, furfuryl, Hal = Cl,Br$$
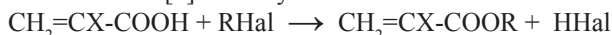
This reaction was carried out in aqueous phase, when acrylic acid is stable [7]. But, it`s known that reaction systems which lack aqueous phase are very attractive to chemists. Therefore, we have tried to carry out reactions with a smaller amount of water (10N), thus having solved also an ecological task. We hope that the proposed synthesis of acrylic esters will give the chance for a choice of optimum variants environmental friendly technology by comparison with existing processes.

Experimental
Synthesis

The synthesis of acrylic esters is carried out by interaction of acrylic acid with alkyl halides in the presence of the sodium hydroxide in water solution (or KOH), the catalytic amounts of quaternary ammonium salts (catamin AB - the mixture of NN-dimethyl-N-benzyl-N-alkyl (C_{12}-C_{18}) ammonium chlorides, industrial SAC), hydroquinone, at the temperature 55-75°C during 1-1,5 hours. The molar ratio of acid : alkyl halide : sodium hydroxide : quaternary ammonium salts – is 1 :1,2 : 1,0 : 0,1. The amount of hydroquinone is 0,5 gram for 0,5 mol of acid. The simplicity of performance and the higher yields (75-90%) of target products can predetermine the application of the present method in industry.

1. Acrylic acid benzyl ester

3,6g (0, 05 mol) of acrylic acid have been placed in a flask, followed by 5ml 10N of a water solution of NaOH, 0,7g (0,001mg) catamin-AB as 50% water solution and 0,05g hydroquinone. At room temperature (18°C) 7,6g (0,06 mol) benzyl chloride were added dropwise during 20 min. The mix was heated up to 75° C and reacted for 40 min. Then the mixture cooled and extracted three times by ether (totally 100ml). Etherial extract was dried up on Na_2SO_4. The product was overtaken under vacuum after removal of the ether. It constitutes 7,3g of benzyl acrilate (90 %, b.p.114-117 °C / 7mm, N^{20}_D = 1, 5243 [7]). IR, $\sqrt{}$, sm-¹: 700,750, 1490,1590,1625 , 1725 , 3030, 3060, 3090. NMR, 5,06s (CH_2) , 5,50 - 6,37m ($CH=CH_2$), 7,11m (C_6H_5). The same processes we make for furfurylic ester of acrylic acid.

2. Acrylic acid allyl ester

Similarly to the above mentioned conditions from 3,6g (0,05mol) acrylic acid, 5ml 10N of a water solution of NaOH, 0,7g (0,001mol) catamin-AB as 50% water solution, 0, 05 g hydroquinone and 7,26g (0,06mol) allyl bromide, 5,11g (91%) allyl acrylate (b.p. 119-120°C/ 680mm, N^{20}_D =1,4335 [7]) have been produced.

3. Acrylic acid n-amyl ester

Similarly to the above mentioned conditions from 3,6g (0,05mol) acrylic acid, 5ml 10N of a water solution of NaOH, 0,7g (0,001mol) catamin-AB as 50% water solution, 0,05 g hydroquinone and 9,1g (0,06mol) n- amyl bromide, 5g (70 %) n-amyl acrylate (b.p. 53-54 °C / 9mm, N^{20}_D =1,4240 [7]) have been produced.

4. Acrylic acid glycidyl ester

Similarly to the above mentioned conditions from 3,6g (0,05mol) acrylic acid, 5ml 10N of a water solution of NaOH, 0,7g (0,001mol) catamin-AB as 50% water solution, 0,05 g hydroquinone and 5,55g (0,06mol) epychlorhydrin, 4,38g (70 %) glycidyl acrylate (b.p. 162-163 °C / 80mm, N^{20}_D =1,4820) have been produced. IR,$\sqrt{}$, sm-¹, 1725. NMR: 1,60-1,68 m (3H, CH-CH_2), 4,21t (2H, OCH_2),, 5,65-6,35m (3H, CH=CH_2).

5. Metacrylic acid n-butyl ester

Similarly to the above mentioned conditions from 4,3g (0,05mol) metacrylic acid, 5ml 10N of a water solution of NaOH, 0,7g (0,001mol) catamin-AB as 50% water solution, 0, 05 g hydroquinone and 8,22g (0,06mol) n-butyl bromide, 3,9g (55%) n-butyl metacrylate (b.p. 60-61 °C / 12mm, N^{20}_D =1,4256 [7]) have been produced.

6. Kinetics

We carried out also the definition of kinetic characteristics of the synthesis of a more interesting monomer - allyl acrylate. The reaction mixture was heated up to necessary temperature, which was kept constant during 1 hour. The analysis was done every 10 minutes. (Figure1). The reaction temperature was varied at the limits of 25-65°C. Activation energy (E) and K_o graphically determined from Arrhenius coordinates:

E = 55625 kjoule/kmol (13,28 kkal / mol)

Ko = 1,922×107 m ³,⁰⁷⁸ / (kmoll, 026 min)

It had been established that the kinetic of reaction acrylic acids with allyl bromide in PTC conditions can be described by the equation:
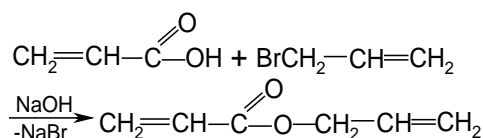
$$-\frac{dC_a}{d\tau} = kC_a^{1,975}C_B^{0,051} ,$$

Where:
$$K = 1,922 \cdot 10^7 e^{-\frac{55625}{8,314 \cdot T}}$$

C_A - concentration of acrylic acid
C_B - concentration of allyl bromide

$$CH_2=CH-\overset{O}{\underset{}{C}}-OH + BrCH_2-CH=CH_2$$
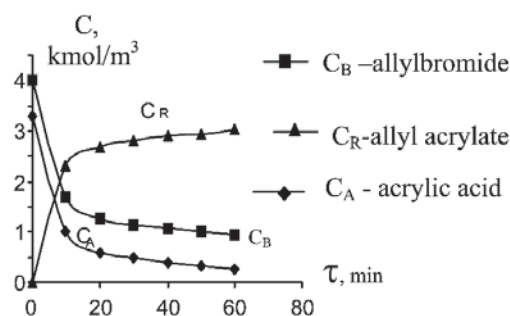$$\xrightarrow[-NaBr]{NaOH} CH_2=CH-\overset{O}{\underset{}{C}}-O-CH_2-CH=CH_2$$

Fig. 1. The kinetic curves of the charge initial substances and accumulation of a product of reaction at the synthesis of allyl acrylate at t=65⁰C.

Results and discussion

The preparation of acrylic esters is an important synthetic reaction for which a variety of procedures have been developed during the last 50-60 years [7]. Traditionally the esters are produced by interaction of carbonic acids with alcohols in the presence of strong acids at higher temperatures – 105-121°C [7], argon current at 90°C [8], and the period of reaction was 55-60 h at 20-25°C [9]. The symmetric ether is formed also from the appropriate alcohol in acidic medium that creates difficulties for isolation of the desirable product [8]. It is necessary to note, that in case of the excess of alkali (the double excess of alkali is usual in alkylation reaction in PTC conditions) the yield of ester falls [3]. The reaction of hydrolysis of an ester takes place in any case.

In the reaction conditions another by-product, the derivative of propionic acid was formed [10]. Environmentally, the strong acidic conditions are less preferable than the basic ones [11]. Besides, as a rule, because of convertibility of the process in acidic medium, it is rather difficult to reach high yields of desirable product, which also requires additional expenses for neutralization of the reaction mixture by alkali materials [12]. Such technology differs by complexity and necessity of huge equipment which is difficult to operate. The ion exchange materials are expensive, quickly fail, require difficult regeneration, during which the huge amount of wastewater is formed [13]. Other method of this ester synthesis consists of interaction of alkyl halogen or other esters with the acrylic acid salts in the presence of organic solvents, acetonitrile, dimethylformamide and other expensive, hazardous and fire-explosive solvents. The toxicity of this solvents in atmosphere within the limits of 10 mg/m³, their accumulation in organism results in a acute poisonings which is observed initialy by narcotic action or excitation, frustration of coordination and spasm infringement of breath.

Obtained kinetic equation allows us to determine the optimum parameters of synthesis of acrylic esters in the simple hashing type reactor.

The greatest disadvantage of acrylic esters synthesis from salts is the formation of metal salts under anhydrous conditions [1, 2]. Acrylic acid is converted into organic salts by the reaction with sodium or sodium hydride. The use of PTC to synthesize acrylic ethers improves the conventional methods since PTC has the advantage that the acrylic salt is synthesized *in situ* directly by the reaction of acid with alkaline solution in the aqueous solution. The final product is readily removed from the organic solvent simply by evaporation of solvent. The solvent in our case is not applied, as an organic phase enters itself. The quantity of used water is reduced also.

The reaction has appeared of the second order under the relation of acrylic acid, and zero - in relation to allyl bromide. Obtained equation allows calculating optimum parameters of process and reactor of ideal mixture for the synthesis of allyl acrylate.

The kinetics of the described synthesis of allyl acrylate testifies for the benefit of the PTC mechanism. Really, the order of reaction for allyl acrylate $\alpha_B = 0,051$ (i.e. very close to zero) shows that the process is determined by the diffusion of acrylate ions from water phase into the organic one, which is consisted only from allyl bromide. The rather loe level of energy of activation also is determined by the contribution of the diffusion factor.

The synthesis of acrylic esters is carried out in a multi section apparatus, filled with strong acidic ion exchanger.

Obtained kinetic equation allows us to determine the optimum parameters of synthesis of acrylic esters in the simple hashing type reactor.

Conclusion

Procedures based on PTC in the substitutions usually excel over traditional methods owing to their simplicity, high yields and quality of final products. This method is especially valuable for reaction with compounds sensitive to water.

The offered method for acrylic ester synthesis in comparison with the traditional methods has more advantages: high speed of process, soft condition of reaction allowing lowering of a power expenses, the complete exception of application of hazardous and dangerous organic solvents, by virtue of – it is sharp reduction of air pollution, much smaller volumes of wastewater. It should be note that the in offered synthesis of acrylates the alkylating agent – allyl bromide is used completely. All of this is devoted to technological problems of the synthesis of ethers in the aspect of protection of environment.

Acknowledgement

References

[1]. Sharma, M. Application of phase transfer catalysis in the chemical industry. Handbook of PTC, Blackie Academic and Profesional, London, Wanheim, New York, Tokyo, Melburne. 1997, pp 168-199.

[2]. Babayan, A.; Torosyan, G., The Stage of PTC development. The Journal of Mendeleev Society, Revue. 1986, 12, 126-135.

[3]. Nazaretyan, A.; Torosyan, G.; Babayan, A. The Journal of Arm.Chim., 1984, 37, 15-17.

[4]. Torosyan, G. Journal of organic chemistry in Russian. 2002, 38, 1542-1543.

[5]. Torosyan, G.; Nazaretyan, A.; Khachatryan, M. Proceedings of Enginering Academy of Armenia, 2006, 3, 651-653.

[6]. Marek, O.; Tomka, M. Acrylic polymers, M-L.in Russian. 1966, p 215.

[7]. Sovetskaja Enciklopedija, M. Polymer Encyclopedy in Russian. 1974, 1, p35.

[8]. Alchinger, H.; Fried, M.; Nestler, G. (1998), BASF AG, - No. 19648743.9, Russian Referative Zournal /RRZ/, (1999), 10H36P.

[9]. Pat.5491244 USA (1995) Acrylic acid ethers, RRZ (1996), 10 Í37 P.

[10]. Siga A. (1975), Acrylic esters, "Seni, Sen," 27, No. 7, 292-306. RRZ (1976), 5H61.

[11]. Makosza, M; Fedorynski PTC catalyzed reactions under basic conditions. Handbook of PTC, Blackie Academic and Profesional, London, Wanheim, New York, Tokyo, Melburne. 1975, pp135-168.

[12]. Pat. 5360926 USA Acrylate synthesis, RRZ in Russian, 1996, 11 Í32 P.

[13]. Osborn, G. Synthetic ion exchange materials, translates from English to Russian by M., Mir. 1986, p 321.

AUTOCATALYTIC REDUCTION AND CHARACTERISTICS OF BORON-CONTAINING COATINGS

Victor Covaliov[a], Olga Covaliova[a]*, Mikhail Ivanov[b], Andrey Drovosekov[b]

[a]*Research Center of Applied and Ecological Chemistry of Moldova State University, 60 Mateevici Street, MD 2009, Chisinau, Republic of Moldova*
[b]*A.N.Frumkin Institute of Physical Chemistry and Electrochemistry, 31 LeninskyProsp., 119071, Moscow, Russia*
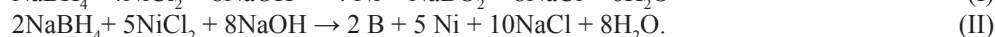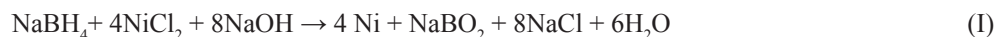**E-mail: covaleva.olga@yahoo.com; Phone/Fax: +37322 577556*

Abstract: The research results of the plating conditions, chemical composition and properties of Ni-B coatings and Ni-Re-B, Ni-Mo-B and Ni-W-B alloys are given. It was shown that introduction of alloying elements (Re, Moand W) in the composition of Ni-containing coatings modifies the catalytic activity of the alloys' surface, with regard to the parallel reactions of dimethylamino-borane(DMAB) heterogeneous hydrolysis, Ni reduction and evolving of the molecular hydrogen. It was found that with the increase in concentration of alloying element, boron contents in the coatings is decreased to the trace amounts. The effect of alloys composition on hydrogen evolving overvoltage was studied. Due to the low overvoltage of hydrogen evolving (HE) on the alloy Ni-Re-B surface (11 at.% Re), it can be used as electrode for hydrogen generation from water in the electrolytic cell with novel design and improved technical-economical indicators.

Keywords: autocatalysis, coatings, alloys, hydrogen generation, electrolytic cell

INTRODUCTION

Since the first publications [1] appeared in the field of chemical-catalytic plating with the obtaining of boron-containing coatings, the essential progress was made both in the theoretical and applied aspect. Due to this, such coatings have been broadly used in industry. This process runs without application of external current and has the autocatalytic nature. The advantage of this plating process is a possibility to metalize the dielectrics, to obtain the uniform layers on details with complex configuration and ensure the co-deposition of boron along with the reduced metals. Boron, under the low-temperature treatment, is involved in the phase interactions with metals, forming the solid functional coatings. These coatings were proposed to be used as substitutes of precious metals in the molding of microelectronics[2,3]. Such new directions have been developed as chemical-catalytic plating with poly-metallic alloys obtaining [4,5], metallization of fine non-metal particles [6], obtaining of composite coatings [7], their applications in photo-catalysis [8].It could be expected that with the development of these processes theory and deeper studies of coatings' properties, they will be used even broader.

On the first stage of this technology development, sodium borohydride ($NaBH_4$) was used as a reducer. It was supposed [9], that during the hydrolytic decomposition of $NaBH_4$the released electron is transferred on the metal surface to the proton - electrons acceptor, resulted from water dissociation: $H_2O \leftrightarrow H^+ + OH^-$.Hydrogen ion is transformed into hydrogen atom:$H^+ + e \rightarrow H$, and then the molecular hydrogen is formed: $H + H \rightarrow H_2$. In the presence of nickel ions, electrons of boron-hydride ions and its hydrolysis products, as well as hydrogen atom's electrons, aregeneralized with metal surface, thus reducing nickel ions to metal, according to the general type reactions:

$$NaBH_4 + 4NiCl_2 + 8NaOH \rightarrow 4\ Ni + NaBO_2 + 8NaCl + 6H_2O \qquad (I)$$
$$2NaBH_4 + 5NiCl_2 + 8NaOH \rightarrow 2\ B + 5\ Ni + 10NaCl + 8H_2O. \qquad (II)$$

Several more mechanisms of these processes have been proposed, including the possibility of electrochemical auto-catalytic reaction, accompanied with the anodic oxidation of BH_4^- andcathodic reduction of Ni. The absence of unified viewpoint may be due to the complexity of phenomena, occurring on the formation of Ni-B coatings. The most justified explanation of these processes mechanism is given in [2],based on the isotopic analysis of hydrogen composition, formed on the reactions running in heavy water, using the chemicals marked with deuterium. It is proposed that the reactions are running following the scheme:

$$BH_4^- + 4OH^- \rightarrow B(OH)_4^- + 4H^+ + 4H + 4e \qquad (III)$$
$$2Ni^{2+} + 4e \rightarrow 2Ni. \qquad (IV)$$

Boron reduction and its inclusion in composition of forming coatings occurs due to the series of other redox-catalytic processes, one of them being the intermediate formation of borine (BH_3)and its decomposition on the catalytically active metal surface:

$$B(OH)_4^- + 3e \longrightarrow B + 4OH^-, \text{ or}(V)$$

$$BH_4^- + H^+ \xrightarrow{\ M\ } BH_3 + H_2 \longrightarrow B + 2,5\,H_2 \qquad (VI)$$
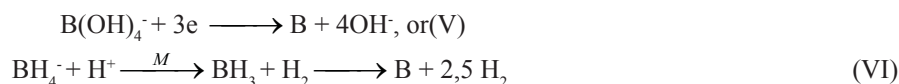
In the last years, the processes of nickel and its alloys chemical-catalytic reduction, using the dimethyl-borane (DMAB) $(CH_3)_2HN\cdot BH_3$ as a reducer, which ismore stable in water solutions, are broadly used [10,11]. Therefore, a deeper study of the reactions mechanism and functional properties of coatings is needed in order to ensure the possibility of governing these processes and broaden the area of their practical applications.

EXPERIMENTAL

The coatings were deposited using $NaBH_4$ and DMAB as reducing agents. To provide comparability of results while studying the effect of doping Ni-B alloys with molybdenum, tungsten or rhenium, pyrophosphate solutions with rather similar compositions were chosen. As a result of the performed optimization of main solution ingredient' concentrations, electrolytes with the following compositions(M/l) have been proposed for deposition of alloys:

1. **Ni-B**: $NiCl_2 \cdot 2H_2O$ … 0,26; Ethylendiamine 50% … 1,03; NaOH … 1,0; $NaBH_4$ … 0,027. $TlCH_3COO - 3,7 \cdot 10^{-4}$. Temperature – 90 °C, pH– 13,5-14,0;
2. **Ni-Re-B**: $NiSO_4 \cdot 7H_2O$ … 0,1; $KReO_4$ …0÷0,018; $K_4P_2O_7$… 0,3; $(CH_3)_2HN\cdot BH_3$ ... 0,05;
3. **Ni-Mo-B**: $NiSO_4 \cdot 7H_2O$…0,1; Na_2MoO_4…0,013; $K_4P_2O_7$…0,15÷0,3; $(CH_3)_2HN\cdot BH_3$... 0,06;
4. **Ni-W-B**: $NiSO_4 \cdot 7H_2O$…0,1; Na_2WO_4…0÷0,02; $K_4P_2O_7$… 0,3; $(CH_3)_2HN\cdot BH_3$ ... 0,06;

The study of structural-phase transformations of Ni-B coatings was performed using the electrohographic, Roenthgenographic and thermoderivatographic methods. To carry out electronographic research, thin 0,1-0,15 mkm films of Ni-B coatings were deposited on the intert acetylcellulose substrate, which has been further dissolved in amylacetate. The measurements were conducted on electrohograph EG, designed and manufactured at the Crystallography Institute of Russian Academy of Sciences. As a standard, NH_4Cl applied by condensation method was used.

Thermoderivatographic analysis was performed on F.Paulik, I.Paulic, L.Erdei derivatograph.The coating was heated either on air, or in vacuum under 10^{-3}mmmercury pressure. Roentgenographic research was carried out both in the chambers РКУ-57 andРКД-114, and on difractometer УРС-50Ион Cu-K_α and Fe-K_α irradiations. Forqualitativemeasurements, microphotometerМФ-4wasused. Quantitative phases ratio, formed as a result of phase-disperse transformations on thermal treatment of boron-containing coatings, was estimated by the intensity comparison of nearby bands.It was considered thus [12], that the intensity of small crystal dispersion in the reflected state is proportional to its volume. The calculations have been performed using the working formula [13]:

$$\frac{I_{hkl}^m}{I_{hkl}^n} = \frac{k_1}{k_2} \cdot \left(\frac{V_2}{V_1} \cdot \frac{F_1}{F} \right)^2 \cdot \frac{P_1 \cdot \rho_2}{P_2 \cdot \rho_1},$$

where$I$ – bands intensity; k- multiplication factor for reflection; F_{hkl}- structural factor for reflection; P- weight; ρ- density; V-total volume of given phase, or, expressed by weight characteristics, $V = \dfrac{P}{\rho}$.

The effect of potassium molybdate, sodium tungstate and potassium perhenate concentration on the basic parameters of chemical-catalytic reduction of metal ions and hydrogen was studied. The chemical state of elementsand composition of the coatings near the surface layers were studied using the method of X-ray photoelectron spectroscopy [14, 15]. The amount of molecular hydrogen evolved was determined volumetrically and that of hydrogen adsorbed by the deposit was measured using vacuum extraction method at 400^0 [16]. DMAB concentration in the solution was determined using the iodometric method [17].

The alloy coatings were plated on 20x10 and 25x5 mm copper and nickel plates. Information on elementary composition was obtained by local spectral analysis, using the scanning electron microscope JSM-3 with energy analyzer WINEDS. Chemical state of the elements and composition of coatings' surface layers was studied by the Roentgen photoelectron spectroscopy (RPES) [18,19]. At the same time, the structure, composition and chemical state of the elements in alloy was determined. To study the composition of near-surface layers of the coatings, the method of layer dissolution (alkalinization) with Ar ions was used with the energy 5 keV and density 60-70 mkA/cm². The dissolution was performed on the surface no less than 1 cm², the analysis was done on the 0,5-0,6 cm² middle part of the surface,

which excluded to use for analysis the non-sprayed portions. The composition of remote layers was determined with «Talystep» profilometer and electron microscopy. Composition of layers, uncovered with the ionic dissolution, was estimated using the method of relative sensitivity factors, considering the ionic spraying coefficients.

The deep layers of deposits have been opened with diamond scribing in preparatory chamber of spectrometer (vacuum 10^{-6}-10^{-7} Pa). Their composition was determined by the same method of relative sensibility factors, and compared with the data of quantitative Roentgeno-spectral analysis. All the data were obtained on spectrometer VG MkII, using the Roentgen Mg k_{α} – irradiation. The calibration of bond energy (E_{bond}) of spectral lines was performed regarding the position of bands Au 4f 7/2 maximum with E_{bond} = 83,8 eV of gold film, sprayed on the coating surface in the preparatory chamber of spectrometer.

Information on chemical composition of elements in studied deposits was obtained from the analysis of form and energy position of bands maximums in the electron spectra of the ground levels Mo2d, W4d, W4f, Ni2p, O1s, B1s, C1s in the spectra of photo-electrons registered for the layers on various coatings' depths.
Nickel-rhenium-boron alloy was selected as the main model system for the study of the effect of doping element concentrations in the alloy on the kinetics of partial reactions of DMAB heterogeneous hydrolysis, reduction of hydrogen, nickel and rhenium ions. The results obtained for this alloy were compared with the specifics of partial reactions, obtained for the alloys Ni-Mo-B and Ni-W-B. It was found that the doping of nickel-boron alloys with rhenium, as well as with wolfram and molybdenum, will sharply hamperthe reaction rate of DMAB catalytic destruction (equation 2), therefore the alloys plated with the inclusions of these elements only contain the trace amounts of boron.

The effect was studied of potassium h sodium molibdate and wolframate in the solution on chemical-catalytic reduction of metal ions and hydrogen: the coatings deposition rate, electrode potential of growing alloy deposit, amount of hydrogen evolved and that of the absorbed by the coating, composition and chemical condition of elements in the alloy. The results of these studies laid in the base of the elaboration of electrode materials with low hydrogen evolving overvoltage and development of the reactor for electrochemical generation of hydrogen, using the flow-through voluminous electrodes with the improved power efficiency.

RESULTS AND DISCUSSIONS
1. The deposition of Ni-B depositsfrom borohydride solutions.

The specifics of the obtained Ni-B coatings' microstructure in the initial state is porous dendritic pillar nanostructure (Fig.1.). Between the dendrites there are vertical zones, which are apparently the places of hydroxide concentration and may appear due to the non-uniform distribution of boron in the deposit.
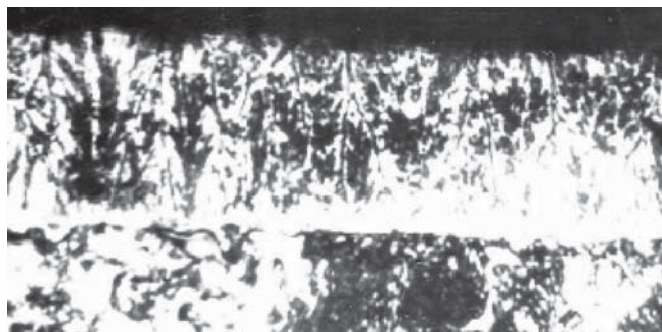

Fig. 1. Microstructure of Ni-B coatings, obtained in the presence of thallium acetate as the solution stabilizer.

On the Debye-grams only the «halo» was detected, specific for the fine or amorphous bodies. Therefore, to reveal the structure of such deposits, the research was performed with electronographic method on ЭГ type Roentgenograph at the Institute of Crystallography RAS. The specimens were prepared by plating of this films of coatings on the inert acetylcellulose substrate with subsequent dissolving in amylacetate. As the standard, NH$_4$Cl was used, applied on the specimens by condensation method.

On the electronograms (Fig.2) of these layers of deposit (less than 0,1 mkm),8 broadened bands of nickel cubic modification are revealed, and additionally –2 very broad bands, which coincide with regard to the inter-planar distances with the strongest bands of nickel hydroxide. This phenomenon is usually observed in the case of the very fine metals [20].

Inter-planar distances and identification of electronogram from Ni-B deposits in the initial state

Nr.	Bands intensity	hkl	Inter-planar distance, experimental	Calculated parameter of Ni	Identification
1.	3		2.862 (2,70 - ref.data)		$Ni(OH)_2$
2.	10	111	2,038	3,54	Ni
3.	1	200	1,771	3,54	Ni
4.	3	220	1.253	3,55	Ni
5.	3	311	1,071	3,55	Ni

The average crystal size was assessed by the breadth of the first band (III)Ni (l_{Ni} = 0,65 mm) and the nearby bands of standard NH_4Cl ($l_{et.}$ = 0,30 mm), neglecting the internal stress effect, which is within the range 40-60 Å. The bond (200) is fuzzy and can hardly be observed, therefore in this direction the size does not exceed 15-20 Å, the effect of packing defects is thus also possible. The signs of amorphous or crystalline boron have not been detected on electronograms, which may be explained by its low contents and low, compared to nickel, scattering power of its atoms.
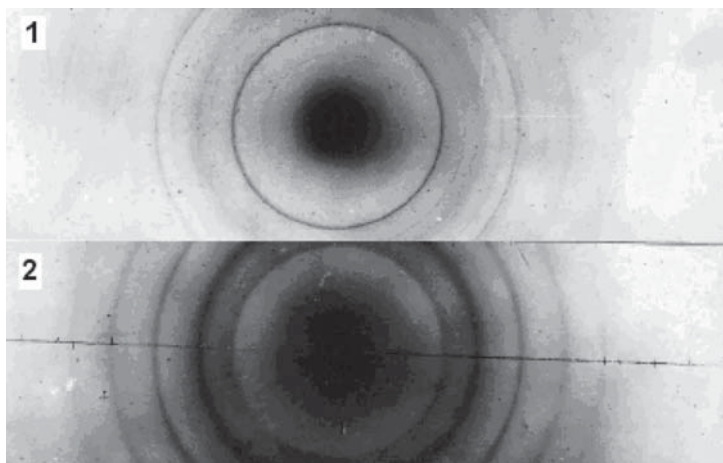
Fig. 2. Electronograms of Ni-B coatings, containing 4,3weight % B (1) and 6,2 weight % B (2).

According to the calculation of nickel cubic lattice, its period turned out to be α = 3,55 ±0,01 Å, which however is 0,03 Å higher, than in accordance to the reference data [10]. This can testify that in the initial state boron is in the form of over-saturated solid solution, as the equilibrium value of boron solubility, making 0,01%, should not have been reflected on the measured value of metal lattice period.

The amount of boron introduced into the coatings, depends on the factors determining the plating rateand other technological factors. As a result of heat treatment, Ni-B coatings undergo the structural-phase transformations and interact with air oxygen, therefore their properties are significantly changed. Thermoderivatographic research of the deposits made it possible to reveal the presence of two rapidly occurring irreversible exothermal effects (Fig.3). The positions of sharp peaks of the coatings with various boron contents on both derivatograms coincide. To clarify the nature of these transformations, 3-min annealing of the deposits was performed each 10 degrees within the intervals close to the transformations temperatures.
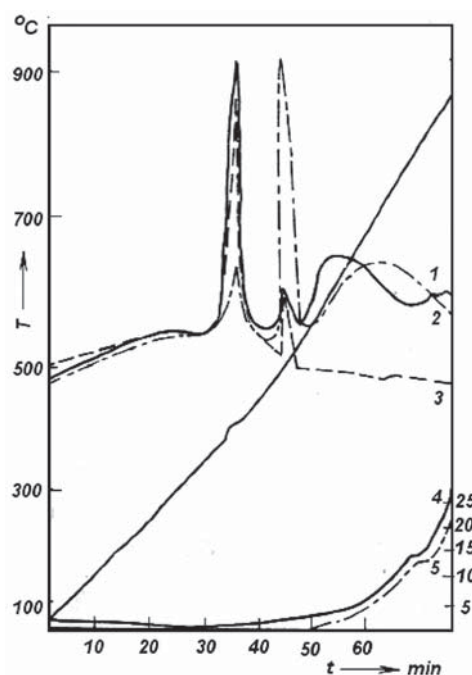
Fig. 3. ThermoderivogramsofNi-Bcoatings: 1, 2; 3 – DTA; 4, 5 – TG, in dependence of boron contents in the coatings;
1,4 – 4,3 weight% B;
2, 5 – 6,2 weight% B;
3 – 4,3 weight % B, annealing in vacuum.
Annealing time – 3 min.

It was found that up to 310 ℃on the samples' roentgenogramsthe weak diffusion bands of cubic nickel are observed against the background of broad bands of the roentgenoamorphous phase. Under the temperature 310 ℃and higher, in the deposits containing 6,2 weight % B, the clear crystalline phases appear, which have been identified as belonging to Ni_3B (main phase), Ni and Ni_2B. When the deposits containing 4,3 weight % of boron, are annealed to 400 ℃, there are weak bands of Ni_3B phase and the intensive amorphous background. Under the higher temperatures of heat treatment, the clear lines of crystalline phases Ni_3B and Ni_2B appear, the free nickel bands thus are absent.

Table 2

Comparative intensity of phase bands in dependence of heat treatment regimes

Temperature, ℃, (duration, min)	Identified phases (reflection bands)				
	Ni (200)	Ni_3B (211)	Ni_7B_3 (102)	Ni_2B (211)	NiO (200)
450 (3)	absent	1,8	5,8	2,4	absent
500 (30)	absent	2,0	1,9	6,1	absent
500 (60)	absent	5,3	absent	4,7	absent
500 (420 vac.)	absent	5,0	absent	5,0	absent
700 (10)	absent	1,3	6,0	2,7	absent
700 (30)	4,1	2,9	absent	3,0	absent
700 (120)	3,4	1,2	absent	0,8	6,6
700 (240)	5,6	1,1	absent	0,2	3,1
700 (420)	8,6	1,4	absent	absent	absent
700 (420 vac.)	absent	4,0	absent	6,0	absent

The bright bands of another phase were not possible to identify with the other well-known compounds of the system Ni– B (Ni_4B_3,NiB, NiB_2). They have been induced as belonging to the hexagonal crystal system with the parameters: a = 6,97±0,01 Å, c = 4,39±0,01 Å, c/a = 0,629. The registered 30 reflections only satisfy to the following rule of reflection:F_{hh2hl} = 0when $l = 2n +1$. These are typical for the following spatial Ferorov's groups: *P6₃/mmc, P6₃/mc, P62c.*

There are only two groups among the binary compounds, possessing the hexagonal cell, which sizes are close (a = 7-8 Å, c = 4,4-5 Å, c/a ≈ 0,629). To the first group belong the transition metal compounds with the elements of II-IV

groups from the Periodic Table: structural type Mn_5Si_3, Fedorov's symmetry group $P6_3/mmc$. The second group involves the borides of some transition metals, structural type Th_7Fe_3, Fedorov's symmetry group $P6_3mc$. Considering that with regard to extinction, the detected compound can only belong to the second type, we have supposed that it's formula is Ni_7B_3. This phase is thermally unstable and will be completely disintegrated within one hour under 400 ºC. Thus, the first exothermal peak on thermograms should be referred to the formation of Ni_3B phase, the second – mainly to the formation of Ni_7B_3. Formation of Ni_2B phase, detected on Roentgenograms as the weak lines, also occurs under this temperature, however, this thermoeffect, apparently, is overlapping by the stronger effect of Ni_7B_3 formation. It was found that the formation of this phase can occur under the lower temperatures, but with the longer exposition. Under 500 ºC and higher, both on the air and in vacuum, the intensity of bands Ni_7B_3 will be sharply decreased, and at the same time the intensity of Ni_3B and especially Ni_2B bands is increasing. With further heat treatment on air, the intensity of Ni_2B lines is decreased more rapidly than that of Ni_3B, the bands of nickel phases thus appear (Table 3). This makes it possible to suppose the reaction: $Ni_7B_3 \rightarrow 2Ni_2B + Ni_3B$.

Table 3

Crystallites size and contents in the free nickel phases under the various treatment regimes

Heat treatment conditions	Phases contents		
	Crystallites size, μ	I_{Ni}/I_{Ni2B}	Free nickel, %
On air			
250 ºC, 7 h	$2,4 \cdot 10^{-2}$	0,7	8
350 ºC, 5 min	$3,5 \cdot 10^{-2}$	0,6	7
350 ºC, 2 h	$4,4 \cdot 10^{-2}$	1,1	12
350 ºC, 4 h	0,2-5	2,3	22
500 ºC, 1 min	$1,5 \cdot 10^{-2}$	0,7	8
500 ºC, 15 min	0,2-5	3,2	28
500 ºC, 4 h	до80	5,1	38
700 ºC, 1 h	до 80	19,7	70
In vacuum			
275 ºC , 7 h	$2,2 \cdot 10^{-2}$	0,7	8
350 ºC ,200 h	0,2-5	0,6	7
500 ºC, 7 h	0,2-5	2,5	23
700 ºC, 1 h	0,2-5	1,8	18

As the thermal annealing, according to the standard technology, is carried out within the longer time – up to 1 hour and more to improve the coatings with metal, this phase cannot be registered.

The data given testify on the essential phase-dispersive transformations of Ni-B coatings under the low-temperature annealing, which may be reflected on their physical-mechanical characteristics. Therefore, the results of the research of polymetal boron-containing alloys may be of certain interest.

2. The deposition of polymetalic alloys from dimethylamine-borane.

The polycomponent nickel alloys with molybdenum, tungsten, rhenium and titan, obtained by autocatalytic (chemical-catalytic, electroless) reduction, have high catalytic activity[12,13]. The different complex experiments have been conducted in order to study the formation conditions and properties of these nanocatalytic systems and metal-oxide autocatalytic coatings with elevated photocatalytical activity for the destruction of high toxic organic pollutants.

The catalytic activity, chemical composition and structure of nickel-molybdenum-boron, nickel-tungsten-boron and nickel-rhenium-boron coatings were studied. Introduction of a doping element into nickel-boron alloy changes the catalytic activity of the alloy surface as regards the concurrent partial reaction of heterogeneous hydrolysis of dimethylamine borane (DMAB) $(CH_3)_2 HN \cdot BH_3$, reduction of nickel ions, evolution of molecular hydrogen, boron and carbon.

The aim of this study was to elucidate the causes for nonlinear, volcano-like dependence of partial rates of DMAB hydrolysis and hydrogen evolution on the concentration of the doping element in the alloy.

The acceleration of the DMAB heterogeneous hydrolysis is explained by the change in the catalytic activity of the coating surface as the result of the subsystem restructuring during the formation of an alloy between nickel and doping element.

It was shown that doping of Ni-B alloys with molybdenum as well as tungsten or rhenium sharply slows down the reaction rate of DMAB catalytic decomposition with the reduction of boron. Therefore the boron contents in the alloys is decreased with increasing of the alloying element concentration. The deposited alloys with the inclusion of rhenium only contain the trace amounts of boron.

The mechanism of autocatalytic reduction of metal ions is based on the catalysis of the reducing agent molecules oxidation (hydrolysis), with electrons transfer to the electrode surface, which shifts its potential to the values sufficient for metal ion reduction [16-19]. For example, if DMAB is used as a reducing agent for metal ions, the electrode potential in alkali solutions is a mixed potential of the following reactions:

1. $(CH_3)_2HN \cdot BH_3 + 3D_2O = 3H^0 + 3e + 3 D^+ + D_3BO_3 + (CH_3)_2HN = 3HD + D_3BO_3 + (CH_3)_2HN$
2. $(CH_3)_2HN \cdot BH_3 + D_2O = BH_3 + (CH_3)_2HND^+ + OD^- = B + 1,5H_2 + OD^- + (CH_3)_2HND^+ = B + 1,5H_2 + D_2O + (CH_3)_2HN$
3. $(CH_3)_2HN \cdot BH_3 + 3D_2O + 1,5 Ni^{2+} = 1,5 Ni^0 + 1,5H_2 + 3D^+ + D_3BO_3 + (CH_3)_2HN$
4. $7(CH_3)_2HN \cdot BH_3 + 12D_2O + 3 ReO_4^- = 3Re^0 + 10,5H_2 + 3OD^- + 7D_3BO_3 + 7(CH_3)_2HN$
5. $ReO_4^- + 4H_2O + 7e = Re^0 + 8OH^-$.
   ("D" means hydrogen from water.)

The first two reactions characterize the possible routes of the DMAB hydrolysis. Out of these, the first reaction is the electron donor. Using mass spectroscopic studies it was shown that oxidation of hydride hydrogen in alkaline media (pH 10) duringheterogeneous DMAB hydrolysis proceeds to atomic hydrogen (reaction (1)). Herewith, three electrons are generated per single dimethylamine borane molecule and molecular hydrogen H_2 formed according to reactions (1) and (3) is a quantitative indicator of occurrence of the DMAB hydrolysis reaction [18].

It was established in the previous studies of the processes of autocatalytic deposition of multicomponent alloys that doping of the nickel-boron coating by molybdenum or tungsten affects significantly the rates of partial coupled reactions: DMAB hydrolysis, hydrogen evolution, and nickel deposition [13,14,19,20]. In the case of molybdenum, a non-monotonous dependence of the rates of partial reactions on the molybdate concentration in the solution and accordingly on molybdenum content in the alloy was found [21]: an increase in the rates of DMAB hydrolysis, nickel ion reduction and molecular hydrogen evolution was observed in the range of sodium molybdate concentrations of 0-4 mM.

Comparison of the research results on the influence of the molybdate concentration on the kinetics of the partial processes of the molecular hydrogen isolation and the deposition of the Ni-Mo-B alloys indicates on a significant role of concentration at kinetic parameters of these reactions.Increasingin $K_4P_2O_7$ concentrations from 0,15 to 0,30 M/l reduces the rate of partial reactions of autocatalytic process and shifts the maximum catalytic activity of the coating in the direction of higher molybdenum contents in the alloy from 6,0 to 9,0 at.%.

There was a significant difference in the nature of rhenium influence on the deposition rate of nickel in comparison with molybdenum or tungsten.
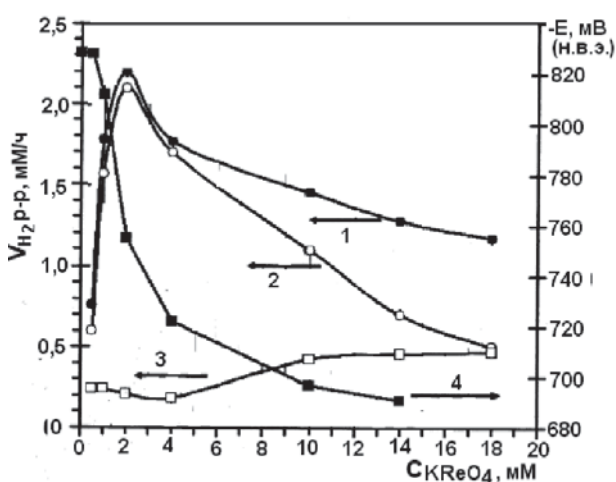

Fig. 4. Effect of potassium perhenate concentration on the kinetic parameters of plating and composition of nickel-rhenium-boron coatings:
 1 – summary amount of hydrogen;
 2 – hydrogen evolved as a result of DMAB hydrolysis;
 3 - hydrogen evolved following the reaction 3 and 4;
 4 – stationery potential of electrode.

With the increase in molybdenum or tungsten contents in the alloy, the deposition rate and rate of hydrogen evolution are changing symbatically. Doping of the same alloy with rhenium at low concentrations, accelerates the process of hydrogen evolution, but also provokes the lowerrate of nickel reduction.The observed features may be connected with the fact that molybdenum and tungsten are not allocated as a separate phase. The reduction rate of ions is determined

by the balance of the rate of hydrolysis DMAB and nickel reduction. The rhenium is emitted in the electrochemical reduction of perhenate in a form of separate phase. Therefore with joint autocatalytic reduction of nickel and rhenium ions, there may be a possible competition of these process (reactions 3 and 5). But rhenium is not a catalyst for the hydrolysis of DMAB, and apparently direct reaction 4 is not realized.Thus, despite the differences in the mechanism of the reactions of co-deposition of molybdenum, tungsten and rhenium with nickel, the processes have common features – namely: the dependence of the rate of the alloying component on the kinetics of the reduction of nickel ions. The rate of rhenium reduction is determined by the kinetics of nickel active surface formation and therefore the composition of the alloy weakly depends on the concentration of perhenate in solution.
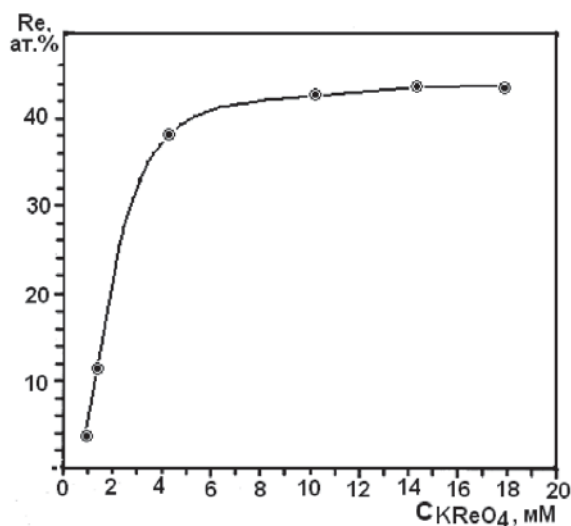
Fig. 5. Effect of perhenate concentration on rhenium contents in the nickel-boron compounds composition

The reaction of hydrogen evolution in acidic and alkaline mediums has been studied by the potentiodynamic polarization curves. Alloying of Ni-B with rhenium (11 wt.%) reduces the overvoltage of hydrogen evolution by 200 mV.

The catalytic activity of alloys for the DMAB hydrolysis reaction has been tested in the solution without the metal ions. Maximum electrode potential for hydrolysis of DMAB is achieved with electrolytic nickel, where hydrogen overvoltage in the system is maximum, too. The lower potential is installed at the electrodes of the Ni-B alloy. For Ni-Re-B alloys with rhenium contents of 11 and 38 at.%, the stationary potential is minimum. The increase of the potentialof the DMAB hydrolysis at the Ni-Mo-B alloy is slightly higher than at the Ni-Re-B alloys.

The only depolarizer in these systems is hydrogen ion (reaction 1). Therefore, stationary potential of theelectrode is determined by the balance of the DMAB hydrolysis rate and discharge of hydrogen ions. Thus, the decreasing of electrode potential with the increase of molybdenum and rheniumcontents in the alloy may be due to either a high rate of hydrogen ions discharge, or decrease in the catalytic activity of alloys in the reaction of heterogeneous DMAB hydrolysis. The overvoltage of hydrogen evolution reaction on the alloy with molybdenum or rhenium varies slightly. Therefore, the decreasing stationary potential of hydrolysis electrode is a result of the decreasing of DMAB heterogeneous hydrolysis rate. This conclusion is confirmed by the studies of DMAB hydrolysis kinetics at the electrodes with different contents of rhenium (11,0, 40,0 and 45,0 at.%) in the solutions without the metal ions.

One reason for the lower efficiency of DMAB at the deposition of nickel-molybdenum, nickel-tungsten-boron and nickel-rhenium-boron alloys is the extremely low overvoltage of hydrogen evolution reaction. For example, the efficiency of DMAB makes 75% during the deposition of nickel-boron coatings and only reaches 17% for nickel-rhenium-boron alloy with 11 at.% of rhenium. Although the dopingof nickel-boron alloy with other metals in low contents dramatically accelerates the hydrolysis of DMAB, the rate of polycomponent deposition is low, as the result of parasitic process of hydrogen ions discharge from water.

Examining the possible causes of the relationship changing between the rate of the partial reactions of hydrogen evolution and the rate of metal ions discharge depending on the contents of the alloying component, the different pH dependence of near-electrode zone of rates of reactions 3 and 5 should be taken in consideration. During the reduction of nickel (reaction 3), the acidification of the reaction zone occurs, and during the reduction of alloying component (reaction 4 or 5) – alkalization.

Since the rate of chemical-catalytic reactions considerably depends on the acidity of the medium, the reactions of nickel reduction and alloying agent reduction are conjugated and determine the partial reduction rate of nickel and molybdenum (tungsten, rhenium).Thus, during the autocatalyticreduction the self-organization occurs of thenext reactions' rate: DMAB hydrolysis, hydrogen ions discharge and metal (nickel, alloying metal) reduction. Therefore, the introduction in the plating solution of ligand-forming complexes with nickel ions, has a significant influence on the kinetics of all

partial reactions. While discussing the possible reasons of catalytic activity of the electrode in the reactions of hydrogen evolution and the DMAB hydrolysis, the surface morphology and phase structure of alloys needs to be considered.

To estimate the effect of these factors on the partial reactions'kinetics of metal ions autocatalytic reduction, the structure of coatings and uniformity of element distribution was studied. According to the results of X-ray analysis, Ni-Mo-B and Ni- Re-B coatings have nanocrystalline structure and Ni-W-B - amorphous structure.

The estimation of nanocrystal size by broadening reflex (111) gives value less than 20 nm. The alloys with this minimal size of nanocrystals have maximum catalytic activity. The several-micron size somatoids, formed from smaller particles, have been found on the coating's surface. The macro-scale distribution of high elements within the volume of coating is uniform, but at the nano-scale the nanocrystals have a bulbous structure with uneven distribution of alloying element on the grain's body. The small size of crystals, a highly developed surface and heterogeneity of composition of coatings (in nano-scale) play an important role in determining of the adsorption heat, the degree of surface coverage, orientation of DMAB molecules and intermediates formed at various stages of oxidation of DMAB.The DMAB adsoption on the electrode surface not only reduces the barrier height of the successive steps ofDMAB oxidation, but,according to the results of a study of the hydrogen evolution kinetics, reduces the rate ofatomic hydrogen recombination as well.

Therefore, the introduction of molybdenum and rhenium into nickel-boron alloys change their catalytic activity in the next reactions: concurrent partial processes of DMAB heterogeneous hydrolysis, reduction of nickel ions, evolution of molecular hydrogen, elemental boron and carbon in the form of alloying metal carbide.

The observed acceleration of DMABheterogeneous hydrolysis is explained by the change in catalytic activity of coatings as the result of the subsystem restructuring during the formation of alloy between nickel and doping element.

To clarify the causes, determining the dependence of DMAB electrocatalytic hydrolysis kinetics, reduction of nickel and hydrogen ions from the concentration of alloying component (molybdate, tungstate, perhenate), the additional studies have been performed.

As soon as rhenium, in contrast to molybdenum and tungsten, do not form passive surface film of semi-product reduction of perhenate, it eliminates the effect of coating passivation during the DMAB hydrolysis. Taking into account that these alloying metals are characterized by low potential of hydrogen evolving, it can be expected that introduction of rhenium in the nickel-boron alloy can affect the rate of nickel and hydrogen ions partial reduction. The development of nickel-rhenium-boron alloys obtaining ways is also a matter of independent interest as a method of a nanocrystalline material with high catalytic activity creating.

At sodium tungstate concentrations of 300 mMand potassium perhenate concentrations of 18 mM, the volcano-like partial rates of Ni-W-B and Ni-Re-B deposition and the molecular hydrogen release rate were revealed. The maximum deposition rate is within the range of tungstate concentrations of around 50 mM and perhenate concentrations of around 2mM, accordingly. At higher concentrations of potassium perhenate, the sharper decrease in partial process rate, compared to the deposition of Ni-W-B alloy, was observed. That may be due to the strong pH increasein the reaction zone due to the high rate of rhenium incorporation in the alloy. Thus, rhenium contents in the deposit reaches 44-54 at.%.
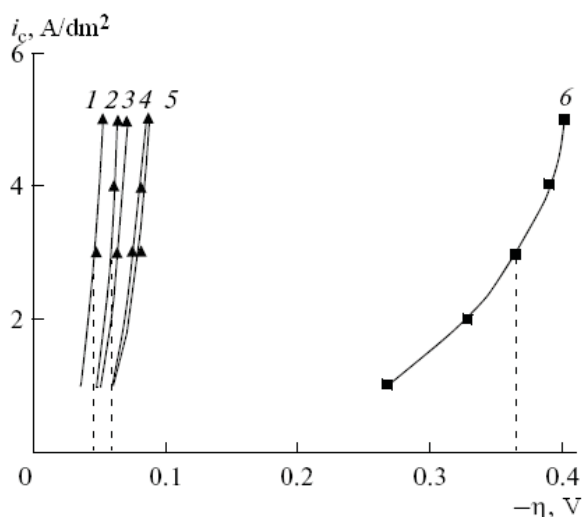

**Fig. 6. Dependence of hydrogen evolving voltage from the cathode current density $i_c$in 0,5 M H$_2$SO$_4$ solution:
1 – Pt-covered platinum(Pt); 2 - Ni-Re (4 at.%)–B; 3 - Ni-Re (4 at.%)–B; 4 - Ni-Re (11 at.%)–B; 4 - Ni-Re (38 at.%)–B; 5 - Ni-Re (45 at.%)–B; 6 - Ni-Re (45 at.%)–B; 6 - Ni–B.**

As follows from the data shown on Fig.6, hydrogen emission overvoltage in 0,5 M H_2SO_4 solution on the surface of Ni-Re-B alloys with the various contents in rhenium essentially decreases (from -0,365 to -0,060-0,080 V under 3 A/dm^2), compared to the Ni-B coating. The lowest overvoltage of hydrogen emission is observed on the alloys with Re contents 4-11 %, the overvoltage values being close to ones on the Pt-coated platinum, making -0,046 V under i_c = 3 A/dm^2. With the increase in rhenium contents in the alloy, hydrogen discharge overvoltage is increased in average by 0,020 V. This can characterize the higher electrocatalytic properties of Ni-re coatings, that can be used, for instance, in hydrogen power engineering [21, 22].

Apparently, for Ni-W-B system, the decrease of partial reaction rates after maximum is associated with the accumulation of W compounds in the reaction zone. With the increase in sodium tungstate concentration in solution, the contents in tungsten in the alloy inreases, reaching the values of 4 ,0 at.% at 200 mM.

We have also studied the theoretical bases of the processes, which lead to photocatalytic activity of some metal oxides. New method of photocatalytically active coatings obtaining, including the deposition of autocatalytic Ni-Ti-B and Ni-Re-B alloys, has been proposed. The deposition occurs on a porous ceramic base from the solution, containing nickel sulfate, titanium lactate or potassium perhenate, lactic or boric acid, thiourea, ammonium hydroxide and dimethylamineborane as reducing agent. After the coatings formation, they were anodized in the electrolyte containing titanium potassium oxalate, oxalic acid and boric acid at the current density of 0,5-1,0 A/dm^2, voltage 27-30 V and electrolysis duration of 30-60 minutes.

In this way, it was found that Ni-B coatings in the initial state represent a solid solution of boron in nickel, whereas the average size of nickel crystallites in the direction (III) is within the range of 40-60 Å. Under the short-term annealing up to 320-350 °C, the phase Ni_3B is formed, and under the further annealing up to 410-420 °C within the several minutes of exposure – phase - фаза Ni_2B, as well as a new phase, which supposed composition is Ni_7B_3. However, this phase is thermally unstable and is decomposed to Ni_2B and Ni_3B the faster, the higher is an annealing temperature.

CONCLUSIONS

1. It was found that the structure of chemically plated Ni-containing coatings obtained from the boron-hydride solutions, represents in the initial state the oversaturated boron interstition solid solution into the nickel crystal lattice, with the dimensions of 40-60 Å in the direction (111), whereas in the direction (200) –no more than 15-20 Å;

2. The nature of structural-phase transitions which occur during the thermal processing of Ni-B coatings was established; the formation of a new intermediate phase was revealed, identified as a Ni_7B_3, which is thermally unstable, and will be decomposed forming Ni_2B and Ni_3B within one hour-time under the temperature $\geq$ 400 °C;

3. The essential reducing of hydrogen evolving overvoltage has been found, due to the alloying of Ni-B coatings with rhenium (11 at.%) in the solutions containing dimethylamine-borane. This effect can be used for the development of a type new reactor for the electrochemical generation of hydrogen.

ACKNOWLEDGEMENT

REFERENCES

[1]. Gorbunova, K.M.; Ivanov, M.V. Application of metal coatings with the help of boron-containing reducers. Science Resume: Electrochemistry, M.: VINITI, 1977, 1970, 12, 122 p.

[2]. Petrov, Yu.N.; Covaliov, V.V.; Marcus, M.M. *Proc. Acad. Sci. USSR*, 1971, 198, Nr.4, pp 118-121.

[3]. Covaliova, O.V.; Covaliov, V.V. Patent Nr.2913 (MD).Method of electrochemical deposition of soldering Ni-Sn-B coatings, BOPI, 2005, 11.

[4]. Covaliova, O.V.; Ivanov M.V.; Covaliov, V.V. Patent Nr.2912(MD). Method of plating of Ni-Cu deposits. BOPI, 2005, 11.

[5]. Covaliova, O.V.; Covaliov, V.V.; Ivanov M.V.; Duca, Gh.G. Patent Nr. 3806 (MD). Method of obtaining of photocatalitically active deposits. BOPI, 2009, 1.

[6]. Covaliova, O.V.; Covaliov, V.V.; Ivanov M.V. Patent Nr.4318 (MD). Chemical deposition of boron-containing metal layers. BOPI, 2007, 10.

[7]. Covaliova, O.V.; Covaliov, V.V.; Ivanov M.V. Patent Nr.244Y (MD). Electrode for electrolytic obtaining of hydrogen and process of its manufacturing. BOPI, 2010, 7.

[8]. Covaliov, V.V.; Covaliova, O.V.; Ivanov M.V. Patent nr.3275 (MD). Device for chemical metallization of fine non-metal particles. BOPI, 2007, 3.

[9]. Covaliova, O.V.; Covaliov, V.V.; Ivanov M.V. Patent Nr.2799(MD). Method of composite chemical coatingsdepositing. BOPI, 2005, 6.

[10]. Markin, L.I. Reference Book on Roentgen-structural analysis, M: Fizmatgiz Publ., 1961.

[11]. Kovba, L.M.; Trunov V.K. Roentgen-Phase analysis. M: MGU Publ., 1969.

[12]. Krutskich, V.M.; Ivanov, M.V.; Drovosekov, A.B.; Polukarov, Yu.M.*Zaschita Met*., 2005, 41, p451.

[13]. Drovosekov, A.B.; Ivanov, M.V.; Krutskich, V.M.; Lubnin, E.N.; Lyakhov, B.F. *Zaschita Met*., 2005, 41, p61.

[14]. A.F.Bogenshyutts, U.George, Electrochemical Alloy Coating. Methods of Analysis, Moscow: Metallurgiya, 1980, p67.

[15]. Homma, T.; Komatsu, I.; Tamaki, A.; Nakai, H.; Osaka, T. *Electrochim. Acta,* 2001, 47, p47.

[16]. Homma, T.; Tamaki, A.; Nakai, H.; Osaka, T. *J. Electroanal. Chem*., 2003, 559, p131.

[17]. Krutskich, V.M.; Ivanov, M.V.; Glazunov, M.P.; Gubin, V.V. *Electrokhimiya*, 1994, 30, p278.

[18]. Drovosekov, A.B.; Ivanov, M.V.; Krutskich, V.M.; Polukarov,Yu. M. *Zaschita Met*., 2005, 41, p4511.

[19]. Krutskich, V.M.; Ivanov, M.V.; Drovosekov, A.B., Polukarov Yu.M. *Electrokhimiya*, 2008, 44, p784.

[20]. Ivanov, M.V.; Covaliov, V.V.; Covaliova, O.V. In: The 3rdIntl.Conf. on Ecological Chemistry. Book of Abstracts. Chisinau, Moldova, 2005, pp 145-147.

[21]. Covaliova, O.V.; Covaliov, V.V.; Ivanov, M.V.; Polukarov. Yu.I. *Studia Universitatis*, Chisinau, 2010, 1 (31), pp 188-198.

[22]. Covaliova, O.V.; Covaliov, V.V.; Duca, Gh.; Ivanov M.V. *Probl. of Reg. Power Eng*., 2011, 1, p1-17.

DINUCLEAR COMPLEXES AS BUILDING BLOCKS FOR TETRA-NUCLEAR MACROCYCLIC COMPLEXES WITH DITHIOLATE MACROCYCLIC LIGAND

Vasile Lozan

Institute of Chemistry ASM, Academiei str., 3, Chisinau, MD 2028, R. Moldova
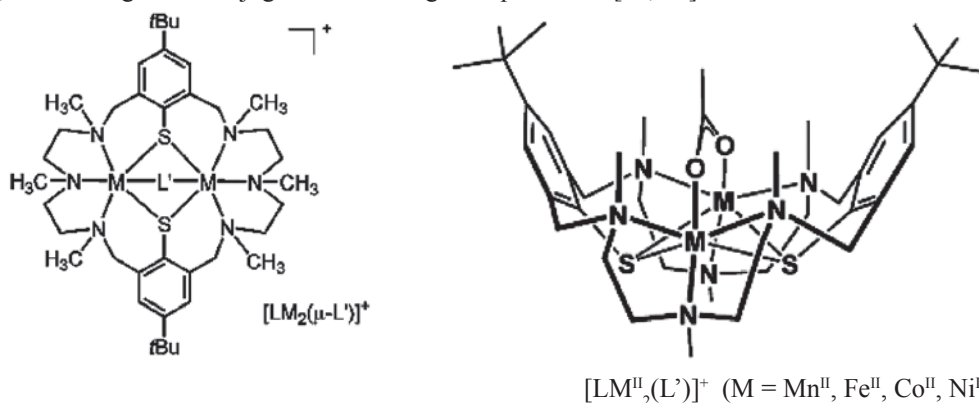e-mail: vasilelozan@gmail.com

Abstract: A series of novel tri-, tetra- and pentanuclear complexes composed of dinuclear LM_2 units (M=Co, Ni, Zn; L=24-membered macrocyclic hexaaza-dithiophenolate ligand) and ferrocene-carboxylate ($[CpFeC_5H_4CO_2]^-$), 1,1'-ferro-cenedicarboxylate($[Fe(C_5H_4-CO_2)_2]^{2-}$), acetylenedicarboxylate, terephthalate, isophthalate, and naphthalene diimide dicar-boxylate groups is reported. The complexes have been synthesized and characterised by UV/Vis-, IR-spectroscopy, and X-ray crystallography. Each dicarboxylate dianion acts as a quadridentate bridging ligand linking two bioctahedral LM_2 units via $\mu_{1,3}$-bridging carboxylate functions to generate discrete dications with a central $LM_2(O_2C-R-CO_2)M_2L$ core.

Keywords: coordination chemistry, amino-thiophenolate ligands, di- and tetranuclear complexes, ferrocene and naphthalene diimide derivatives, polynuclear complexes

1. Introduction

The chemistry of container molecules has developed extensively over the past two decades. Many container molecules such as calixarenes, resorcarenes, cyclodextrins, carcerands and glycourils have been invaluable in studying the fundamental principles of inclusion phenomena and consequently their use in separation science or drug delivery, as two examples of application. Importantly, the area has attracted interest in the field of supramolecular chemistry because the properties of such host–guest compounds are often different from those of their constituent components. By adjusting the size and form of the binding cavity it is often possible to complex co-ligands in unusual coordination modes, to activate and transform small molecules, or to stabilize reactive intermediates [1, 2]. One subclass are the metallated container molecules, in which metal ions and clusters are used as both a point of recognition and to give the container a well-defined structure. Such compounds also allow for an interplay of molecular recognition and transition-metal catalysis, and for the construction of more effective enzyme mimics. Of interest to the present work is the ability of metallocavitands to recognize and encapsulate difunctionalised molecules towards stabilising or enhancing the optical and electronic properties of redox- and photo-active compounds within a confined environment set up by two hemispheres.

The carboxylate group, RCO_2^-, can bind to transition metals in a variety of coordination modes giving rise to complexes of great structural diversity [3]. Current activities focus on the coordination chemistry of polycarboxylate ligands, as these offer great potential in the construction of polynuclear aggregates [4] and extended coordination polymers with micro- and mesoporous structures [5–8] or catalytic properties [9]. In addition, polycarboxylate ligands are of importance as spin-coupling bridging ligands [10–17] in the rapidly expanding field of molecular magnetism [18, 19]. In this context, an enormous amount of literature has been generated concerning the distance dependence of magnetic exchange interactions between metal atoms linked by extended dicarboxylate ligands. Dinuclear copper complexes bridged by oxalate [20, 21] and terephthalate [22–24] dianions form, by far, the largest group of such systems, and it appears that the exchange interactions depend on the M···M distance [25], the relative orientation of the magnetic orbitals [26], and the degree of conjugation of the organic spacer unit [27, 28].
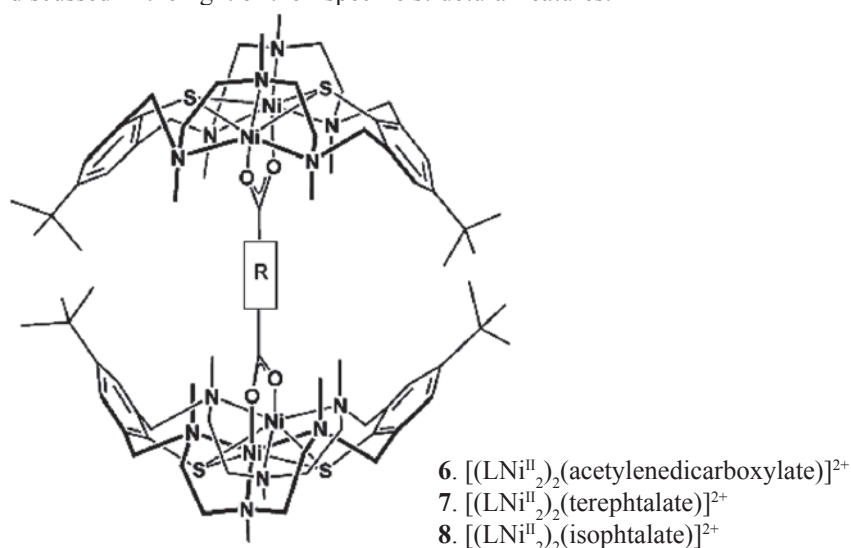

$[LM_2(\mu\text{-}L')]^+$ $[LM^{II}_2(L')]^+$ (M = Mn^{II}, Fe^{II}, Co^{II}, Ni^{II})

1. $[(LNi^{II}_2(\mu\text{-}Cl)]^+$ **2**. $[(LCo^{II}_2(\mu\text{-}Cl)]^+$ **3**. $[(LZn^{II}_2(\mu\text{-}OAc)]^+$ **4**. $[(LCo^{II}_2(\mu\text{-}OAc)]^+$ **5**. $[(LNi^{II}_2(\mu\text{-}OAc)]^+$
Scheme 1. Dinuclear acetate-bridged complexes of the hexaaza-dithiophenolate ligand L^{2-} and their label.

Recently, we reported the structures and magnetic properties of an isostructural series of bioctahedral $[LM^{II}_2(OAc)]^+$ complexes, where L^{2-} represents a macrodinucleating N_6S_2 supporting ligand (Scheme 1) [29]. Intramolecular antiferromagnetic exchange interactions are present in the Mn^{II}_2, Fe^{II}_2 and Co^{II}_2 complexes of this series with J values of -5.1, -10.6, and -2.0 cm^{-1}(H = $-2JS_1S_2$). In contrast, in the corresponding Ni^{II}_2 complex a ferromagnetic exchange interaction is present with $J = +6.4$ cm^{-1}.

2. Dicarboxylate dianions as a tetradentate bridged ligands.

In view of the increasing interest in the targeted assembly of molecular-based magnetic materials using high-spin molecules of higher nuclearity [30–36], we considered it worthwhile to examine the possibility of linking pairs of dinuclear $[LNi^{II}_2]$ units by dicarboxylate dianions to form tetranuclear species. In the present contribution we report the synthesis and crystallographic characterization of three tetranuclear nickel (II) complexes of the type $[LNi^{II}_2$dicarboxylate$Ni^{II}_2L]$, where "dicarboxylate" stands for acetylenedicarboxylate, terephthalate, or isophthalate dianions. A schematic representation of these complexes is shown in Scheme 2. These complexes differ by the distance between the centre of the Ni···Ni axis of the isostructural LNi_2 subunits, their relative orientation, and the nature of the bridging ligands. The ability of the dicarboxylate dianions to mediate magnetic exchange interactions between the dinuclear subunits is examined and discussed in the light of their specific structural features.

6. $[(LNi^{II}_2)_2(\text{acetylenedicarboxylate})]^{2+}$
7. $[(LNi^{II}_2)_2(\text{terephtalate})]^{2+}$
8. $[(LNi^{II}_2)_2(\text{isophtalate})]^{2+}$

Scheme 2. Complexes prepared and their labels.

The complexes $[(LNi^{II}_2)_2(\text{acetylenedicarboxylato})]^{2+}$ (**6**),$[(LNi^{II}_2)_2(\text{terephthalato})]^{2+}$ (**7**), and $[(LNi^{II}_2)_2$ (iso-phthalato)$]^{2+}$ (**8**) were readily prepared from the reaction of the dinuclear complex $[LNi^{II}_2(\mu\text{-Cl})]^+$ (**1**) and the corresponding triethylammonium dicarboxylate, prepared in situ from the acid and triethylamine in methanol in a 1:2 molar ratio, and isolated in high yield as the perchlorate or tetraphenylborate salts. The transformations are not simple substitution reactions, because simultaneous conformational changes of the supporting ligand L^{2-} from the folded (C_s-symmetric) to the "bowl-shaped" (C_{2v}-symmetric) conformation take place (see Scheme 3) [37].
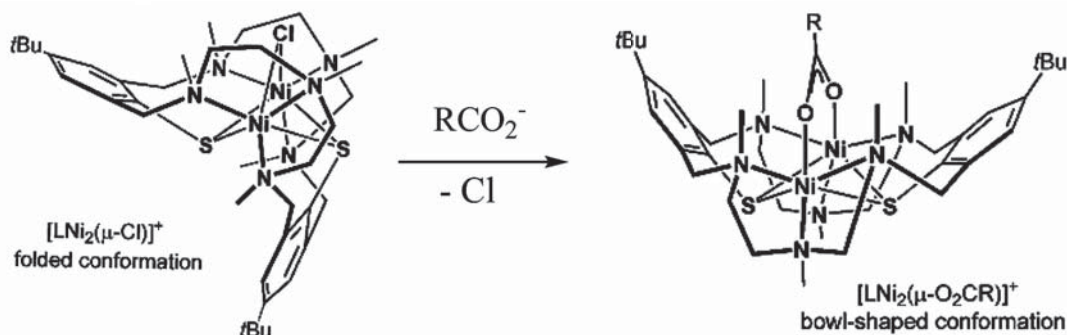
Scheme 3. Schematic representation of the two ligand conformations in the chloro- and carboxylato-bridged complexes of (L)$^{2-}$. For these conformational changes metal–ligand dissociations are required.

Nonetheless, linking of two $[LNi_2]^{2+}$ fragments by the carboxylato ligands is a clean and facile step driven by the low solubility of the products.

All compounds gave satisfactory elemental analyses and their IR spectra are marked by the prominent asymmetric and symmetric carboxylate stretching frequencies around 1580 cm^{-1} and 1420 cm^{-1}, diagnostic of $\mu_{1,3}$-bridging carboxylate functions [38]. The UV/Vis spectra of **6–8** in acetonitrile display two weak bands above 500 nm typical of octahedral Ni^{2+} (d^8, S = 1) ions. The observed values compare closely with those of the acetato-bridged complex [LNi$^{II}_2$(OAc)]$^+$ [29], indicative of a pseudo-octahedral N$_3$S$_2$O coordination environment about the metal ions. This is confirmed by single-crystal X-ray crystallography.

Crystals of **6**[BPh$_4$]$_2$·2MeCN·0.5H$_2$O were obtained by slow evaporation of an acetonitrile/ethanol (1:1) solution of **6**[BPh$_4$]$_2$. The crystal structure is composed of tetranuclear [(LNi$^{II}_2$)$_2$(acetylenedicarboxylate)]$^{2+}$ dications, tetraphenylborate anions and acetonitrile and water solvates. Perspective drawings of the structure of **6** are depicted in Figure 1.
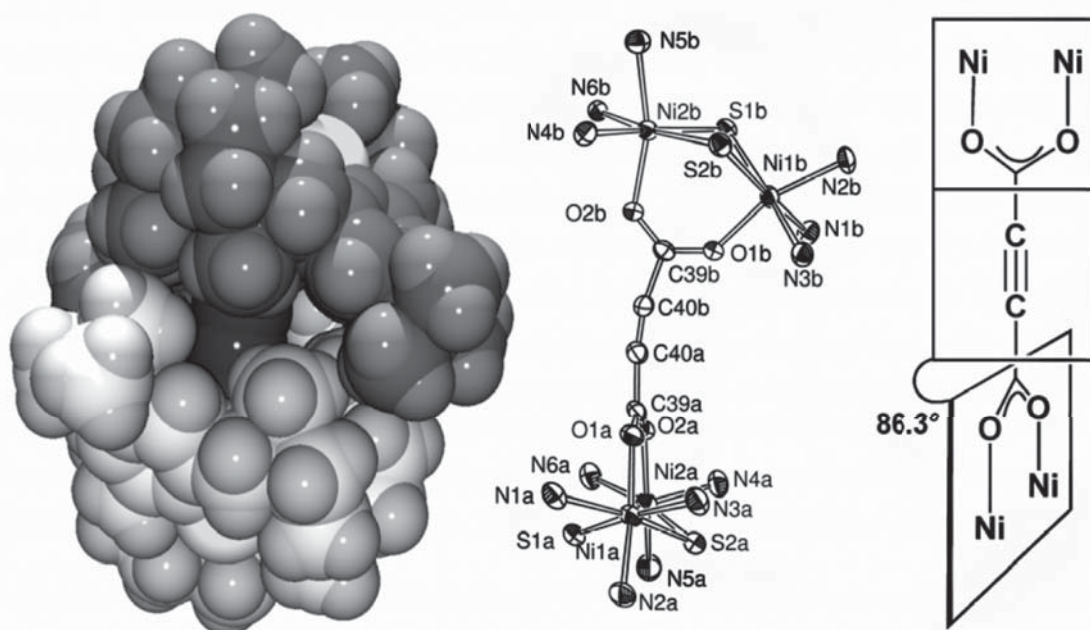
Figure 1. Left: Van der Waals plot of the [(LNi$^{II}_2$)$_2$(μ-acetylenedicarboxylato)]$^{2+}$ dication in crystals of **6**[BPh$_4$]$_2$·2MeCN·0.5H$_2$O. Middle: ORTEP representation of the core structure of **6** with the atom labeling scheme. Ellipsoids are represented at the 50% probability level. Right: Mutual orientation of the Ni$_2$carboxylato planes in **6**.

The acetylenedicarboxylate dianion acts as a tetradentate bridging ligand joining two dinuclear [LNi$^{II}_2$]$^{2+}$ fragments through its carboxylate functions to give a tetranuclear Ni$_2$-(O$_2$CC≡CCO$_2$)-Ni$_2$ array. Each nickel atom is surrounded in a highly distorted octahedral fashion by two sulfur atoms and three nitrogen atoms from the supporting ligand, and one oxygen atom from the acetylenedicarboxylate moiety. The Ni$_2$carboxylato planes are necessarily twisted by 86.3° about the C≡C bond to relieve the unfavourable steric interactions between the bulky *t*Bu groups of the two opposing [LNi$^{II}_2$]$^{2+}$ subunits. The coligand is also slightly bent (C≡C 1.185(6) Å) such that the intramolecular distances between two nickel atoms of different dinuclear subunits within the tetranuclear complex range from 8.623(1) to 9.769(1) Å. The only system comparable to that of **6** is provided by the complex [{Mo$_2$(DAniF)$_3$}$_2$(O$_2$CC≡CCO$_2$)], where DAniF = N,N'-di-*p*-anisylformamidinate, for which an intramolecular Mo···Mo distance of 9.537 Å has been reported [39]. There are no significant intermolecular interactions between the Ni$^{II}_4$ complexes within the lattice. The shortest intermolecular Ni···Ni distance is at 7.470(1) Å.

Figure 2 shows the structure of the tetranuclear nickel(II) complex **7** in crystals of **7**[BPh$_4$]$_2$·2EtOH·0.5MeCN·H$_2$O. Again, the terephthalato ligand acts as a bifunctional linker coordinating to two bioctahedral [LNi$^{II}_2$]$^{2+}$ entities via the carboxylate functions to generate a twisted Ni$_2$-O$_2$C–C$_6$H$_4$–CO$_2$-Ni$_2$ motif.

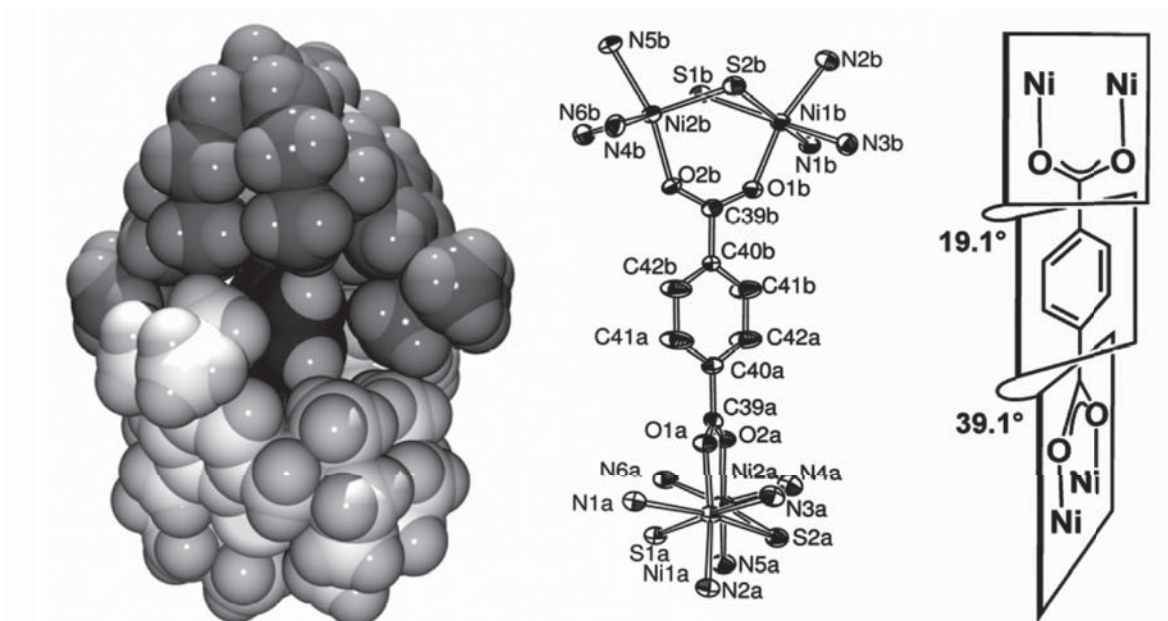**Figure 2. Left: Van der Waals representation of the [(LNi$^{II}_2$)$_2$(μ-terephthalato)]$^{2+}$ dication in crystals of 7[BPh$_4$]$_2$·2EtOH·0.5MeCN·H$_2$O. Middle: ORTEP representation of the core structure of 7 with the atom labeling scheme. Ellipsoids are represented at the 50% probability level. Right: Relative orientation of the Ni$_2$carboxylato planes in 7.**

The [LNi$_2$]$^{2+}$ subunits in **6** and **7** are structurally very similar, and the Ni–N, Ni–O, and Ni–S distances lie within very narrow ranges. As in **6**, the *t*Bu groups of the two opposing Ni$_2$ clusters are forced to interlock to accommodate the terephthalato ligand. This causes tilting of the carboxylato planes that are rotated by 58.2° with respect to each other and by 19.1° and 39.1° with respect to the aromatic ring of the terephthalato coligand. Again, there are no intermolecular interactions between the tetranuclear complexes other than van der Waals contacts. The intramolecular Ni···Ni distances between the two dinuclear subunits are within the range 10.833(1) –11.155(1) Å (mean 10.990(1) Å). This is a typical value for terephthalato-bridged nickel(II) complexes [40,41].

Crystals of **8**[BPh$_4$]$_2$·4MeCN·EtOH are triclinic, space group P1. ORTEP views of the structure of the dication **8** and the central core are provided in Figure 3.
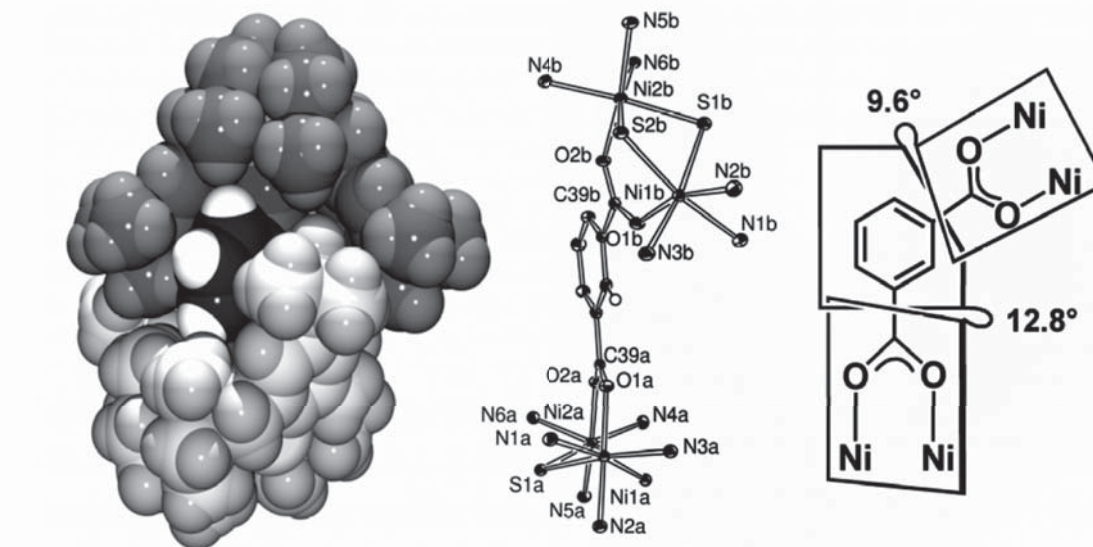

Figure 3. Left: ORTEP view of the [(LNi$^{II}_2$)$_2$(μ-isophthalato)]$^{2+}$ dication in crystals of 8[BPh$_4$]$_2$·4MeCN ·EtOH. Middle: ORTEP representation of the core structure of 8 with the atom labeling scheme. Ellipsoids are represented at the 50% probability level. Right: Tilting of the Ni$_2$carboxylato planes in 8.

The isophthalate dianion is bonded to two [LNi$^{II}_2$]$^{2+}$ units through $\mu_{1,3}$-bridging carboxylate functions. The metal–ligand bond lengths within **8** reveal no anomalies and are very similar to those in **6** and **7**. Strangely, the twisting of the carboxylato planes is less pronounced than in the previous cases. In fact, the two planes are almost coplanar with the phenyl ring of the bridging isophthalate dianion. The geometrical requirements of the isophthalate moiety with the two carboxylate functions in *meta* orientation leads to a distance of 9.561 Å between the center of the Ni···Ni axes of the dinuclear units. This value should be compared with that of 10.712 Å in **7**, where the two carboxylate functions are in *para* positions. The present coordination mode of the isophthalate dianion forming a discrete Ni$^{II}_4$ cluster is without precedence in the literature [42–44].

The magnetic properties of the three carboxylato-bridged complexes were examined in view of literature reports that conjugated dicarboxylate ligands are able to mediate long-range magnetic exchange interactions between paramagnetic metal ions [45]. The variable-temperature magnetic susceptibility data for **6**[BPh$_4$]$_2$, **7**[BPh$_4$]$_2$, and **8**[BPh$_4$]$_2$ were measured over the range 2.0-295 K using a SQUID magnetometer and an applied external magnetic field of 0.2 T. Plots of the temperature dependence of the effective magnetic moment for μ_{eff} the three compounds are shown in Figure 4. The complexes have similar magnetic properties. At room temperature, the respective values of μ_{eff} are 6.91 μ_B, 6.82 μ_B, and 7.13 μ_B per tetranuclear complex. With decreasing temperature the μ_{eff} values increase steadily to maximum values of 7.85 μ_B (15 K), 7.71 μ_B (15 K), and 8.03 μ_B (25 K) for **6**[BPh$_4$]$_2$, **7**[BPh$_4$]$_2$, and **8**[BPh$_4$]$_2$, respectively. On lowering the temperature to 2.0 K, these values decrease slightly down to 7.57 μ_B, 7.02 μ_B, and 5.78 μ_B at 2 K, presumably due to saturation effects or the zero-field splitting of nickel(II).
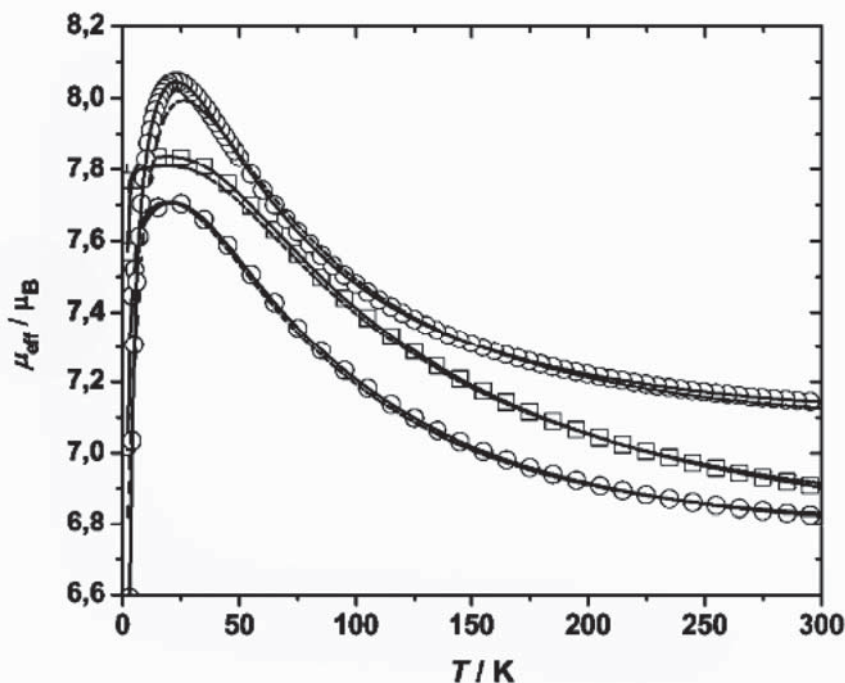

Figure 4. Temperature dependence of μ_{eff} (per tetranuclear complex) for 6[BPh$_4$]$_2$ (open squares), 7[BPh$_4$]$_2$ (open triangles), and 8[BPh$_4$]$_2$ (open circles). The full lines represent the best theoretical fits.

In all cases the maximum value of the effective magnetic moment is lower than expected for a spin-only value of 9.84 μ_B for $S_T = 4$ resulting from ferromagnetic coupling of four Ni^{II} ($S_i = 1$, g = 2.20) ions. However, the values are also significantly larger than the value of 6.22 μ_B calculated for completely uncoupled spins. The overall behaviour indicates the presence of weak ferromagnetic exchange interactions between the Ni^{2+} ions within the dinuclear subunits, but negligible, if any, coupling across the dicarboxylate bridges. The latter behaviour can be attributed to the long distance between the Ni^{2+} ions spanned by the dicarboxylates. In this regard, it is worthwhile noting that very weak exchange interactions have indeed been reported for other terephthalato- or isophthalato-bridged nickel(II) complexes [28,46,47].

In summary, all three new compounds are discrete tetranuclear nickel(II) complexes composed of pairs of bioctahedral [LNi$^{II}_2$]$^{2+}$ units united by a tetradentate dicarboxylate anion. The calixarene-like conformation adopted by the supporting ligand leads to an almost complete encapsulation of the Ni$_2$(O$_2$C–R–CO$_2$)Ni$_2$ core. As a consequence the Ni$^{II}_4$ clusters are well-separated from each other in the solid state, featuring only intermolecular van der Waals contacts.

3. Redox-active ferrocenecarboxylates anions coordinated by dinuclear aminethiolate complexes

Polynuclear complexes composed of classical and organometallic complex fragments have attracted considerable attention in recent years [48, 49], owing to their rich redox chemistry [50, 51], the search for novel magnetic and electronic materials [52, 53], and potential applications in catalysis [51]. In addition, the presence of redox-active signalling groups and open coordination sites enables these compounds to be used as selective sensor molecules for target guest species [54–59]. So far, research in this area has mainly focused on conjugates built up of mononuclear LM complexes (L = chelate ligand) and suitably functionalized ferrocene derivatives [60–63]. Less attention has been paid to the use of discrete dinuclear LM$_2$ building blocks. The tetranuclear Mo$_4$ complexes containing two quadruply bonded Mo$_2$-formamidinate units linked by 1,1'-ferrocenedicarboxylate dianions may serve as rather rare examples of this class of compounds [64].

Recently, we described a series of dinuclear transition metal complexes supported by the macrocyclic hexa-azadithiophenolate ligand L^{2-} (Scheme 4). These complexes have a rich coordination chemistry since the [LM$_2$]$^{2+}$ fragments are able to coordinate a large variety of coligands such as Cl$^-$ [65], OH$^-$ [66], NO$_2^-$, NO$_3^-$, N$_3^-$ [67], BH$_4^-$ [68], and various carboxylates [69–71]. The extensive redox chemistry exhibited by dinuclear aminethiolate complexes [29] and the possibility of coupling these units into polynuclear arrays, led us to synthesize derivatives bearing ferrocenemono- and ferrocenedicarboxylate anions ([CpFeC$_5$H$_4$CO$_2$]$^-$ and [Fe-(C$_5$H$_4$CO$_2$)$_2$]$^{2-}$, Cp = cyclopentadienyl) as coligands. Our first attempts afforded a series of trinuclear [LM$_2$(O$_2$CC$_5$H$_4$FeCp)]$^+$ and pentanuclear [(LM$_2$)$_2$-(O$_2$CC$_5$H$_4$)$_2$Fe]$^{2+}$ complexes. To our knowledge, these complexes represent the first class of compounds containing dinuclear aminethiolate complexes and redox-active ferrocenecarboxylates in the same molecule [72–75].

It was our aim to synthesize polynuclear complexes containing classical and organometallic complex fragments. Two types of complexes were considered: trinuclear [LM$^{II}_2$(O$_2$CC$_5$H$_4$FeCp)]$^+$ complexes and pentanuclear [(LM$^{II}_2$)$_2$(O$_2$CC$_5$H$_4$)$_2$Fe]$^{2+}$ compounds (here after abbreviated as M$^{II}_2$Fe and M$^{II}_4$Fe), respectively. Scheme 4 shows the complexes prepared and their labels.
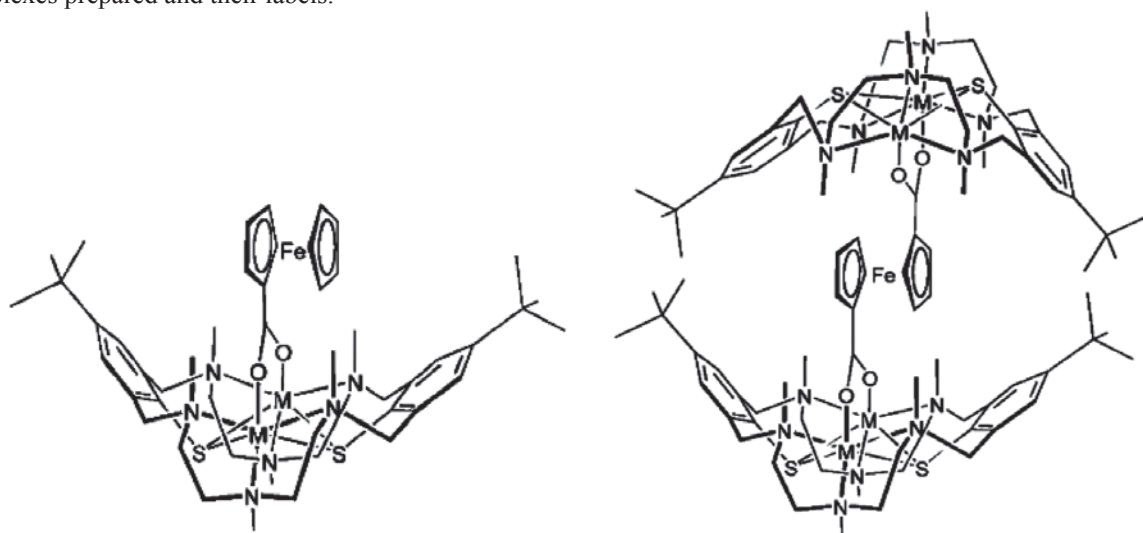
9. [LCo$^{II}_2$(O$_2$CC$_5$H$_4$FeCp)]$^+$ **10**. [LNi$^{II}_2$(O$_2$CC$_5$H$_4$FeCp)]$^+$ **11**. [LZn$^{II}_2$(O$_2$CC$_5$H$_4$FeCp)]$^+$
12. [(LCo$^{II}_2$)$_2$(O$_2$CC$_5$H$_4$)$_2$Fe)]$^{2+}$ **13**. [(LNi$^{II}_2$)$_2$(O$_2$CC$_5$H$_4$)$_2$Fe)]$^{2+}$ **14**. [(LCo^{II}Co^{III})$_2$(O$_2$CC$_5$H$_4$)$_2$Fe)]$^{4+}$

Scheme 4. Complexes prepared and their labels.

The trinuclear Co$_2$Fe and Ni$_2$Fe complexes, **9** and **10**, were obtained in almost quantitative yield by reaction of the corresponding chloride complex [LM$_2$(μ-Cl)]$^+$ (M=Ni **1**, Co **2**) with triethylammonium ferrocenylmono-carboxylate (prepared in situ from CpFeC$_5$H$_4$CO$_2$H and triethylamine) in a 1:3 ratio in methanol at room temperature and isolated as perchlorate salts upon addition of LiClO$_4$. It should be noted that these reactions are not simple substitution reactions, because a simultaneous conformational change of the supporting ligand from a "partial-cone" to a "bowl-shaped" conformation takes place [76]. Since a chloro-bridged dizinc complex [LZn$^{II}_2$(μ-Cl)][ClO$_4$] is not yet known, the synthesis of the Zn$_2$Fe complex **11**[ClO$_4$] required another starting material. Complex [LZn$^{II}_2$(μ-OAc)][ClO$_4$] (**3**[ClO$_4$]) was chosen due to its proven ability to readily exchange its acetato group for more hydrophobic carboxylate anions [71]. Indeed, when **3**[ClO$_4$] is treated with a 10-fold excess of triethylammonium ferrocenecarboxylate in methanol at room temperature an exchange reaction takes place and **11**[ClO$_4$] can be isolated as an analytically pure yellow powder after workup. The three perchlorate salts **9**[ClO$_4$]–**11**[ClO$_4$] are air-stable solids that are readily soluble in polar aprotic organic solvents such as dimethylformamide, dichloromethane, acetone and acetonitrile but only slightly soluble in methanol or ethanol. The corresponding tetraphenylborate salts **9**[BPh$_4$]–**11**[BPh$_4$] are formed within a few minutes upon addition of ethanol solutions of NaBPh$_4$ to acetonitrile solutions of the ClO$_4^-$ salts.

The pentanuclear Ni^{II}_4Fe and Co^{II}_4Fe complexes $[(LM_2)(\mu\text{-}O_2CC_5H_4)_2Fe]^{2+}$ (M=Co (**12**), Ni (**13**)) were prepared in much the same way as **9** and **10**: the chloride complexes **1** and **2** reacted smoothly with half an equivalent of triethylammonium 1,1'-ferrocenedicarboxylate (prepared in situ from the free acid and triethylamine) in methanol to give red-brown **12**$[ClO_4]_2$ and green **13**$[ClO_4]_2$, respectively, in nearly quantitative yields. The coupling of the dicarboxylate dianions with the $[LM_2]^{2+}$ fragments is a clean and facile step driven forward by the low solubility of the products. The complexes are only slightly soluble in polar aprotic organic solvents such as DMF, dichloromethane, and acetonitrile and virtually insoluble in methanol or ethanol. Addition of $NaBPh_4$ to suspensions of the perchlorate salts in acetonitrile/ ethanol followed by concentration in vacuum provided the corresponding tetraphenylborate salts as analytically pure products.

We have also been able to isolate the two-electron-oxidized $Co^{II}Co^{III}$ form **14**$[ClO_4]_4$ of compound **12**$[ClO_4]_2$. This mixed-valent complex was prepared as a black powder in good yields by oxidation of **12**$[ClO_4]_2$ with 1 equiv of bromine in acetonitrile at 0^oC followed by addition of a saturated ethanol solution of $LiClO_4$ and low-temperature vacuum concentration. In contrast to **12**$[ClO_4]_2$, **14**$[ClO_4]_4$ exhibits excellent solubility in acetonitrile. Such solutions can be stored for several days at ambient temperature without noticeable decomposition. Attempts to prepare the analogous $[(LNi^{II}Ni^{III})_2(\mu\text{-}O_2CC_5H_4)_2Fe]^{4+}$ complex were not successful.

All compounds gave satisfactory elemental analyses and were characterized by appropriate spectroscopic methods (IR, NMR, UV/Vis -spectroscopy). The infrared spectra of the new complexes display absorptions due to the $[LM_2]^{2+}$ fragments, the counter ions (ClO_4^- or BPh_4^-), and the ferrocene derivatives. The ferrocene-carboxylates in **9**–**13** give rise to two characteristic bands, as in other carboxylato-complexes [38, 77], in the 1575–1565 cm^{-1} and 1435–1425 cm^{-1} ranges; these are assigned to the asymmetric and symmetric carboxylate stretching modes, respectively. These values are very similar to those in **3**–**5** indicative of $\mu_{1,3}$-bridging carboxylate functions [69, 70]. The oxidation of **12** to **14** is accompanied by a shift of the asymmetric stretching mode by ≈ 18 cm^{-1} to lower wavenumbers. A similar behaviour was observed for the acetato-bridged Co^{II}_2 complex **4** [70].The data are thus in good agreement with the formulation of complex **14** as a mixed-valent $Co^{II}Co^{III}$ species.

The diamagnetic Zn_2Fe complex **11** was characterized by NMR spectroscopy to determine its structure in solution. The ^1H NMR spectrum shows the characteristic signal patterns for the $[LZn_2]^{2+}$ [78], and $[CpFe(C_5H_4CO_2)]^-$ [79], units indicating local C_{2v} symmetry for **11**. Particularly indicative of a stable 1:1 complex is the upfield shift of the *tert*-butyl resonance of the $[LZn_2]$ unit (0.25 ppm relative to **3**). The resonances of the ferrocenecarboxylate are observed at δ 3.40 for the unsubstituted Cp ring, δ 3.90 for the two *meta*-H and δ 4.04 for the two *ortho*-H of the substituted Cp ring. These values are also significantly shifted to higher field when compared with the corresponding resonances of uncomplexed ferrocenmonocarboxylate [80, 81]. The ^{13}C NMR spectrum is also in accord with the proposed formulation showing five signals for the $[CpFe(C_5H_4CO_2)]^-$ unit and only 13 signals for the $[LZn_2]^{2+}$ moiety. The local C_{2v} symmetry is suggestive of a dynamic averaging process in solution. A rapid rotation of the ferrocenyl group about the $CpFeCp\text{-}CO_2Zn_2L$ bond seems most likely. This motion would result in the coalescence of the respective signals and the time averaged C_{2v} symmetry of the complex. The crystal structure determinations of **9** and **10** support this assumption.

The UV/Vis spectra of **9, 10, 12,** and **13** display several weak bands above 500 nm typical of octahedral high-spin Co^{II} (d^7, S = $^3/_2$) and Ni^{II} (d^8, S=1) ions, respectively. The observed values closely compare with those of **4** and **5** again consistent with pseudo-octahedral N_3S_2O coordination environments around the metal atoms [69, 70]. For the Zn_2Fe species **11**$[ClO_4]$ two absorptions bands are detected at 342 and 440 nm; these are readily assigned to the d–d transitions of the coordinated $[CpFe(C_5H_4CO_2)]^-$ unit. The feature at 440 nm is also evident in the electronic absorption spectrum of the Ni_2Fe complex **10**. In the UV spectrum of **11**, this band is obscured by an intense ligand-to-metal charge-transfer transition ($RS \rightarrow Co^{II}$). The d–d transitions of the $[Fe(\eta^5\text{-}C_5H_4CO_2)]^{2-}$ unit in **12, 13** and **14** could not be located.

The UV/Vis spectrum of the mixed-valent $Co^{II}Co^{III}$ complex **14** is dominated by two very intense absorptions at ≈ 449 and 681 nm; these are attributable to $RS \rightarrow Co^{III}$ charge-transfer transitions. Such intense LMCT transitions are characteristic of thiolato-bridged $Co^{II}Co^{III}$ complexes. The corresponding absorptions in $[LCo^{II}Co^{III}(\mu\text{-}OAc)]^{2+}$, for example, were observed at 460 and 710 nm [70]. It should be noted that the UV/Vis spectrum of **14** reveals no bands attributable to intervalence transfer (IT) bands. Complex **14** is therefore presumably class I in Robin and DayOs classification of mixed-valence species with distinct localized high-spin Co^{II} and low-spin Co^{III} sites [82]. This is confirmed by the crystal structure determination of **14**$[ClO_4]_4$.

Crystals of **9**$[BPh_4]\cdot 3MeCN$ suitable for X-ray crystallography were grown by slow evaporation of a dilute 1:1 acetonitrile/ethanol solution of **9**$[BPh_4]$. The X-ray structure revealed the presence of well-separated $[LCo^{II}_2(\mu\text{-}O_2CC_5H_4FeCp)]^+$ cations, tetraphenylborate anions, and acetonitrile molecules of solvent of crystallization. An ORTEP representation of the molecular structure of **9** is shown in Figure 5.
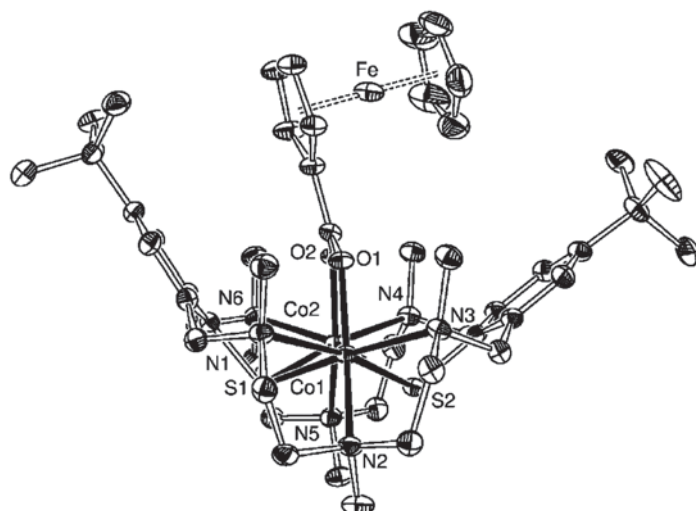
Figure 5. Structure of the cation 9 in crystals of 9[BPh$_4$]·3MeCN. Thermal ellipsoids are drawn at the 30% probability level. Hydrogen atoms are omitted for reasons of clarity. Only one orientation of a rotationally disordered *t*Bu group is shown.

The ferrocenecarboxylate bridges the two Co atoms in a $\mu_{1,3}$-fashion, resulting in nonbonded Co···Fe separations of 5.884(1) and 5.753(1) Å. The Co···Co distance of 3.448(1) Å is the same as that in **4** [67]. The Cp rings are nearly parallel (angle between the normals of the Cp planes = 1.8(1)°) and adopt an almost eclipsed conformation, with the torsional angle τ (defined as "CO$_2$-centroid-centroid-C(45)") being 6.4(1)°. The carboxylato plane is slightly twisted by 9.7° with respect to the Cp ring to which it is attached. The Fe–centroid distances are 1.656(6) and 1.646(6) Å for the carboxylated and the unsubstituted Cp rings, respectively; the mean Fe–ring (centroid) distance of 1.651(6) Å is, within experimental error, the same as that of 1.645(2) Å for ferrocene [83]. The bond lengths and angles around the Co atoms within the [LCo$^{II}_2$]$^{2+}$ unit reveal no unusual features. The average Co–S, Co–N and Co–O bond lengths are at 2.018(3), 2.291(3), and 2.517(1) Å, respectively. Virtually the same distances are seen in the acetato-bridged complex **4** [67]. A large number of metal complexes containing ferrocenecarboxylate ligands have been structurally characterized [84–86]; to our knowledge, **9** is the first such complex supported by a dinuclear aminethiolate metallo ligand.

In contrast to the compound above, **10**[BPh$_4$] recrystallized from acetonitrile/ethanol 1:1 with only one acetonitrile solvate molecule. Figure 6 shows the ferrocenecarboxylate to be coordinated to the [LNi$^{II}_2$] unit in a manner identical to the situation found in **9** (Figure 5).
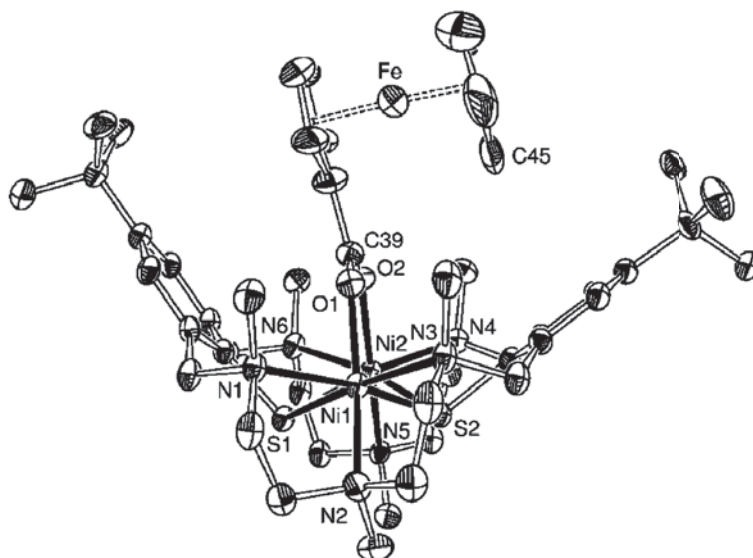

Figure 6. Structure of the cation 10 in crystals of 10[BPh$_4$]·MeCN. Thermal ellipsoids are drawn at the 30% probability level. Hydrogen atoms are omitted for reasons of clarity. Only one orientation of a rotationally disordered *t*Bu group is shown.

Thus, both Ni^{II} ions are six coordinate with three N and two S atoms from L^{2-} and one O atom of a $\mu_{1,3}$-bridging ferrocenyl carboxylate group. In comparison to **9**, the two Cp rings are perfectly eclipsed (tilt angle = 0.6(1)°) and the carboxylato plane is now coplanar with the Cp ring (τ = 2.88). The different τ values may be taken as evidence for an unhindered rotation of the coordinated ferrocene moiety about the O_2C–Cp bond in the solution state. It should be noted in this respect that there are no intramolecular steric interactions between the ferrocene group and the *t*Bu substituents. The short distances between C(45) and the *p*-electrons of the adjacent phenyl ring (d(C45)···centroid = 3.518 Å in **10** and 3.991 Å in **9**) may be considered as weak CH···π hydrogen bonds. The Ni–O, Ni–N, and Ni–S distances of the [LNi_2carboxylate] subunit in **10** are unexceptional and are very close to the corresponding distances in **5**. Overall, the two structures clearly show that the [LM_2]$^{2+}$ units can expand their binding pockets sufficiently to accommodate $\mu_{1,3}$-bridging ferrocenecarboxylate ions.

Single crystals of the two compounds **12**[BPh_4]$_2$·$2^2/_3$MeCN·$^1/_3H_2O$ and **13**[BPh_4]$_2$·1.75MeCN·EtOH· $0.25H_2O$ suitable for X-ray crystallography were each obtained by slow evaporation from an acetonitrile/ethanol/ CH_2Cl_2 solution. The crystal structures consist of isolated [($LM_2)_2(O_2CC_5H_4)_2Fe$]$^{2+}$ dications (Figure 7), tetraphenylborate anions and various solvate molecules (MeCN, H_2O, and EtOH), of which some are either severely disordered or not fully occupied.
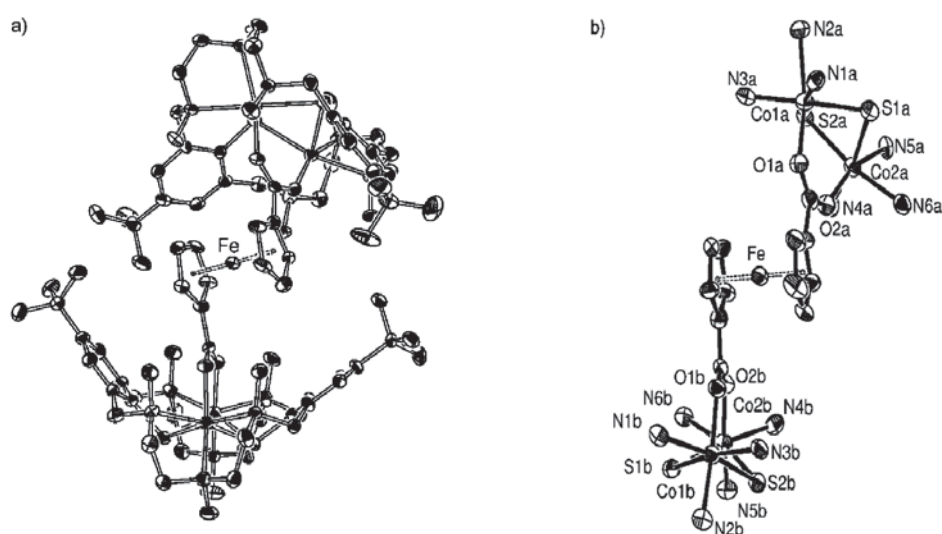

Figure 7. a) ORTEP view of the [($LCo^{II}_2)_2(\mu-O_2CC_5H_4)_2Fe$]$^{2+}$ dication 12 in crystals of 12[BPh_4]$_2$· $2^2/_3$MeCN ·$^1/_3H_2O$. Hydrogen atoms are omitted for clarity. b) ORTEP representation of the core structure of 12 with the atom labelling scheme. Ellipsoids are represented at the 30% probability level.

The two compounds were found to be isomorphous in spite of differences in the number and type of solvate molecules. The following discussion will focus on the $Co_4^{II}Fe$ complex **12**. Metrical details for the $Ni_4^{II}Fe$ complex **13** are reported in square brackets.

As can be seen in Figure 7b, the ferrocenyldicarboxylate dianion links two [LCo^{II}_2]$^{2+}$ units via two $\mu_{1,3}$-bridging carboxylate functions. The [LCo_2]$^{2+}$ subunits in **12** and **4** are structurally very similar, and the Co–N, Co–O, and Co–S distances lie within very narrow ranges. The carboxylato groups on the Cp rings assume an *anti*-eclipsed conformation as manifested by a torsional angle τ (CO_2-centroid-centroid-CO_2) of 148.4° [148.3°]. The distance d between the centre of the Co···Co axes of the binuclear subunits amounts to 10.751 Å [10.749 Å], which is slightly smaller than the corresponding distance in [$Mo_2(DAniF)_3$]$_2$ [ferrocendicarboxylate] [64]. It should be noted that the Co_2carboxylato planes are considerably tilted against each other (32.3°, [33.1°]) and also with respect to their corresponding Cp rings (22.4°, 10.1°; [22.4°, 10.0°]). This distortion from coplanarity relates to steric interactions between the *t*Bu groups of the two opposing [LCo^{II}_2]$^{2+}$ subunits. The *tert*-butyl groups must interlock to accommodate the dicarboxylate ion. In ferrocenedicarboxylato complexes of sterically less encumbered supporting ligands the carboxylato planes are both coplanar with their parent Cp rings [87, 88].

The crystal structure of **14**[ClO_4]$_4$·$4H_2O$ consists of [($LCo^{II}Co^{III})_2(\mu-O_2CC_5H_4)_2Fe$]$^{4+}$ cations (Figure 8), ClO_4^- anions and water solvate molecules. There are two crystallographically independent but chemically almost identical molecules (labelled A and B) in the asymmetric unit; both have crystallographically imposed C_2 symmetry with the iron atoms residing on crystallographic two-fold axes. The overall structure of complex **14** is very similar to that of its parent **12**, featuring two binuclear LCo_2 subunits linked by a tetradentate ferrocenedicarboxylate ion. Again, the carboxylato

groups are *anti*-eclipsed (τ = 148.6° [136.9° (molecule B)] and considerably tilted against each other (48.2°, [25.2°]) and by 24.1° [12.6°] with respect to their corresponding Cp rings. The distance *d* between the centre of the Co⋯Co axes is 10.770 Å in molecule A and 10.322 Å in molecule B.
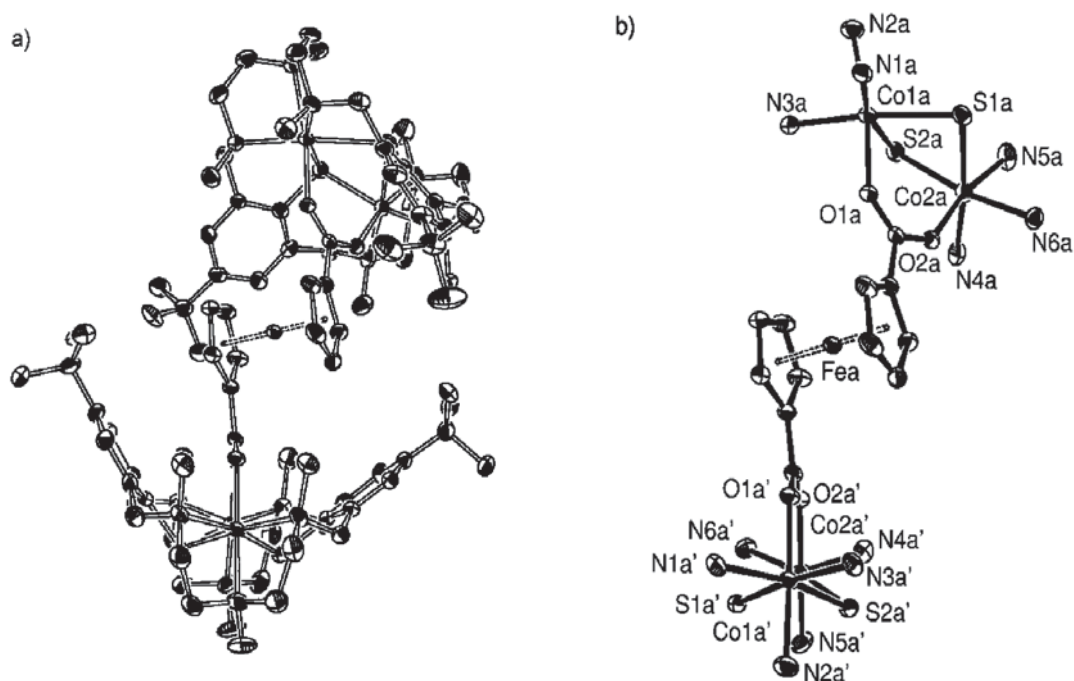

Figure 8. a) ORTEP view of the [(LCo^{III}Co^{II})$_2$(µ-O$_2$CC$_5$H$_4$)$_2$Fe]$^{4+}$ tetracation (molecule A) in crystals of 14[ClO$_4$]$_2$·4H$_2$O. Hydrogen atoms are omitted for clarity. b) ORTEP representation of the core structure of 14 with the atom labelling scheme. Ellipsoids are drawn at the 30% probability level.

The oxidation of **12** to **14** is accompanied by a significant shortening of the metal–ligand bond lengths around one Co atom in each binuclear subunit. This is in accord with the mixed-valent nature of **14** and the metal-centred nature of the oxidation of **12**. Assignments of the trivalent and divalent Co ions are based on the bond distances around the cobalt atoms. Co1a [Co1b in molecule B] is assigned an oxidation state +II (d^7, high-spin), because the bond lengths are very similar to those in **12**. The average Co–O, Co–N and Co–S bond lengths around Co2a [Co2b] are all significantly shorter at 1.884(4), 2.122(6), and 2.311(2) Å, respectively. These distances are too short for a six-coordinate Co^{II} complex, but are in excellent accord with those of related low-spin Co^{III}N$_{6-x}$S$_x$ [89, 90] and Co^{III}N$_3$S$_2$O [67] complexes. Interestingly, the oxidation of **12** is accompanied by an opening up of the Co-S-Co angle to 93.56(7)° causing a slight increase of the intramolecular Co⋯Co distance to 3.523(1) Å. The Fe-Cp-ring (centroid) distances (1.653(6) Å and 1.651(6) Å) are not affected by the oxidation.

Evidently, the crystal structures of **12–14** clearly show that dinuclear LM$_2$ units can be coupled together by the 1,1'-ferrocendicarboxylate dianion. Moreover, the pentanuclear Co$_4$Fe complex **12** is even accessible in another oxidation state. The oxidation is metal-centered and occurs without gross structural changes of the parent complex **12**. This finding paves the way for novel multi-redox systems composed of binuclear complex units and multifunctional metalorganic linkers which may find applications due to novel chemical or physico-chemical properties that are not seen for the individual components [91].

One facet of the present complexes is the presence of a redox-active ferrocene unit in close proximity to one or two redox-active [LM$_2$]$^{2+}$ groups. This feature suggests that electron transfer events can influence one another owing to the short distance (5.6±0.2 Å) between the redox centres. To determine whether this is the case, cyclovoltammetric studies have been carried out on the M$_2$Fe complexes **9**[ClO$_4$]–**11**[ClO$_4$] and the Co$_4$Fe compound **14**[ClO$_4$]$_4$. The cyclic voltammograms (CV's) have been recorded in acetonitrile solution with tetra-*n*-butylammonium hexafluorophosphate as the supporting electrolyte. The electrochemical results are shown in Figure 9, and the redox potentials referenced versus SCE are collected in Table 1.
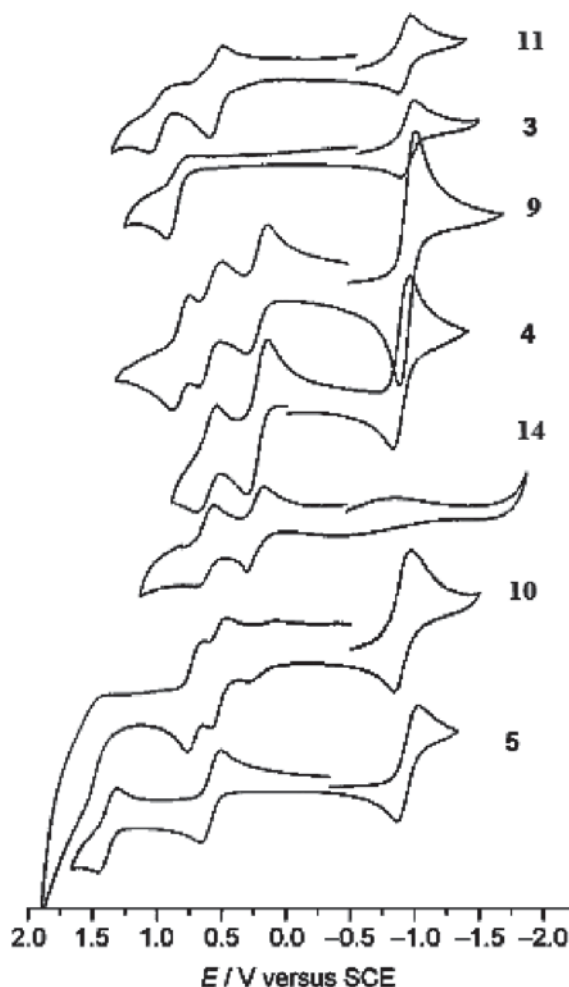
Figure 9. Cyclic voltammograms of the perchlorate salts of complexes 3–5, 9-11 and 14 in CH₃CN solution at 295K. Experimental conditions: 0.1M [ⁿBu₄N][PF₆] supporting electrolyte, ca. 1x10⁻³ M sample concentration, Pt disk working, Pt wire auxiliary electrodes, Ag wire reference electrode, scan rate=100 mV s⁻¹ . [Co(Cp)₂][PF₆] internal standard (E[CoCp₂⁺/CoCp₂]= − 0.94 V versus SCE).
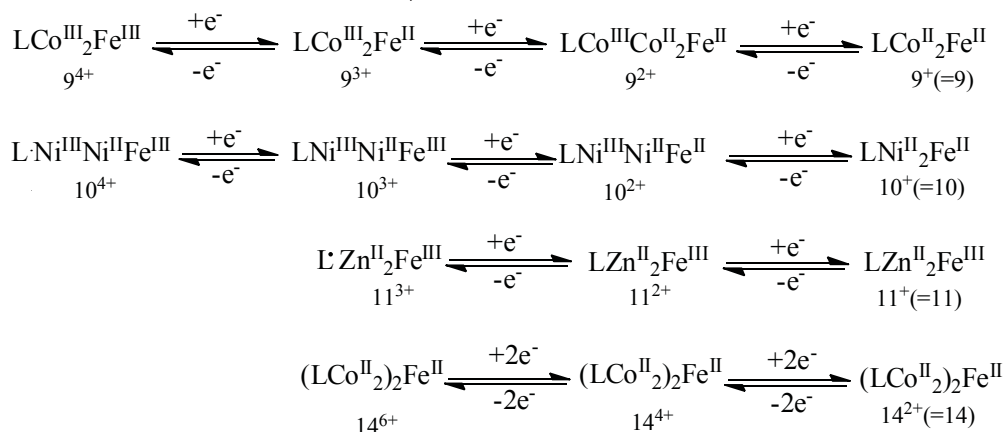
Table 1

Electrochemical data, E[V] vs SCE, for the compounds examined in this study.[b]

Compound	Solvent	Fe^{III}/Fe^{II}	$E_{1/2}$ [V] (ΔEp [mV])^b $M^{III}M^{II}/M^{II}$,	$M^{III}_2/M^{III}M^{II}$	RS^-/RS
3·[ClO₄][29]	CH₃CN				0.92(irr.)[d]
4·[ClO₄][29]	CH₃CN		0,22(118)	0,60 (147)	
5·[ClO₄][29]	CH₃CN		0,56(140)	1,36(140)	
9·[ClO₄]	CH₃CN	0,81(120)	0,20(150)	0,59(170)	
10·[ClO₄]	CH₃CN	0,55(120)	0,74(120)	1,54(irr.)[d]	
11·[ClO₄]	CH₃CN	0,54(100)			1.06(irr.)[d]
14·[ClO₄]	CH₃CN	Obsc.	0,23(140)	0,61 (120)	
	DMF	Obsc.	0,17(120)	0,52(120)	
[FeCp₂][55]	CH₃CN	0,40			
[CpFe(C₅H₄CO₂H)][91]	aq.CH₃CN	0,53			
	CH₃CN	0,63(50)			
[CpFe(C₅H₄CO₂)]⁻[c][91]	aq.CH₃CN	0,34			
	CH₃CN	0,44			
[CpFe(C₅H₄CO₂H)₂]	DMF	0,80(0.10)			

[a] The CV's were recorded at ambient temperature using 0.10 M [ⁿBu₄N][PF₆] as supporting electrolyte at a scan rate of 100 mV s⁻¹. The data refer to the perchlorate salts. Sample concentration was ca. 1.0x10⁻³ M. All potentials are referenced versus the saturated calomel electrode (SCE). [b] Separation between the anodic (Eᵖᵃ) and cathodic peaks (Eᵖᶜ) of the redox wave (ΔE_p =Eᵖᵃ–Eᵖᶜ). [c] Sodium salt. [d] Peak-potential value for irreversible processes.

The electrochemical data of **3–5**, ferrocenecarboxylic acid and 1,1'-ferrocenedicarboxylic acid have been included for comparative purposes [92]. The CV of the Zn_2Fe complex **11**[ClO_4] shows one reversible redox wave at +0.54 V that can be readily assigned to the oxidation of the ferrocene moiety, since it its absent in the CV of [$LZn_2(OAc)$][ClO_4] (**3**[ClO_4]). Interestingly, the complexation of [$CpFe(C_5H_4COO)$]⁻ causes an anodic potential shift of 90 mV in the reversible redox wave of the ferrocene moiety. It is assumed that this potential shift results from the electrostatic repulsion (Coulomb) effect between the two Zn^{2+} ions bonded by the macrocycle and the positively charged ferrocenium centre. Thus complexation of [$CpFe(C_5H_4COO)$]⁻ by the dipositively charged [LZn_2]²⁺ unit makes the ferrocenyl group more difficult to oxidize. Curiously, an anodic shift of ≈ 140 mV for the peak potential for the second, irreversible ligand-based oxidation (formally a RS⁻→RS· transition) [29] that follows the ferrocenyl centred oxidation is also evident. In this case it is the additional positive charge on the ferrocene that causes the thiolate sulfur atoms to be oxidized at a higher potential. The redox-processes for **11**[ClO_4] are summarized in Scheme 5.

$$LCo^{III}_2Fe^{III} \underset{-e^-}{\overset{+e^-}{\rightleftharpoons}} LCo^{III}_2Fe^{II} \underset{-e^-}{\overset{+e^-}{\rightleftharpoons}} LCo^{III}Co^{II}_2Fe^{II} \underset{-e^-}{\overset{+e^-}{\rightleftharpoons}} LCo^{II}_2Fe^{II}$$
$$9^{4+} \qquad\qquad 9^{3+} \qquad\qquad 9^{2+} \qquad\qquad 9^+(=9)$$

$$L^{\cdot}Ni^{III}Ni^{II}Fe^{III} \underset{-e^-}{\overset{+e^-}{\rightleftharpoons}} LNi^{III}Ni^{II}Fe^{III} \underset{-e^-}{\overset{+e^-}{\rightleftharpoons}} LNi^{III}Ni^{II}Fe^{II} \underset{-e^-}{\overset{+e^-}{\rightleftharpoons}} LNi^{II}_2Fe^{II}$$
$$10^{4+} \qquad\qquad 10^{3+} \qquad\qquad 10^{2+} \qquad\qquad 10^+(=10)$$

$$L^{\cdot}Zn^{II}_2Fe^{III} \underset{-e^-}{\overset{+e^-}{\rightleftharpoons}} LZn^{II}_2Fe^{III} \underset{-e^-}{\overset{+e^-}{\rightleftharpoons}} LZn^{II}_2Fe^{III}$$
$$11^{3+} \qquad\qquad 11^{2+} \qquad\qquad 11^+(=11)$$

$$(LCo^{II}_2)_2Fe^{II} \underset{-2e^-}{\overset{+2e^-}{\rightleftharpoons}} (LCo^{II}_2)_2Fe^{II} \underset{-2e^-}{\overset{+2e^-}{\rightleftharpoons}} (LCo^{II}_2)_2Fe^{II}$$
$$14^{6+} \qquad\qquad 14^{4+} \qquad\qquad 14^{2+}(=14)$$

Scheme 5. Assignment of redox processes in 9-11 and 14

The CV of the Co_2Fe complex **9** exhibits three reversible one-electron redox waves which can be assigned to i) a metal-centered $Co^{II}Co^{II}\rightarrow Co^{II}Co^{III}$ oxidation yielding the mixed-valent dication [$LCo^{III}Co^{II}(O_2CC_5H_4FeCp)$]²⁺ (**9²⁺**) at 0.20 V, ii) a metal-centered $Co^{III}Co^{II}\rightarrow Co^{III}Co^{III}$ oxidation at 0.59 V forming tricationic [$LCo^{III}_2(O_2C_5H_4FeCp)$]³⁺ (**9³⁺**), and iii) oxidation of the metalorganic unit generating tetracationic [$LCo^{III}_2(O_2CC_5H_4Fe^{III}Cp)$]⁴⁺ (**9⁴⁺**) at 0.81 V. These assignments are supported by the electronic absorption spectra of the corresponding di-, tri- and tetracations generated in situ by successive chemical oxidations of **9⁺** with 0.5, 1.0, and 1.5 equiv of bromine in acetonitrile solution (Figure 10); the characteristic absorption maxima at 388 and 467 nm of the ferrocinium ion are not observed before the third oxidation step.
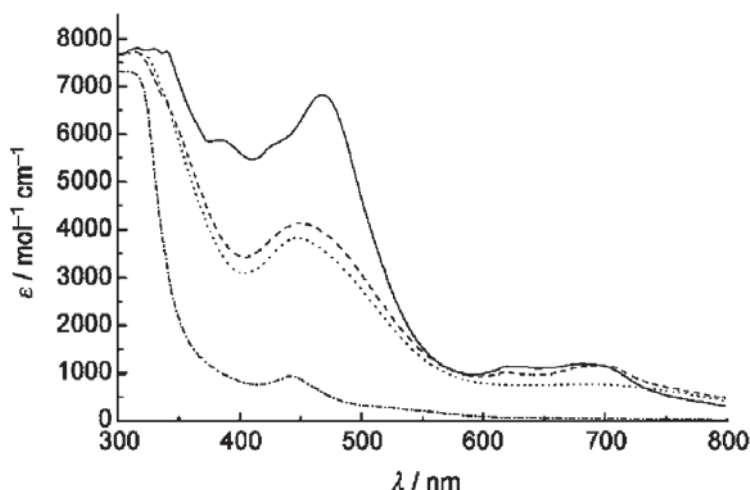

Figure 10. UV/Vis spectra of 9 (-·-·-·), 9²⁺ (·····), 9³⁺ (-----), and 9⁴⁺ (——) in acetonitrile generated by chemical oxidation of [$LCo^{II}_2(\mu\text{-}O_2CC_5H_4FeCp)$][$ClO_4$] (9[$ClO_4$]) with 0.5, 1.0, and 1.5 equiv of Br₂, respectively.

The potential shift for the oxidation of the ferrocenyl unit in **9³⁺** (ΔE = +0.37 V) is significantly larger than in **11⁺**. The significantly larger shift is likely to be a result of the higher positive charge of the [LCo^{III}_2]⁵⁺ fragment to which the $Fe^{II}(Cp)(C_5H_4COO^-)$ unit is attached in **9³⁺**.

The CV of Ni_2Fe compound **10** reveals two electrochemically reversible and one irreversible redox waves, which by comparison with the CV of **5** [29] are tentatively assigned to i) a metal-centred $Ni^{II}Ni^{II} \rightarrow Ni^{II}Ni^{III}$ oxidation yielding the mixed-valent dication $[LNi^{III}Ni^{II}(O_2CC_5H_4Fe^{II}Cp)]^{2+}$ (**5^{2+}**) at 0.53 V, ii) the oxidation of the metal organic unit forming $[LNi^{III}Ni^{II}(O_2CC_5H_4Fe^{III}Cp)]^{3+}$ (**5^{3+}**) at 0.71 V, and iii) the oxidation of the thiophenolate sulfur atoms yielding a nickel bound thiyl radical at 1.59 V. Anodic shifts in the second and third redox waves are clearly discernible, confirming the above findings that the electron transfer events of the ferrocenyl moiety and the binuclear subunit influence one another. The fact that the potential shifts are not so pronounced than in **9** is in good agreement with the smaller positive charges of the participating species. It should be noted that all oxidation products of **9** and **10** are only stable on the time scale of a cyclic voltammetry experiment. Attempts to prepare these compounds by electrochemical or chemical oxidation led to unidentified decomposition products. Thus, while some of the above oxidations appear electrochemically reversible, they are all chemically irreversible.

Of the tetranuclear complexes, only complex **14**$[ClO_4]_4$ had sufficient solubility (due to its higher charge) to examine its electrochemical properties by cyclic voltammetry. The CV shows two quasi-reversible redox waves. On the basis of the crystal structure of **14**$[ClO_4]_4$, the first redox wave at 0.22 V can be assigned to a two-electron reduction of **14^{4+}** yielding the fully-reduced Co^{II}_4Fe form **14^{2+}** (which is assumed to be identical with **12**). The other wave at 0.53 V can be attributed to a metal-centred two-electron oxidation process yielding the fully oxidized Co^{III}_4Fe form $[(LCo^{III}_2)_2(Fe(Cp))]^{6+}$ (**14^{6+}**). The observed potential values are almost identical with those in **4** [67], indicating that the oxidation/ reduction processes at one $[LCo_2]$ unit do not influence the ones that occur at the other. In other words, the two dinuclear cobalt(II) subunits behave as two independent redox-groups. That is fully consistent with the large distance between the two subunits and the fact that the electrostatic (Coulomb) interactions decrease rapidly with increasing distance between the redox sites. The redox wave for the oxidation of the $[Fe(C_5H_4CO_2)_2]^{2-}$ unit in **14** could not be detected. We assume that it is obscured by the redox waves at 0.53 V.

There have been many reports in the literature that a charged subunit can influence the redox properties of an adjacent ferrocene group [93]; to our knowledge, complexes **9–11** represent the first examples for a system in which the redox properties of a ferrocenecarboxylate-based ligand is modified by dinuclear aminethiophenolate complexes.

The magnetic properties of the pentanuclear Ni_4Fe complex **13**$[BPh_4]_2$ were examined in view of literature reports that conjugated dicarboxylate ligands can mediate long-range magnetic exchange interactions [45]. Figure 11 displays the temperature dependence of the effective magnetic moment for **13**$[BPh_4]_2$. The effective magnetic moment increases from 6.88 μ_B at 295K to a maximum value of 7.70 μ_B at 25K. On lowering the temperature further the magnetic moment decreases to 7.08 μ_B at 2 K. Although the effective magnetic moment at 25K is smaller than expected for the spin-only value of 9.84 μ_B for $S_T = 4$ resulting from the ferromagnetic coupling of four Ni^{II} ions ($S_i = 1$, g = 2.20), it is larger than the value of 6.22 μ_B calculated for four noninteracting Ni^{II} ions. This behaviour indicates the presence of weak ferromagnetic exchange interactions between the Ni^{II} ions in the binuclear subunits but negligible - if any - coupling across the metallocene dicarboxylate bridge. Considering the long distance between the nickel(II) ions, this is not surprising.
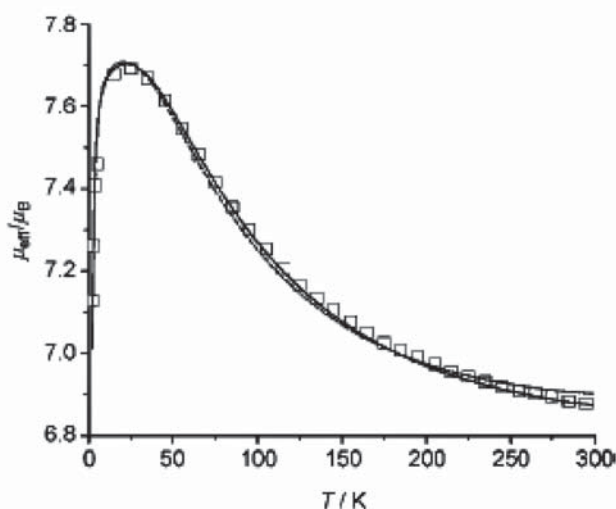

Figure 11. Temperature dependence of μ_{eff} (per tetranuclear complex) for 13[BPh$_4$]$_2$. The full line represents the best theoretical fit. The dashed line represents the best fit to the dimer model.
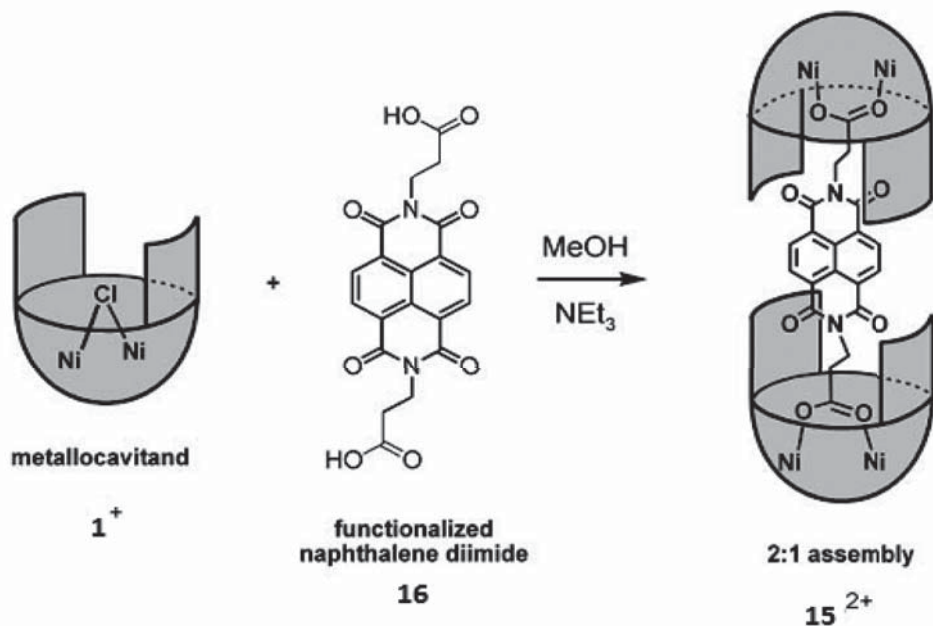
4. Functionalized naphthalene diimide as a bifunctional linker

We and others have been working with naphthalene diimides as a suitable class of chemically robust redox- and photo-active units with which to explore molecular electronic applications [94, 95].

The naphthalene diimides are a compact, electron-deficient class of aromatic compounds that allow further fine-tuning of their optical properties (absorbance and emission) via suitable core functionalization [95]. The consideration that naphthalene diimides can act as ideal components for the creation of supramolecular functional materials has transpired as a result of their more desirable electronic and spectroscopic properties relative to pyromellitic diimides and better fabrication properties than the perylene diimide dyes, the latter being a result of their enhanced solubility properties. Naphthalene diimides (NDI) undergo single reversible one-electron reduction (chemically and electrochemically) at modest potentials (NDI: $E^1_{red} \approx 1.1$ V vs.Fc/Fc$^+$) to form stable radical anions in high yield [96]. They are seen as attractive redox-active units because of their electronic complementarity to ubiquinones [97] which make them excellent components for studying photoinduced electron transfer [98]. Here we examine the interplay of a binucleating nickel(II) cavitand [LNi$_2$(μ-Cl)][ClO$_4$](1) [1] with a naphthalene diimide **16** bearing two β-alanyl groups [99, 100] (Scheme 6).

To our knowledge, complex **15** represents the first example of a supramolecular ensemble containing dinuclear amine-thiolate complexes and redox-active organic components within the same molecule.

Reaction of **1** with half an equivalent of **16** with NEt$_3$ in MeOH at r.t. leads to the immediate formation of a green solution. After the addition of a ten-fold excess of LiClO$_4$ a green microcrystalline solid, characterized as the 2:1 complex **15**[ClO$_4$]$_2$, is obtained in 72% yield. The perchlorate salt of **15**$^{2+}$ is an air-stable solid that is readily soluble in polar aprotic solvents such as N,N-dimethylformamide, dichloromethane and acetonitrile, but virtually insoluble in methanol and water. The electrospray ionization mass spectrum (ESI-MS, positive mode)

Scheme 6. Schematic representation of the encapsulation of the di-functionalised naphthalene diimide **16** by a binucleating metallocavitand **1** to yield the complex **15**[ClO$_4$]$_2$.

of a dilute CH$_2$Cl$_2$ solution of **15** [ClO$_4$]$_2$ exhibits a molecular ion peak with the correct isotopic distribution for the dication **15**$^{2+}$ (m/z = 989.36). Two prominent vibration bands are seen in the IR, as in other carboxylato-bridged Ni$_2$ complexes of (L)$^{2-}$, at 1583 and 1423 cm^{-1} [65, 67]. These are assigned to the antisymmetric and symmetric carboxylate stretching modes, respectively, of a $\mu_{1,3}$-bridging carboxylate function. The ν(CO) stretching frequencies of the carboxamide functions of [**16**-2H]$^{2-}$ are also clearly visible at 1706 and 1669 cm^{-1}.

The dual coordination mode of the naphthalene diimide unit is further demonstrated by UV/Vis spectroscopy. The UV/Vis spectrum of a solution of **15**[ClO$_4$]$_2$ in CH$_2$Cl$_2$ is displayed in Figure 12 and that of [LNi$_2$(OAc)][ClO$_4$] **5**[ClO$_4$] is shown for comparison. Complex **15**$^{2+}$ reveals five well-resolved UV bands at 272, 306, 336, 360 and 380 nm, the former three of which are attributable to the π–π* transitions within the thiophenolate units of the [Ni$_2$L]$^{2+}$ fragments. Their intensity is approximately twice as large as those of the model compound **5**$^+$, which is in good agreement with the formulation of compound **15**$^{2+}$ as a 2:1 complex.
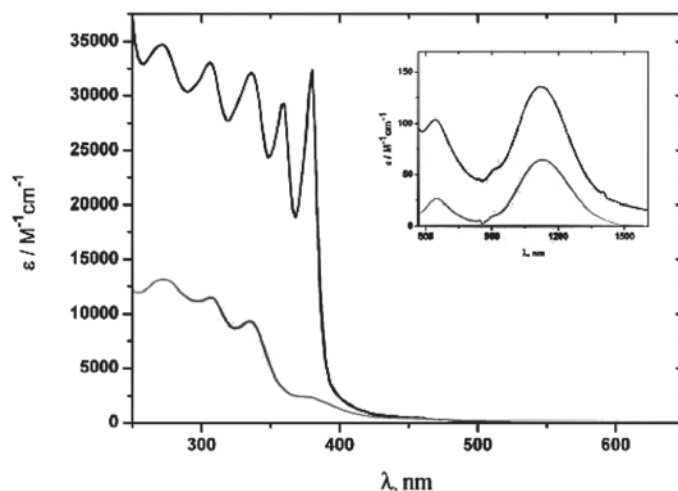
Figure 12. Electronic absorption spectra of 15[ClO₄]₂ (black) and model 5[ClO₄](grey) in CH₂Cl₂ solution (sample concentration = 10⁻⁴ M). The inset shows the absorptions of 15[ClO₄]₂ and 5[ClO₄] attributed to weak d–d absorptions (sample concentration = 10⁻³ M).

The low energy bands at 360 and 380 nm which are typical for naphthalene diimides [96] further confirm the identity of complex 15^{2+}. The UV/Vis spectrum also reveals two weak d–d absorption bands at 644 and 1122 nm typical of octahedral Ni^{II} in an $N_3S_2O^{carboxylate}$ environment. The observed values closely compare with those of 5^+ (see inset in Fig. 12) again consistent with pseudo-octahedral N_3S_2O coordination environments around the metal atoms. All these findings strongly indicate that the tetranuclear complex 15^{2+} retains its integrity in solution.

To determine whether 15^{2+} exhibits electron transfer events due to the NDI unit and the $[Ni_2L]^{2+}$ groups, cyclic voltammetric studies have been carried out on $15[ClO_4]_2$ in DMF solution using 0.10 M $[^nBu_4N][PF_6]$ as the supporting electrolyte (Fig. 13). The CV of the Ni_4 complex $15[ClO_4]_2$ shows three redox waves at - 1.62, -1.04 and 0.15 V, respectively, vs. ferrocenium /ferrocene (Fc^+/Fc). The processes at -1.04 and -1.62 V correspond to the reduction of the dication 15^{2+} to 15^+ (bearing the radical anion 16^-) and the reduction of 15^+ to neutral 15 (bearing the doubly reduced NDI ligand), respectively. Upon reduction of 15^{2+} by either electrochemical or chemical means ($Na_2S_2O_4/H_2O$) the colour of the complex changes to deep mauve which (in the absence of air) persists in solution over 3 h indicative of radical anion formation. The redox wave located at 0.15 V on the other hand is tentatively assigned to a two-electron metal-centered $Ni^{II}Ni^{II} \rightarrow Ni^{II}Ni^{III}$ oxidation yielding the mixed-valent tetrametallic tetracation $[(Ni^{III}Ni^{II}L)_2(16)]^{4+}$ (15^{4+}). The redox-wave for the oxidation of the tetracation 15^{4+} to the hexacation 15^{6+} (formally a $Ni^{II}Ni^{III} \rightarrow Ni^{III}Ni^{III}$ process as seen for complex $5[ClO_4]$) could not be detected. We assume that it is obscured by the redox-waves associated with the oxidation of the solvent.
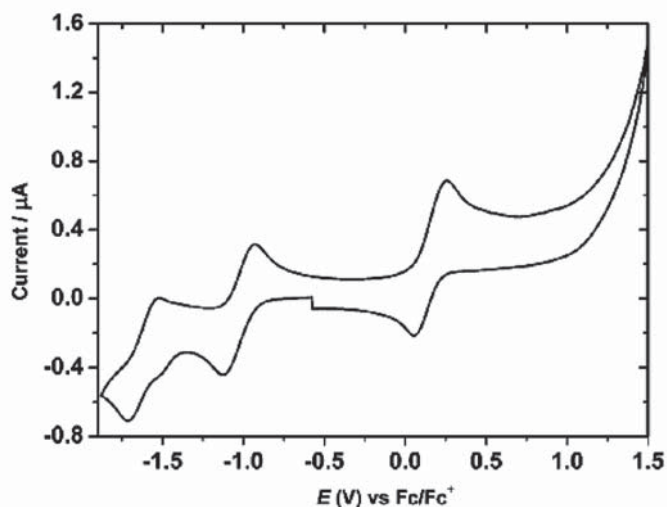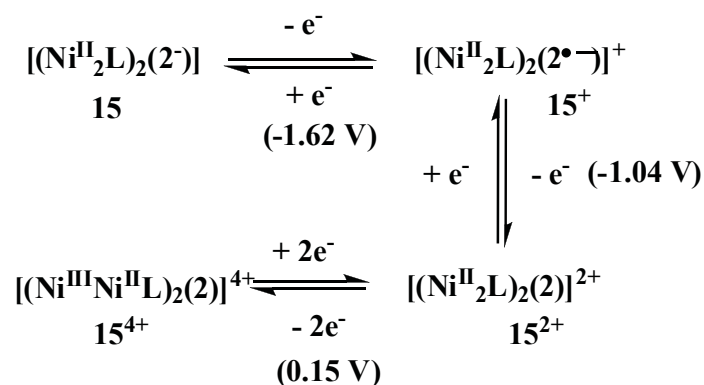

Figure 13. Cyclic voltammogram of 15[ClO₄]₂ in DMF at 295K. Experimental conditions: [15(ClO₄)₂] = 10⁻³ M, Pt-disk working electrode, Ag wire reference electrode, 0.1 M [ⁿBu₄N][PF₆], scan rate = 200 mV s⁻¹.

The redox-processes are summarised in Scheme 7.

$$[(Ni^{II}_2L)_2(2^-)] \underset{\substack{+ e^- \\ (-1.62\text{ V})}}{\overset{- e^-}{\rightleftharpoons}} [(Ni^{II}_2L)_2(2^{\bullet-})]^+$$

15   15^+

$+ e^- \| - e^-$ (-1.04 V)

$$[(Ni^{III}Ni^{II}L)_2(2)]^{4+} \underset{\substack{- 2e^- \\ (0.15\text{ V})}}{\overset{+ 2e^-}{\rightleftharpoons}} [(Ni^{II}_2L)_2(2)]^{2+}$$

15^{4+} 15^{2+}

Scheme 7. Assignment of redox processes for 15[ClO$_4$]$_2$.

The observed potentials for the reduction of the naphthalene diimide ligand **16** are ca. 100 mV more negative than those reported for other N-alkylated naphthalene diimides [95]. Though there are many factors that could contribute to this significant effect, a simplistic thermodynamic view would argue that the influence of the aromatics within the cavitand structure on the NDI upon encapsulation is a strong contributor. The single peak value of 0.15 V measured for the $Ni^{II} \rightarrow Ni^{III}$ oxidation steps is almost identical to that observed for the model **5**[ClO$_4$] (E = 0.11 V vs. Fc$^+$/Fc) [29], indicating that the oxidation/reduction process on one [Ni$_2$L] unit does not influence the processes that occur at the other site [75]. In other words, the two dinuclear nickel(II) subunits behaveas two independent redox-groups. This observation is consistent with the large distance of ca. 19 Å between the two subunits (see Fig. 14(a)) and the fact that the electrostatic (Coulombic) interactions decrease rapidly with increasing distance between two redox-sites.

The radical anion of the NDI within **15$^+$** is characterised by a set of intense and characteristic visible and near-infrared (NIR) absorption bands. Thus, the electronic spectrum of a solution of **15$^+$** in DMF (generated by reduction of **15^{2+}** with an aqueous Na$_2$S$_2$O$_4$ solution) shows bands at 270 (50236), 283 (26840), 329 (28917), 373sh (1072), 400sh (8360), 474 (31586), 607 (9019), 682 (4738) and 756 nm (6618 M^{-1} cm^{-1}). Similar values have been reported for other NDI radicals [95].
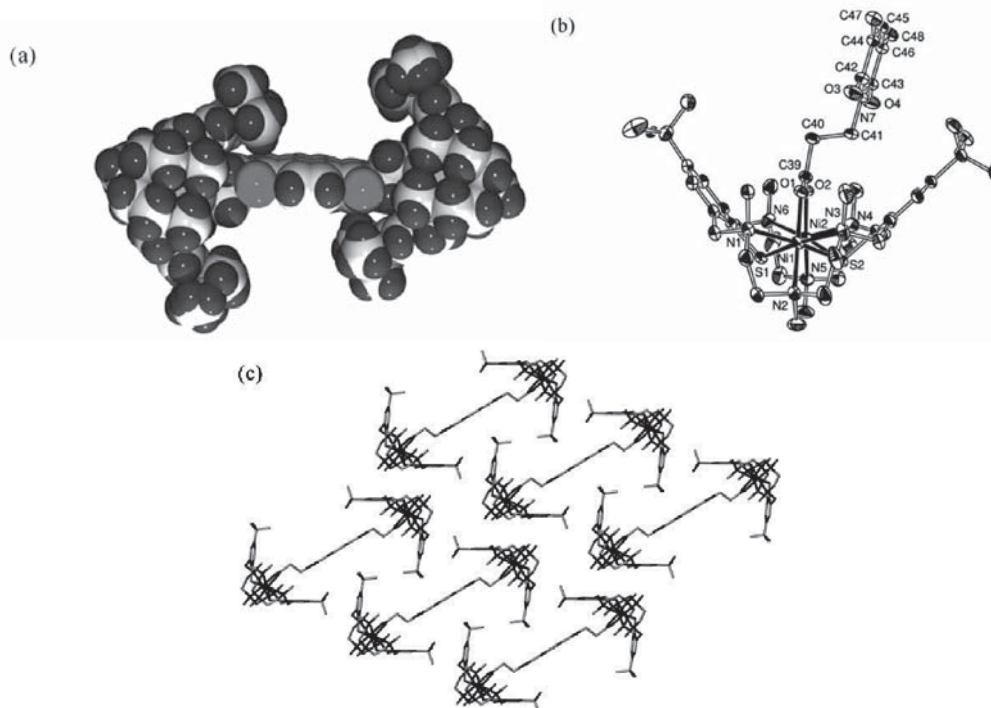
Figure 14. (a) van derWaals representation of the molecular structure of the dication 15^{2+} in crystals of 15[BPh$_4$]$_2$. (b) Asymmetric unit of 15^{2+} with thermal ellipsoids drawn at the 30% probability level, hydrogen atoms and MeCN solvent are omitted for clarity. (c) Packing of individual molecules in the crystal lattice of 15[BPh$_4$]$_2$ (BPh$_4$$^-$ anions and solvent acetonitrile molecules are omitted for clarity).

The composition of the assembly as $\mathbf{15}^{2+}$ was confirmed by a single-crystal X-ray structure determination, as the tetraphenylborate salt $\mathbf{15}[BPh_4]_2$ (prepared by salt metathesis of $\mathbf{15}[ClO_4]_2$ with $NaBPh_4$). Crystals of $\mathbf{15}[BPh_4]_2 \cdot xCH_3CN$ suitable for X-ray crystallography were grown by recrystallisation from MeCN. Fig. 14 displays a van der Waals representation of the centrosymmetric dication $\mathbf{15}$ formed within a triclinic crystal with space group P$\underline{1}$. The dicarboxylate acts as a tetradentate bridging ligand joining two dinuclear $[LNi^{II}_2]^{2+}$ fragments through its carboxylate functions. Each Ni atom is thus surrounded in a highly distorted octahedral fashion by two sulfur atoms and three nitrogen atoms from the supporting ligand L^{2-}, and one oxygen atom from the carboxylate groups of $[\mathbf{16}\text{-}2H]^{2-}$.

The macrocycle assumes a rigid bowl-shaped conformation very similar to that found for $[Ni_2L(\mu\text{-OAc})][ClO_4]$ ($\mathbf{5}$) [29]. As a consequence, the $[Ni_2L]^{2+}$ subunits in $\mathbf{15}$ and $\mathbf{5}$ are structurally very similar, and the Ni–N and Ni–S distances lie within very narrow ranges. The NDI ligand assumes a planar conformation and the Ni_2O_2 planes are only slightly folded with respect to the NDI plane (folding angle = 15.1°). The NDI unit is not coplanar with the aromatic rings of the cavitand, the folding angles between the planes of the two aromatic rings of the cavitand and the plane through the NDI unit being 31.8° and 53.9°, respectively. The Ni···Ni distance of 3.481(1) Å is practically the same as that in $\mathbf{5}$. The distance between the center of the Ni···Ni axes of the binuclear subunits are amounts to 19.010(1) Å.

Complex $\mathbf{15}$ is unique in the sense that its naphthalene diimide coligand is included within the two metallocavitands. To the best of our knowledge, this is the first structural report of such an inclusion complex. In contrast to 'free' NDI compounds, no π–π-stacking interactions involving the NDIs are present in $\mathbf{15}$, a fact attributable to the steric shielding of the $[Ni_2L]^{2+}$units. This feature is no doubt responsible for the enhanced solubility of the complex $\mathbf{15}$ over $\mathbf{16}$. Furthermore, limiting the ability for NDIs to stack has important implications for their use in molecular electronics by limiting aggregation and hence the excimer emission found in many systems [101–103].

The structure is stabilised by intermolecular CH···π interactions as indicated by relatively short distances between the *t*Bu methyl groups and the naphthalene rings (d (C^{tBuMe}···centroids naphthalene ring): 3.618 Å (C36'···X1a), 3.979 Å (C37''···X1a), 3.663 Å (C37'···X1b), 3.902 Å (C36''···X1b) [104]. These interactions lead to a two-dimensional interdigitated packing of the molecules as shown in Figure 14(c). The shortest intermolecular Ni···Ni distance is at 7.470(1) Å. The structure lacks any intermolecular or intramolecular π–π stacking interactions. The closest distances between the centre of the NDI unit and the centre of the aromatic rings are 7.633 and 10.018 Å, respectively. The BPh_4^- counterions are well separated from the dication $\mathbf{15}^{2+}$.

5. Conclusions

In summry, a series of novel tri-, tetra- and pentanuclear complexes composed of dinuclear LM_2 units (M=Co, Ni, Zn; L^{2-} = represents a macrocyclic hexaazadithiophenolate ligand) and ferrocenecarboxylate ($CpFeC_5H_4CO_2^-$), 1,1'-ferrocenedicarboxylate($Fe(C_5H_4\text{-}CO_2)_2^{2-}$), acetylenedicarboxylate, terephthalate, isophthalate, and naphthalene diimide dicarboxylate groups is reported. The complexes, have been synthesized and characterised by UV/Vis-, IR-spectroscopy, and X-ray crystallography. Each dicarboxylate dianion acts as a quadridentate bridging ligand linking two bioctahedral LM_2 units via $\mu_{1,3}$-bridging carboxylate functions to generate discrete dications with a central $LM_2(O_2C\text{-}R\text{-}CO_2)M_2L$ core. The structures differ mainly in the distance between the center of the Ni···Ni axes of the isostructural LNi_2 units (8.841(1) Å in $\mathbf{6}[BPh_4]_2$, 10.712(1) in $\mathbf{7}[BPh_4]_2$, and 9.561(1) in $\mathbf{8}[BPh_4]_2$) and the tilting angle between the two Ni_2O_2 planes (86.3° in $\mathbf{6}[BPh_4]_2$, 58.2° in $\mathbf{7}[BPh_4]_2$, 20.9° in $\mathbf{8}[BPh_4]_2$). Magnetic susceptibility measurements on the complexes over the range 2.0 -295K reveal the presence of weak ferromagnetic exchange interactions between the Ni^{II} ions within the dinuclear subunits with values for the magnetic exchange constant J_1 of 23.10, 18.06, and 14.16 cm^{-1} for $\mathbf{6}[BPh_4]_2$, $\mathbf{7}[BPh_4]_2$, and $\mathbf{8}[BPh_4]_2$, respectively (H = -2JS_1S_2). The magnitude of the exchange interaction J_2 across the dicarboxylate bridges is in all cases less than 0.1 cm^{-1}, suggesting that no significant interdimer exchange coupling occurs in $\mathbf{6}[BPh_4]_2$ – $\mathbf{8}[BPh_4]_2$.

The first members of a new class of polynuclear transition metal complexes composed of classical $[LM_2]$ units (M=Co, Ni, Zn) and ferrocenylcarboxylate groups were synthesised and characterized. Mixed-valent $[(LCo^{II}Co^{III})_2\text{-}(O_2CC_5H_4)_2Fe]^{4+}$ ($\mathbf{14}$) was prepared by oxidation of $\mathbf{12}$ with bromine. X-ray crystal determination of complexes $\mathbf{9}[BPh_4]$, $\mathbf{10}[BPh_4]$, $\mathbf{12}[BPh_4]_2$, $\mathbf{13}[BPh_4]_2$, and $\mathbf{14}[ClO_4]_4$ show, that the ferrocenyl carboxylates act as bidentate ($\mathbf{9}$, $\mathbf{10}$) or bis-bidentate ($\mathbf{12}$–$\mathbf{14}$) bridging ligands towards one or two bioctahedral LM_2 subunits, respectively. The structures are retained in solution as indicated by NMR spectroscopic studies on the diamagnetic ferrocenylcarboxylate $[ClO_4]$. All complexes were found to exhibit a rich redox chemistry. Complexation of the ferrocenylcarboxylates by the LM_2 fragments results in large potential shifts of the ferrocenyl-centred redox process. The redox processes of the LM_2 units are also affected upon complex formation, showing that the electron transfer events of the ferrocenyl moiety and the binuclear subunit influence one another. In $\mathbf{14}$, however, the two dinuclear cobalt(II) subunits behave as two independent redox-groups owing to the large distance between them. Additionally, we found that the magnetic properties in the pentanuclear Ni_4Fe complex $\mathbf{13}$ are based on the ferromagnetic exchange interactions between the Ni^{II} ions in the binuclear subunits. The coupling across the metallocene dicarboxylate bridge is negligible. These results can now be used as a guide for further studies aimed at the synthesis of polynuclear complexes with novel electronic and magnetic properties.

The first member of a new class of inclusion complex composed of encapsulating metallocavitands and naphthalene diimide units **15** were found to exhibit a rich redox chemistry. Complexation of the naphthalene diimide dicarboxylate **16** by the Ni_2L fragments results in a cathodic potential shift of the diimide-centered redox process. The two dinuclear nickel (II) subunits behave as two independent redox-groups owing to the large distance of ca. 19 Å between them. These results can now be used as a guide for further studies aimed at a more complete encapsulation of the naphthalene diimide subunits, its photochemical properties and future developments in optoelectronics.

Acknowledgements

References

[1]. Lozan, V.; Loose, C.; Kortus J.; Kersting, B. Coord. Chem. Rev., 2009, 253, 2244-2260.
[2]. Kersting, B. Z. Anorg. Allg. Chem., 2004, 630, 765–780.
[3]. Cotton, F.A.; Wilkinson, G.; Murillo, C.A.; M. Bochmann, M. Advanced Inorganic Chemistry, 6th ed., John Wiley & Sons, Weinheim, 1999, p. 486.
[4]. a) Cotton, F.A.; Donahue, J.P.; Murillo, C.A. J. Am. Chem.Soc. 2003, 125, 5436–5450.
    b) Cotton, F.A.; Donahue, J.P.; Murillo, C.A.; Perez, L.M. J. Am. Chem. Soc. 2003, 125, 5486–5492.
[5]. A) Eddaoudi, M.; Moler, D.B.; Li, H.; Chen, B.; Reineke, T.M.; O'Keefe, M.; Yaghi, O.M. Acc. Chem. Res. 2001, 34, 319–330; b) Eddaoudi, M.; Kim, J.; Wachter, J.B.; Chae, H.K.; O'Keefe, M.; Yaghi, O.M. J. Am. Chem. Soc. 2001, 123, 4368–4369; c) Rowsell, J. L. C.; Milward, A.R.; Park, K.S.; Yaghi, O.M. J. Am. Chem. Soc. 2004, 126, 5666–5667; d) Barton, T.J.; Bull, L.M.; Klemperer, W.G.; Loy, D.A.; McEnaney, B.; Misono, M.; Monson, P.A.; Pez, G.; Scherer, G.W.; Vartuli, J.C.; Yaghi, O.M. Chem. Mater. 1999, 11, 2633–2656.
[6]. Rao, C. N. R.; Natarajan, S.; Choudhury, A.; Neeraj, S.; Ayi, A.A. Acc. Chem. Res. 2001, 34, 80–87.
[7]. Moulton, B.; Zaworotko, M.J. Chem. Rev. 2001, 101, 1629–1658.
[8]. Kitagawa, S.; Kitaura, R.; Noro, S. Angew. Chem. 2004, 116, 2388–2430; Angew. Chem. Int. Ed. 2004, 43, 2334–2375.
[9]. Kitagawa, S.; Noro, S.; Nakamura, T. Chem. Commun. 2006, 701–707.
[10]. Kahn, O. Molecular Magnetism, VCH, Weinheim, 1993.
[11]. Magneto-Structural Correlation in Exchange Coupled Systems (Eds.: Willet, R.D.; Gatteschi, D.; Kahn, O.), NATO ASI Series, Redidel, Dordrecht, 1985.
[12]. Miller, J.S.; Epstein, A.J. Angew. Chem. 1994, 106, 399–432; Angew. Chem. Int. Ed. Engl. 1994, 33, 385–418.
[13]. Julve, M.; Faus, J.; Verdaguer, M.; Gleizes, A. J. Am. Chem. Soc. 1984, 106, 8306–8308.
[14]. a) Girerd, J.J.; Kahn, O.; Verdaguer, M. Inorg. Chem. 1980, 19, 274–276; b) Bakalbassis, E.; Bergerat, P.; Kahn, O.; Jeannin, S.; Jeannin, Y.; Dromzee, Z.; Guillot, M. Inorg. Chem. 1992, 31, 625–631; c) Kahn, O.; Martinez, C.J. Science 1998, 279, 44–48.
[15]. Deakin, L.; Arif, A.M.; Miller, J.S. Inorg. Chem. 1999, 38, 5072–5077.
[16]. Mukherjee, P.S.; Maji, T.K.; Mostafa, G.; Ribas, J.; Fallah, M.S.E.; Chaudhuri, N.R. Inorg. Chem. 2001, 40, 928–931.
[17]. Gatteschi, D.; Sessoli, R.; Cornia, A. Chem. Commun. 2000, 725–732.
[18]. Gatteschi, D.; Sessoli, R. Angew. Chem. 2003, 115, 278–309; Angew. Chem. Int. Ed. 2003, 42, 268–297.
[19]. Sato, O.; Tao, J.; Zhang, Y.-Z. Angew. Chem. 2007, 119, 2200–2236; Angew. Chem. Int. Ed. 2007, 46, 2152–2187.
[20]. Felthouse, T.R.; Laskowski, E.J.; Hendrickson, D.N. Inorg. Chem. 1977, 16, 1077–1089.
[21]. a) Julve, M.; Verdaguer, M.; Gleizes, A.; Philoche-Levisalles, M.; O. Kahn, O. Inorg. Chem. 1984, 23, 3808–3818; b) Alvarez, S.; Julve, M.; Verdaguer, M. Inorg. Chem. 1990, 29, 4500–4507.
[22]. Verdaguer, M.; Gouteron, J.; Jeannin, S.; Jeannin, Z.; Kahn, O. Inorg. Chem. 1984, 23, 4291–4296.
[23]. a) Bakalbassis, E.G.; Tsipis, C.A.; Mrozinski, J. Inorg. Chem. 1985, 24, 4231–4233; b) Bakalbassis, E.G.; Mrozinski, J.; Tsipis, C.A. Inorg. Chem. 1986, 25, 3684–3690; c) Xanthopoulos, C.A.; Sigalas, M.P.; Katsoulos, G.A.; Tsipis, C.A.; Terzis, A.; Mentzafos, M.; Hountas, A. Inorg. Chem. 1993, 32, 5433–5436.
[24]. Chaudhuri, P.; Oder, K.; Wieghardt, K.; Gehring, S.; Haase, W.; Nuber, B.; Weiss, J. J. Am. Chem. Soc. 1988, 110, 3657–3658.
[25]. Coffman, R.E.; Buettner, G.R. J. Phys. Chem. 1979, 83, 2387–2392.
[26]. Burger, K.S.; Chaudhuri, P.; Wieghardt, K.; Nuber, B. Chem. Eur. J. 1995, 1, 583–589.
[27]. Erasmus, C.; Haase, W. Spectrochim. Acta, Ser. A 1994, 50,2189–2195.
[28]. Cano, J.; De Munno, G.; Sanz, J.L.; Ruiz, R.; Faus, J.; Lloret, F.; Julve, M.; Caneschi, A. J. Chem. Soc. Dalton Trans. 1997, 1915–1923.
[29]. Journaux, Y.; Glaser, T.; Steinfeld, G.; Lozan, V.; Kersting, B. Dalton Trans. 2006, 1738– 1748.

[30]. Magnetism: Molecules to Materials (Eds.: Miller, J.S.; Drillon M.), Wiley-VCH, Weinheim, 2001.

[31]. Coronado, E.; Delhaes, P.; Gatteschi, D.; Miller, J.S.; Eds., Molecular Magnetism: From Molecular Assmblies to Devices, NATO ASI Series, Kluwer, Dordrecht, The Netherlands, 1995, vol. 321.

[32]. Watton, S.P.; Fuhrmann, P.; Pence, L.E.; Caneschi, A.; Cornia, A.; Abbati, G.L.; Lippard, S.J. Angew. Chem. 1997, 109, 2917–2919; Angew. Chem. Int. Ed. Engl. 1997, 36, 2774–2776.

[33]. Larionova, J.; Gross, M.; Pilkington, M.; Andres, H.; Stoeckli-Evans, H.; Güdel, H.U.; Decurtins, S. Angew. Chem. 2000, 112, 1667–1672; Angew. Chem. Int. Ed. 2000, 39, 1605–1609.

[34]. Dearden, A.L.; Parsons, S.; Winpenny, R.E.P. Angew. Chem. 2001, 113, 155–158; Angew. Chem. Int. Ed. 2001, 40, 151–154.

[35]. Demeshko, S.; Leibeling, G.; Dechert, S.; Meyer, F. Dalton Trans. 2006, 3458–3465.

[36]. Kersting, B.; Steinfeld, G.; Siebert, D. Chem. Eur. J. 2001, 7, 4253–4258.

[37]. a) Gressenbuch, M.; Kersting, B. Eur. J. Inorg. Chem. 2007, 90–102. b) Klingele, J.; Klingele, M.H.; Baars, O.; Lozan, V.; Buchholz, A.; Leibeling, G.; Plass, W.; Meyer, F.; Kersting, B. Eur. J. Inorg. Chem. 2007, 5277–5285.

[38]. Nakamoto, K. Infrared and Raman Spectra of Inorganic and Coordination Compounds, John Wiley & Sons, New York, 1986.

[39]. Cotton, F.A.; Donahue, J.P.; Lin, C.; Murillo, C.A. Inorg. Chem. 2001, 40, 1234–1244.

[40]. Bakalbassis, E.G.; Bozopoulos, A.P.; Mrozinski, J.; Rentzeperis, P.J.; Tipsis, C.A. Inorg. Chem. 1988, 27, 529–532.

[41]. Hong, C.S.; Yoon, J.H.; Lim, J.H.; Ko, H.H. Eur. J. Inorg. Chem. 2005, 4818–4821.

[42]. Shakhatreh, S.K.; Bakalbassis, E.G.; Bruedgam, I.; Hartl, H.; Mrozinski, J.; Tsipis, C.A. Inorg. Chem. 1991, 30, 2801–2806.

[43]. Ma, C.; Chen, C.; Liu, Q.; Chen, F.; Liao, D.; Li, L.; Sun, L. Eur. J. Inorg. Chem. 2004, 3316–3325.

[44]. Bourne, S.A.; Lu, J.J.; Mondal, A.; Moulton, B.; Zaworotko, M.J. Angew. Chem. 2001, 113, 2169–2171; Angew. Chem. Int. Ed. 2001, 40, 2111–2114.

[45]. Bayly, S., McCleverty, J.A., Ward, M.D., Gatteschi, D., Totti, F. Inorg. Chem. 2000, 39, 1288–1293.

[46]. Li, L., Liao, D., Jiang, Z., Yan, S. Inorg. Chem. 2002, 41, 421–424.

[47]. Deng, Z.L., Shi, J., Jiang, Z.H., Liao, D.Z., Yan, S.P., Wang, G.L., Wang, H.G., Wang, R.J. Polyhedron 1992, 11, 885–887.

[48]. Ferrocenes (Eds.: Togni, A.; Hayashi, T.), VCH, Weinheim, 1995.

[49]. a) Cotton, F.A.; Donahue, J.P.; Murillo, C.A. Inorg. Chem. 2001, 40, 2229 – 2233; b) Cotton, F.A.; Lin, C.; Murillo, C.A. Inorg. Chem. 2001, 40, 478–484.

[50]. Astruc, D. Electron Transfer and Radical Processes in Transition-Metal Chemistry, Wiley-VCH, Weinheim, 1995.

[51]. Hall, C.D.; Truong, T.-K.-U.; Tucker, J. H. R.; Steed, J.W. Chem. Commun. 1997, 2195– 2196.

[52]. a) DeBlass, A.M.; DeSantis, C.; Fabrizzi, L.; Liccheli, M.; Pallavicini, P.; Poggi, A. in Supramolecular Chemistry (Eds.: Balzani, V.; DeCola L.), Kluwer Academic Publishers, London, 1995, 87 –93; b) Steed, J.W.; Atwood, J.L. Supramolecular Chemistry, Wiley, Chichester, 2000, 224 – 230, 574 – 639.

[53]. Christie, S.D.; Subramanian, S.; Thomson, L.K.; Zaworotko, M.J. Chem. Commun. 1994, 2563 – 2564.

[54]. Metzler-Nolte, N.; Severin, K. in Concepts and Models in Bioinorganic Chemistry (Eds.: Kraatz, H.-B.; Metzler-Nolte, N.), Wiley-VCH, Weinheim, 2006, 113 –133.

[55]. Matsue, T.; Evans, D.H.; Osa, T.; Kobayashi, N. J. Am. Chem. Soc. 1985, 107, 3411–3417.

[56]. a) Beer, P.D. Chem. Commun. 1996, 689 –696; b) Beer, P.D.; Keefe, A.D.; Slawin, A. M.Z.; Williams, D.J. J. Chem. Soc. Dalton Trans. 1990, 3675– 3682; c) Beer, P.D. Acc. Chem. Res. 1998, 31, 71– 80.

[57]. Medina, J.C.; Goodnow, T.T.; Rojas, M.T.; Atwood, J.L.; Lynn, B.C.; Kaifer, A.E.; Gokel, G.W. J. Am. Chem. Soc. 1992, 114, 10583 –10595.

[58]. Atwood, J.L.; Holman, K.T.; Steed, J.W. Chem. Commun. 1996, 1401 – 1408.

[59]. M'hamed Chahma, Lee, J.S., Kraatz, H.-B. J. Organomet. Chem. 2002, 648, 81–86.

[60]. a) Harriman, A.; Ziessel, R. Chem. Commun. 1996, 1707 –1716; b) Buda, M.; Moutet, J.-C.; Saint-Arman, E.; DeCian, A.; Fischer, J.; Ziessel, R. Inorg. Chem. 1998, 37, 4146–4148; c) Ion, A.; Moutet, J.-C.; Saint-Aman, E.; Royal, G.; Tingry, S.; Pecaut, J.; Menage, S.; Ziessel, R. Inorg. Chem. 2001, 40, 3632 –3636; d) Moutet, J.-C.; Saint-Aman, E.; Royal, G.; Tingry, S.; Ziessel, R. Eur. J. Inorg. Chem. 2002, 692–698.

[61]. Butler, I.R.; Kalaji, M.; Nehrlich, L.; Hursthouse, M.; Karaulov, A.I.; Abdul Malik, K.M. J. Chem. Soc. Chem. Commun. 1995, 459 – 460.

[62]. Houlton, A.; Jasim, N.; Roberts, R.M.G.; Silver, J.; D. Cunningham, D.; McArdle, P.; Higgins, T. J. Chem. Soc. Dalton Trans. 1992, 2235– 2241.

[63]. Beer, P.D.; Nation, J.E.; McWhinnie, S.L.W.; Harman, M.E.; Hursthouse, M.B.; Ogden, M.I.; White, A.H. J. Chem. Soc. Dalton Trans. 1991, 2485– 2492.

[64]. a) Cotton, F.A.; Lin, C.; Murillo, C.A. Inorg. Chem. 2001, 40, 472 – 477; b) Cotton, F.A.; Donahue, J.P.; Lin, C.; Murillo, C.A. Inorg. Chem. 2001, 40, 1234 –1244.

[65]. Kersting, B.; Steinfeld, G. Chem. Commun. 2001, 1376 –1377.

[66]. Klingele, M.H.; Steinfeld, G.; Kersting, B. Z. Naturforsch. 2001, 56b, 901 – 907.

[67]. Hausmann, J.; Klingele, M.H.; Lozan, V.; Steinfeld, G.; Siebert, D.; Journaux, Y.; Girerd, J.J.; Kersting, B. Chem. Eur. J. 2004, 10, 1716 –1728.

[68]. Journaux, Y.; Lozan, V.; Hausmann, J.; Kersting, B. Chem. Commun. 2006, 83–84.

[69]. Kersting, B. Angew. Chem. 2001, 113, 4110 – 4112; Angew. Chem. Int. Ed. 2001, 40, 3988 – 3990.

[70]. Kersting, B.; Steinfeld, G. Inorg. Chem. 2002, 41, 1140 –1150.

[71]. Steinfeld, G.; Lozan, V.; Kersting, B. Angew. Chem. 2003, 115, 2363 – 2365; Angew. Chem. Int. Ed. 2003, 42, 2261 – 2263.

[72]. Churchill, M.R.; Li, Y.-J.; Nalewajek, D.; Schaber, P.M.; Dorfman, J. Inorg. Chem. 1985, 24, 2684– 2687.

[73]. Costa, R.; Lopez, C.; Molins, E.; Espinosa, E. Inorg. Chem. 1998, 37, 5686 – 5689.

[74]. Klingert, B.; Rihs, G. Organometallics 1990, 9, 1135– 1141.

[75]. Lozan, V.; Buchholz, A.; Plass, W.; Kersting, B. Chem.Eur. J., 2007,13, 7305–7316.

[76]. Gressenbuch, M.; Lozan, V.; Steinfeld, G.; Kersting, B. Eur. J. Inorg. Chem. 2005, 2223–2234;

[77]. Lang, H.; Kзhler, K.; Zsolnai, L. Chem. Ber. 1995, 128, 519 –523.

[78]. Lozan, V.; Kersting, B. Eur. J. Inorg. Chem. 2005, 504 –512.

[79]. Tao, J.; Xiao, W. J. Organomet. Chem. 1996, 526, 21– 24.

[80]. Sabbatini, M.; Franco, M.A.; Psaro, R. Inorg. Chim. Acta 1980, 42, 267 – 270.

[81]. Wang, X.-B.; Dai, B.; Woo, H.-K.; Wang, L.-S. Angew. Chem. 2005, 117, 6176 –6178; Angew. Chem. Int. Ed. 2005, 44, 6022 – 6024.

[82]. Robin, M.B.; Day, P. Adv. Inorg. Chem. Radiochem. 1967, 10, 247–422.

[83]. Takusagawa, F.; Koetzle, T.F. Acta Crystallogr. Sect. B 1979, 35, 1074 – 1081.

[84]. Cooke, M.W.; Cameron, T.S.; Robertson, K.N.; Swarts, J.C.; Aquino, M.A.S. Organometallics 2002, 21, 5962 –5971.

[85]. Aquino, M.A.S. Coord. Chem. Rev. 1998, 170, 141 –202.

[86]. Lopez, C.; Costa, R.; Illas, F.; Molins, E.; Espinosa, E. Inorg. Chem. 2000, 39, 4560–4565.

[87]. Takusagawa, F.; Koetzle, T.F. Acta Crystallogr. Sect. B 1979, 35, 2888 – 2896.

[88]. Palenik, G.J. Inorg. Chem. 1969, 8, 2744 –2749.

[89]. Tyler, L.A.; Noveron, J.C.; Olmstead, M.M.; Mascharak, P.K. Inorg. Chem. 2000, 39, 357– 362.

[90]. Higgs, T.C.; Ji, D.; Czernuszewicz, R.S.; Matzanke, B.F.; V. Schünemann, V.; Trautwein, A.X.; Helliwell, M.; Ramirez, W.; Carrano, C.J. Inorg. Chem. 1998, 37, 2383 –2392.

[91]. a) Cotton, F.A.; Donahue, J.P.; Murillo, C.A.; Perez, L.M. J. Am. Chem. Soc. 2003, 125, 5486 –5492; b) Chisholm, M.H.; Pate, B.D.; Wilson, P.J.; Zalewski, J.M. Chem. Commun. 2002, 1084 – 1085.

[92]. De Santis, G.; Fabrizzi, L.; Licchelli, M.; Pallavicini, P. Inorg. Chim. Acta. 1994, 225, 239 – 244.

[93]. Beer, P.D. Chem. Soc. Rev. 1989, 18, 409 –450.

[94]. Katz, H.E.; Lovinger, A.J.; Kloc, C.; Slegrist, T.; W. Li, W.; Lin, Y.-Y.; Dodabalapur, A. Nature, 2000, 404, 478–481.

[95]. Bhosale, S.V.; Jani, C.H.; Langford, S.J. Chem. Soc. Rev., 2008, 37, 331–342.

[96]. Andric, G.; Boas, J.F.; Bond, A.M.; Fallon, G.D.; Ghiggino, K.P.; Hogan, C.F.; Hutchison, J.A.; Lee, M. A.-P.; Langford, S.J.; Pilbrow, J.R.; Troup, G.J.; Woodward, C.P. Aust. J. Chem., 2004, 57, 1011–1019.

[97]. Bauscher, M.; Mantele, W. J. Phys. Chem, 1992, 96, 11101–11108.

[98]. Langford, S.J.; Latter, M.J.; Woodward, C.P. Photochem. Photobiol., 2006, 82, 1530–1540.

[99]. Fallon, G.D.; Lee, M.A-P.; Langford, S.J. Acta Crystallogr., Sect.E, 2004, 60, o542–o543.

[100]. Lee, K.A.; Lozan, V.; Langford, S.J.; Kersting, B. Dalton Trans., 2009, 7481-7485.

[101]. Liu, S.-G.; Sui, G.; Cormier, R.A.; Leblancand, R.M.; Gregg, B.A. J. Phys. Chem. B, 2002, 106, 1307–1315.

[102]. Lee, H.N.; Xu, Z.; Kim, S.K.; Swamy, K.M.K.; Kim, Y.; Kimand, S.-J.; Yoon, J. J. Am. Chem. Soc., 2007, 129, 3828–3829.

[103]. P. Ganesan, P.; Van Lagen, B.; Marcelis, A.T.; Sudhlter, E.J.R.; Zuilhof, H. Org. Lett., 2007, 9, 2297- 2300.

[104]. Meyer, E.A.; Castellano, R.K.; Diederich, F. Angew. Chem., 2003, 115, 1244–1287; Angew. Chem., Int. Ed., 2003, 42, 1210–1250.

SYNTHESIS AND CRYSTAL STRUCTURE OF A NEW Fe(II) α-DIOXIMATE WITH TRIAZINE

O. Ciobanica[a], P. Bourosh[b*], O. Bologa[a], I. Bulhac[a], V. Lozan[a], V. Shofransky[a]

[a]Institute of Chemistry, Academy of Sciences of Moldova, 3, Academiei str.,
MD-2028, Chisinau, R. Moldova; E-mail : ionbulhac@yahoo.com, Phone :+(373 22) 73 97 90
[b]Institute of Applied Physics, Academy of Sciences of Moldova, 5, Academiei str., MD-2028,Chisinau,
R. Moldova;E-mail : bourosh.xray@phys.asm.md, Phone : +(373 22) 73 81 54

Abstract: The interaction of $[Fe(DfgH)_2Py_2]$ (where DfgH=monodeprotonated diphenylglyioxime, Py-pyridine) and 1,3,5-triazine (Trz) in chloroform resulted in a new coordination compound with the composition $[Fe(DfgH)_2(Trz)_2]\cdot 2CHCl_3$ (**1**). The crystal structure of **1,** determined by single crystal X-ray diffraction, revealed that Fe(II) atom is coordinated by four oximic nitrogen atoms of two DfgH and two nitrogen atoms of two Trz ligands resulting in octahedral surrounding.

Keywords: synthesis; Fe(II)dioxime; 1,3,5-triazine, crystal structure

Introduction

The inner-sphere substitution of apical ligands in $[M(DioxH)_2A_2]$ complexes (M = metal ion, DioxH = monodeprotonated α-dioxime and A = neutral apical ligand) represents an attractive procedure for obtaining new complexes with polyfunctional ligands such as bridgind exo-bidentate or polydentate species. Aromatic [1] and heterocyclic [2, 3] amines, thio- and seleno-carbamides [4, 5] readily enter the inner coordination sphere of dioximates. Generally, such compounds reveal an octahedral surrounding of the metal ion with a stable square-planar $M(DioxH)_2$ building block consolidated by two strong intramolecular hydrogen O–H···O bonds [6]. Various binuclear and polymeric coordination compounds based on Co(III), Cu(II), Cd(II) and Zn(II) dioximates and 4,4'-bipyridyl bridging ligands have been reported [7-10]. It was of particular interest to investigate the complexation process and coordination ability of potentially polydentate heterocyclic amines, in particular, 1,3,5-triazine (Trz). The CSD [11] statistics indicates that the architecture of the molecule Trz, which contains three donor nitrogen atoms, facilitates the formation of polynuclear complexes, three-dimensional networks, various nanoporous materials with Cu(II) [12-14], Ru(II) [15, 16], Pt(II) [17] and Ag(I) [18, 19] transition metal ions.

Our contribution describes the reaction of Trz molecule with $[Fe(DfgH)_2(Py)_2]$ which results in the formation of a new compound $[Fe(DfgH)_2(Trz)_2]\cdot 2CHCl_3$ (**1**) and X-ray study of these crystals.

Results and discussion

We recently reported Co(III) and Fe(II) dioximates with pyridine and its derivatives, pyrazine and isonicotinamide ligands [3, 20-22]. We have shown the specificity of formation of metal coordination polyhedron, the connection features of these ligands to the central atom and their mutual positions in the complexes. These results demonstrated that various heterocyclic amines coordinate in dioximate-based complexes to the metal ion through one nitrogen atom. The structural studies of (**1**), which results from the interaction of $[Fe(DfgH)_2(Py)_2]$ with Trz, confirmed the substitution of coordinated Py by Trz molecules. It was determined that the crystal consists of molecular centrosymmetric Fe(II) complexes and crystallization molecules of $CHCl_3$. The metal ion in the complex has a *trans*-octahedral coordination, similar to those found in transition metal complexes of the general formula $[M(DioxH)_2A_2]$ [3, 6, 20].

The coordination polyhedron of the Fe(II) ion is formed by six nitrogen atoms (Figure 1), four of which belong to two bidentate monoprotonated dioxime (DfgH⁻) ligands, and two of monodentate Trz molecules. The CSD analysis [11] showed that in Cu(II), Ru(II), Pt(II) and Ag(I) complexes Trz molecules are quite frequently involved in coordination as tridentate ligands coordinating to the metal atoms through three nitrogen atoms. Thus, trinuclear (e.g. Pt(II) complex [17]), tetra- and hexanuclear complexes (Cu(II) complexes [12]) or polymeric structures (Cu(II), Ru(II) and Ag(I) complexes [13, 15, 18, 19]) are formed. However Trz molecules can also act as bidentate bridging ligands (Cu(II) complexes [13, 14]), as well as monodentate ligands (complex of Ru(II) [16]). In the mononuclear molecule of compound (**1**), two Trz molecules are coordinated to the Fe(II) ion in a monodentate mode. The equatorial plane of the octahedron is defined by two monoprotonated DfgH⁻ residues, coordinated in a N,N-type chelate mode. The Fe-N distances in the basal plane have the values of 1.898 (7) and 1.911 (7) Å, and the distance to the apical Trz nitrogen atom is 1.990 (6) Å (Table 1). In coordination environment of copper, two monoprotonated oxime residues are linked by the intramolecular O-H···O hydrogen bonds (O(2)–H···O(1)(–x+1, –y, –z) 1.75, 2.541(9)Å, 161°), resulting in the alternation of five-membered chelate rings and six-membered hydrogen-bonded rings (Figure 1).

Figure 1. The molecular structure of [Fe(DfgH)₂(Trz)₂]·2CHCl₃

The dihedral angle between the plane of the Trz ring and the equatorial plane of the coordination polyhedron is equal to 95.3°. Similar arrangement of monodeprotonated α-dioximes and neutral ligands which contain nitrogen atoms was also found in iron complexes with imidazole [23, 24], β-picoline [25], pyrazine [26] and isonicotinamide [3]. The values of interatomic distances and angles for coordinated Trz molecules do not differ significantly from those found in similar complexes of Cu(II), Ru(II), Pt(II) and Ag(I) [13-19].

Table 1

Bond lengths (Å) and angles (deg) for compound (1).

Atom-atom	d, Å	Atom-atom	d, Å
Fe(1)-N(2)	1.898(7)	C(6)-Cl(2)	1.740(9)
Fe(1)-N(1)	1.911(7)	C(6)-Cl(1)	1.774(9)
Fe(1)-N(3)	1.990(6)	C(6)-Cl(3)	1.777(9)
N(1)-C(1)	1.291(10)	C(11)-C(16)	1.32(1)
N(1)-O(1)	1.361(8)	C(11)-C(12)	1.33(1)
N(2)-C(2)	1.296(11)	C(12)-C(13)	1.37(2)
N(2)-O(2)	1.397(8)	C(13)-C(14)	1.32(2)
N(3)-C(5)	1.343(9)	C(14)-C(15)	1.31(2)
N(3)-C(3)	1.382(9)	C(15)-C(16)	1.41(2)
N(4)-C(3)	1.397(10)	C(21)-C(22)	1.38(1)
N(4)-C(4)	1.426(11)	C(21)-C(26)	1.39(1)
N(5)-C(4)	1.390(11)	C(22)-C(23)	1.38(2)
N(5)-C(5)	1.409(10)	C(23)-C(24)	1.38(3)
C(1)-C(11)	1.47(1)	C(24)-C(25)	1.31(3)
C(1)-C(2)	1.492(11)	C(25)-C(26)	1.45(2)
C(2)-C(21)	1.50(1)		
Atom-atom-atom	ω, grad	Atom-atom-atom	ω, grad
N(1)-Fe(1)-N(2)	79.8(3)	N(3)-C(3)-N(4)	122.8(8)
N(1)-Fe(1)-N(2)#1	100.2(3)	N(5)-C(4)-N(4)	119.1(7)
N(1)-Fe(1)-N(3)	90.0(3)	N(3)-C(5)-N(5)	124.0(7)
N(1)-Fe(1)-N(3)#1	90.0(3)	Cl(2)-C(6)-Cl(1)	110.4(5)
N(2)-Fe(1)-N(3)	88.9(3)	Cl(2)-C(6)-Cl(3)	111.4(5)
N(2)-Fe(1)-N(3)#1	91.1(3)	Cl(1)-C(6)-Cl(3)	109.1(4)
C(1)-N(1)-O(1)	119.7(7)	C(16)-C(11)-C(12)	117.3(11)
C(1)-N(1)-Fe(1)	118.9(6)	C(16)-C(11)-C(1)	119.8(10)

O(1)-N(1)-Fe(1)	121.1(6)	C(12)-C(11)-C(1)	122.9(8)
C(2)-N(2)-O(2)	119.3(7)	C(11)-C(12)-C(13)	121.8(11)
C(2)-N(2)-Fe(1)	118.0(6)	C(14)-C(13)-C(12)	120.5(12)
O(2)-N(2)-Fe(1)	122.7(6)	C(15)-C(14)-C(13)	119.2(12)
C(5)-N(3)-C(3)	117.3(7)	C(14)-C(15)-C(16)	119.8(11)
C(5)-N(3)-Fe(1)	122.3(5)	C(11)-C(16)-C(15)	121.2(12)
C(3)-N(3)-Fe(1)	120.2(5)	C(22)-C(21)-C(26)	120.9(11)
C(3)-N(4)-C(4)	118.3(8)	C(22)-C(21)-C(2)	118.8(9)
C(4)-N(5)-C(5)	118.4(8)	C(26)-C(21)-C(2)	120.4(11)
N(1)-C(1)-C(11)	125.1(8)	C(21)-C(22)-C(23)	121.5(13)
N(1)-C(1)-C(2)	110.6(8)	C(24)-C(23)-C(22)	118(2)
C(11)-C(1)-C(2)	124.2(9)	C(25)-C(24)-C(23)	122(2)
N(2)-C(2)-C(1)	112.6(8)	C(24)-C(25)-C(26)	122(2)
N(2)-C(2)-C(21)	123.5(8)	C(21)-C(26)-C(25)	116(1)
C(1)-C(2)-C(21)	123.9(9)		

Symmetry transformations used to generate equivalent atoms: #1 -*x*+1, -*y*, -*z*.

The crystal packing of compound **1** is shown in Figure 2. The structure is molecular; the complexes are located close to the center of the symmetry of the orthorhombic *Pbca* space group, forming channels with a 27% of the total crystal volume. In these channels, the solvate $CHCl_3$ molecules are encapsulated and linked to the complexes by weak hydrogen-bond interactions (C(6)–H···O(1) (*x, y, z*) 0.98, 2.27, 2.966 Å, 127°) (Figure 2).
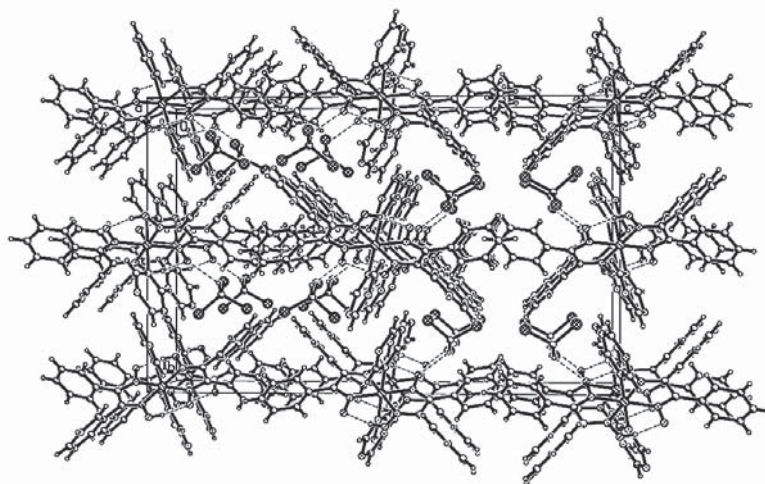

Figure 2. Fragment of crystal packing in 1.

The IR spectrum of **1** confirms the presence of all organic ligands used in the synthesis process [27, 28]. The characteristic bands of the Trz ligands were assigned as following: the weak intensity band at 3054 cm^{-1} was attributed to $\nu(= C$-$H)$ vibration; a series of six weak intensity bands within 2000-1660 cm^{-1} – to overtones and vibrations typical to mono- and 1,3,5-substituted aromatic; 1069 cm^{-1} - to (δ_{plane} (CH) of mono- and 1,3,5-substituted aromatic. The presence of DfgH$^-$ is documented by the characteristic oscillations $\nu_{as}(CH_2)$= 2931, $\delta(OH)$= 1730, $\delta_{as}(CH_2)$=1450 and $\delta(C$=N-$O)$=731 cm^{-1}.

Experimental

All reagents and solvents were obtained from commercial sources and were used without further purification. Elemental analysis was performed on an Elementar Analysensysteme GmbH Vario El III elemental analyzer. The IR spectra were obtained in Vaseline on a FT IR Spectrum-100 Perkin Elmer spectrometer in 400-4000 cm^{-1} range.

Synthesis. To [Fe(DfgH)$_2$Py$_2$] (0.17 g, 0.245 mmol) dissolved in 20 mL of chloroform Trz (0.05 g, 0.615 mmol) dissolved in 10 mL of methyl alcohol was added. The resulted crystals of hexagonal habitus were collected from the dark-cherry solution. Yield: ~ 60%. The crystals are insoluble in water and alcohol. Anal. found for $C_{36}H_{30}Cl_6Fe_1N_{10}O_4$, %: Fe 6,05; C 46,28; H 3,18; N 14,75. Calculated: Fe 5,97; C 46,23; H 3,23; N 14,98.

X-ray Crystallography. Diffraction measurement for **1** was carried out at room temperature on a STOE IPDS diffractometer equipped with a graphite monochromator utilizing MoKα (λ = 0.71073Å) radiation and ω scans. Final unit cell dimensions were obtained and refined on an entire data set. The crystal structure was solved by direct methods. All calculations to solve the structures and to refine the models were carried out with the programs SHELXS97 and SHELXL97 [29]. The C–bound H atoms were placed in calculated positions and were treated using a riding model approximation with $U_{iso}(H)=1.2U_{eq}(C)$, while the O–bound H–atoms were found from differential Fourier maps at intermediate stages of the refinement and their positions were constrained using the AFIX 83 instruction in SHELXL for oxime groups. These hydrogen atoms were refined with isotropic displacement parameter $U_{iso}(H)=1.5U_{eq}(O)$. Crystal data and details on the structure refinement are given in Table 2. Selected geometric parameters for **1** are given in Table 1. CCDC 933171 contains the supplementary crystallographic data for **1**.

Table 2

Crystal data and structure refinement for compound (1).

Empirical formula	$C_{36}H_{30}Cl_6Fe_1N_{10}O_4$
Formula weight	935.25
Crystal system	orthorhombic
Space group	*Pbca*
Unit cell dimensions	
a, Å	8.957(2)
b, Å	17.231(3)
c, Å	27.285(5)
V, Å^3	4211.1(14)
Z	4
ρ(calc), mg/m^3	1.475
μ, mm^{-1}	0.790
F(000)	1904
Crystal size, mm^3	0.2 x 0.12 x 0.04
θ range for data collection, deg	2.99 – 25.05
Index ranges	$-10 \leq h \leq 10, -20 \leq k \leq 20, -32 \leq l \leq 32$
Reflections collected	64661
Independent reflections	3685 (*R*(int) = 0.32650
Completeness to θ = 25.05°, %	98.6
Data / parameters	3685 / 259
GOOF	1.019
Final R indices (*I*>2σ(*I*))	*R*1 = 0.0983, *wR*2 = 0.2002
R indices (all data)	*R*1 = 0.2074, *wR*2 = 0.2428
Largest diff. peak and hole, e·Å^{-3}	0.338 / -0.407

References
[1]. Melnic, E. Bourosh P.; Rija, A.; Lipkowski, J.; Bologa, O.A.; Bulhac, I.; Coropceanu, E.; and Shafranski, V.N. Rus. J. Coord. Chem. 2012, 38(9), 623-633.
[2]. Coropceanu, E.B.; Rija, A.P.; Lozan, V.I.; Bologa, O.A.; Boldisor, A.A.; Bulhac, I.I.; Kravtsov, V. Ch.; Bourosh, P.N. Russ. J. Coord. Chem. 2012, 38(8), 545-551.
[3]. Bulhac, I.I.; Bourosh, P.N.; Schollmeyer, D.; Zubareva, V.E.; Suwinska, K.; Ciobanica, O.; and Simonov, Yu.A. Russ. J. Coord. Chem. 2009, 35(5), 352-359.
[4]. Bourosh, P.N.; Coropceanu, E.B.; Rija, A.P.; Bologa, O.A.; Gdaniec, M.; Bulhac, I.I. J. Mol. Struct. 2011, 998, 198-205.
[5]. Rija, A.P.; Nicolescu, A.; Soran, A.; Coropceanu, E.B.; Bulhac, I.I.; Bologa, O.A.; Deleanu, C.; and Bourosh, P.N. Rus. J. Coord. Chem. 2011, 37(10), 757-765.
[6]. Botoshanskii, M.M.; Dvorkin, A.A.; Simonov, Yu.A.; Malinowskii, T.I. Stroenie dimethylglioximatov

perehodnykh metallov. In Kristallicheskie struktury neorganicheskikh soedinenii. Izd-vo. Shtiintsa: Kishinev, 1974; 26-61.

[7]. Bourosh, P.; Coropceanu, E.; Kravtsov, V.; Bologa, O.A.; Shafranski, V.N.; Bulhac, I. The XVII-th International Conference „Physical Method in Coordination and Supramolecular Chemistry", Book of Abstracts, P13, Chisinau, October, 24-26, 2012, p. 61.

[8]. Coropceanu, Ed. B.; Croitor, L.; Botoshansky, M. M.; Siminel, A. V.; Fonari, M. S. Polyhedron. 2011, 30, 2592-2598.

[9]. Croitor, L.; Coropceanu, Ed. B.; Siminel, A.V.; Kravtsov, V. Ch.; Fonari, M.S. Cryst. Growth& Design, 2011, 11, 3536-3544**.**

[10]. Croitor, L.; Coropceanu, Ed.B.; Siminel, A.V.; Kulikova, O.; Zelentsov, V.I.; Datsko, T.; Fonari, M.S. CrystEngComm. 2012, 14, 3750-3758.

[11]. Allen, F.H. Acta Crystallogr. 2002, 58B(3-4), 380-388.

[12]. Pike, R.D.; Borne, B.D.; Maeyer, J.T.; Rheingold, A.L. Inorg. Chem. 2002, 41**,** p. 631-633.

[13]. Blake, A.J.; Brooks, N.R.; Champness, N.R.; Cooke, P.A.; Deveson, A.M.; Fenske, D.; Hubberstey, P.; Li, W.-Sh.; Schroder, M. J. Chem. Soc., Dalton Trans. 1999, 2103-2110.

[14]. Maeyer, J.T.; Johnson, T.J.; Smith, A.K.; Borne, B.D.; Pike, R.D.; Pennington, W.T.; Krawiec, M.; Rheingold, A.L. Polyhedron. 2003, 22, 419-431.

[15]. Furukawa, S.; Ohba, M.; Kitagawa, S. Chem. Commun. 2005, p. 865-867.

[16]. Garcia, M.H.; Morais, T.S.; Florindo, P.; Piedade, M.F.M.; Moreno, V.; Ciudad, C.; Noe, V. J. Inorg. Biochem. 2009, 103, 354 -361.

[17]. Kaufman, W.; Venanzi, L.M.; Albinati, A. Inorg.Chem. 1988, 27, 1178-1187.

[18]. Venkataraman, D.; Lee, S.; Moore, J.S.; Zhang, P.; Hirsch, K.A.; Gardner, G.B.; Covey, A.C.; Prentice, C.L. Chem. Mater. 1996, 8, 2030-2040.

[19]. Bertelli, M.; Carlucci, L.; Ciani, G.; Proserpio, D.M.; Sironi, A. J. Mater. Chem. 1997, 7, 1271-1276.

[20]. Bulhac, I.; Bouros, P.N.; Bologa, O.A.; Lozan, V.; Ciobanica, O.; Lipkowski, J.; Mitina, T.F.; Simonov, Yu.A. Rus. J. Inorg. Chem. 2010, 55(7), 1042-1051.

[21]. Chiobenika, O.; Bourosh, P.; Lozan, V.; Bologa, O.; Bulhak, I.; Wicher, B.; Simonov, Yu. Rus. J. Inorg. Chem. 2011, 56(7), 1054-1063.

[22]. Bourosh, P.; Ciobanica, O.; Lozan, V.; Bulhac, I. Rus. J. Coord. Chem. 2012, 38(7), 461-470.

[23]. Bowman, K.; Gaughan, A.P.; Dori, Z. J. Am. Chem. Soc. 1972, 94(3), 727-731.

[24]. Prout, C.K.; Wiseman, T.J. J. Chem. Soc. 1964, No1, 497-504.

[25]. Dvorkin, A.A.; Simonov, Yu.A.; Malinovskii, T.I.; Bulgak, I.I.; Batir, D.G. Dokl. Akad. Nauk SSSR(Russ.)(Proc. Nat. Acad. Sci. USSR), 1977, 234(6), 1372-1375.

[26]. Kubel, F.; Strahle, J. Z. Naturforsch. B: Chem. Sci. 1983, 38(2), 258-259.

[27]. Bellami, L. Infrakrasnye spektry slozhnykh molecul. Izd-vo inostr. lit. Moskva. 1963. 590 p.

[28]. Khakanisi, K. Infrakrasnye spektry i stroenie organicheskikh soedinenii. Izd-vo "Mir". 1965. 216 p.

[29]. Sheldrick, G.M. Acta Cryst. 2008, A64, 112-122.

SYNTHESIS AND BIOLOGIC PROPERTIES OF SOME1-(ALCHYL) PHENYL-3-(4-(3-(PYRIDIN-2-IL)ACRYLOYL)PHENYLTHIOUREA

Popusoi Ana[1], Barba Nicanor[1], Gulea Aurelian[1], Roy Jenny[2],
Poirier Donald[2], Prisacari Viorel[3]

[1] Moldova State University, Chisinau, 2009, 60 Mateevici Str., Moldova
[2]Laboratory of Medicinal Chemistry, CHUQ (CHUL) - Research Center and Université Laval, 2705 Boulevard Laurier, Québec City, G1V 4G2, Canada
[3]Microbiological Laboratory, Moldova State Medicinal and Pharmacy University, 2009, Stefan cel Mare Str., Moldova
Tel +373-22-57-76-96, E-mail: popusoi.ana@gmail.com

Abstract: This paper describe the synthesis of some 1-(alchyl)aril-3-(4-(3-pyridin-2-il) acryloyl)phenylthiourea obtained by condensation of 2-pyridincarboxaldehyde with some derivatives of 4-acetylphenilthioureas in basic medium or by addition of aliphatic and aromatic amines to the correspondingisothiocyanatopropenones. 12 new compounds were obtained and their biological properties were analysed. The substituted thioureas by pyridine radicals, morpholine and phenol show a maximum bacteriostatic activity for Gram positive microorganisms like: *Staphylococcus Aureus* and *Enterococcus Faecalis* at the minimum inhibitory concentration 9.37-37.5 µM. Antifungal activity for *Candida Albicans*, *Aspergillus Niger*, *AspergillusFumigatus, Penicillium* is weak, in minimum inhibitory concentration 600->600 µM. The leukemia activity like inhibitor (HL-60), is 84-96.9% at the concentration 10^{-5}mol/l and 15-20% and at the concentrations 10^{-6}, 10^{-7}mol/l.

Keywords: chalcones, isothiocyanatopropenones, thioureas, antibacterial activity, antifungal activity, antiproliferative activity

Introduction

Some chalcones, arylheterilpropenone and their derivatives posses divers biological properties: inflammatory [1, 2], antioxidative [3], antituberculosis [4], anti malaria [5], antifungal and antibacterial [6, 7], anticancer [8-12] etc. The testation of chalcones [8] like proliferates inhibitors of cancer cells showed that their activity depend by the substituent (OH, OCH_3) position on the benzene nuclei. Some chalcones [13] with thioamids groups exhibit higher anticancer action then in those without sulphur. For chalcones with thioureea groups was detected a pronounced antinociceptive activity [14]. The chalcones [15] (with OH, OCH_3, $OCH_2=CH_2$ groups) extracted from Chinese Licorice roots have a strong antileishmanial activity. Robinson et all. [11], showed that the enon fragment of the chalconesincrease the biological activity.

Some derivatives, obtained from chalcones through chemical transformations are also biologically active compounds. The modification of the chalcones on the carbonyl group with some hydrazine derivatives, followed by cyclisation [16], leads to 1,3,5-substituted pyrazolines with anticonvulsant and antidepressant properties. Were identified bacterial species which can modify and cyclisedchalcones in biologically active flavonoids [17].

In the literary sources mentioned above, the chalcones are obtained through the condensation of the aromatic and heterocyclic aldehides with acetyl arenes or by modifying the functional groups [18]. 1,3-Pyridylphenylpropenones with thiourea groups are less studies and became our object of study.
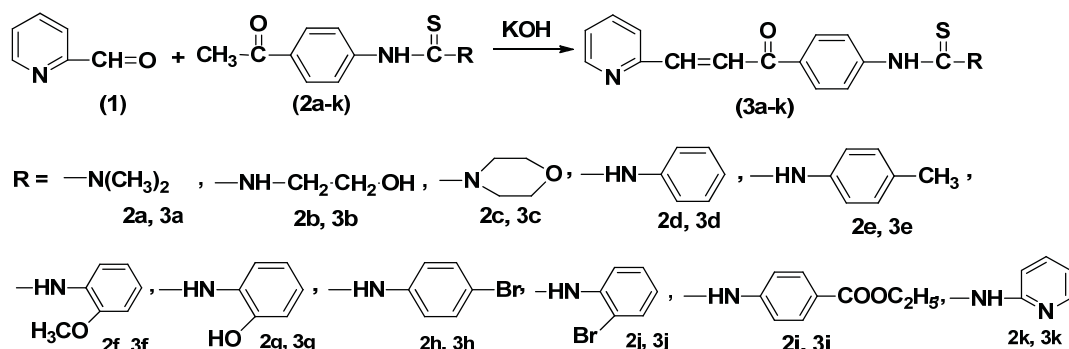
Results and discussion
Chemistry

The first chalcones [14] with thiourea groups were obtained by Claisen-Schmidt condensation of a 1-(4-acetylphenyl)-3-(4-clorophenyl)thiourea with different aromatic aldehides:
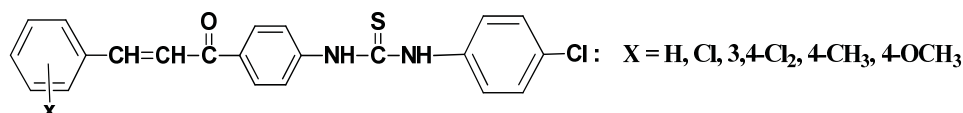

We obtained 3-(4-(3-pyridin-2-il)acryloyl)phenyl-1-(alchil)arilthiourea with similar structure as illustrated below:

4-Acetylphenylthiourea 2a was obtained [19] by heating 1-(4-aminophenyl)ethanonewith tetramethyltiuram disulphide (DTMT) in dimethylformamide (82%, m.p.= 175-176°C).4-Acetylphenylthioureas**2b-k** were synthesised by addition of the corresponding amines to the4-isothiocyanatoacetophenone [20].
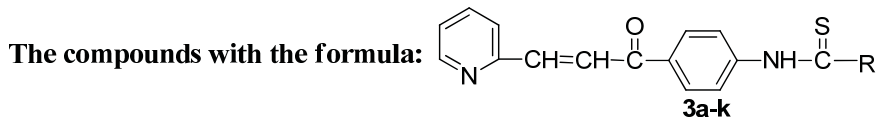
The condensation of the thioureas **2a-k** with 2-pyridincaboxaldehide**1** in alkaline catalysis lead to 1,3-arilpyridil-propenones**3a-k** with thioureas groups. Silofol thin layer chromatography showed that the reactions take place easy, with good yields, but with small quantities of secondary products which can be isolated by recristallisation from ethanol.

Alternative method of synthesis of thiourea **3b** was investigated following the transformations:
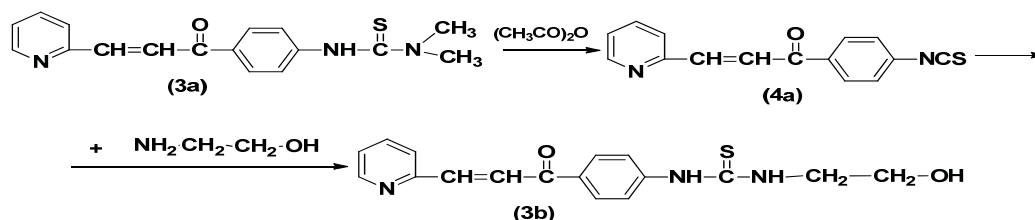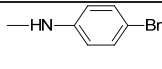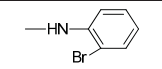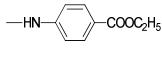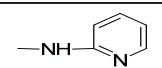

By heating the thiourea **3a**withaceticanhydride is obtained the 1-(4-isothiocyanatophenyl)-3-(pyridin-2-il)prop-2-en-1-one**4a** with 53% of yield. The addition of the monoethanolamine to the isothiocyanate **4a**, lead to thiourea **3b** with 92% of yield. The synthesis of thioureas **3b-k** in this way is less convenient because of low yield (53%) of the isothiocyanate **4a**. The solvents and reagents were purified in the usual manners where necessary. The structure of the compounds**3a-k** and **4a** were confirmed by the elemental and spectral analysis (^{13}C, ^{1}H-NMR).The NMR (^{13}C, ^{1}H-NMR) spectra were recorded on a Bruker DRX-400spectrometer at room temperature. All chemical shifts (^{1}H, ^{13}C) are given in ppm versus $SiMe_4$ using DMSO – d_6 as solvent.

Table 1

The compounds with the formula:

Nr.	R	Formula	Found/Calculated, %			M. P., 0C	Yield, %
			C	**H**	**N**		
3a	—N(CH3)2	$C_{17}H_{17}N_3OS$	65.03/65.57	5.98/5.50	14.00/13.49	180-182	89
3b	—NH–CH2·CH2·OH	$C_{17}H_{17}N_3O_2S$	62.31/62.36	5.20/5.23	12.80/12.83	124-125	80
3c	—N morpholine	$C_{19}H_{19}N_3O_2S$	64.92/64.57	6.35/5.42	11.72/11.89	145-146	89
3d	—HN–phenyl	$C_{21}H_{17}N_3OS$	70.52/70.17	4.81/4.77	11.64/11.69	155-156	75
3e	—HN–C6H4–CH3	$C_{22}H_{19}N_3OS$	70.93/70.75	5.29/5.13	11.38/11.25	134-136	82
3f	—HN–C6H4, H3CO	$C_{22}H_{19}N_3O_2S$	67.90/67.84	4.89/4.92	10.81/10.79	142-143	79
3g	—HN–C6H4, HO	$C_{21}H_{17}N_3O_3S$	67.26/67.18	4.50/4.56	11.38/11.19	163-165	68

3h		$C_{21}H_{16}BrN_3O_2S$	57.19/57.54	4.84/3.68	9.69/9.59	149-150	82
3j		$C_{21}H_{16}BrN_3O_2S$	57.22/57.54	4.90/3.68	9.64/9.59	159-162	79
3i		$C_{24}H_{21}N_3O_3S$	66.00/66.80	5.18/4.91	9.34/9.74	123-125	78
3k		$C_{20}H_{16}N_4OS$	65.49/66.65	5.14/4.47	15.75/15.54	197-199	87

Elemetal analyses (C, H, N) were performed on a Elemental Analyza Vario EL (III).

The melting points were determined with a Melting point meter A. KRUSS OPTRONIC Germania KSP-1N 90-26V/Al.

Antibacterial activity

The antibacterial activity (bacteriostatic and bactericidal) of the **3a-k** substances was investigated for the micro-organisms: *Staphylococcus Aureus, Enterococcus Faecalis, Esscherichia coli, Proteus Vulgaris, Pseudomonas Aeruginosa* by serial dilution method in liquid nutrient medium (meat peptone broth 2%, pH = 7,0).

For sowing were used cultures of indicated microorganisms, grown on agar during 18 hours and washed with isotonic solution of sodium chloride. Insemination dose is 500 thousand copies for 1 mL of nutrient medium. The tubes were shaken and thermostated at 37°C during 24 hours. As control were used nutrients media inoculated with the same strains but without investigated substances. Evaluation of bacteriostatic activity (CMI) was carried out visually, as lack of growths of microorganisms in the broth. Bacterial activity (CMB) was determined based on the lack of growth of microorganisms after repeated seeding on peptone agar with subsequent thermostating for 24, 48 hours.

The obtained results are presented in Table 2.

Table 2

Antibacterial activity of compounds 3a-k

Nr.	Microorganisms. Antibacterial activity for the – Tests (mcg/ml)									
	Staphylococcus Aureus		*Enterococcus Faecalis*		*Escherichia Coli*		*Proteus Vulgaris*		*Pseudomonas Aeruginosa*	
	*CMI	**CMB	CMI	CMB	CMI	CMB	CMI	CMB	CMI	CMB
3a	>300	>300	>300	>300	>300	>300	>300	>300	>300	>300
3b	>300	>300	>300	>300	>300	>300	>300	>300	>300	>300
3c	37,5	>300	37,5	>300	>300	>300	>300	>300	>300	>300
3d	>300	>300	>300	>300	>300	>300	>300	>300	>300	>300
3e	>300	>300	>300	>300	>300	>300	>300	>300	>300	>300
3f	>300	>300	>300	>300	>300	>300	>300	>300	>300	>300
3g	>300	>300	>300	>300	>300	>300	>300	>300	>300	>300
3h	>300	>300	>300	>300	>300	>300	>300	>300	>300	>300
3j	9,37	>300	>300	>300	>300	>300	>300	>300	>300	>300
3i	>300	>300	>300	>300	>300	>300	>300	>300	>300	>300
3k	>300	>300	>300	>300	>300	>300	>300	>300	>300	>300
Furaci-uyline	18,7	37,5	37,5	75	18,7	37,5	150	>300	>300	>300

*MIC – minimum inhibitory concentration. **MBC – minimum bactericide concentration.

The investigation results show that the substance **3c** posses bacteriostatic activity for Gram-positive microorganisms: Staphylococcus Aureus and Enterococcus Faecalis at concentration of 37.5 mcg/mL. The substance **3j** show bacteriostatic activity for S. Aureus (minimum inhibitory concentration is 9.37 μM) which prevail furaciline activity 2 times; minimum antibacterial concentration of this substance for Staphylococcus Aureus and for the other test bacterial cultures (Table 2) investigated is more than 300 μM.

Bacteriostatic and bactericidal action of substances **3a, 3b, 3d-f,3h,3i,3k** for all test bacterial cultures investigated is at concentrations above 300 μM.

Antifungal activity

Antifungal activity of compounds **3a-k** was investigated for fungi: *Candida Albicans, Aspergillus Niger, Aspergillus Fumigatus, Penicillium*. Initially, the substances were dissolved in dimethylformamide (concentration 10 mg/mL) and subsequent concentrations were obtained using serial dilution method in broth (broth Saburo). The inoculates were prepared from cultures of fungi. After mixing the inoculates with the solutions of investigated substances, the tubes were exposed in thermostat at 28°C during 14 days (Candida Albicans during 48 hours). Antifungal activity was determined by the absence of the fungal growth in a repeated sowing on Saburo agar with incubation during 7 days (Candida albicans during 48 hours).

The investigation results show that the substances **3a-k** possess antifungal activity for Candida albicans, Aspergillus Niger, Aspergillus Fumigatus, Penicillium in minimum inhibitory concentration of 600 and…>600 µM.

Antileukemia activity (HL-60)

Cell culture. Human promyelocytic leukemia cells HL-60 (ATCC, Rockville, MD, USA) were routinely grown in suspension in 90% RPMI-1640 (Sigma, Saint Louis, USA) containing L- glutamine (2 nM), antibiotics (100 IU penicillin/mL, 100 mg streptomycin/mL) and supplemented with 10% (v/v) foetal bovine serum (FBS), in a 5% CO_2 humidified atmosphere at 37°C. Cells were currently maintained twice a week by diluting the cells in RPMI 1640 medium containing 10% FBS. Cellproliferation assay. The cell proliferation assay for compounds and ligands was performed using 3-(4,5-dimethylthiazol-2-yl)-5-(3-carboxymethoxyphenyl) 2-(4-sulfophenyl)-2H-tetrazolium (MTS) (Cell Titer 96 Aqueous, Promega, USA), which allowed us to measure the number of viable cells. In brief, triplicate cultures of 10,000 cells in a total of 100 mL medium in 96-well microtiter plates (Becton Dickinson and Company, Lincoln Park, NJ, USA) were incubated at 37°C, 5% CO_2. Compounds were dissolved in ethanol to prepare the stock solution of 1 J 1022 M. These compounds and doxorubicin (Novapharm, Toronto, Canada), as a positive control, were diluted at multiple concentrations (1 and 10 µM) with culture media, added to each well and incubated for 3 days. Following each treatment, MTS (20 µL) was added to each well and the mixture incubated for 4 hours. MTS is converted to water-soluble colored formazan by dehydrogenase enzymes present in metabolically active cells. Subsequently, the plates were read at 490 nm using a microplate reader (Molecular Devices, Sunnyvale, CA).

Table 3

Antiproliferative activity of thioureas onhuman leukemia (HL-60) cells at two concentrations

Nr.	Compound	Inhibition of cell proliferation (%)		
		Concentrates, mol/l		
		10^{-5}	10^{-6}	10^{-7}
3a		84.0	6.2	0
3g		92.6	22.8	15.7
3f		84.2	23.0	17.8
3h		92.6	19.8	18.7
3k		96.9	13.7	18.4
6a		24.0	23.8	10.8
7a		0	0	0
8a		0	0	0
Dox	**Dox-** doxorubic	100	100	100

[a]SEM <± 4% of a single experiment in triplicate, **Dox** – doxorubicin of a single experiment in triplicate,

*7a and **8a**are known [22, 23]

If we look at the compounds **3a**, **3g**, **3f**, **3h**, **3k** like derivatives of thiourea, we observe that their anticancer activity depends strongly on structure and varies from 0...96.9% for the compound concentration 10^{-5}mol/L and from 0...23.8% for concentrations 10^{-6}, 10^{-7}mol/L. The introduction of a 2 pyridincarbonil radical in the thiourea molecule (compound **3a**) increase suddenly the activity from 0 to 84%, which is also mentioned for the other inhibitors with the

enon structure [11]. Replacing methyl groups in thiourea **3a** with the rest of phenol compound**3g** increases activity, but is reduced by ~8% for thiourea **3f**, when the hydroxyl group is methylated. The compounds **3g** and **3h** have almost the same activity, which is maximal for thiourea **3k** (96.9%), which contain in his structure two pyridine residues. A. Gulea et all. [21] explain the activity of anticancer inhibitors by the formation of hydrogen bonds with ADN cancerous cells. Indeed this type of interaction can be maximum for thiourea 3k with two pyridine nuclei. For compound 3k, when the structural fragment of 2-pyridil acryloyl is replaced by 4-dimethylaminophenyl-(thiourea**6a**), the activity decrease to 24%. In the case of compounds **7a** and **8a** with more pronounced hydrophobic character when the hydrogen bonds with the substrate are weaker, the activity is zero.

Conclusion

1-(alkyl)aryl-3-(4-(3-pyridin-2-yl)phenylthioureas **3a-k** are obtained with better efficiency by condensation of 4-acetilfenilthioureas derivatives with 2-pyridincarboxaldehide in the basic medium. The synthesis of this thioureas by the addition of aliphatic or aromatic amines to 1-(4-isothiocyanatophenyl)-3-(pyridin-2-il)prop-2-en-1-one is inconvenient; the respective isothiocyanate with rest of pyridine is unstable and is isolated with a relatively low yield.

The biological research has shown:

- The thioureas with the rest of morpholine **3c** and o-bromfenil **3j**possess bacteriostatic activity   more pronounced for microorganisms Staphylococcus Aureus and Enterococcus Faecalis.

- The antifungal activity of compounds **3a-k** is weak.

- The antileukemia activity (HL-60) depends on the compounds structure; inhibition ranging from 24...96.9% for concentrations 10^{-5} mol/l. The thiourea,**3k** with two pyridine nuclei have maximal activity.

Experimental section

Synthesis   of   1,1-dimethyl-3-(4-(3-(pyridin-2-il)-acryloyl)-phenyl)thiourea   (3a). To   the   solution   of 3-(4-Acetylphenyl)-1,1-dimethylthiourea**2a** (2.22 g, 0.01 mol) and 6 mL of dimethylformamide was added under stirring potassium hydroxide (1 g, 0.02 mol) dissolved in 4 mL of ethanol. After, the 2-pyridincarboxialdehide (1.28 g,0.012mol) in 4 mL of ethanol was added dropwise and the temperature maintained at 5-10°C. The resulting mixture was keep at room temperature for 12 hours. The impurities was isolated by filtration and the resulting solution was neutralized until pH = 7-8 to afford 2.78 g (89%) of thiourea**3a**, m.p. = 180-182°C. ¹H-NMR (DMSO-d_6), ppm: 3.30 (s, 6 H, N(CH$_3$)$_2$), 7.43-8.19 (m, 10H, =CH, Ar-H), 9.36 (s, 1H, NH). ¹³C-NMR (DMSO-d_6), ppm: 187.82 (C=O), 181.39 (C=S), 144.47 (C-N), 144.73 (-**CH**=CH), 126.97 (-CH=<u>CH</u>), 154.79, 136.82, 131.37, 131.11, 128.84, 40.44, 40.23.

Synthesis of 1-(2-hidroxietil)-3-(4-(3-(piridin-2-il)acryloyl)phenyl)thiourea (3b)

a) To the solution of 1-(4-acetylphenyl)-3-(2-hydroxyethyl)thiourea 0.64 g, (0.002 mol) dissolved in minimum quantity of DMF was added potassium hydroxide 0.27 g(0.0048 mol) dissolved in 4 mL of ethanol. After, a solution of 2-pyridincarboxialdehide0.2 g, (0.002 mol) in 2.5 mL of ethanol was added under vigorous stirring at 10-20°C. The resulting mixture was neutralized with hydrochloric acid until pH = 7 and cooled down to room temperature. The yellow crystals was isolated by filtration 0.52 g (80%), m.p. = 124-125°C.

b) The mixture of 1-(4-isothiocyanatophenyl)-3-(pyridin-2-il)prop-2-en-1-one **4a**0.53 g, (0.002 mol), mono-ethanolamine 0.12 g, (0.002 mol) and 2 mL of acetone was kept at room temperature for 30 minutes, after boiled for 5 minutes and then cooled down to room temperature. The resulting crystals were isolated by filtration,to obtain 0.60 g (92%) of thiourea**3b**,m.p. = 124-125°C. ¹H-NMR (DMSO-d_6), ppm: 7.41-8.69 (m, 13H, =CH, Ar-H), 10.08 (s,1H, <u>NH</u>-C$_6$H$_4$), 10.00 (s, 1H, <u>NH</u>-CH$_2$), 3.6(m, 4H, N-CH$_2$-CH$_2$-O), 4.09 (s, 1H, OH). ¹³C- NMR (DMSO, d_6), ppm: 188.26 (C=O), 180.65 (C=S), 143.40 (-CH=CH), 126.67 (-CH=CH), 46.95 (-<u>CH$_2$</u>-CH$_2$-OH), 59.48 (-CH$_2$-<u>CH$_2$</u>-OH).

The 3c-k thioureas were obtained in the similar way.

N-(4-(3-(Pyridin-2-yl)acryloyl)phenyl)morfoline-4-carbothioamide 3c.¹H-NMR (DMSO-d_6), ppm: 7.42-8.70 (m, 10H, =CH, Ar-H), 9.72 (s, 1H, NH-C$_6$H$_4$), 3.66-3.93(m, 8H, N-(CH$_2$-CH$_2$)$_2$O). ¹³C-NMR (DMSO, d_6), ppm: 188.42 (C=O), 181.72 (C=S), 142.88 (-<u>CH</u>=CH), 125.67 (-CH=<u>CH</u>), 146.47 (C-N), 66.26 (-O-<u>CH$_2$</u>), 49.36 (-N-<u>CH$_2$</u>), 153.39, 137.67, 132.70, 129.42, 125.30, 123.48.

1-Phenyl-3(4-(3-(pyridin-2-yl)acryloyl)phenyl)thiourea 3d. ¹H-NMR (DMSO-d_6), ppm: 8.71-7.14 (m, 15H, =CH, Ar-H), 10.14 (s,1H, <u>NH</u>-C$_6$H$_4$), 10.09 (s, 1H, <u>NH</u>-C$_6$H$_5$). ¹³C-NMR (DMSO-d_6), ppm: 188.39 (C=O), 179.79 (C=S), 142.97 (-<u>CH</u>=CH), 125.67 (-CH=<u>CH</u>),   137.69 (C$_6$H$_5$-<u>NH</u>), 145.12 (C-N), 153.37, 150.48, 132.93, 129.84, 122.17, 124.16.

1-(4-(3-(Pyridin-2-yl)acryloyl)phenyl)-3-(p-tolyl)thiourea 3e.¹H-NMR (DMSO-d_6), ppm: 7.20-8.71 (m, 14H, =CH, Ar-H), 9..25 (s, 1H, 2<u>NH</u>-C$_6$H$_4$), 9.22 (s, 1H, <u>NH</u>-C$_6$H$_4$)3.62 (s, 3H, CH$_3$).¹³C-NMR (DMSO-d_6), ppm: 188.37 (C=O), 179.62 (C=S), 142.90 (-<u>CH</u>=CH), 144.38 (C$_6$H$_5$-<u>NH</u>)**,** 122.14, 127.3, 137.26, 131.05.

1-(2-Methoxyphenyl)-3-(4-(3-(pyridin-2-yl)acryloyl)phenyl)thiourea 3f.^{1}H-NMR (DMSO-d$_6$), ppm: 3.75 (s, 3H, OCH$_3$), 6.83-8.71 (m, 14H, =CH, Ar-H), 9.77 (s, 1H, NH-C$_6$H$_4$), 10.21 (s, 1H, NH-C$_6$H$_4$). ^{13}C-NMR (DMSO, d$_6$), ppm: 188.38 (C=O), 180.68 (C=S), 142.85 (-CH=CH), 126.65 (-CH=CH), 153.31 (-C$_6$H$_4$-OCH$_3$), 144.38 (C-N), 59.93 (-O-CH$_3$), 153.31, 150.40, 145.15, 137.78, 130.90, 129.81, 125.33, 122.22, 121.75.

1-(2-Hydroxyphenyl)-3-(4-(3-(pyridin-2-yl)acryloyl)phenyl)thiourea 3g.^{1}H-NMR(DMSO-d$_6$), ppm: 8.71-6.56 (m, 13H, =CH, Ar-H), 10.17 (s,1H, NH-C$_6$H$_4$), 9.52 (s, 1H, NH-C$_6$H$_4$-OH). ^{13}C-NMR (DMSO-d$_6$), ppm: 188.40 (C=O), 179.38 (C=S), 142.88 (-CH=CH), 153.35 (-C$_6$H$_4$-OH), 157.99 (C-N), 127.09 (-CH=CH), 145.11, 140.59, 137.74, 132.86, 125.75, 122.20, 114.39.

1-(4-Bromophenyl)-3-(4-(3-(pyridin-2-yl)acryloyl)phenyl)thiourea 3h.^{1}H-NMR (DMSO-d$_6$), ppm: 8.7-7.41 (m, 14H, -C$_6$H$_3$ and =CH), 10.32 (s,1H, NH-C$_6$H$_4$), 10.22 (s, 1H, NH-C$_6$H$_4$-Br). ^{13}C-NMR (DMSO-d$_6$), ppm: 188.49 (C=O), 179.83 (C=S), 143.00 (-CH=CH), 126.07 (-CH=CH), 122.42 (C$_6$H$_4$-Br), 153.40, 149.37, 144.76, 131.80, 133.18, 129.83, 137.61, 137.27.

1-(2-Bromophenyl)-3-(4-(3-(pyridin-2-yl)acryloyl)phenyl)thiourea 3j.^{1}H-NMR (DMSO-d$_6$), ppm: 8.7-7.41 (m, 14H, -C$_6$H$_3$ and =CH), 10.32 (s,1H, NH-C$_6$H$_4$), 10.22 (s, 1H, NH-C$_6$H$_4$-Br). ^{13}C-NMR (DMSO-d$_6$), ppm: 188.49 (C=O), 179.83 (C=S), 143.00 (-CH=CH), 126.07 (-CH=CH), 122.42 (C$_6$H$_4$-Br), 153.40, 149.37, 144.76, 131.80, 133.18, 129.83, 137.61, 137.27.

Ethyl 4-(3-(4-(3-(pyridin-2-yl)acryloyl)phenyl)thioureido)benzoate 5i.^{1}H-NMR (DMSO-d$_6$), ppm: 6.55-8.70 (m, 14H, =CH, Ar-H), 10.53 (s, 1H, NH-C$_6$H$_4$), 10.46 (s, 1H, NH-C$_6$H$_4$), 4.33-4.28(m, 2H, -CH$_2$-O), 1.34(m, 3H -CH$_3$). ^{13}C-NMR (DMSO, d$_6$), ppm: 188.47 (C=O), 179.58 (C=S), 165.78 (C=O-O-C$_2$H$_5$), 144.30 (-CH=CH), 125.67 (-CH=CH), 144.61 (C-N), 60.99 (-O-CH$_2$), 14.68 (-CH$_3$), 153.38, 150.50, 137.66, 133.29, 130.24, 129.87, 125.30, 122.55.

1-(Pyridin-2-yl)-3-(4-(3-(pyridin-2-yl)acryloyl)phenyl)thiourea   3k.^{1}H-NMR (DMSO-d$_6$), ppm: 7.13-8.71 (m, 14H, =CH, Ar-H), 10.53 (s, 1H, **NH**-Py), 10.46 (s, 1H, NH-C$_6$H$_4$). ^{13}C-NMR (DMSO, d$_6$), ppm: 188.59 (C=O), 178.39 (C=S), 143.27 (-CH=CH), 125.59 (-CH=CH), 143.85 (C-N), 153.84, 153.31, 150.51, 137.67, 134.21, 129.75, 125.39, 122.55.

Synthesis of 1-(4-isothiocyanatophenyl)-3-(pyridine-2-yl)prop-2-en-1-one 4a. The mixture of 1,1-dimethyl-3-(4-(3-(pyridin-2-il)-acryloyl)-phenyl)thiourea (0.6 g, 0.02 mol), acetic anhydride (0.2 g, 0.002 mol) and 7 mL ethyl acetate was stirred at 60-65°C during 3 hours. The end of the reaction was follow by the totally consumption of the thiourea**3a**. The mixture was stirred until the thiourea 3a was totally consumed. The resulting product was washed with NaHCO$_3$ solution and after dried with anhydrous Na$_2$SO$_4$. The organic layer was diluted with hexane (2:1) and chromatographed on Silica Gel (eluent hexane/benzene 1:1). The solvent was removed *in vacuo* to afford 0.28 g (53%) of isothiocyanatopropenone **4a**, m.p. = 124-126°C.Elemental and spectral analysis: Found, %: C, 67.75; H, 3.88; N,10.62. Calculated, %: C, 67.65; H, 3.78; N,10.52.^{1}H-NMR(DMSO-d$_6$), ppm: 7.37-8.70 (m, 10H, =CH, Py-H, Ar-H). ^{13}C-NMR (DMSO-d$_6$), ppm: 189.34 (C=O), 181.39 (C=S), 143.96 (-CH=CH), 126.89 (-CH=CH).

References

[1].   Lee S. K., Jeon T. W., Basnet A., Lee E. S., Jeong T. C., Journal of Chromatography B, 837, 2006, pp. 108-111.
[2].   Zarghi A., Zebardast T., Hakimian F., Farshad H. Shirazi, P. N. Bioorganic Medicinal Chemistry 14, 2006, pp. 7044-7050.
[3].   Xiaolin Z., Simoneau A. R., Flavokawain A, Cancer Research 65, 2005, p. 3479-3486.
[4].   Mohamed A.A., Shaharyar M., Siddiqui A. A., European Journal of Medicinal Chem. 42, 2007, pp. 268-275.
[5].   Chen M., Brogger S. C., Zhai L., Rasmussen M. H., Theander T. G., Journal of Infectious Diseases 176(5), 1997, pp. 1327-1333.
[6].   Kalirajan R., Sivakumar S.U., Jubie S., Gowramma B., Suresh B., International Journal of ChemTech. Research, Vol.1, No.1, 2009, pp. 27-34.
[7].   Konieczny M.T., Konieczny W., Sabisz M., Skladanowski A., Wakiec R., Augustynowicz-Kopec E., Zwolska Z., Chemical and Pharmaceutical Bulletin 55 (5), 2007, p. 817-820.
[8].   Daszkiewicz J. B., Comte G., Barron D., Thomasson F., Tetrahedron Letters 40, 1999, pp. 7095-7098.
[9].   Tabata K., Motani K., Takayanagi N., Nishimura R., Aşami S., Kimura Y., Ukiya M., Biological Pharmaceutical Bulletin, 28(8), 2005, pp. 1404-1407.
[10]. Nishimura R., Tabata K., Arakawa M., Ito Y., Kimura Y., Biological Pharmaceutical Bulletin, 30(10), 2005, pp. 1878-11883.
[11]. Robinson T. P., Hubbard R. B., Ehlers T. J., Arbiser J. L., Goldsmithd D. J., Bowen J. P, Bioorganic Medicinal Chemistry 13, 2005, pp. 4007-4013.

[12]. Vijaya Bhaskar Reddy M., Chung-Ren Su, Wen-Fei C., Yi-Nan L., Yin-Hwa R. C., Bioorganic Medicinal Chemistry 16, 2008, pp. 7358-7370.

[13]. Patil C. B., Mahajan S. K., Suvarna A. K., Journal of Pharmaceutical Sciences and Research, vol. 1(3), 2009, pp. 11-22.

[14]. Santos L., Lima L.A., Cechinel-Filho V., Correa R., Buzzi F. C., Nunes R. J., Bioorganic Medicinal Chemistry 16, 2008, pp. 8526-8534.

[15]. Zhai L., Chen M., Blom J., Theander T. G., Journal of Antimicrobial Chemotherapy 43, 1999, p. 793-803.

[16]. Ozan Ruhoglu, Zuhal O. Unsal C., Arzneim-Forsch/Drug Res. 55, No. 8, 2005, p. 431-436.

[17]. Sanchez-Gonzalez M., Rosazza J. P. N., Journal of Natural Products, 67 (4), 2004, pp. 553-558.

[18]. Horakova K., Drobnica L., Nemec P., Neoplasma 18 (1971), pp. 355-359.

[19]. Barbă N., Dragalina G., Vieru R., Popuşoi A., Brevet de invenţie MD 3684 G2, 2008.

[20]. Doub L., Richardson L. M., Herbst D. R., Black M. L., Stevensona O. L., Bambas L. L., Youmans G. P., Youmans A. S., Journal of the American Chemical Society 80, 1958, pp. 2205-2217.

[21]. A. Gulea, D. Poirier, J. Roy, V. Stavila, I. Bulimestru, V. Ţapcov, M. Bârcă, L. Popovschi, Journal of Enzyme Inhibition and Medicinal Chemistry 23, 2008, pp. 806-818.

[22]. Barbă N., Luchiţa G., Barbă A., Vieru R., Brevet de invenţie MD 2985, 2004.

[23]. Nair V. G., Journal Indian Chemical Society 42B, (6), 1965, pp. 359-366.

THE INFLUENCE OF THE POROUS STRUCTURE OF LOCAL ACTIVATED CARBONS ON THE IMMOBILIZATION OF THE CONGO RED DYE AND VITAMIN B$_{12}$

Țîmbaliuc Nina, Lupașcu Tudor

Institute of Chemistry of the ASM
3 Academiei str., MD 2028, Chişinău, R. Moldova
E-mail: timbaliuc_nina@yahoo.com

Abstract: The adsorption properties of activated carbons, obtained from local raw materials (nut shells, peach and plum stones), towards Congo Red and vitamin B$_{12}$ have been studied. The values of adsorption of these marker-substances are in direct correlation with the structural characteristics of the studied samples of activated carbons, in particular, with their mesopore volume**.**

Keywords: activated carbons, adsorption, mesopore volume, Congo Red, vitamin B$_{12}$

Introduction

Environmental Protection is now one of the primary problems of mankind as ecological systems can hardly adapt to anthropogenic factors pressure [1, 2]. One of the consequences of environmental degradation caused by intensive development of industry, excessive chemical agriculture and food processing industry is the radically worsening health status of the population. These factors are responsible for the considerable increase of diseases and medical conditions of people, increase of exogenous intoxications. Currently are successfully used several methods of detoxification of the body, but one of the simplest and most efficient methods is entherosorption. The most required entherosorbents are those made of activated carbons. A special role in this respect lies with activated charcoal made from fruit stones, nut shells, grape seeds [3-5]. This is due to the fact that morphological structure of nut shells and fruit stones favors the production of activated carbon with high mechanical strength and increased adsorption capacity. Significant adsorption properties of these activated carbons offer wide possibilities for their use [6-8], including in the complex treatment of poisoning and medical conditions to immobilize, neutralize and eliminate toxic substances from the body through different mechanisms (ions exchange or complexation).

The aim of this study was to estimate the adsorption properties of local activated carbon obtained from the waste products of local food industry towards toxic substances with an average molecular weight (MM 500-1500) as oligopeptides, lipopolysaccharides. As test compounds for adsorption were selected Congo Red dye and vitamin B12, substances frequently used as markers in modeling states of intoxication of the human body [9, 10].

Materials and methods

For this research were selected local active carbons obtained from nut shells - CAN-8, peach kernels - CAS-23, plum kernels – CAP, considering the further perspective of their use for medicinal purposes, and the industrial activated carbon - BAU. In accordance with the requirements of the modern Pharmacopoeia Monograph, approved for the medicinal carbon Medicas E, heavy metals content shall not exceed 0.001% (specification for iron content - not more than 0.06%), ash residues - 5% and the amount of substances dissolved in hydrochloric acid solution - 2.5%. To obtain these quality indices of activated carbons, selected samples were treated with 6% HCl solution at boiling temperature for 2 hours. Afterwards, the coal was washed with distilled water until a solution pH of 5 was reached. Finally, the coal was dried in an oven at 110 ^{0}C until a constant mass was reached. The content of heavy metals, ash residues for selected coal samples were determined in the atomic spectroscopy testing laboratory of the Institute of Chemistry. The concentrations of heavy metals, calcination residues and substances dissolved in hydrochloric acid solution were within the requirements of Pharmacopoeia Monograph for all selected coal samples.

The porous structure of investigated activated carbons was determined from nitrogen adsorption-desorption isotherms (N$_2$, 77 K) obtained using the AUTOSORB-1MP automatic analyzer (Quantachrome, USA).

As a marker substance was used vitamin B$_{12}$ (Cyanocobalamin) with MM 1355.38 c.u. (Figure 1) and Congo Red dye (Panreac Quimica PA, Analytical Reagents & Fine Chemicals) with MM 696.66 c.u. (Figure 2).
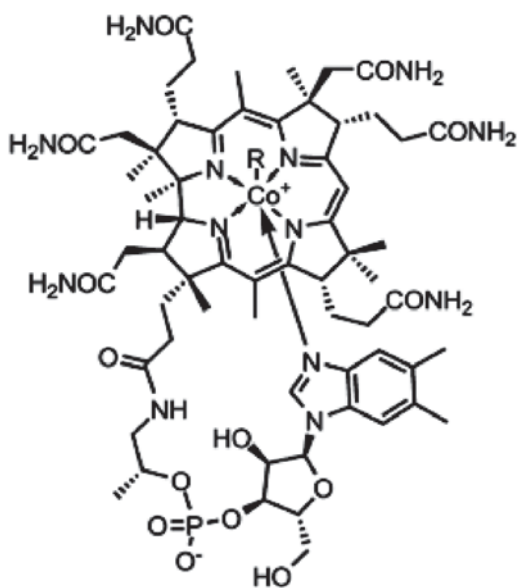
R = 5'-deoxyadenosyl, Me, OH, CN

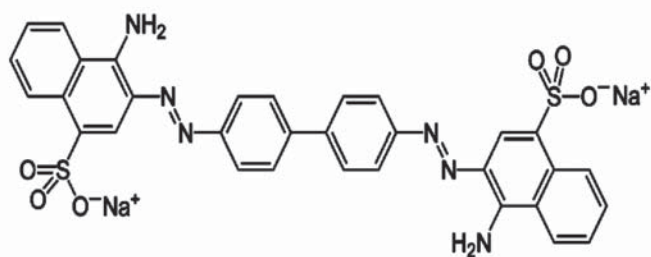**Figure 1. Vitamin B12 ($C_{63}H_{88}CoN_{14}O_{14}P$)**

**Figure 2. Congo Red dye ($C_{32}H_{22}N_6Na_2O_6S_2$)**

Adsorption processes were investigated under static conditions. Adsorption isotherms were measured at a temperature of 22 °C, after the process equilibrium was reached. Equilibrium concentrations were determined using the UV/Vis spectrophotometer, Jenway model 6505. The used experimental method consists in dosing, at known quantities of activated carbon with constant mass *m* of fixed volume *V* of solutions with known concentrations C_0 and stirring maintained for sufficient time to reach chemical equilibrium at constant temperature.

Results and Discussion

To assess the immobilizing potential towards studied compounds, structure parameters were determined and adsorption capacity of selected activated carbons. The nitrogen adsorption-desorption isotherms for investigated coal samples are shown in Figure 3.
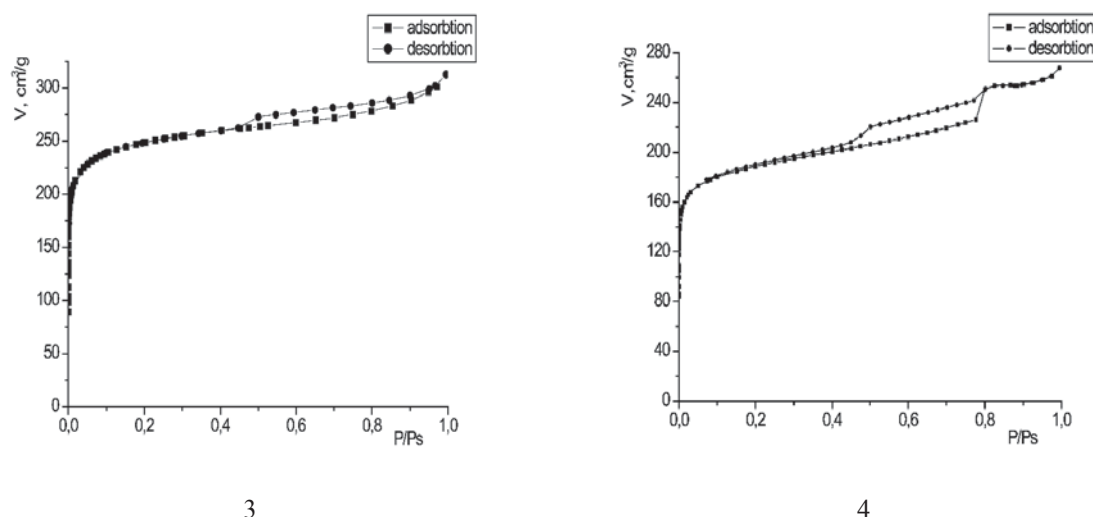

1

2

3

4
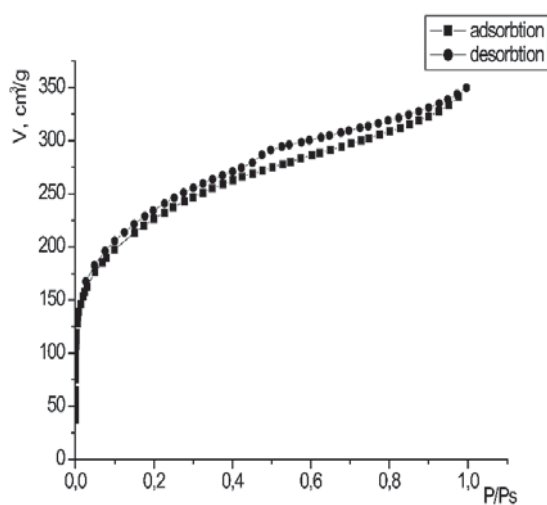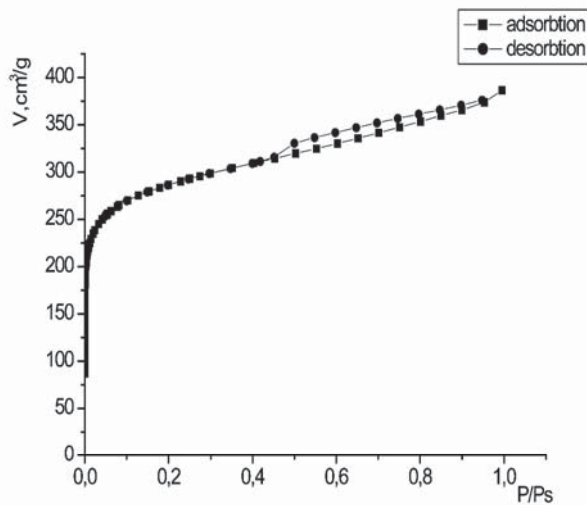
Figure 3. Adsorption-desorption isotherms of nitrogen (77 K) for activated carbons CAP (1), CAN-8 (2), CAS-23 (3) and BAU (4).

Geometric surface and structure parameters of studied activated carbons were determined from adsorption-desorption isotherms of nitrogen using the BET equation and the method NLDFT ((Non-Local Density Functional Theory) [11]. The results are presented in Table 1.

Analysis of the results suggests that the most effective carbonic adsorbent for immobilization of investigated substances could be the activated carbon CAN-8, with the highest value of S_{geom} (1071 m²/g). But if we take into account the size of B_{12} molecules (1.83 x 1.41 x 1.14 nm) and Congo red dye (2.8 x 1.1 x 0.5 nm) [10] then we can assume that predominantly the mesoporous structure of coal CAP (V_{me} = 0.239 cm³/g) will be the crucial feature in the immobilization of investigated substances.

Table 1

Structural parameters of activated carbons CAN-8, CAS-23, CAP and BAU

AC sample	V_S, cm³/g	W_{01}, cm³/g	S_{geom}, m²/g	Vme, cm³/g	Vme/ V_S, %
CAN-8	0,598	0,413	1071	0,185	30.9
CAS-23	0,484	0,376	945	0,108	22.3
CAP	0,541	0,302	769	0,239	44.2
BAU	0,41	0,28	713	0,13	31.7

V_S- sorption volume of pores; W_{01}- micropores volume; S_{geom}- geometrical surface of pores; **Vme** –mesopores volume.
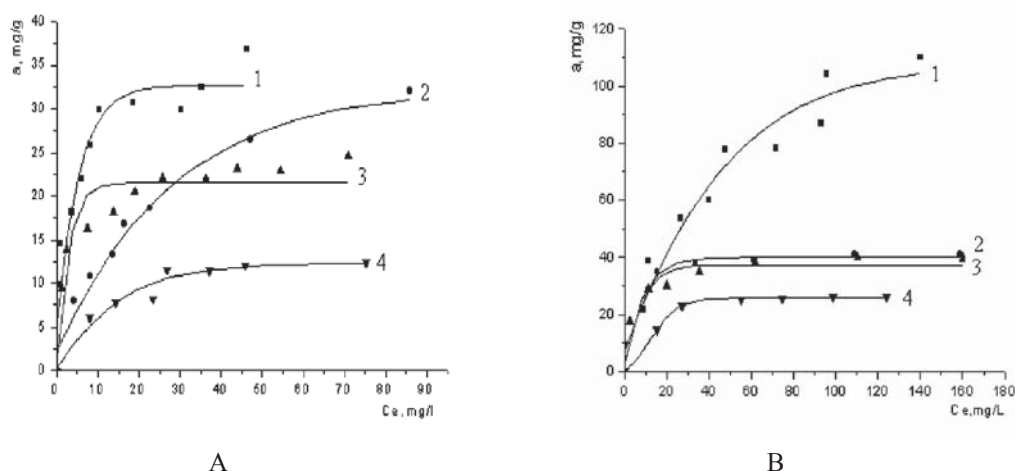

A

B

Figure 4. Adsorption isotherms of vitamin B_{12} (A) and Congo Red dye (B) on activated carbons CAP (1), CAN-8 (2), BAU (3) and CAS-23 (4).

Absorption of studied substances was determined according to the equation (1):

$$a = \frac{(Co - Ce)V}{m} \ , \tag{1}$$

where: a - adsorption, mg/g; C_0- initial solution concentration, mg/L; Ce – equilibrium concentration, mg/L; V- solution volume, L; m – sorbent quantity, g.

Adsorption isotherms of Congo Red dye and vitamin B_{12} on investigated activated carbons are shown in Figure 4.

The results confirm the hypothesis of more effective activated carbon CAP at immobilizing investigated substances. This allows us to conclude that the determinant role in the adsorption of vitamin B_{12} and Congo Red dye was played by structural parameters of studied carbons, and especially the value of mesopores volume which is in direct correlation with the value of maximum adsorption (Figure 5).
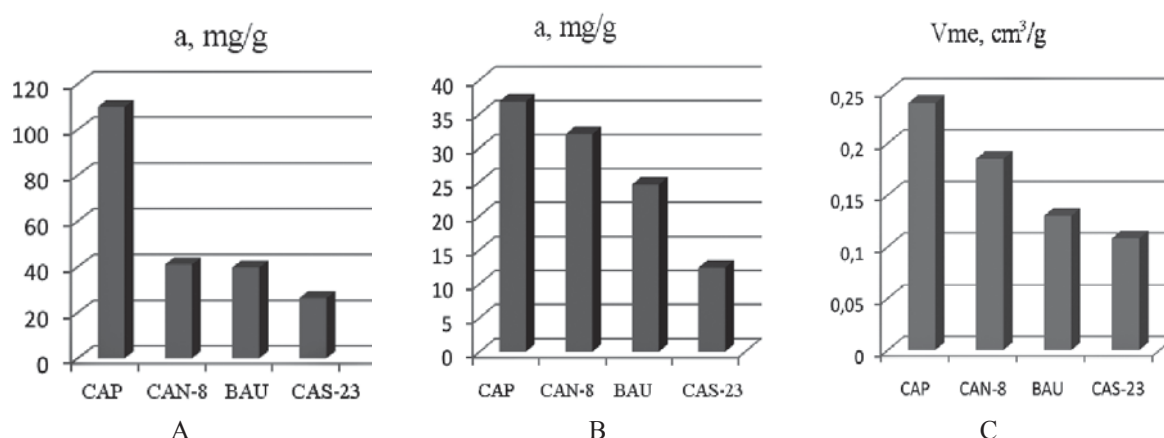

Figure 5. Correlation between the values of maximal adsorption of Congo Red dye (A), vitamin B_{12} (B) and the values of mesopores volume (C) of studied activated carbons.

Pore volume occupied by molecules of Congo Red dye and vitamin B_{12} in investigated activated carbon pores was determined from equation (2):

$$V_{S}^{*} = a_m \cdot V^{*}, \tag{2}$$

where: V_{S}^{*} - pore volume occupied by molecules in the pores of activated carbon adsorbents, cm³/g; a_m - maximal adsorption value of adsorption on active carbons, mmol/g; V^{*} - molar volume of adsorbents calculated from the values of length and Van der Waals angles between molecules' atoms.

Values V^{*}, calculated according to [10], are 2.94 nm³ for B_{12} and 1.54 nm³ for Congo Red. Table 2 presents the results of estimating the pore volume V_{S}^{*} occupied by molecules of investigated substances on investigated carbon samples and the rate of use of mesopores G%, calculated according to equation 3.

$$G\% = (V_{S}^{*}/Vme) \cdot 100, \tag{3}$$

Table 2

Pore volume V_S and the rate of use of mesopores G% for activated carbons CAN-8, CAS-23, CAP and BAU

AC sample	Vme, cm³/g	Vitamin B_{12}			Congo Red		
		a_m, mmol/g	V_{S}^{*}, cm³/g	G, %	a_m, mmol/g	V_{S}^{*}, cm³/g	G, %
CAN-8	0,185	0,0236	0,0418	22,59	0,0574	0,0533	28,81
CAS-23	0,108	0,0096	0,0170	15,74	0,0316	0,0293	27,13
CAP	0,239	0,0295	0,0523	21,88	0,1579	0,1465	61,29
BAU	0,13	0,0177	0,0314	24,15	0,0560	0,0519	39,92

The obtained data show higher indices for mesopores use in the case of Congo Red dye, which is due to the smaller size of the dye molecule opposite the vitamin B_{12} molecule size.

There have been studies on the influence of increasing temperature and decreasing pH on the immobilization process of marker substances. Adsorption isotherms were determined for investigated substances at t = 38 ° C and in solution with pH 2. It was found that increase of temperature to 38 ° C and pH decrease to 2 is accompanied by an increase in the rate of immobilization of the dye Congo Red and vitamin B_{12} on average by 10% (Figure 6, 7).
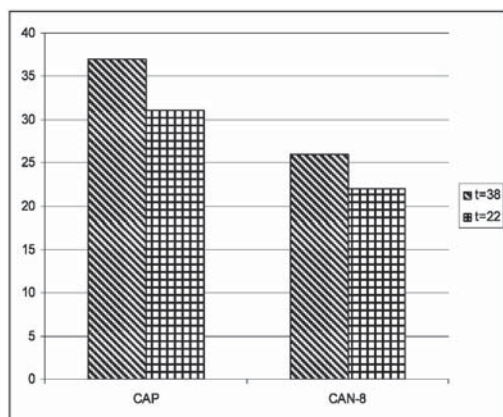
Figure 6. Influence of temperature on vitamin B$_{12}$ adsorption from aqueous solutions
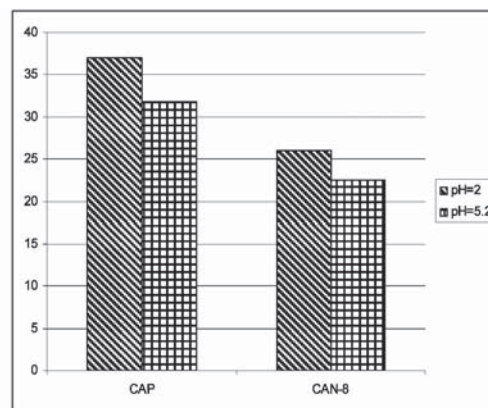

Figure 7. Influence of pH on vitamin B$_{12}$ adsorption from aqueous solutions

Conclusions

1. It was established that the immobilization of the Congo Red dye and vitamin B$_{12}$ depends directly on the structural parameters of activated carbons, in particular, the volume of mesopores, and the structure and molecular weight of the adsorbed substance. The adsorption highest values were recorded for activated carbons from plum stones, with a mesopores volume practically twice higher than of the other carbons.

2. Increase of temperature to 38 ° C and pH reduction to 2 probably enhances the diffusion of adsorbed molecules in the pores of the adsorbent, which increases adsorption with around 10%.

References

[1]. Duca, Gh.; Scurlatov, Iu.; Misiti, A.; Macoveanu, M.; Surpăţeanu, M. Ecological chemistry./In romanian. Bucharest: Matrix Rom., 1999, pp 305.

[2]. Negulescu, M.; Vaicum, L.; Pătru, C.; ş. a. Environment protection. /In Romanian. Bucharest, 1995, pp 204.

[3]. Lupaşcu, T. Activated carbon from vegetal raw materials. Monograph/ In Romanian L.: ÎEP: Ştiinţa, Chişinău, 2004, pp 224.

[4]. Lupaşcu, T. Modern technologies for obtaining activated carbons and its use for the environment protection and human health. /In Romanian. Buletinul ASM, Seria ŞBCA, 2004, nr 1, pp 170-175.

[5]. Rodriguez-Reinoso, F.; Lopez-Gonzalez, I. Activated carbons from almond shells. Caracterization of the pore structure. Carbon, 1984, vol. 22, pp.13-18.

[6]. Lupaşcu, T.; Ciobanu, M.; Ţîmbaliuc, N. Uze of oxidized activated carbon in water treatment processes. Environmental Engineering and Managament Journal. September, 2002. vol.1.№2, pp.169-176.

[7]. Lupaşcu, T.; Ciobanu, M.; Ţîmbaliuc, N. Adsorption of dyes and surfactants from aqueous solutions on activated carbons. /In Romanian. Journal of chemistry, 2007, v. 58, nr.10, pp. 905 -908.

[8]. Lupaşcu, T.; Ţîmbaliuc N. Elaboration of technological scheme of sewage treatment at the textile industries. / In romanian. Materials of the Conference INECO 15 years "Ecology and environment - research, implementation and management". 29 December, Chisinau, 2006, pp.201-204.

[9]. Shen, W.Z.; Zheng, J.T.; Zhang, Y.L.; Wang, J.G.; Qin Z.F. The effect of pore structure of activated carbon on the adsorption of Congo red and vitamin B12. Studies in Surface Science and Catalysis. Volume 146, 2003, pp 779-782.

[10]. Wenzhong Shen, Jingtang Zheng, Zhangfeng Qin, Jianguo Wang, Yihong Liu. Preparation of mesoporous activated carbon fiber by steam activation in the presence of cerium oxide and its adsorption of Congo red and Vitamin B12 from solution. Journal of Materials Science, vol. 39, no.13, 2004 July, pp. 4693 – 4696.

[11]. AUTOSORB AS-1. AS1Win. GAS SORPTION SYSTEM. OPERATION MANUAL. Firmware: ver 2.55. AS1Win Software: ver 2.0 and newer. Quantachrome Instruments, 2008.

NONEXPERIMENTAL SCREENING OF THE WATER SOLUBILITY, LIPOPHILICITY, BIOAVAILABILITY, MUTAGENICITY AND TOXICITY OF VARIOUS PESTICIDES WITH QSAR MODELS AID

O.G. Kolumbin[a], L.N. Ognichenko[b], A.G. Artemenko[b], P.G. Polischuk[b],
M.A. Kulinsky[b], E.N. Muratov[b], V.E. Kuz'min[b], V.A. Bobeica[c]

[a]*Tiraspol State University of T.G.Shevchenko, Moldova, Tiraspol, 3300, 25 October, 128,*
[b] *Department of Molecular Structure and Chemometrics, A.V. Bogatsky Physical-Chemical Institute National Academy of Science of Ukraine, Ukraine, Odessa, 65080, LustdorfskayaDoroga 86,*
[c]*Moldova State University, Department of Industrial and Ecological Chemistry, Republic of Moldova, Kishinew, 2009, 60 Mateevich Str. *Corresponding author: valentinbobeica@rambler.ru*

Abstract: In our study the dataset containing 489 pesticides and their active substances of different classes of organic compounds was used for analysis. For compounds of analyzed dataset the values of lipophilicity, water solubility, toxicity, bioavailability and mutagenicity were predicted by developed QSAR models. The most environmentally hazardous substances were identified using prediction of QSAR models for pesticides. The satisfactory coincidence between the experimental values of investigated properties and their predicted values by QSAR models was obtained (coefficient of determination in the range 83-94%).

Keywords: pesticides, toxicological analysis, QSAR, lipophilicity, RF method

Introduction

The prognosis of dangerous xenobiotics and elaboration of new methods of their toxic evaluation is getting more actual when the growing amount of new pesticides outnumbers the possibilities of their experimental toxic evaluation. Terefore, different mathematical models based on the relationship between biological activity and physical-chemical properties of compounds are used for predicting toxic parameters of new pesticides, their teratogenesis and mutagenesis and for installing the calculation methods of the corresponding normatives. This approach of nonexperimental screening can considerably reduce the number of experimental researches of new pesticides and use of time and materials in these investigations. The goal of this study is to determine mathematical QSAR effective application for prognosis of ecological danger caused by pesticides on mammals using such properties as the lipophilicity, water solubility, bioavailability, mutagenicity and toxicity calculations.

Materials and Methods

In this study a dataset[1] containing information about solubility, lipophilicity and toxicity for 489 pesticides and their active substances of different classes of organic compounds was used for research. Similar researches and analysis had been done using HiT QSAR software [1, 2]. Experimental values of lypophilicity are known for 334 molecules and are varied in the range of -4 till 8,39. Values for water solubility are known for 371 molecules of the analyzed database and are varied from -7,8 till 1,57.

All the 489 compounds were analyzed using previously developed models for lypophilicity [3], solubility [4], bioavailability [5], mutagenicity [6] and toxicity on *Tetrahymenapyritormis*[7]. All these 5 models were built using simplex representation of molecular structure (SiRMS) and the statistic method of random forest (RF) [8]. CAS numbers of investigated molecules are presented in Table 1.

In this study Simplex Representation of Molecular Structure (SiRMS) QSPR approach [1] was used for calculation of structural descriptors of molecules. Main concept of this approach is that any molecule can be represented as a system of different simplexes (tetratomic fragments with fixed composition and topological structure). At the 2D level, the connectivity of atoms in simplex, atom type and bond nature (single, double, triple, aromatic) are taking into consideration. In the present study, only bounded 2D simplex descriptors were used for molecular structure representation.Not only atom type but also other physical-chemicalcharacteristics of an atom such as: partial charge, lipophilicity, refraction and the ability for an atom to be a donoror acceptor in hydrogen bond formation were used for atomdifferentiation. The usageof sundry variants of differentiation of simplex vertexes(atoms) represents the principal feature of the proposedapproach. LogP, molecularrefraction, electronegativity of the molecule and its mass were used as integral descriptors in addition to calculated 2D simplex descriptors.Although the developed in our laboratory SiRMS method is novel, it has been employed successfully in several studies to differentiate ''structure-activity'' relationships [9-11]. The main advantages of SiRMS are the possibilityof analysis of molecules with noticeable structural differencesas well as the possibility to reveal individual molecularfragments (simplex combinations) promoting or interferingwith investigated property.

---

[1] http://chem.sis.nlm.nih.gov/chemidplus/chemidlite.jsp

Such approach avoids additive contributions of structural fragments, because the contributions of atom/or structural fragment depend on their surrounding. SiRMS methodology does not have many of the restrictions of such well-known and widely used approaches as CoMFA, CoMSIA, HASL, in which the application is limited to a structurally homogeneous set of molecules only. SiRMS approach is similar to HQSPR approach but has not its limitations (consideration of atom type only) and deficiencies (an ambiguity of descriptor formation during the hashing of molecular holograms).

Results and Discussion

As early mentioned the experimental lipophilicity values were found only for 334 compounds (68% from all molecules). Using the lipophilicity RF model [3] LogP values were predicted for all 489 molecules. RF model for calculation of lipophilicity was built on the base of more than 10,000 molecules. Simplex descriptors were calculated for studied 489 molecules using such tuning parameters which were used for the construction of lipophilicity RF model. For molecules of analyzed dataset with known LogP values the model predictive ability was assessed. The coefficient of determination (R^2) between the observed experimental values of Log P and predicted Log P for RF model equals 0.94 and the standard error (SE) equals 0.46.

For water solubility (LogS$_w$) a model was built on dataset consisting of more than 1200 compounds [12]. Statistical characteristics of the RF model for water solubility are quite adequate: R^2 for the training set is 0.99 and for *out-of-bag* set equals 0,91. For 489 molecules simplex descriptors were calculated considering the same tuning parameters which were used to build the RF model for solubility. It should be noted that only 312 of the molecules (64% from the dataset) with known experimental values LogSw get in the model domain applicability. The other 59 molecules (12%) are out the range of applicability. Using the molecules that are in the domain applicability of the model with known Log Sw values the predictive ability of the model was estimated. The coefficient of determination (R^2) between the observed experimental Log Sw values and the predicted Log S$_w$ by RF model is 0.83 and the standard error (SE) = 0.85. Among the remaining 118 molecules for which experimental Log Sw values aren't known only 90 molecules are in the domain applicability of the model and 28 outside of the domain applicability.

Table 1

CAS – numbers of analysed compounds

100-02-7	108-34-9	116-29-0	126-22-7	1563-66-2	2310-17-0	327-19-5	520-45-6
100-52-7	108-35-0	116-52-9	126-61-4	1582-09-8	2312-35-8	327-98-0	524-40-3
101-05-3	1085-98-9	117-18-0	126-75-0	1596-84-5	2314-09-2	330-54-1	524-42-5
101-20-2	108-60-1	117-26-0	127-21-9	1610-17-9	2425-06-1	330-55-2	52-46-0
101-21-3	108-62-3	117-52-2	127-63-9	1610-18-0	2425-10-7	330-64-3	52-51-7
101-27-9	108-80-5	117-80-6	127-90-2	1646-87-3	2431-96-1	333-41-5	52-60-8
101-42-8	108-91-8	117-81-7	130-15-4	1646-88-4	2439-01-2	3337-71-1	52-68-6
1014-69-3	108-94-1	118-52-5	130-86-9	1689-83-4	2463-84-5	3347-22-6	52-85-7
1014-70-6	108-95-2	1186-09-0	131-11-3	1689-84-5	2497-07-6	3383-96-8	53-19-0
101-99-5	109-84-2	118-74-1	131-89-5	1689-99-2	2511-10-6	350-46-9	532-54-7
102-60-3	109-94-4	118-75-2	131-91-9	1696-17-9	2540-82-1	3566-00-5	533-74-4
102-71-6	109-97-7	118-96-7	132-66-1	1698-60-8	2587-90-8	3615-21-2	534-52-1
1031-47-6	110-12-3	119-12-0	133-06-2	1702-17-6	2593-15-9	366-18-7	535-89-7
103-17-3	110-44-1	119-27-7	133-07-3	1836-75-5	2595-54-2	3689-24-5	54-11-5
103-18-4	110-85-0	119-38-0	133-32-4	1836-77-7	2597-03-7	371-62-0	542-75-6
103-33-3	1113-02-6	1194-65-6	133-90-4	1861-32-1	262-20-4	371-86-8	545-06-2
1034-01-1	1113-14-0	119-89-1	133-91-5	1861-40-1	2631-37-0	3740-92-9	54-62-6
104-01-8	111-44-4	120-23-0	136-25-4	1897-45-6	2631-40-5	420-04-2	551-06-4
104-04-1	1114-71-2	120-32-1	136-45-8	1912-24-9	2636-26-2	470-90-6	55-38-9
105-13-5	112-12-9	120-36-5	137-18-8	1912-26-1	2642-71-9	477-27-0	555-37-3
105-28-2	1121-30-8	120-51-4	137-26-8	1918-00-9	2655-14-3	485-31-4	555-77-1
105-67-9	112-24-3	120-57-0	139-40-2	1918-02-1	2686-99-9	494-52-0	556-61-6
105-99-7	112-27-6	120-60-5	1397-94-0	1918-13-4	2797-51-5	495-73-8	558-25-8
106-24-1	112-30-1	120-62-7	139-94-6	1918-16-7	288-32-4	499-75-2	563-12-2
106-46-7	112-38-9	120-80-9	140-57-8	1929-77-7	2921-88-2	50-00-0	584-79-2
106-50-3	112-42-5	120-83-2	141-03-7	1929-82-4	297-97-2	500-28-7	60-51-5
106-51-4	112-56-1	120-93-4	141-27-5	1943-79-9	298-00-0	50-14-6	60-57-1
106-89-8	1129-41-5	121-21-1	141-43-5	1982-47-4	298-01-1	50-18-0	60-80-0

106-93-4	1134-23-2	121-29-9	141-66-2	1982-49-6	298-02-2	502-55-6	615-15-6
106-95-6	113-48-4	1214-39-7	141-78-6	2008-41-5	298-03-3	50-29-3	61-82-5
106-96-7	114-26-1	121-75-5	141-84-4	2032-59-9	298-04-4	50-31-7	62-56-6
107-02-8	1146-99-2	122-10-1	1420-06-0	2032-65-7	299-85-4	504-24-5	62-73-7
107-04-0	114-83-0	122-14-5	1420-07-1	2104-64-5	299-86-5	50-65-7	63-25-2
107-06-2	1149-23-1	122-15-6	142-46-1	2104-96-3	300-76-5	506-77-4	63-74-1
107-07-3	115-26-4	122-17-8	1444-64-0	2164-09-2	301-11-1	50-71-5	64-00-6
107-13-1	115-29-7	122-34-9	145-73-3	2164-17-2	301-12-2	510-15-6	640-15-3
1071-83-6	115-31-1	122-39-4	148-01-6	2212-67-1	305-85-1	51-03-6	645-05-6
107-18-6	115-32-2	122-42-9	148-24-3	2227-13-6	3060-89-7	51-14-9	65-85-0
107-19-7	115-90-2	122-88-3	148-79-8	2227-17-0	311-45-5	51-17-2	66-02-4
107-21-1	115-91-3	123-09-1	149-30-4	2255-17-6	311-47-7	51-18-3	66-27-3
107-22-2	115-92-4	123-33-1	1498-64-2	2274-67-1	312-73-2	512-56-1	66-76-2
107-31-3	115-93-5	123-54-6	149-91-7	2275-18-5	314-40-9	51-28-5	66-81-9
107-49-3	116-01-8	124-17-4	150-50-5	2303-16-4	314-42-1	513-49-5	67-63-0
1079-33-0	116-06-3	124-28-7	150-68-5	2303-17-5	321-54-0	518-20-7	67-66-3
1081-34-1	116-16-5	126-15-8	152-20-5	2307-68-8	3244-90-4	518-75-2	67-72-1
67-99-2	731-27-1	759-94-4	78-87-5	84-74-2	91-20-3	94-96-2	97-23-4
680-31-9	732-11-6	76-03-9	79-00-5	85-34-7	919-86-8	950-10-7	973-21-7
68-11-1	73-24-5	76-06-2	79-01-6	86-29-3	92-52-4	950-35-6	97-53-0
694-59-7	741-58-2	76-22-2	79-09-4	86-50-0	92-67-1	950-37-8	97-77-8
70-30-4	74-59-9	76-44-8	79-11-8	867-27-6	92-84-2	95-14-7	98-64-6
70-34-8	74-60-2	77-06-5	79-19-6	86-87-3	934-32-7	953-17-3	98-95-3
70-38-2	74-83-9	77-09-8	79-21-0	86-88-4	934-87-2	95-50-1	991-42-4
70-43-9	74-85-1	77-47-4	79-34-5	869-29-4	93-65-2	95-57-8	99-30-9
709-98-8	74-90-8	77-49-6	79-40-3	87-51-4	93-72-1	95-65-8	99-92-3
71-23-8	75-01-4	77-92-9	79-46-9	87-68-3	93-76-5	957-51-7	99-93-4
71-43-2	75-09-2	780-11-0	79-57-2	87-86-5	94-09-7	95-80-7	75-99-0
71-55-6	75-15-0	78-34-2	81-81-2	88-06-2	941-69-5	95-93-2	786-19-6
72-20-8	75-21-8	78-48-8	82-68-8	886-50-0	944-22-9	95-95-4	84-65-1
72-33-3	75-56-9	78-52-4	834-12-8	88-85-7	947-02-4	96-12-8	91-15-6
72-43-5	75-75-2	78-53-5	83-79-4	89-78-1	94-74-6	96-24-2	94-82-6
72-54-8	757-58-4	78-57-9	841-06-5	90-43-7	94-75-7	96-45-7	97-17-6
72-56-0							

Table 2

Predicted and observed values of lipophilicity, water solubility, toxicity and bioavailability for 14 the most environmentally hazardous soluble in water substances analysed with QSAR-models

№	CAS number	Structure formula	LogP		Log (IGC50-1)	Bioavailability (Pred.)			LogS$_w$	
			Pred.	Exp.	Pred.	low	average	high	Pred.	Exp.
1	70-34-8		1.67		1.44	1	2	2	-2.15	-2.67
2	1929-82-4		3.15	3.41	1.28	1	2	2	-3.63	-3.51
3	86-88-4		1.96	1.65	1.06	1	2	2	-3.15	-2.53
4	92-67-1		2.94	2.86	1.06	1	1	2	-3.66	-
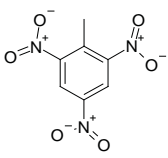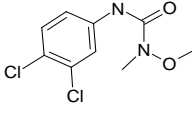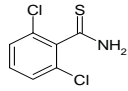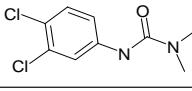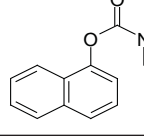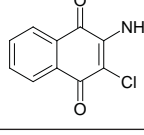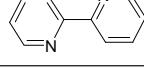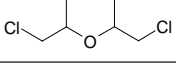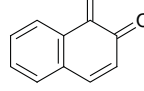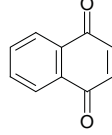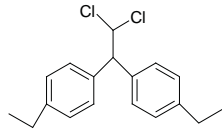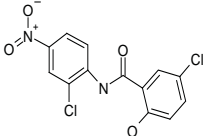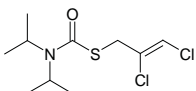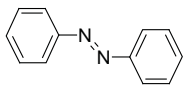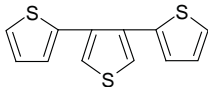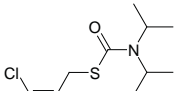
№	CAS number	Structure formula								
5	118-96-7		1.82	1.60	0.97	1	2	2	-2.43	-3.24
6	330-55-2		3.09	3.20	0.94	1	1	2	-3.31	-3.52
7	1918-13-4		2.12	2.96	0.92	1	1	2	-2.78	-2.34
8	330-54-1		2.78	2.68	0.86	1	1	2	-3.16	-3.74
9	63-25-2		2.49	2.36	0.85	1	1	2	-3.20	-3.26
10	2797-51-5		1.88	2.12	0.43	1	1	1	-2.35	-
11	366-18-7		1.61	1.50	0.41	1	1	2	-1.60	-1.42
12	108-60-1		2.32	2.48	0.37	1	2	2	-1.57	-2.00
13	524-42-5		1.72		0.22	1	1	2	-2.11	-
14	130-15-4		1.77	1.71	0.20	1	1	2	-2.15	-

Table 3

Predicted and observed values of lipophilicity, water solubility, toxicity and bioavailability for 6 the most environmentally hazardous lipophilic substances from analysed dataset with QSAR-models

№	CAS number	Structure formula	LogP		Log (IGC50-1)	Bioavailability (Pred.)			LogS$_w$	
			Pred.	Exp.	Pred.	low	average	high	Pred.	Exp.
1	72-56-0		5.39		1.63	1	1	2	-6.78	-6.49
2	50-65-7		4.74		1.49	1	2	2	-4.65	-5.31

3	2303-16-4		4.25	4.49	1.02	1	1	2	-4.26	-4.29
4	103-33-3		3.80	3.82	1.34	1	1	2	-4.25	-4.45
5	1081-34-1		3.45	5.57	1.18	1	2	2	-4.37	
6	2303-17-5		4.42	4.60	1.04	1	1	2	-4.72	-4.88

In the result of the analysis of the 489 molecules of the studied dataset according to the developed three models for bioavailability [5], it was found that 116 of them (34%) are not bioavailable molecules, 25 molecules (5%) - with high bioavailability, 124 molecules (25%) - with average and 175 molecules (36%) - with low bioavailability. In these models, if the molecule is assigned 1 - the substance is bioavailable, and 2 – not bioavailable.

For 489 molecules of the dataset using the RF model for calculation of mutagenicity [6] it was predicted that 392 molecules (80% of all the molecules of dataset) are part of the class of non-mutagenic, while the remaining 97 molecules (20%) are dangerous mutagenic substances, which were used to find the most environmentally hazardous substances.

Using the RF model of toxicity on Tetrahymenapyriformis organisms [7] toxicity values (Log(IGC50-1)) for all 489 molecules of dataset were predicted. 339 molecules (69%) concern the area of applicability of the model, their predicted values are varied in the range of -1.6 till 2.4. The remaining 150 molecules (31%) are not part of domain of applicability of the model.

In the result of the data analysis the most environmentally hazardous substances which are bioavailable, mutagenic, toxic, having proper water solubility and have a high lipophilicity were selected. Mutagenic, bioavailable and toxic substances were selected for which the values of solubility in water and fats were analyzed. In particular, there were selected 14 compounds well soluble in water and 6 with large lipophilicity value. The predicted LogP, $LogS_w$, Log (IGC50-1) values and bioavailability for most environmentally hazardous molecules from the dataset are presented in Table 2 and 3.

Conclusion

Non- experimental screening of the lipophilicity, solubility in water, toxicity, bioavailability and mutagenicity was carried out for the database consisting of 489 pesticides and their active substances of different classes of organic compounds. For prediction of oral human bioavailability of pesticides the previously developed RF model was used. Using screening results the most environmentally hazardous substances which are mutagenic, bioavailable, toxic, having high water and fats solubility were identified.

The satisfactory coincidence between the experimental data and predicted by QSAR models was revealed (coefficient of determination in the range 83-94 %). Thus, this allows the use of these models as a non experimental, ecotoxicity prior prediction calculation tool for new pesticides.

References
[1]. Kuz'min, V. E.; Artemenko, A. G.; Muratov, E. N.; Polischuk, P. G.; Ognichenko, L. N. Liahovsky, A. V.; Hromov, A. L.; Varlamova, E. V. InRecentAdvancesinQSARStudies. Puzyn,T.; Cronin, M.; Leszczynski, J. (eds), **2009**, Springer, NewYork.
[2]. Kuz'min, V. E.; Artemenko, A. G.; Muratov, E. N. *J. Comp. Aid. Mol. Des.* **2008**, *22*, pp. 403–421.
[3]. Ognichenko, L. N.; Kuz'min, V.E.; Gorb, L.; Hill, F.C.; Artemenko, A.G.; Polischuk, P.G.; Leszczynski, J. *Mol. Inf.*, **2012**, *31*, pp. 273-280.
[4]. Kovdienko, N. A.; Polishchuk, P. G.; Muratov, E. N.; Artemenko, A. G.; Kuz'min, V. E.; Gorb, L.; Hill, F.; Leszczynski, J.*Mol. Inf.* **2010**, *29*, pp. 394 – 406.

[5]. Golovenco, M.Ja.; Kuz'min, V. E.; Artemenko, A. G.; Kulinskii, M.A.; Polishchuk, P.G.; Borisiuk, J.Ju. Prognozirovanie biodostupnosti likarskih zasobiv metodom klasificatsiinih modelei.*Jurnal kliniceskaia informatica i telemeditsina*, **2011**, *8*, 88-92 (in ukrainian).

[6]. Sushko, Yu.; Novotarskyi, S.; Korner, R.; Pandey, A. K. et al.*J. Chem. Inf. Model.* **2010,** *50,* pp. 2094–2111.

[7]. Polishchuk, P. G.; Muratov, E. N.; Artemenko, A. G.; Kolumbin, O. G.; Muratov, N. N.; Kuz'min, V. E. ApplicationofRandomForestApproachtoQSARPredictionofAquaticToxicity.*J. Chem. Inf. Model.* **2009,** *49,* pp.2481–2488.

[8]. Breiman, L. *Machine Learning.* **2001**, *45*, pp. 5-32.

[9]. Artemenko, A. G.; Muratov, E. N.; Kuz'min,V. E.; Kovdienko, N. A.; Hromov, A. I.; Makarov,A. A.; Riabova, O. B.; Wutzler, P.; Schmidtke, M. *J. Antimicrob. Chemother.* **2007**, *60*, pp. 68–77.

[10]. Kuz'min, V. E.; Artemenko, A. G.; Muratov, E. N.; Volineckaya, I. L.; Makarov, V. A.; Riabova, O. B.; Wutzler, P; Schmidtke, M.*J. Med. Chem.* **2007**, *50*, pp. 4205–4213.

[11]. Kuz'min, V. E.; Muratov, E. N.; Artemenko, A. G. Gorb, L.; Qasim, M.; Leszczynski, J.*J. Comp. Aid. Mol. Des.* **2008**, *22*, pp. 747–759.

[12]. Tetko, I. V.; Tanchuk, V. Y.; Villa, A. E. P. *J. Chem. Inf. Comp. Sci.* **2001**, *41*(5), pp. 1407-1414.